INVESTIGATIONS ON PERFORMANCE CHARACTERISTICS OF A CENTRIFUGAL SLURRY PUMP HANDLING WATER AND ASH

A thesis submitted in fulfillment of the

requirements for the award of the degree of

DOCTOR OF PHILOSOPHY

in

Mechanical Engineering

Submitted by

Satish Kumar

Roll No: 90708502

DEPARTMENT OF MECHANICAL ENGINEERING

THAPAR UNIVERSITY, PATIALA-147004

PUNJAB-INDIA

CERTIFICATE

Certified that the thesis entitled **"INVESTIGATIONS ON PERFORMANCE CHARACTERISTICS OF A CENTRIFUGAL SLURRY PUMP HANDLING WATER AND ASH"**, being submitted by Satish Kumar, to Mechanical Engineering Department, Thapar University, Patiala, in fulfillment of the requirements for the award of the degree of **DOCTOR OF PHILOSOPHY**, is a record of bonafide research work carried out by him under my guidance and supervision. The matter presented in the thesis has not been submitted in part or full to any other University or Institute for the award of any degree.

SUPERVISORS

Dr. B. K. Gandhi

Professor

Department of Mechanical and Industrial Engineering

Indian Institute of Technology Roorkee

Dr. S. K. Mohapatra

Senior Professor

Department of Mechanical Engineering

Thapar University, Patiala

DECLARATION

I hereby declare that the research work presented in this thesis entitled "**INVESTIGATION ON PERFORMANCE CHARACTERISTICS OF A CENTRIFUGAL SLURRY PUMP HANDLING WATER AND ASH**", submitted for the award of the degree of Doctor of Philosophy in the Department of Mechanical Engineering, Thapar University, Patiala is original and my own account of research. This research work is independent and its main content work has not previously been submitted for degree at any university in India or Abroad.

(Satish Kumar)

ACKNOWLEDGEMENT

This note of acknowledgement is my sincere appreciation to all those who stand out most notably in my mind as contributing directly or indirectly to this research effort.

I am greatly indebted to my revered supervisor, Dr Bhupendra Kumar Gandhi, Professor, Department of Mechanical and Industrial Engineering, Indian Institute of Technology, Roorkee and Dr S. K. Mohapatra, Senior Professor, Department of Mechanical Engineering, Thapar University, Patiala for his invaluable guidance, prudent advice and encouragement in accomplishing this research work. His expertise, innovative ways of thinking, constant interest and follow up were the crucial factors in enabling this research work to take its final shape. I extend my heartfelt thanks to my supervisor forever.

I express my regards and gratitude to Dr Ajay Batish, Professor and Head, Mechanical Engineering Department, Thapar University, Patiala for providing requisite facilities, unfailing support, inspiration and ingenuous suggestions.

A sincere token of gratitude is paid to my wife and son for their enormous patience, sustained encouragement and eternal support throughout the research work.

Lastly, on a personal note, I would also like to express my gratitude to all my wonderful students and colleagues of Mechanical Engineering Department, Thapar University, Patiala for their great support, conscientious advice, encouragement and inspiration throughout this research.

(Satish Kumar)

ABSTRACT

Power generation in India is primarily coal based in the present scenario. Coal used in our thermal power plants produces a large amount of ash. Currently, bottom ash is being transported hydraulically from thermal power plant to ash ponds through pipelines at low solid concentration. The operation of ash disposal pipelines is therefore highly uneconomical due to requirement of large quantity of water and increase in power consumption for pumping water.

The basic parameters for the design of any slurry transportation system are hydraulic parameters, which include properties of carrier fluid, particle size, solid concentration, slurry rheology, specific gravity of the solids etc. The fly ash and bottom ash from different power plants differ greatly in their characteristics and hence the design of ash disposal system needs to take in to account these variations. It is therefore necessary to have knowledge of the properties of fly ash, bottom ash and their slurries. Pump is the heart of any ash disposal system. Coal ash is generally transported to the ash pond using slurry pumps and pipelines in the thermal power plant. Bottom ash particles are coarser without much fine particles. The Indian coal ash having higher specific gravity and also content large amount of non-combustible matter. Further, these also differ widely in their physical and chemical characteristics depending on the coal mines. Therefore in order to optimize the hydraulic design procedure for transporting bottom ash (B.A.) at higher concentrations, it is essential to carry out basic investigation using bench scale tests and pilot plant loop to develop the required technology.

As rheology of the slurry plays a major role in flow, the rheological characteristics of the bottom ash in the concentration range of 10-50% (by weight) with and without the addition of fly ash has been studied to facilitate conveying of bottom ash slurry at higher concentrations. Addition of fly ash in the bottom ash has been varied from 10 to 30% (by weight). The flow behaviour of all the slurries was observed as Newtonian. It is seen that the shear stress value increases monotonically with increase in the solid concentration. The value of relative viscosity increases with increase in the proportion of fly ash in the bottom

ash slurry. The rheology of the slurry suspension was evaluated with the variation of the temperature from 26ºC to 41ºC at different shear rates. The temperature of the slurry suspension was increased in step of 5ºC at concentration of 20% (by weight). The relative viscosity gets reduced with increase in the temperature of the bottom ash slurry, with and without addition of fly ash. The optimum modification in viscosity was found as temperature of 36 ºC.

The performance characteristics of the centrifugal slurry pump have been evaluated at four different speeds namely 1000, 1150, 1300 and 1450 rpm with clear water and bottom ash slurry with and without addition of fly ash. Experiments were conducted with bottom ash slurry at four concentrations for each speed. Addition of fly ash in the bottom ash has been varied from 10 to 30% (by weight). Similarly, the experiments with addition of the fly ash in the bottom ash mixture in different ratios namely 9:1, 8:2 and 7:3 were conducted at four concentrations in the range of 12 to -48% to evaluate the performance characteristics of the pump at all four speeds.

The pump total head, overall efficiency and pump input power at different flow rates have been evaluated. The performance characteristics results show that the values of head and the efficiency of the pump depend on the solid concentration. It was also observed that the performance parameter of the pump strongly depends on slurry concentration. The addition of fine particles of fly ash in the coarser particles of bottom ash slurry, leads to reduce the additional head losses in the pump. The pump performance in terms of head and efficiency has been found to improve with addition of fly ash in bottom ash slurry.

The solid-liquid two-phase flow behavior in the centrifugal slurry pump has been numerically simulated using Computational Fluid Dynamics (CFD) code FLUENT for the design condition and also off-design conditions. The mixture model has been used for the simulation of the solid-liquid two-phase flow of bottom ash and water mixture. The performance characteristics of the centrifugal slurry pump are numerically predicted with water and bottom ash slurry at different speed 1000, 1150, 1300 and 1450 rpm. The solid concentration of the bottom ash slurry varied from 0% to 45% by weight. The numerical

results are compared with the experimental measurements. The CFD-results show satisfactory agreement with experimental data in a complete operating range of the pump with water. The predicted simulation results show that performance characteristics of the centrifugal slurry pump are the function of concentration and viscosity of the bottom ash slurry. The deviation of predicted value of head ratio and power ratio with experimental data is lie within the limits of ±8%.

Both the pump head and the efficiency are reduced with concentration of solid-liquid mixture. The flow separation has been found near the volute tongue and becomes more remarkable with increasing solid phase concentration. The predicted numerical results are helpful for improvement in the hydraulic design of centrifugal slurry pumps. The present study can be useful for transporting coarser particles like bottom ash with the addition of fine particulate fly ash at higher concentrations, so that large amount of water and power can be saved.

CONTENTS

NOMENCLATURE

$\vec{a}$	Secondary-phase particle's acceleration, m/ s^2
C_D	Drag coefficient
C_v	Volume concentration of solid in fraction
C_w	Concentration of solid (by weight) ,%
d_{50}	Median particle diameter, mm
d_{wm}	Weighted mean diameter, mm
d_i	Average diameter of the two successive size of sieves, mm
d_s	Diameter of the particles of secondary phase , mm
D_1	Impeller diameter at inlet, mm
D_1	Impeller diameter at outlet, mm
$\frac{du}{dy}$	Shear rate, s^{-1}
ER	Efficiency ratio
e_{ss}	Coefficient of restitution for particle collisions
F	External body forces, N
f_i	Fraction of solid retained on a particular sieve
g	Gravitational acceleration, m/ s^2
$g_{o.ss}$	Radial distribution function
H	Total head, m
H_s	Head developed of slurry, m

H_w	Head developed of water, m
HR	Head ratio
J_f	Mass flux through face f
k	Thermal conductivity, W/ m K
K	Turbulence kinetic energy, Ns/m^2
N	Impeller speed, rpm
N_s	Non dimensional specific speed
P_{out}	Output power, kW
P_{in}	Input power of pump, kW
$\frac{P}{\rho g}$	Pressure reading at delivery side, m
$\frac{P}{\rho g}$	Pressure reading at suction side, m
PR	Power ratio
Q	Flow rate, $m^{3/}sec$
Q_r	Flow ratio
Q_{ea}	Equi-size skew
Re_p	Particle Reynolds number
$\vec{r}$	Position vector in the rotating frame
S	Specific gravity of solid
sH	Specific head
sQ	Specific discharge

sP	Specific power
Se	Maximum area in 2-dimensional or volume in 3-dimensiona
S_i	Heat generation, J/m^3
T	Terminal energy per unit volume, J/m^3
U_1	Peripheral velocity at impeller inlet, m/s
U_2	Peripheral velocity at impeller outlet, m/s
V_d	Velocity of fluid in delivery pipe , m/s
V_s	Velocity of fluid in suction pipe, m/s
$\vec{v}_{dr}$	Drift velocity, m/s
$\vec{v}_{kc}$	Relative velocity of solid particle, m/s
W	Particle settling velocity, m/s
w	Turbulence frequency, s^{-1}
Z_d	Delivery height, m
Z_s	Suction lift, m
α_s	Packing limit
θ_{max}	Maximum angles between the edges of the element, degree
θ_{min}	Minimum angles between the edges of the element, degree
θ_{eq}	Angle corresponding to an equilateral cell of similar form, degree
τ	Shear stress, N/m^2
τ_y	Yield stress, N/m^2

$\bar{\bar{\tau}}$	Stress tensor
τ_s	Particle relaxation time, sec
ψ	Pressure loss index
φ	Flow index
Φ	Dissipation
Θs	Granular temperature,^oC
δ_{ij}	Stain rate, s^{-1}
Ω_{ij}	Mean rate of rotation tensor
μ_m	Mixture viscosity, Ns/m^2
μ_t	Turbulence viscosity, Ns/m^2
ν_t	Eddy diffusivity, m^2/sec
η_{Pump}	Efficiency of pump
η	Coefficient of rigidity, Ns/m^2
ρ	Mass density of water, kg/m^3
ρ_s	mass density of solid material, kg/m^3
ρ_l	mass density of liquid, kg/m^3
ρ_m	Mass density of slurry, kg/m^3
ρg	Gravitational force, N
$\vec{\omega}$	Angular velocity vector, rad/s
Suffix	
50	Median

d	Delivery
f	Friction
in	Input to pump passage
l	Liquid
m	Mixture
max	Maximum
min	Minimum
out	Output from the pump
s	Solid phase
w	Water
w_n	weight mean

CHAPTER 1

INTRODUCTION

Slurry transportation system is used to transport solids through pipeline by mixing them with water or any other carrier liquid. Transportation of solids through pipelines are used in many industrial application like mineral ores of processing plants, coal transportation to thermal power plants, transportation of waste materials like fly ash and bottom ash, tailing materials etc. Pipeline transportation is very popular due to its economy, reliability, low maintenance cost, round the year availability at the user's end. It is also extremely safe and leads to minimum environmental pollution. The following advantages are associated with the pipeline transportation of solids.

- Installation is very simple as compared to the road and railway track.
- Possibility of complete automation.
- Elimination of traffic problem.
- Low construction, operation and maintenance.
- Air pollution reduction,
- Noise reduction
- Accident reduction
- Least ecological balance
- Saving on energy consumption

Some of the investigators (Link et al. 1974 and Aude et al.1974 & 1975) have reported that transportation of solid with pipeline is more economical as compared to any other mode of transportation. However, the pipe line transportation system has some limitations as listed below:

- Very high initial capital cost.

- Single purpose utility.
- This system requires large quantity of water or other liquid as the carrier fluid which may not be easily available at all the time and all the places.
- This system also needs strict quality control for the efficient pipeline operation.

1.1 BASIC SLURRY TRANSPORTATION SYSTEM

The schematic diagram of the basic slurry transportation system is shown in Figure 1.1. As shown in Figure 1.1, the slurry transportation system can be broadly classified into three sub-systems namely:

1. Slurry preparation facility
2. Main pipeline and pumps
3. Terminal facility

In the first sub system the solids are reduced to the convenient size by crushing and grinding so as to enable the transportation through pipeline. The solids are then mixed with the carrier fluid and the proportion of solid to liquid is adjusted to an optimum value before pumping the slurry. Chemical treatment is provided in this subsystem for corrosion control and drag reduction.

The second sub- system consists of a pump and pipeline depending on the distance and to polygraphs over which transportation is to be affected. The total pumping requirements is provided from either one or more than one point along the length of pipeline. For systems where intermediate pumping is provided, sometimes additional facilities like intermediate storage, corrosion and product quality control may to be provided on a smaller scale as compared to these at starting point.

At the terminal end, the slurry is received in storage tanks. This slurry then needs to be dewatered, filtered and dried to the extent as desired for the end utilization of the solids. In some cases, special processing usually required for hydraulic transportation at both the starting and terminal ends can be avoided. The

design of the basic transportation system involves the design of all the subsystems. The technology of the design of first and third sub system are fairly well developed and understood whereas the design of the main pipeline and pump depends on the number of parameters and still considerable technology input is needed for an optimized design.

1.2 ASH DISPOSAL SYSTEM

Power generation in India is primarily coal based in the present scenario. Coal used in our thermal power plants produces a large amount of ash, which is around 200 million tons per year**.** Out of this, around 130 million tons will be fly ash and the remainder will be bottom ash (Naik et al. 2011).

Currently, bottom ash is being transported hydraulically from thermal power plant to ash ponds through pipelines at low solid concentrations. The operation of ash disposal pipelines is therefore highly uneconomical due to requirement of large quantity of water and increase in power consumption for pumping water. Further, bottom ash particles are coarser as compared to fly ash particles. The transportation of bottom ash at low concentration also requires higher flow velocity and results in development of highly skewed concentration profile across the pipe cross-section.

This causes excessive erosion wear of the components of ash disposal system and therefore reduces their working life. Studies carried out for transportation of different solid materials at higher concentration in pipeline shows reduced skewness in concentration profile and flow velocity. These results reduce the pipeline erosion wear and hence increase the pipeline life.

These are expected to reduce the erosion wear. Besides these technical advantages, Seshadri et al. (2008) elaborated that transporting ash at higher concentrations is expected to lead to the following additional advantages.

- The amount of water required decreases considerably, resulting in faster drying & settling of ash.

- Due to reduced water consumption, ground water is not polluted to some extent. Air pollution also gets reduced due to retention of the binding characteristics of fly ash which otherwise gets washed away when transported at low concentration.
- Due to reduced erosion wear of pipeline, life of the pipeline is increased.
- Reduction in specific power consumption for transportation due to decrease in transportation velocity.
- The recirculation of water from the ash ponds can be avoided.

The design of existing ash disposal systems is highly conservative and no emphasis has been given on the optimization of various parameters like water and energy consumption, economic considerations etc. The present design procedure results in excessive wastage of water and energy. It has become imperative to optimize the design methodology of these systems, as this procedure of ash handling will be going to remain the primary method for many more years to come. In order to optimize the design a detailed knowledge of the parameters affecting its operation is essential.

The basic parameters for the design of any slurry transportation system are, hydraulic parameters, which include properties of carrier fluid, optimum particle size, optimum solid concentration in the slurry, rheology of the slurry, specific gravity of the solids and material properties. It is well known that the properties of the ash produced depends on various factors such as properties of coal, combustion process and its efficiency, methodology of ash collection etc. The bottom ash and fly ash from different thermal power plants differ greatly in their characteristics and hence the design of ash disposal system has to take in to account these variations. It is therefore necessary to have knowledge of the extent of variation in the properties of fly ash, bottom ash and their slurries.

It is economical to have the concentration of ash as high as possible. Sive and Lazarus (1987) found that the bottom and fly ash slurries can be easily transported using centrifugal slurry pump having solid concentration up to 40% by weight or

even higher. Laboratory tests have shown that at solid concentration above 40% by weight, bottom ash slurries behave like pseudo-homogeneous suspensions.

Thus the pipeline can be operated at much lower velocity since the critical deposition velocity for these slurries are lower. In fact at higher solid concentration, it is possible to operate the pipeline in laminar conditions since the slurry becomes non-settling.

This condition would occur, if the solid concentration approaches the static settled concentration level (maximum achievable concentration under gravity settling process). Bunn and Chambers (1993) found that the ash slurries behave like non-Newtonian fluids with rheological characteristics of either Bingham or yield pseudo-plastic type.

The values of rheological parameters i.e. yield stress and Bingham plastic viscosity have been found to vary over a wide range for various samples of fly ash collected from different thermal power plants (Biswas et al.2000). Once the rheological characteristics of the slurry suspension at higher concentration are established then it is simple to calculate the head requirements.

Further, most of the mineral industries which are using slurry pipelines for disposal of tailings and slime materials are also going for concentrated tailings disposal system because they offer various advantages over lean phase or medium phase disposal systems.

1.3 CENTRIFUGAL SLURRY PUMP

Pump is the heart of the any ash disposal system. The slurry pumps are classified into two categories namely centrifugal pump and positive displacement pump. In positive displacement pumps, a fixed volume of the fluid is positively displaced in the confined space to raise the pressure where as in the centrifugal pump, rotodynamic action develops the pressure.

The choice of pump or pumping system for slurry transportation depends not only on the flow rate, head required, suction conditions, type of installation and

location, but also on the slurry flow regime and its properties, like mixture concentration, particle size distribution, apparent viscosity, and abrasivity of solid materials etc. Hence, the range of affecting parameters is quite large and thus the selection depends heavily on the experience of the designer.

Centrifugal pump is used for slurry transportation purpose at low head and moderate flow rate, where as a positive-displacement pump is used for the low flow rate and high pressure applications. In some of the cases moderately high pressures may also be achieved with centrifugal pumps, by arranging them in series. For a given duty, centrifugal pumps are usually cheaper with better operational stability, occupy less space and have low maintenance costs compare to the positive displacement pumps. Also they can handle bigger solid particles. Dobson (1960) found that the centrifugal pumps are used for over 97% of all short distance slurry pipelines. Few investigators (Bain et al.1970and Walker1985) pointed out some of the main advantages of rotodynamic slurry pumps compared to positive displacement pumps. Though the centrifugal pump discharge pressure is relatively low, but they can also be used for moderate pressure requirements when used in series.

The design of a centrifugal pump for slurry handling system needs special consideration to ensure that the flow passages do not offer any restriction to the passage of solids. The efficiency of centrifugal slurry pump is lower as compared to that of a conventional centrifugal pump because of robust impeller and nearly concentric casing design, large running clearances and relatively wide throat-impeller clearance.

It may not be feasible to determine the performance characteristics of each pump at all the operating speeds whereas the pump needs to be operated at different value of rotational speeds in the field. At any operating speed, pump head with water can be evaluated using affinity relationship as under:

$$\text{Specific head } sH = \left(\frac{gH}{N^2 D^2} \right) \tag{1.1}$$

Specific discharge $sQ = \left(\frac{Q}{N\ D^3} \right)$ (1.2)

Specific power $sP = \left(\frac{Pin}{\left(\rho N^3 D^5\right)} \right)$ (1.3)

The dimension less parameter specific head, specific discharge and specific power, given in Equations (1.1) to (1.3), are applicable to conventional centrifugal pump handling water (Stepanoff 1957 and Wilson et al. 1992).

In centrifugal slurry pumps, the performance characteristics of pump is generally estimated with water and then the performance characteristics with slurry suspension is determined using suitable correction factors as below:

$$\text{Head ratio(HR)} = \frac{\text{Head developeded by slurry at a given flow rate(m)}}{\text{Head developed by water at a given flow rate(m)}} \quad (1.4)$$

$$\text{Power ratio(PR)} = \frac{\text{Input power drawn by slurry at a given flow rate (kW)}}{\text{Input power drawn by water at a given flow rate(kW)}} \quad (1.5)$$

$$\text{Efficiency ratio(ER)} = \frac{\text{Efficiency of the pump for slurry at a given flow rate}}{\text{Efficiency of the pump for water at a given flow rate}} \quad (1.6)$$

During the last few years, design and performance analysis of turbo machinery have experienced great progress with the availability of less expensive high performance computers and user friendly computational fluid dynamics (CFD) software's. The numerical simulation can provide information about the fluid flow characteristics inside the pump, and thus helps the design engineer to optimize the design of a particular pump. This will reduce the cost and time of trial-and-error process of fabricating and testing of the prototype/ model pumps which reduces the profit of the pump manufacturers. For this reason, CFD simulation is being used by many pump designers to estimate the pump performance and flow field analysis.

Many researchers **(**Gayo et al.2002; Gonz´alez et al. 2002; Byskov et al. 2003;Asuaje et al.2005; Gonzalezand Santolaria.2006) have studied the performance analysis of conventional centrifugal pumps using commercial CFD code. Generally pressure and velocity distribution, reverse flow inside the impeller and casing at design and off-design conditions have been predicted through simulation.

1.4 MOTIVATION OF THE PRESENT STUDY

Centrifugal slurry pumps are being normally used to transport the solid liquid mixture in slurry transportation system. Due to incomplete understanding of complex solid-liquid flow phenomena in the impeller and casing, and limited data base, there is no well-established method available to predict the performance of these pumps for liquid as well as solid –liquid mixtures. The empirical correlations developed for prediction of the pump performance are generally applicable for particular type of slurry and cannot predict reasonably the pump performance with other types of slurries.

It is needless to say that the present state of knowledge on the characteristics of the solid suspensions containing multisized irregular particles at high concentrations is at best incomplete. The limited data on the centrifugal slurry pumps has motivated the author to undertake a systematic study to generate data on the centrifugal slurry pumps performance characteristics while transporting coarse slurry with and without fine particles at moderate solid concentrations.

Hence, the present study is aimed to investigate the effect of physical and chemical properties of ash slurries on its rheological characteristics and the pump performance. The rheological characteristics of each sample were obtained at various concentrations of solids with varying temperature environment. The rheology of the coarse particulate bottom ash suspension is also measured with and without addition of the finer particles of fly ash in different proportion. Also, the centrifugal slurry pump performance characteristics are investigated with water and

coal ash slurries at different operating speeds. The effect of coal ash properties, solids concentration and rheological parameters on the pump performance has been investigated.

Efforts have been made to carry out the detailed analysis of hydraulic losses in the case of both pure liquid and slurry flowing through this pump for identifying a methodology for evaluating the performance. Numerical simulation makes it possible to visualize the flow conditions inside a centrifugal pump, and provides valuable information about the hydraulic design of the pumps. By using simulation results, one can predict the centrifugal slurry pump performance to reduce number of experiments in the process of pump design.

This also motivated the author to numerical study the flow field of pump using CFD tools. Flow behavior inside the pump passages was analyzed through simulation studies and numerical model is validated with the experimental data. Further, some design modifications have been suggested for the existing pump for better hydraulic performance.

1.5 ORGANISATION OF THE THESIS

The work carried out in the present investigation is presented in different chapters as given below.

Chapter 1 : introduces the various aspects of ash disposal system.

Chapter II: contains a survey of the available literature on the rheology of suspensions. Experimental performance of the centrifugal slurry pumps and numerical performance of the centrifugal slurry pump. Scope of the present study is also given.

Chapter III: presents the details of bench scale test procedure and their test result with coal ash and range of parameters of the present slurries. The experimental investigation of the physical /chemical / rheological properties of bottom ash slurry with and without addition of fly ash is also given.

Chapter IV: deals with the experimental set up, measuring instruments, experimental procedure and results on the centrifugal slurry pump performance while handling bottom ash slurries with and without addition of fly ash. The performance of the pump has been also discussed in terms of head ratio, power ratio and efficiency ratio.

Chapter V: presents the numerical modeling and simulation of the centrifugal slurry pump using commercial Computational Fluid Dynamics Code FLUENT. It also gives the comparison of the measured performance with the numerically predicted performance.

Chapter VI: lists the conclusions drawn based on the present investigation and suggestions for the pump operation for better hydraulic performance.

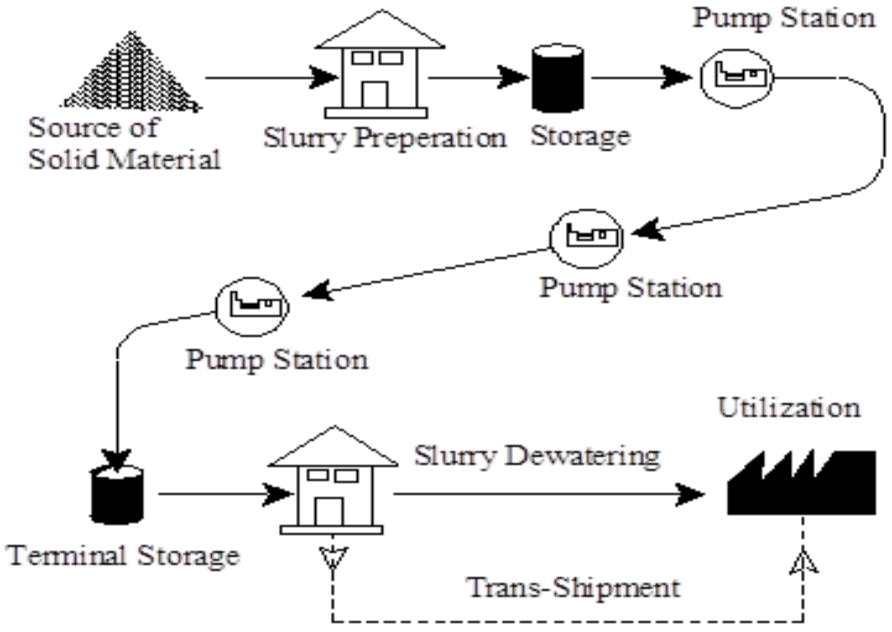

Figure 1.1: Basic slurry transportation system

CHAPTER 2

LITERATURE REVIEW

The ash disposal system of the thermal power plant can be classified into three sub-systems namely slurry transportation facility, pipeline and pumps, and terminal facility as highlighted in the previous chapter. The pump and pipeline is the main component of the transportation system and its proper design contributes significantly to the overall performance of the complete system. Centrifugal pump is used generally for ash disposal system as they can handle bigger solid particles. Centrifugal slurry pump performance characteristics plays very important role in the successful operation of the ash disposal system.

The design of a centrifugal pump for ash handling system need special consideration to ensure that the flow passages do not offer any restriction to the passage of solids. The efficiency of centrifugal slurry pump is lower as compared to that of a conventional centrifugal pump because of robust impeller and nearly concentric casing design, large running clearances and relatively wide throat impeller clearance. Over the years, efforts have been made to estimate the effect of suspended solids on the performance characteristics of the centrifugal slurry pump. Attempts have been made to estimate the performance of the pump handling slurries based on its clear water performance. A review of important works in this area has been presented in this chapter to give an insight into the present state of knowledge.

2.1 RHEOLOGICAL BEHAVIOUR OF SLURRY

Rheology is defined as the study of deformation and the flow of matter under the action of shear forces. Several investigators (Moreland 1963; Horsley 1982; Sive et al. 1987; Mishra et al. 1998; Verma et al. 2006; Parida et al. 2006 ; Senapati et al. 2010; Kumar et al. 2013a) have studied the rheology of suspensions of different materials. However no universal correlation for the prediction of the rheological parameters of a suspension is available. This is mainly due to the fact that a large

number of factors affect the rheological behavior of the suspension. When a liquid containing solid particle is subjected to shear, additional energy dissipation takes place. This dissipation is dependent on parameters like the rate of shear, the volume fraction of solid particles and other various solid properties.

The rheological characteristics of the slurry suspension play a very important role in design of the slurry transportation system. On the basis of the rheological data of suspension, head loss can be calculated on the basis of flow rate-pressure drop relationship of the pipeline for the flow of solid–liquid mixture. It also helps in determining the wear rate and life of the pipeline. Based on the knowledge of suspension rheology the stable and energy efficient pipeline transportation system can be designed. The rheological behaviour of the slurry suspension depends on several parameters such as particle size distribution, concentration of solid and fluid properties etc. The particle size distribution is also important for the dewatering of solid. If the solids are coarse then the cost of dewatering is less but the flow becomes more heterogeneous. If the particles are fine then the flow is homogenous but the slurry becomes non-Newtonian and the cost of dewatering also increases.

The presence of solid particle in the fluid invariably results is an increase in the viscous resistance of the suspension. At the same time it may also result in a change in the character of the liquid from that of a Newtonian fluid to that of a non-Newtonian fluid.

Many investigators (Mooney 1951; Roscoe 1952; Williams 1953; Einstein 1956; Rutgers 1962; Moreland 1963; Landel et al. 1965; Thomas 1965; Krieger 1968; Schrick et al. 1972 and Wilson 1982) have studied the rheological behavior of the different slurries. Moreland (1963) studied the particle shape effect on the slurry rheology and found that the non-sphericity enhances the non-Newtonian behaviour of the slurry. Einstein (1956) proposed a linear correlation for estimating the suspension viscosity. Unfortunately, the commercial slurries handled are completely different from the one for which the equation was developed and consequently, the applicability of the Einstein's equation of viscosity is limited.

Thomas (1965) carried out a critical analysis of the relative viscosity of the suspension of uniform spherical particles. The coefficient in the power in relationship was related to relative viscosity and solid volume fraction was determined using least squares procedure and a new expression for viscosity containing six terms was proposed.

The rheological characteristics of the solid –liquid suspension depends on the concentration, particle size distribution, particle shape, viscosity, and yield stress of the slurry(Moreland 1963; Horsley 1982; and Sive et al. 1987).

Gay et al. (1969) studied the rheological behaviour of slurries of different solids e.g. nickel, alumina, copper, and glass in suspending media such as liquid sodium, m-xylene and glycerin and found yield-pseudo plastic behaviour of slurry. They proposed a correlation, for the viscosity and yield stress of the slurry based on yield pseudo plastic model. However Cheng (1980) observed that the viscosity of the suspension is independent of the particle size.

Darby et al. (1981) studied the non-Newtonian viscosity of methanol using methanol as suspending liquid. He observed that both Bingham plastic and power law model can be used to represent the apparent viscosity. Lazarus and Sive (1984) investigated the rheological characteristics of suspension of fly ash slurry collected from South African power stations using a balanced beam viscometer. The rheology results indicated that the fly ash slurries may follow the Bingham plastic model. Gahlot et al. (1988) studied the rheological characteristics of coal water and zinc tailing slurries containing large sized particles which tend to settle during the experiments. They have scalped the larger size particle from original sample and rheological behavior performed with the residual finer sized particulate suspensions. They proposed the criteria to determine the viscosity of the coal water and zinc tailing slurries containing the large sized particles with the finer particles.

Kawatra and Eisele (1988) proposed that major variables affecting the slurry viscosity are solid concentration, particle size distribution, environment temperature and chemical composition. Bunn et al. (1990 and 1991) and Bunn and Chamber (1993) have studied the rheological characteristics of high concentration

fly ash slurry of the Australian power stations. The rotary viscometers and tube viscometers were used for rheological measurements of ash slurry at concentration of 60 to 80% (by weight). The fly ash slurry suspension showed the non-Newtonian behavior above the solid concentration of 60% (by weight).

Turian et al. (1992) observed that the settling concentration, yield stress and relative viscosity of the slurry suspension are the function of the solid concentration. Heywood et al. (1993) studied the pulverized coal ash slurry rheological behaviour at solid concentrations of 68 to 70 % (by weight). A power law model was used to predict the rheological characteristics of coal ash slurry. The exponent value 'n' of the power law relationship was found as 0.46. Reddy et al. (1994) investigated the rheological properties of coal- oil mixtures and determined the effect of coal properties such as moisture content on the slurry behavior. The data of particle size distribution were fitted into the Rosin-Rammler model. The results showed that coal oil mixtures with high ash content were less viscous and the viscosity decreased with the increase in the moisture content of the coal. Roh et al.(1994) studied the effect of particle size distribution on the rheology of coal water mixtures. Rheological test were conducted using Haake RV-12 viscometer. They found that all the slurries exhibited pseudo plastic behaviour. The blending with coarse coal fraction was useful in reducing the viscosity of finer coal.

Parida et al. (1995) investigated the rheological behavior of fly ash slurry. They found that the fly ash slurry exhibited Newtonian nature up to the concentration of 50% (by weight) and at higher concentrations it showed non-Newtonian behaviour.

Ahmad et al. (1995) studied the rheology of two multi-sized particulate slurries namely iron ore and zinc tailings. They found that slurry rheology is a functioning solid concentration, chemical and physical properties of the solid suspensions.

Biswas et al. (2000) evaluated the rheological properties of slurries of coal ash produced from various thermal power plants of India. They found that the

rheological and other physical properties of the Indian coal ash collected from different thermal power plants vary over a wide range.

Mishra et al. (2002) studied the influence of concentration, temperature and ash content on the rheological characteristics of coal- water slurry. They found that coal water slurry exhibits pseudo plastic behavior. The viscosity of slurry dependent on the solid concentration of slurry, pH and temperature.

Boylu et al. (2004) studied the influence of volume fraction, particle size distribution and rank on the rheological characteristics of coal water slurry suspension. They prepared coal water mixture with three types of coals having different rank but similar particle size distribution. They found that apparent viscosity of the slurries decreases from the lower to higher quality coals.

Senapati et al. (2005) investigated rheological characteristics of fly ash slurry with and without addition of bottom ash using a Haake rotational viscometer. They found that fly ash slurry exhibits pseudo plastic nature and the viscosity of the fly ash and mixture of fly ash and bottom ash slurry could be modeled by applying power law equation.

Verma et al. (2006) investigated the influence of particle size distribution on rheological characteristics of fly ash slurry at high concentrations. They prepared five fly ash samples having different particle size distribution and from each sample, six suspensions of different solid concentrations were prepared. They found that the fly ash slurries exhibit non-Newtonian behaviour above concentration of 40% (by weight).

Branganca et al. (2009) found that viscosity of the coal ash depends on a number of factors such as chemical composition, solid concentration and particle size distribution of fine and medium particles. Senapati et al. (2010) investigated the rheological characteristics of fly ash slurry at high concentrations. They took the five different samples of fly ash with volumetric concentration of 0.32 to 0.4945 and shear rate of 10 to 200 s^{-1}. They found that relative viscosity of fly ash is function of solid concentration and particle size distribution.

The investigators (Ahmad et al. 1995 and 1997; Mishra et al. 1998 and 2001; Usui and Suzuki 2001;Maclnnes 2002; Seshadri et al. 2005 ;Verma et al. 2006; Parida et al. 2006 ; Senapati et al. 2010 ; Convery et al. 2010 and Kumar et al. 2013a) found that fly ash slurry exhibit non-Newtonian nature above solid concentration of 40% (by weight). They also observed that the yield stress and Bingham plastic viscosity of slurry suspension increases rapidly with increase in solid concentrations.

The above review shows that rheological characteristics of bottom ash has not been studied extensively and differ for the different power plants. Investigation has not been carried over so far.

2.2 EFFECT OF ADDITIVES ON THE RHEOLOGICAL BEHAVIOUR OF SLURRY

Centrifugal slurry pump performance characteristics predictions are different from conventional centrifugal pump because the presence of solid particles leading to change the flow structure, which in turn affects the head loss. The fine particulate slurry suspensions show non-Newtonian nature at operational solid concentrations whereas the coarse particulate slurry suspensions require high flow velocity resulting in higher power consumption.

For reducing the head loss in slurry transportation system, numbers of techniques were employed. These techniques were able to reduce the frictional losses either by reducing the slurry rheological characteristics or by reducing the impact of adverse flow characteristics. The direct methods for reducing slurry viscosity are addition of fibers of high aspect ratio, soaps and higher molecular weight polymers.

The present literature review focuses on techniques where rheological characteristics of given slurry are directly affected. A large variety of chemical compounds were used as additives to modify the slurry suspension characteristics.

The chemical additives may be categorized as ionic & non-ionic, dispersants, polymeric, surfactant, deflocculates etc. The most desirable

characteristics of additive are low viscosity and high stability. The influence of an additive on the rheology of slurry suspension depends on the particle size distribution, solid concentration, chemical and physical properties of the solid.

The following discussions describe different ways to improve the rheological characteristics of slurry suspension using different additives. The details summery of the rheology of the fly ash slurry with bottom ash and different additive are presented in the Table 2.1.

Saeki et al. (1999) investigated the effect of eight commercially available surfactants, five newly synthesized surfactants and four stabilizers on coal water slurry. The coal-water slurry was prepared from Indonesian coal of 60% solid concentration (by weight). The dispersing additive and stabilizing additive concentration was taken as 0.03% and 0.005% (by weight). They found that Naphthalene Sulfonate formaldehyde (NSF-Na+) was the most effective additive to decrease the apparent viscosity of the coal-water mixture. The most effective stabilizer was found as bio-polysaccharide.

Kumar et al. (2000) studied the rheology of the bottom ash, fly ash and mixture of fly ash and bottom ash using a Weissenberg rheogoniometer. They found that the addition of bottom ash in the fly ash suspension improve the rheological behavior of the fly ash slurry.

The influence of solid concentration, particle size distribution, and surface characteristics on the viscosity of the suspension was investigated by Ghanta et al. (2002) using two different solid mineral namely coal and copper ore. They observed that coarse size coal-water slurry exhibit lower viscosity as compared to finer size coal-water slurry, whereas copper ore showed reverse rheological behaviour due to its opposite surface characteristics. They have also observed that mixing of coarse particles in the finer particles improves the rheology of the finer particle suspension.

Senapati et al. (2005) investigated the rheological characteristics of fly ash slurry using a Haake Rotational viscometer with and without addition of bottom ash .They found that fly ash slurry exhibits a pseudo plastic nature and the

viscosity of the fly ash and mixture of fly ash and bottom ash slurries could be modeled using power law equation.

Vlasak et al. (2007) conducted pipe loop test study on fly ash bottom ash mixture slurry with concentration of 45-55% (by weight). It was found that the addition of bottom ash reduces the head loss of fly ash slurry. Seshadri et al. (2008) studied the rheological behavior of fly ash slurry with and without additives for different particle size distributions and concentrations of the solid-liquid mixture. They used 0.1% (by weight) solid concentration of sodium-hexa-metaphosphate as additive. They found that the solid concentration and particle size distribution influence more to the rheological characteristics of slurry of non-Newtonian as compared to the Newtonian nature.

Senapati et al. (2008) studied the rheological behavior of coal water mixture using a natural additive. The rheological measurements were carried out using HAAKE RV 30 rotational viscometer. The coal water slurry concentration was taken between 55-63.7 % (by weight). The concentration of the additive was varied from 0.4–1.2 % (by weight). They found that the coal water slurry in the presence of natural additive exhibited Bingham plastic behavior.

Das (2008) studied the rheological behavior of coal water mixture using saponin as a natural additive. They investigated the rheology coal-water mixture as a function of ash content, pH, temperature, coal loading and concentration of saponin. The rheological measurements were performed using HAAKE (Model RV 30) rotational viscometer. The coal water slurry concentration was taken between 55-64% (by weight). The additive concentrations were varied from 0.4-1.2% (by weight). They found that the optimum value of the saponin as additive is 0.8% for coal-water slurry

Naik et al. (2009a) studied the effect of drag reducing polymers on the rheology of fly ash slurry at various temperatures. The rheology of the fly ash was evaluated in shear rate range of 25 to 500 $s^{-1}$and temperature range of 20°C to 40 °C with additive cetyl-trim-ethyl ammonium bromide. They found that the addition of the additive improves the rheological characteristics of the ash slurry. Vlasak et

al. (2009) studied the rheology of fly ash slurry with addition of sodium hexametaphosphate as additive. They found that small proportion of the additive reduces the slurry viscosity significantly.

Chandel et al. (2009a) studied the effect of sodium-hexa-meta phosphate and Henko detergent (in the ratio of 5:1) as an additive on the rheological behavior of fly ash slurry at higher concentrations. Using the rheology data, the flow behaviour of ash slurry was predicted using the Bingham plastic model. They found that the additive improve the rheology of the ash slurry, results in lower pressure drop and power consumption.

Naik et al. (2011) studied the rheological behavior of fly ash at 40% solid concentration (by weight) with and without additives with variation of temperature from 20ºC to 40ºC. They used cetyltrimethyl ammonium bromide as an additive and NaSal as a counter ion. They found that all the slurry shows the Newtonian flow behavior. It was also observed that with addition of the additive, viscosity of the slurry reduced.

Buranasrisak et al. (2012) studied the influence of particle size distribution on the rheology of coal-water mixture. The samples were classified into six particle size ranges. Naphthalene sulfonate formaldehyde (NSF) and Na-CMC were used as the dispersing agent and stabilizer. The coal water slurry concentration was taken between 60-65% (by weight). The different packing characteristics of the coal samples were defined by making monomial, bimodal and multimodal distributions at different coarse to fine ratios. They observed that maximum coal loading was possible when coal water slurry was made from bimodal particle size distribution.

Senapati et al. (2013) investigated rheology of highly concentrated coal ash slurry containing fine particulate fly ash and coarse particulate bottom ash. They have measured the rheology data using a HAAKE Rotational Viscometer (Model RV 30). The slurry concentration was taken between 62-65% (by weight). The pH value was measured around 5.6. The fly ash slurry showed the non-settling nature of the pseudo-homogeneous flow behaviour whereas mixture of fly ash and bottom ash exhibits the non- Newtonian nature.

Kumar et al. (2013a) studied the effect of addition of fly ash on the rheological characteristics of bottom ash slurry. Addition of fly ash in the bottom ash was varied from 10 to 30% (by weight). They found that the addition of finer particles of fly ash with coarser particles of bottom ash improves the rheological characteristics of bottom ash slurry suspension which will result in substantial saving in power consumption.

Above studies reveal that the addition of the small proposition of the additive is capable to improve the rheology of the slurry suspension. The selections of the additive agent depends on the physical/chemical and minerogical nature of the solid-liquid suspension.

2.3 PERFORMANCE CHARACTERISTICS OF SLURRY PUMP

2.3.1 Experimental Work

The variation of head, power and efficiency with flow rate at a constant speed is called the operating or simply the pump performance characteristics. Experimental studies on the centrifugal slurry pumps have generally been conducted to evaluate the performance characteristics of pump and to determine their dependence on various geometrical and operating parameters. The effect of presence of solids on the pump performance has been studied by several researchers. The details of the centrifugal slurry pump performance with solid material properties are given in the Table 2.2.

2.3.1.1 Parametric Study

Fairbank (1942) developed an expression to estimate the theoretical head developed by a centrifugal pump handling slurry as well as water using Euler's equation. He assumed that the solid particles leave the impeller with a greater velocity (relative to blade) as compared to water. The predicted head showed higher deviation as compared to the measured head with increase in concentration and particle size.

Ippen(1946) conducted the pilot plant test on the centrifugal pumps handling oil of different viscosities. He found that the head, efficiency and input power can be determined by distinct curves plotted against Reynolds number.

A general conclusion drawn on the effect of presence of solids on the pump performance is that the head and efficiency of the pump decreases with increase in solid concentration whereas input power increases with increase in solid concentration (Stepnoff 1957 and 1965).

Herbitch (1962); and Itaya and Nishikawa (1964) determined the path of the solid particles in the impeller to handle solid-liquid mixtures using high speed camera. The head developed through the pump was also determined using the velocity triangles for water and solid particles at pump outlet.

Hunt and Faddick (1971) studied the performance of three different size centrifugal pumps handling aqueous solution of chip shaped particles. They found that the head developed and the efficiency of the pump depends on the pump size. Wilson (1982) reported that the volute tongue causes large energy losses and wear in the pump casing when operating at off-designed conditions.

The effect of higher viscosity of homogeneous slurries on the pump performance can be estimated using the viscosity correction charts prepared by Hydraulic Institute of Standards (1974).

Vocaldo et al. (1974) studied the performance characteristics of rubber-lined and metal type centrifugal slurry pump for transporting sand material with different particle sizes and clay. They found more head loss with rubber-lined pump as compare with the metal pump. The loss in the head and the efficiency of the pump

was found equal for variation in concentration. However, clay suspension did not show any significant effect on the pump performance up to concentrations of 8% by volume.

Burgess and Reizes (1976) found that the relative reduction in head ratio and efficiency ratio is proportional to the flow coefficient, solid concentration, particle size, specific gravity of solid and the pump size. An empirical expression was developed as,Head ratio $= \frac{H_s}{H_w} = \left(1\text{-}C_w\right) n$ (2.1)

A detailed analysis of the experimental data of Burgess and Reizes (1976) was made by Cave (1976) to determine the effect of solid concentration, specific gravity of solids and the particle size on the relative reduction in head. He showed that Head ratio varied linearly with concentration. The effect of specific gravity of solids on pump performance studied by comparing the plot of (Head ratio - Concentration) curves for two materials whose particle size was almost identical.

Wiedenroth (1978) calculated the velocity of solid particles entering and leaving the pump by measuring the time taken by solids when passing a concentrated cloud of solid matter or a salt solution between two fixed electrodes. However, he found that the solid matter entered the pump with a slip. He also evaluated experimentally the performance of two centrifugal pumps handling coarse solid materials at different speeds. He reported that the deterioration in the pump performance due to presence of solid particles depends largely on the friction paths in the pump, and the head and efficiency reduce with increase in particle size and solid concentration as reported earlier by Fairbank (1942).

Sellgren (1979) studied the effect of particle shape, particle size distribution and particle terminal velocity on the drag coefficient C_D . He concluded that the head reduction factor is a function of drag coefficient, specific gravity of solid(s) and the solid concentration. From the experimental results and the functional relationship between variables, an expression for head reduction factor was developed as

$$1 - HR) = k = 0.32 C_w^{0.7} (s - 1)^{0.7} C_D^{0.25} \quad (2.2)$$

C_D is the drag coefficient and is given as

$$C_D = \frac{4g}{3}\frac{dwm(s-1)}{w^2} \tag{2.3}$$

Neerken (1979) suggested a derating factor for performance characteristics of centrifugal slurry pump. He plotted the variation of derating factor with average particle size and specific gravity of solid suspension. The plot can be used to find the value of derating factor directly for any solid of specific gravity between 1.1 to 6.0 and average particle size between 0.01 to 8.0 mm.

Murakami et al. (1980) measured the flow patterns in centrifugal pump impellers with three and seven blades, by use of cylindrical yaw probe and an oil surface flow method. The measured distribution of velocities and pressure for the seven (sufficient number) blade impeller at the design flow rate showed good agreement with the numerical predictions. The flow pattern of the three (insufficient number) blade impeller deviated largely from those of the seven-blade impeller both at design and off- design conditions.

Johnson (1981) studied the centrifugal slurry pump performance with heterogeneous slurries. He found the deterioration in the pump performance is due to the inability of the coarse particles to absorb or store pressure energy and to convert the kinetic energy into the useful pressure energy. A major part of kinetic energy is lost and therefore the head developed by slurry is lower than that of clear water.

Gillies et al. (1982) found that centrifugal slurry pump efficiency is reduced with increase in solid concentration.

Remisz (1983) presented a method of transforming the pump performance characteristics from clear water to solid-liquid flow. He derived an expression for head ratio which depends on non-dimensional flow rate and non-dimensional mass density of the mixture. The shift in the BEP point observed was related to the ratio of peripheral and meridional velocity components at the impeller exit. He also presented graphically the efficiency ratio as a function of the impeller geometry and non-dimensional mass density.

Roco et al. (1984) suggested an empirical model, to predict the effect of solid properties effect on the pump head of dredge pump. A computer programme was also generated to evaluate the head- flow rate characteristics as a function of slurry properties and pump dimensions. Based on experimental data on irrigation pump handling muddy water, Baiz (1984) derived the expression for head ratio and efficiency ratio as

$$HR = 1 - 0.02\,Cv\,(1 + Q_r^2) \tag{2.4}$$

$$(1 - ER) = \frac{Cv}{(1.02 - 0.12\,Q_r)^{16}} \tag{2.5}$$

Maz (1984) investigated the influence of specific weight, particle size distribution and solid concentration of solid on the performance of slurry pump with 150 mm diameter centrifugal pump with channel type impeller. The solid materials clean coal, raw coal and gravel of maximum particle size of 125 mm were selected for experimental investigations up to a solid concentration of 40% (by volume). The measured pump reduction factor was compared with the predicted results obtained using available correlations. It was observed that the predicted results were generally lower than the measured values. His findings were in agreement with the (Vocaldo et al. 1974) and showed linear dependence of head drop with solid concentration and its proportional increase with the difference in specific gravity of solids and carrier liquid.

Walker and Goulas (1984) reported that the reduction in the head and the efficiency depends on the rheological properties of slurry and the Reynolds number. They selected two centrifugal slurry pumps having different specific speeds (n_s = 0.27 & 0.57) to handle non - Newtonian slurries of coal dust and kaolin clay. They reported that the pump with higher specific speed had a better performance which showed the dependence of head loss on pump friction paths as reported by Widenroth (1978).

Chand et al. (1985) studied the effect of solid particles on the performance characteristics of centrifugal slurry pump. They evaluated the pump performance with various solid materials such as fly ash, sand iron ore and coal dust with solid concentration up to 26% by volume. The pump was operating at three different speeds namely 1000, 1200 and 1400 rpm. They reported that decrease in head and efficiency of the pump with increase in concentrations of solids.

Roco et al. (1986) studied the performance characteristics of centrifugal slurry pumps with different geometrical configurations for handling of silica sand slurry. They divided the head losses into three categories namely local loss, secondary flow loss and frictional loss. They found that the different head losses in the pump are the function of solid material properties and flow rate.

Roco et al. (1989) measured the velocity distribution of liquid and solid particles leaving the impeller for very dilute suspension (Cv=0.002) of 0.08 mm particle size glass beads using Laser Doppler velocimeter (LDV). From the velocity distribution, they found that the solids were generally leading the liquid in radial direction and lagging in circumferential direction. They also proposed a correlation between velocity distribution and the overall pump performance.

Wilson et al. (1992) reported the flow behaviour of homogeneity or heterogeneity in the pump depending on the particle size and flow conditions. The finer particles are homogeneously distributed in the solid - liquid mixture, whereas larger particles are heterogeneously distributed.

Cader et al. (1992) investigated the solid-liquid mixture flow velocities at the impeller outlet of centrifugal slurry pump using Laser Doppler Velocimetry (LDV). They observed that the solid particles have larger radial velocity than the carrier liquid at the impeller outlet, but they lag the water in the circumferential direction.

Gahlot et al. (1992) studied the centrifugal slurry pump performance characteristics with two types of slurries namely zinc tailing and coal. They proposed a correlation for predicting the reduction in pump head due to slurry. They also observed that the head and the efficiency of the pump decreases with

increase in solid concentration, particle size and specific gravity of solids at any flow rate.

Walker et al. (1993) studied the effect of impeller geometry on the centrifugal slurry pump performance with sand slurries. They found that except the blade shape, other parameters do not have any significant effect on the head or the efficiency.

Cader et al. (1994) studied the velocity distribution and performance characteristics of centrifugal slurry pump using LDA (Laser Doppler Anemometer). They evaluated the liquid and solid velocity distribution in the pump. The reported that the fluctuations produced in the flow rate, head and efficiency due to particle slip.

Ni et al. (1996) studied the centrifugal slurry pump performance with concentrated slurry of narrowly graded sands. They found that pump head, efficiency and input power are function of solid concentration and sand properties.

Kazim et al. (1997) studied the performance of a centrifugal slurry pump handling slurries of coal, zinc, iron ore and six types of sands containing different particle sizes. They observed that the higher reduction in the efficiency compared to the head for increase in solid concentration, particle size and density of the solids. They found that the Gahlot's correlation gives reasonable accuracy for his experimental data. They also proposed a new correlation for greater accuracy in prediction of head with an error of $\pm$ 10 %.

Gandhi et al. (1998) presented a methodology to predict the performance characteristics of centrifugal slurry pumps with water based on loss analysis procedure. Prediction of head-capacity curve showed reasonable agreement with their experimental water data over the full range of operating condition. Based on investigation they concluded that the hydraulic losses in centrifugal slurry pumps can be calculated from the knowledge of its geometry. The leakage loss plays a major role in the performance of centrifugal slurry pump.

Engin and Gur (2001) studied the influence of tip clearance on the performance of a centrifugal slurry pump. The performance characteristics of the

pump was evaluated with four different solid materials, namely casting sand, beach sand, perlite-A and perlite B. Measurements were made with two different concentrations of each solid material for four different tip clearance settings of 1.25 mm, 2.5 mm, 5.5 mm, and 8 mm at 1250 rpm. They found that the pump performance decreased steadily as the tip clearance increased and this was attributed to the tip leakage loss that increases with the increase in tip clearance due to an increase in flow passage.

Sellgren and Addie (2002) studied the performance characteristics of centrifugal pump for highly concentrated tailing slurries (C_w=50% by volume). They observed that the power consumption increases more than slurry to water density ratio at higher concentrations. Xu et al. (2002) studied the performance characteristics of centrifugal slurry pump handling Newtonian and non-Newtonian slurries. The clay free slurry with water showed the Newtonian flow behaviour whereas kaolin clay in water showed the non-Newtonian s flow behaviour. They found that more derating of pump performance occurred with clay free slurry as compared to clay free with water.

Engin and Gur (2003) studied the centrifugal slurry pump performance and proposed a correlation to predict the head reductions of pump. They studied the influence of particle size, particle size distribution, specific gravity, solid concentration and impeller diameter on the pump performance. The correlations already developed in literature were also validated and showed good agreement with errors in the permissible range.

Pullum et al. (2007) studied the performance characteristics of centrifugal slurry pump with non-Newtonian slurry suspension using Hydraulic Institute method. Solid liquid suspensions were taken up to 38% (by volume) with mean diameters of 1.1 to 3.4 mm. They observed that the decrease in the head is the function of solid concentration of the slurry suspension.

Yassine (2010) studied the performance characteristics of centrifugal slurry pump with sand slurry. The concentration of the sand varies from 0 to 15% (by weight).It was observed that the head and the efficiency of a centrifugal pump with

slurries are lower than that of the water due to the presence of solids. They have also observed that the head ratio, power ratio, and efficiency ratio variation is within ± 9% at any sand concentration with flow rate. Khalil et al. (2013) studied the performance characteristics of centrifugal pump with soft slurry. The solid concentration of the soft slurry varied from 0 to 18% (by weight). They a developed the empirical correlations, to predict the performance characteristics with slurry using the experimental data.

A close scrutiny of all these studies show that the centrifugal slurry pump performance characteristics are greatly influenced with solid concentration, particle size distribution and specific gravity of the material, rheological characteristics of slurry suspension.

2.3.1.2 Affinity Law

The centrifugal slurry pump may be operated at different operating speeds in the field to achieve the required head and flow rate. Generally affinity laws have been used to estimate the performance characteristics of conventional pump at different speeds. The applicability of these laws to centrifugal slurry pump has been investigated.

Fairbank (1942) observed that the affinity laws are applicable for changing the pump speed from 1000 to 1200 rpm for sand and mud slurry in the concentration range of 0 - 25% (by volume). Vocaldo et al. (1974) conducted the laboratory tests on rubber lined and metal centrifugal slurry pumps for transporting silica sand with solid concentration of 6 - 30% (by weight) at two speeds, 1180 and 1780 rpm. They found that the affinity laws hold well for changing the pump speed but not applicable for changing the diameter of impeller.

Sutton(1968) and Osterwalder et al. (1777) found that affinity laws are not applicable for the Newtonian fluids. They recommended that the applicability of affinity laws for the pumps handling slurries requires that the head ratio or efficiency ratio for slurries are not be a function of either the pump speed or the impeller outlet

diameter for transferring the test data for one pump to another pump size or rotational speed.

Burgress and Riezes (1976) experimentally evaluated the pump performance for slurries at various pump speeds. They found that the head loss is a function of particle size, solid concentration and specific gravity of solids.

Walker and Goulas (1984) studied the performance characteristics of pump on two centrifugal slurry pumps with non -Newtonian homogeneous slurries of coal and kaolin clay at three pump speeds namely 800, 1000 and 1200 rpm. They reported that non-applicability of the affinity laws for pumps handling non-Newtonian slurries.

Sellgren (1979) studied the performance characteristics of centrifugal slurry pump handling ores and industrial minerals at two rotational speeds namely 760 and 1140 rpm. He found that the head reduction correlation does not depend either on pump speed or impeller diameter. He also reported that non-applicability of the affinity laws for mineral suspensions. Maz (1984) investigated the pump performance of 150 mm centrifugal slurry pump at two speeds namely 740 and 870 rpm for concentrations of coal up to 40% (by weight) . His data also confirmed the validity of affinity laws for slurries.

Kazim (1997) reported the performance of a centrifugal slurry pump at two speeds namely 1000 and 1400 rpm for narrow sized sand slurries (d_{50} = 230 μ and d_{wn} = 328 μm) for concentration range of 0 - 44.84% (by weight) . He compared the head ratio and the efficiency ratio values for the two speeds which imply that the affinity laws are applicable for speed variation.

Gandhi et al. (2001) studied the centrifugal slurry pump performance characteristics with three solid materials bottom ash, fly ash and zinc trailing having different particle size distribution (PSD). They found that the head and efficiency ratio values are not only function of solid concentration but also affected by PSD of the solids and properties of slurry. They also observed that the head and efficiency of the pump decreases with increase in solid concentration, particle size

and slurry viscosity. The presences of fine particulate in coarse particulate slurry improved the pump performance in terms of head and efficiency.

Gandhi et al. (2002) studied the centrifugal slurry pump performance characteristics at different operating speeds with water and solid-liquid mixture. They observed that the affinity relations applicable to conventional pumps for head and flow rate can be applied to slurry pumps handling water and slurries at low concentrations. These relationships need to be corrected at higher solids concentrations.

2.3.1.3 Effect of additive

The above review of investigation shows that the rheology of the slurry suspension has improved with addition of some drag reducing agents. The addition of the additive reduces the viscosity of the slurry suspension which helps in the improvement of the slurry pump performance. The following discussion describes the investigation on the centrifugal slurry pump performance characteristics with different additives.

Chand et al. (1985) studied the centrifugal slurry pump performance with and without additive. They performed the experimentation with various solid materials such as iron ore, fly ash, sand and coal dust at solid concentrations up to 26% (by volume). The experimentation carried out at three different operating speeds namely 1000, 1200 and 1400 rpm. The guar gum was used as a drag reducing polymer additive. They observed that the pump head and efficiency improved with the use of polymer additives.

Sellgren et al. (2000) studied the centrifugal slurry pump performance characteristics with addition of clay as an additive for handling three narrow graded sand slurry. They found that addition of clay to sand slurry reduces the pumping head and power consumption. Ogata et al. (2006) studied the centrifugal pump performance characteristics with aqueous solutions of Oreyl-bishydroxyethylmethyl-ammonium. They performed the experimentation with volumetric concentration of 200, 500, and 1000 ppm (part per million). They found

that total pump head and efficiency increased and the shaft input power decreased with addition of surfactant solution.

Some of the investigators (Vlasak et al. 2002; Thomas and Sobota, 2002 ;Frei and Huber 2005; Seshadri et al. 2005; Chandel et al. 2011) also observed that addition of coarser particles in the slurry of fine material leads to reduction in the additional losses. Chandel et al. (2011) studied the centrifugal slurry pump performance characteristics with fly ash slurries at speeds 1450 rpm in the concentration range of 50 to 70% (by weight). The bottom ash mixed as an additive in the fly ash slurry in the ratio of 4:1 (fly ash +bottom ash) by weight. They also found that pump head, efficiency and input power is the function of the flow rate. The performance of the pump improved with mixing of the coarser bottom ash in the fly ash slurry.

Kumar et al. (2014) evaluated the performance characteristics of the centrifugal slurry pump with multi sized particulate slurry of bottom ash and fly ash mixtures. The performance characteristic of the pump was experimentally evaluated at rotational speed of 1450 rpm for bottom ash slurries with and without addition of fly ash in the concentration range of 10 to 50% (by weight). Addition of fly ash in the bottom ash was varied from 10 to 30% (by weight). The performance characteristics results showed that the value of head and the efficiency of the pump depend on the solid concentration. It was also observed that the performance parameter of the pump strongly depends on slurry properties. The addition of fine particles of fly ash in the coarser particles of bottom ash slurry, leads to reeducation the additional head losses in the pump. The pump performance in terms of head and efficiency improved with addition of fly ash in bottom ash slurry.

The literatures review reveals that due to incomplete understanding of complex solid-liquid flow phenomena in the impeller and casing, there is no well-established method available to predict the performance centrifugal slurry pumps for liquid as well as solid –liquid mixtures. The empirical correlations developed experimentally for prediction of the pump performance are applicable of the particular slurry and cannot predict reasonable pump performance with other

slurries. The addition of additive has improved slurry pump performance characteristics. Few studies have been conducted on the centrifugal slurry pump performance handling fine particles with addition of coarse particles. The effect of fine particles in such coarse slurry has not been investigated so far.

2.3.2 Numerical Work

In the recent years, Computational fluid dynamics (CFD) is being increasingly applied to design of the pumps. Simulation study makes it possible to visualize the flow characteristics inside the centrifugal pump passage and provides the valuable information for hydraulic design. Several investigators have used different commercial CFD packages like FLUENT, STARCD, CFX, and PHOENICS to analyze the flow distribution inside the centrifugal pump. A summary of the numerical simulation of the centrifugal performance with water and solid –liquid mixtures have been listed in the Table 2.3 and Table 2.4.

2.3.2.1 Parametric Study with water

Roco and Reinhart (1980) developed a numerical method for calculating the distribution of solid concentration in centrifugal slurry pump. They used finite element method to solve the convection-diffusion differential equation between blades. By using this method they predicted best optimum impeller design of pump.

Das et al. (1998) presented a computer-aided design method for centrifugal pump impellers with blades of single curvature. The effect of blade shape, blade outlet angle and number of blades on hydraulic loss was studied using computer program. The predicted value showed good agreement with the general observations of the pump designers.

Jude and Covshi (1998) developed numerical code to determine the pressure distributions along the impeller blade of pump. The flow through two-dimensional centrifugal impeller was investigated using of conformal mapping and boundary element method. Pagalthivarthi et al. (1998) developed a 2-dimensional computer program using finite element method to investigate turbulent flow in a

centrifugal pump. The mixing length model was used as turbulence model. Through the program they found 2.5% difference in inflow to the impeller and outflow of the casing. They also determined the recirculation in casing of pump at design flow rate condition.

Miner (2000) studied the flow distribution inside the axial flow pump and a mixed flow pump using FLOTRAN. The standard k-ε model was used. He took fine and coarse meshes for his study. He found that the computational results obtained from coarse meshing closely match with the experimental results and proposed that it can be used to predict the performance.

Sun and Tuskamoto (2001) studied the performance characteristics of centrifugal pump using CFD code FLUENT. The simulation results was used to determine the flow distribution inside the pump over the entire flow range. They observed back flow at small flow rates, however no back flow was observed at higher flow rate.

Some of the investigators (Gayo et al. 2002; Hornsby 2002; Gonz´alez et al. 2002; Byskov et al. 2003; Asuaje et al. 2005; Wang et al.2005; Cao and Peng, 2005 ; Gonzalez and Santolaria 2006) studied the performance analysis of conventional centrifugal pumps used for pumping water only using commercial CFD code.

Byskov et al. (2003) validated the design and off-design simulation results performance with the experimental result collected by particle image velocimetry (PIV) and laser Doppler velocimetry (LDV) systems.

Asuaje et al. (2005) carried out the numerical simulation of centrifugal pump using CFX code with different turbulent models and observed that standard k-ε model showed rescannable agreement with the experimental results.

Addie et al. (2007) studied the effect of slurry on pump performance, net positive suction head required and wear using the ANSI/HI standard developed by the hydraulic institute.

Cheah et al. (2007) performed the numerical simulation of centrifugal pump by using commercial code CFX. The unstructured mesh with tetrahedral element

was used for meshing of the centrifugal pump component. The internal flow characteristics inside the pump passage were analyzed with the simulation results.

Spence et al. (2008) studied the influence of geometrical variations on performance characteristics of a centrifugal pump. They used CFD code TASCFLOW to investigate the time variation of pressure pulsation in the centrifugal pump. The pressure pulsations were evaluated at fifteen different location of the pump with three mass flow rate conditions. They observed that the transient flow simulation results show reasonable agreement with the experimental result.

Yang et al. (2011) studied the flow distribution in the volute section of pump using CFD code FLUENT. The simulation study carried out with k- € turbulence modeling scheme. The flow distribution was evaluated with different cross-section shape of the volute, throat area of volute and radial gap between volute tongue and impeller. When throat area increases, pump efficiency drops in very small quantity. The maximum efficiency of the pump observed with round volute shape and spiral volute area.

2.3.2.2 Number of Blades

Some of the investigators (Zhou et al. 2003; Cui et al. 2006; Liu et al. 2010; Behrouz et al. 2010; and Jafarzadeh at al. 2011; Yang et al. 2013) studied the influence of performance characteristics of the centrifugal pump by changing the number of impeller blades of the impeller. It was found that the optimum number of impeller blades produces maximum head and efficiency of the pump.

Houlin et al. (2010) studied the influence of number of blade on the centrifugal pump performance characteristics using CFD code FLUENT. In the simulation, number of impeller blade varies from 4 to7. They analyzed the flow characteristics inside the pump for cavitations and non-cavitations conditions. As the number of blades increase, head of the pump increases but the efficiency and NPSHR value decreased. They observed that the impeller with 5 blades has the maximum efficiency.

Shojaeefard et al. (2012) studied the influence of the passage width of the impeller using CFD code FLUENT. The simulation study was performed using k -€ and SST turbulence modeling scheme. They found that the increasing of passage width of the impeller from 17 to 21 mm increases the head and hydraulic efficiency due to reduction of the friction losses.

Chakraborty et al. (2012) studied the effects of number of blade variations on the centrifugal pumps performance at different rotational speeds using CFD code FLUENT. The number of blade varies from 4 to 12. The simulation study performed at different operating speed of 2900, 3300 and 3700 rpm. They found that the head and efficiency of the pump increases with the increase in rotational speed. Due to increase in the number of blade, centrifugal pump head increases but the efficiency decreases. The optimum number of blade was found 10.

Chakraborty et al. (2013) studied the influence of number of blade on the centrifugal pump performance characteristics using CFD code FLUENT at operating speed 3000 rpm. Number of blades varied from 5 to 7. They found that the static pressure and head increases with the increase in the number of blades but the maximum efficiency of centrifugal pump is observed for 7 number of blade.

2.3.2.3 Two phase flow

Some of the authors (Liu et al. 2011; Yi et al. 2011;Wang et al. 2012; Yuliang et al. 2013) studied the two-phase solid-liquid flow distribution inside the centrifugal pump passage using CFD code.

Guan et al. (2007) studied the two-phase flow phenomena in the chemical pump using CFD code FLUENT. Simulation was carried out with standard k-ε turbulence model at different operating conditions. The velocity and pressure profiles, secondary flow distribution inside the pump passage analyzed with the help of simulation result. They proposed some design modification in the pump component on the basis of observed phenomena.

Liu et al. (2011) evaluated the two-phase flow distribution of sewage pump using CFD code FLUENT. They used Eulerian mixture model and k-ε- turbulence

modeling scheme for numerical simulation. The distribution of the solid particles between the impeller was observed. They analyzed the influence of outlet blade angle of impeller on the pump efficiency. They observed that the internal hydraulic losses inside the pump passages increase with outlet blade angle of impeller. With the decrease in the outlet blade angle, internal hydraulic losses decreases hence improve the impeller wear and efficiency.

Yi et al. (2011) studied the solid-liquid two-phase flow abrasion characteristic inside the centrifugal pump using CFD code FLUENT. They used two phase flow mixture model and RNG k-ε- turbulence modeling scheme. They found that the effect of solid phase on the abrasive characteristics of centrifugal pump is very small when volume fraction is less than the 2.5% afterwards abrasive wear rate increases rapidly. They also observed that the wear characteristic can be minimizing by reducing the blade outlet angle.

Wang et al. (2012) studied the solid-phase particles effect on the performance characteristics of pump using CFD code FLUENT. They found that the same particle size, the head decreases and shaft power increases due to increase in concentration of solid phase. They also observed very low solid-phase concentration at the pressure side and high solid-phase concentration on the suction of the pump.

Liu et al. (2012) studied the solid-liquid two-phase distribution in chemical process pump. The two phase simulation study was performed using mixture model and k -€ turbulence modeling scheme. They found that the solid phase distribution in the pump passage changes with particle concentration. The solid concentration near the back side of the impeller was higher than the face side.

Yi et al. (2012) performed the numerical simulation of two phase solid-liquid characteristics on the centrifugal pump performance. They compared the numerical result with the experimental data. The two-phase numerical simulation was carried out with different solid particle diameter and mixture concentration. They found that the influence of the solid phase characteristics is the function of

flow rate. The best efficiency point of the pump also shifted with increase in solid particle diameter and volume fraction.

Yuliang et al. (2013) numerically evaluated the centrifugal pump performance using CFD code FLUENT. They used the mixture model for the simulation of two phase flow analysis. They found that solid concentration, diameter of particle and density have strong influence on the pump hydraulic performance. They also observed that head and efficiency are decreased with increase in particle diameter and solid concentration.

Kumar et al. (2013 b) studied the centrifugal slurry pump performance using CFD code FLUENT at design and off-design conditions. Steady state simulation with Moving Reference Frame (MRF) model was used to consider impeller-volute interaction. Different turbulence models like standard k- ε, RSM, k-ώ and RNG k- ε were applied for simulation of flow through the pump, which showed reasonably close prediction of head –flow characteristics of pump by k-ε model. Performance characteristics of the pump was numerically predicted at four different operating speeds namely 1000, 1150, 1300 and 1450 rpm with water. The numerical results were compared with the experimental measurements. The comparison indicates that the specific head, specific power and efficiency characteristics prediction are within an error of 5 %.

From the literature review, it can be clearly seen that the performance of a conventional pump has been predicted using numerical technique and limited studies have been carried out for centrifugal slurry pump handling solid –liquid mixtures.

2.4 GAPS IN KNOWLEDGE

Based on literature review, following gaps in knowledge on the centrifugal slurry pump performance characteristics are observed. Few studies have been conducted on the performance of the pump handling concentrated multi size particulate slurries.

1. Due to incomplete understanding of complex solid-liquid flow phenomena in the impeller and casing, and limited data base, there is no well-established method available to predict the performance of these pumps for liquid as well as solid –liquid mixtures.
2. The empirical correlations developed experimentally for prediction of the pump performance are applicable to particular slurry and cannot predict reasonably the pump performance with other slurries.
3. The understanding of the flow mechanism of multi-sized particulate slurries is limited.
4. Extensive investigations have not been carried out to establish effect of solids on different energy losses.
5. Bottom ash does not contain much fine particles and the effect of fine particles in such coarse slurry has not been investigated so far. Only few studies were reported on the pump handling only bottom ash slurries.
6. The numerical investigations on the pump for solid-liquid flows are limited and no such investigation has been carried out for this type of slurries.

2.5 OBJECTIVES OF THE PRESENT WORK

The limitations of the available experimental data, correlations and numerical simulation have motivated the author to undertake the present study. The efforts of the present study are as below:

1. Determine the physical and chemical characteristics of bottom ash, fly ash and mixture of bottom and fly ash in different proportions.

2. Investigate the effect of addition of fly ash on the rheology of bottom ash slurry at varying temperature environment.
3. Experimentally evaluate the centrifugal slurry pump performance characteristics with water and ash at different operating speeds and solid concentrations.
4. Simulate the flow field inside the pump for flow of water and ash by simulation models and to validate the numerical model with the measured performance.
5. Determine the additional hydraulic losses due to solid suspension in the centrifugal slurry pump.
6. Suggestion for transportation of ash at moderate concentration through centrifugal slurry pump.

The scopes of the present study as well as range of the parameters covered are summarised in the Table 2.5.

Table 2.1: Rheological characteristics of coal ash with additives

Author	Type of Slurry	Concentration (%)	shear rate (1/s)	Additives	Additive concentration (% by weight)	Specific Gravity	Rheometer	Temperature range (°C)
Kumar et. al. (2000)	Fly ash(F.A), Bottom ash (B.A), and FA+BA	0-60 (by weight)		Addition of bottom ash in the fly ash slurry	Fly ash and Bottom ash mixture in the ratio of 9:1,8:2,7:3	Fly ash: 2.08, Bottom ash: 2.11	Weissenberg Rheogoniometer	21
Usui et al. (2001)	Fly ash	70 (by weight)	0.01-1000	Polystyrene sulfuric acid	0.3		Iwamoto Seisakusho Rheometer	25
Seshadri et al. (2008)	Fly ash	60-68 (by weight)	20 - 120	Sodium hexametaphosphate	0.1		WeissenbergRheogoniometer R 18	32
Chandel et al.(2009)	Fly ash	60-70 (by weight)	0-120	Mixture of sodium carbonate and Henko detergent	0.2		WeissenbergRheogoniometer	25
Naik et al. (2009a)	Fly ash	30 (by weight)	25-500	Cationic surfacant and NaSal	0.1-0.5	2.2	Anton Paar Rheometer model MCR 101	20-40
Naik et al. (2009b)	Fly ash	20 (by weight)	100-500	Cetyltrimethyl ammonium bromide, sodium salicylate	0-.5	2.2	Anton Paar Rheometer model MCR 101	20-35

Author	Type of Slurry	Concentration (%)	shear rate (1/s)	Additive	Additive concentration (% by weight)	Specific Gravity	Rheometer	Temperature range (°C)
Naik et al. (2011)	Fly ash	40 % (by weight)	100-1000	Cetyltrimethyl ammonium bromide and sodium salicylate	0.1-0.5	2.2	Anton Paar Rheometer model Physica MCR 101	20-40
Senapati et. al. (2013)	Fly ash	62.5 to 67.5 % (by weight)	0-200	Addition of bottom ash in the fly ash slurry	--------		HAAKE Rotational Viscometer (Model RV 30)	30
Kumar et. al. (2013)	Bottom ash(B.A), Fly ash ash (B.A), and BA+FA	0-60 % (by weight)	50-300	Addition of fly ash in the bottom ash slurry	Bottom ash and Fly ash mixture in the ratio of 9:1,8:2,7:3	Fly ash: 2.01 Bottom ash: 2.25	Anton Paar Rheometer (Rheoplus)	26-41

Table 2.2: Centrifugal slurry pump performance with slurry materials properties

Author	Solid Material	Material properties	Pump specification	Speed Range (rpm)
Fairbank (1942)	Mud and two Sized sand	Specific gravity: 2.65, d50: sand:34 and 800μ m, Concentration(by volume): 0.05-0.20	Conventional centrifugal pump, 75mm impeller diameter, logarithmic spiral shaped vanes	1000 & 1200
Wiedenroth (1970)	Sand	Specific gravity: 2.7, Concentration(by volume): 0.05-0.30	Two solid handling type metal centrifugal pump	500-1250
Vacaldo et al. (1974)	Silica sand	Specific gravity: 2.64, Concentration(by volume): 6-30%	Rubber lined and hard metal centrifugal slurry pump, 75mm impeller diameter	1180 & 1780
Baiz (1984)	Mud	Concentration(by volume): 0-15%	Conventional centrifugal pump, 150 mm impeller diameter	
Maz (1984)	Coarse particulate slurry	dmax.<125mm Concentration(by volume) :40%	Centrifugal pump with channel type impellers, 150mm and 300 mm impeller inlet and outside diameter	
Chand et al. (1985)	Fly ash, sand, iron ore and coal dust	Concentration(by volume): 26%	Centrifugal slurry pump	1000, 1200 1400
Roco et al. (1986)	Sand in narrow sized distribution	Specific gravity : 2.65, Concentration(by volume): 0 - 0.31	Seven solid handling metal centrifugal Pump, 675 mm impeller diameter	
Gahlot et al. (1992)	Coal and Zinc Tailings	Specific gravity: 1.48 and 2.45, Concentration(by weight): 0 - 0.57	Two WILFlEY Rubber lined and Ni hard material centrifugal slurry pump with open and closed impeller respectively, 50mm impeller diameter	1450

Author	Solid Material	Material properties	Pump specification	Speed Range (rpm)
Kazim et al. (1997)	Six types of sand, mild steel, coal zinc, iron ore	Specific gravity: sand-2.65, mild steel 6.24, coal 1.49, zinc 5.51, iron ore-4.35, d50: sand A: 180, B: 230, C:460, sand D:230, E:230, F:362 coal: 185, zinc: 455, Steel:230, iron ore: 663µm, Concentration(by weight): sand A:0-30%, B: 0-30%, C:0-25%, sand D:0-57.8 %, E:0-10%, coal: 0-57.8%, zinc: 0-57.8%, Steel: 0-20%, iron ore: 0-25%	Centrifugal pump with Ni-hard metal, 270mm impeller diameter	1000
Sellgren et al. (1999)	Red mud clay and scrubber sludge	Density: Scrubber sludge:2650, red mud clay: 3200 kg/m^3, Concentration(by volume): Scrubber sludge-31-35 %, Red mud clay-26% Temperature: Scrubber sludge 45-48 ºC, Red mud clay-32-36 ºC	Centrifugal slurry pump with 0.63m impeller diameter, 4 vanes	650-850
Sellgren et al. (2000)	Mixture of sand and clay	Sand to clay mass ratios between 4:1 and 6:1, d50 of sand: 0.64, 1.27, 2.2 mm, Concentration(by volume): 0-35% Temperature: 30-40 ºC	Radial type 4 vane metal pump with 0.625m impeller diameter	500 to 900
Gandhi et al. (2001)	Fly ash, bed ash and zinc tailing	Specific gravity: fly ash-2.08, bed ash-2.44, zinc tailing-2.82, d50: fly ash:42, bed ash:135, zinc tailing: 145µ m, Concentration(by weight): 0-60% pH: fly ash: 7-7.3, bed ash: 7-7.74, zinc tailing: 7-7.3	Two pumps A&B With Ni-hard material and impeller eye diameter 114 &190 mm respectively with single volute casing	1450 and 1250
Engin and Gur (2001)	Casting sand, beach sand, perlite-A& B	Specific gravity: casting sand-2.10, beach sand 2.64, perlite-A-2.34, perlite-B-2.34, d50: casting sand:0.4, beach sand:0.413, perliteA: 0.27, perliteB: 1.39mm, Concentration(by weight): casting sand 5.54-28.42%, Perlite-A: 8.45-20.42%, perlite-B: 8.47-23.39%	Centrifugal pump with inlet diameter 134.5mm, 7 backward curved blades	1250

Author	Solid Material	Material properties	Pump specification	Speed Range (rpm)
Gandhi et al. (2002)	Fly ash and zinc tailing	Specific gravity: fly ash-2.08 and zinc tailing-2.82, d50: fly ash:42, zinc tailing:145μm, Concentration(by weight): zinc tailing-15.1-45 %, fly ash- 15.7-61.9% pH: 7-7.3	centrifugal slurry pump with close impeller having 5 vanes, single volute casing, 114mm impeller eye diameter, Ni-hard material	1150, 1450, 1750
Kadambi et al. (2004)	NaI and glass beads	Particle size: glass beads:500 Concentration(by volume): 1-3%	centrifugal slurry pump	725 & 1000
Ogata et al. (2006)	Ethoquad O/12 and sodium silicate in the molar ratio of 1:1	Concentration: 200, 500, 1000 Temperature- 6-60ºC	centrifugal pump with inlet diameter 80mm	1300
Benretem et al. (2007)	Slurry of washed phosphate	Density: 2800kg/m^3, dmax: 0.2mm, Concentration(by weight): 30%	centrifugal pump with 6 blades, closed impeller	2900
Yassine et al. (2010)	Sand	Specific gravity: 1.602, d50: 0.4mm, Concentration(by weight): 0-15 %	centrifugal pump with closed impeller, 6 vanes and 38mm eye diameter made of brass materials , single volute casing made of cast iron	2900
Chandel et al. (2011)	Fly ash	specific gravity: 1.992, d50: 25μm, Concentration(by weight): 50-70 %	centrifugal slurry pump with volute casing, 5 vanes, 32mm impeller eye diameter, material Ni-hard	1450
Khalil et al. (2013)	Aquatic weeds (mixture of water hyacinth and cattails)	specific gravity: Water hyacinth-0.096, Cattails-0.15 concentration(by weight): 0-18%	centrifugal pump with single volute casing, semi open impeller, 6 vanes, 101.6 mm inlet impeller diameter	2900
Kumar et al.(2014)	Bottom ash, mixture of bottom and fly ash in the ratio of 9:1, 8:2, 7:3	Specific gravity: Fly ash: 2.01 bottom Ash: 2.25 Concentration (by weight): 0- 48% Temperature: 26ºC, pH:7. 4-7.72	centrifugal slurry pump with Ni-hard material, 263 mm impeller diameter	1000-1450

Table 2.3 : Simulation of centrifugal pump performance with water

Author	Turbulence modeling scheme	No. of element	Mesh type	Speed (rpm)	Convergence control	CFD Code	Pump specification
Dick et al. (2001)	k-ϵ	300000 and 550000	Hybrid Mesh	620 and 2190	---	FLUENT	Centrifugal pump, 4 and 5 number of blade
Gonzalez et al. (2002)	Standard k-ϵ	89712	Unstructured tetrahedral	1620	10-5	FLUENT	Centrifugal pump, Single tongue volute, 7 number of blade
González et al. (2006)	Standard k-ϵ	335,000	Structured hexahedral	1620	10-5	FLUENT	Centrifugal pump, Single tongue volute, 200 mm impeller diameter,7 number of blade
Cheah et al. (2007)	Standard k-ϵ	100 4139	Unstructured tetrahedral	1450	10-4	FLUENT	Centrifugal pump, Spiral volute casing, 356 mm impeller diameter, 6 number of blade
Feng et al. (2007)	K-ϵ	1 585 494	Hexahedral	1450	----	CFX	Centrifugal pump, 80 mm impeller diameter, 6 number of blade
Patidar et al. (2007)	Standard k-ϵ, RNG, RSM and LES	890000	Unstructured tetrahedral and coarse finer	3480	10-5	FLUENT	Centrifugal pump, Single volute, 90 mm impeller diameter, 6 number of blade
Spence et al. (2008)	K-ϵ	870500	Hexahedral	1400	------	TASC flow	Centrifugal pump, Double volute,366 mm impeller diameter, 6 number of blade
Wu et al. (2008)	K-ϵ	375000	Hexahedral	3550	-----	TASCflow	Centrifugal pump, 160 mm impeller diameter, 6 and 8 number of blade

Author	Turbulence modeling scheme	No. of element	Mesh type	Speed (rpm)	Convergence control	CFD Code	Pump specification
Bacharoudis et al. (2009)	k-ϵ	432000	Structured and unstructured hexahedral	925	---	FLUENT	Centrifugal pump
Ozturk et al. (2009)	RNG k-ϵ	209546	Unstructured hexahedral and tetrahedral	890	10^{-4}	FLUENT	Centrifugal pump, volute casing, 203.2 mm, impeller diameter, 5 number of blade
Houlin et al. (2010)	Standard K-ϵ	480000	Unstructured tetrahedral	2900	10^{-4}	FLUENT	Centrifugal pump, Volute casing, 168 mm impeller diameter, 4 , 5 and 6 number of blade
Aman et al. (2011)	Standard K-ϵ	724000	Triangular	2900	-----	FLUENT	Centrifugal pump, 52 mm impeller diameter, 6 number of blade
Yang et al. (2011)	RNG k-ϵ	100000	Structural hexahedral	3000	------	FLUENT	Centrifugal pump, 100 mm impeller diameter, 7 number of blade
Chakraborty et al. (2012)	Standard k-ϵ	316789	Structured hexahedral	3000	10^{-5}	FLUENT	Centrifugal pump, Semi volute type, 80 mm impeller diameter, 4 to 12 number of blade
Ge et al. (2012)	k-ϵ	631800	Unstructured tetrahedral and structured hexahedral	600	10^{-4}	FLUENT	Centrifugal pump, 7 number of blade
Kumar et al. (2013)	Standard k-ϵ, RNG, RSM and k-ω	1400503	Unstructured tetrahedral and hexahedral	1000, 1150,1300, 1450	10^{-5}	FLUENT	Centrifugal slurry pump, 26 5 impeller diameter, 5number of blade

Table 2.4 : Two phase flow simulation of centrifugal pump performance using FLUENT

Author	Properties of material	Simulation Parameters	Speed (rpm)	Convergence control	Pump specification
Kee et al. (2002)	Particle diameter (μm) = 150 and 250 Concentration (%) = 56(by weight)	Modeling scheme = mixture model, k-ϵ Flow rate (m3/s) = 0.015	1540	----	Two centrifugal pump with 3 and 6 number of blades
Wang et al. (2003)	Particle diameter (μm) = 87, Concentration (%) = 5 and 20	Modeling scheme = mixture model, k-ϵ	800	10-^{3}	Centrifugal pump,
Benretem et al. (2007)	Types of slurry = sand beach, stream sand and heavy ore, Particle diameter (μm) = 300, Concentration (%) = 15 and 35 (by weight)	Modeling scheme = Mixture model, k-ϵ Flow rate (m3/s) = 0.0055	2900	10^{-4}	Centrifugal pump,400 mm impeller diameter, 6 number of blade
Liu et al. (2009)	Types of slurry = CaCO3, Particle diameter (μm) = 50,100 and 150, Concentration (%) = 5, 15 and 25	Modeling scheme = Mixture model, standard k-ϵ, No. of cells = 1224808, Mesh type =Hexahedral and Hybrid, Flow rate (m3/s) = 0.677	990	10^{-3}	Centrifugal pump, 340 mm impeller diameter, 6 number of blade
Yi et al. (2011)	Particle diameter (μm) = 100, 250, 500 and 1000, Concentration (%) = 1, 2.5, 4 and 5.5	Modeling scheme = Mixture model, RNG k-ϵ, Flow rate (m3/s) = 0.00236	2900	10^{-4}	Centrifugal pump
Liu et al. (2011)	Types of slurry= solid liquid, Particle diameter (μm) = 20000	Modeling scheme = Mixture model, k-ϵ, No. of cells = 220286, Flow rate (m3/s) = 0.00416	2900	10^{-3}	Centrifugal pump,
Li et al. (2011)	Types of slurry = water oil	Modeling scheme = Mixture model, Flow rate (m3/s) = 0.00694	2900	-----	Centrifugal pump,62 mm impeller diameter, 5 number of blade

Author	Properties of material	Simulation Parameters	Speed (rpm)	Convergence control	Pump specification
Wang et al. (2012)	Particle diameter (μm) = 200, Concentration (%) = 3, 6 and 10	Modeling scheme = Euler model, No. of cells = 421345, Mesh type = Tetrahedral and Mixed, Flow rate (m3/s) = 0.01388	1650	10^{-4}	Centrifugal pump,
Liu et al. (2012)	Particle diameter (μm) = 50, 100, 200 and 300, Concentration (%) = 2.5, 5, 7.5 and 10	Modeling scheme = Mixture model, k-ϵ, No. of cells = 2472624, Mesh type = Tetrahedral		----	Centrifugal pump, 5 number of blade
Yang et al. (2013)	Particle diameter (μm) = 19, 36 and 76	Modeling scheme = Euler-Lagrange multiphase flow model, RNG k-ϵ, No. of cells = 1387564, Mesh type = Unstructured, Flow rate (m3/s) = 0.00711	1480	-----	Centrifugal pump,142 mm impeller diameter,
Cheng et al. (2013)	Mean diameter of particle (μm) = 76, Concentration (%) = 5, 10 and 15	Modeling scheme = Mixture model, RNG k-ϵ, No. of cells = 100000, Flow rate (m3/s) = 0.01	1460	----	Three centrifugal pump with 4, 6 and 8 number of blade
Yuliang et al. (2013)	Particle diameter (μm) = 10, 50, 100, 150 and 200, Concentration (%) = 5, 7, 10 and 15	Modeling scheme = Mixture model, RNG k-ϵ, No. of cells = 508792, Mesh type = Tetrahedral Flow rate (m3/s) = 0.00166	1450	10^{-4}	Centrifugal pump, 48 mm impeller diameter,

Table 2.5: Scopes of the Present Study

S. no.	Nature of work	Parametric study	Range of parameters
1.	Experimental	Physical and chemical characteristics of bottom ash, fly ash and mixture of bottom and fly ash in the ratio of 9:1.8:2 and 7:3.	Concentration range: 0 to 60% (by weight)
2.	Experimental	The rheological characteristics of bottom ash (B.A) slurry at varying temperature environment with and without addition of fly ash (F.A).	Concentration range: 0 to 60% (by weight) Temperature range- 26 ºC to 41 ºC
3.	Experimental	Performance characteristics of centrifugal slurry pump with Bottom ash, B.A+FA (9:1), B.A+FA (8:2), B.A+FA (7:3).	Concentration range: 0 to 48% (by weight) ,Speed range-1000-1450 rpm, Complete head-flow and efficiency-flow characteristics
4.	Numerical	Simulation study of flow field inside the pump for flow of water using commercial computational Fluid Dynamics code FLUENT.	Fluid –waterSpeed range-1000-1450 rpm Turbulence model- standard k- ε, RSM, k- ώ and RNG k- ε
5.	Numerical	Simulation of Two phase solid –liquid flow through a centrifugal slurry pump with Bottom ash, B.A+FA(9:1), B.A+FA (8:2), B.A+FA(7:3).	Concentration range: 0 to 45% (by weight) , Speed range-1000-1450 rpm, Complete head-flow and efficiency-flow characteristics

CHAPTER-3

PHYSICAL AND RHEOLOGICAL PROPERTIES OF FLY ASH AND BOTTOM ASH

The flow behaviour of solid-liquid mixtures depends on the large number of parameters. These parameters are interdependent which complicates the design process. For the hydraulic design of the slurry pump, the designers need extensive data covering all aspects of two-phase solid –liquid flow. The extensive literature shows that enough data is not available to support the design methodology for all solid materials. So it is essential to establish the flow characteristics of a particular slurry flow for making the design methodology suitable for it. For any slurry suspension, the flow properties data has been generated by conducting the experiments. Bench scale tests are required to establish the physical properties of the solids and solid –liquid mixtures.

3.1 BENCH SCALE TESTS

The material chosen for the study of the physical, chemical and rheological characteristics of the particulate materials are (i) fly ash and (ii) bottom ash. Both the samples of bottom ash (B.A) and fly ash (F.A) were collected from Guru Gobind Singh thermal power plant, Ropar, Punjab. The fly ash was collected directly from the electrostatic precipitators (ESPs) and bottom ash from the hoppers. Various bench scale tests were carried out on ash collected to determine the specific gravity, particle size distribution, (PSD) of the solid materials, pH value and static settling characteristics of slurries at various concentrations. A brief description of these tests is presented here.

3.1.1 Particle Size Distribution

The variation of the particles size and the percentage of particles present in the solid materials are determined to establish the particle size distribution (PSD). The sieve

analysis method is used to get the particle size distribution of the bottom ash and fly ash samples.

A known weight of fly ash and bottom ash samples of solid particles were taken and dried in an oven.

The dried ash samples are sieved through a set of standard sieves. Special care is taken to ensure that both the ash samples are properly dried. The coal ash samples retained on each sieve are collected and the percentage retained on each sieve is calculated using the standard method.

Data from sieve analysis of different materials were plotted between percentages finer vs. particle diameter. The differential analysis of the size distribution was done and weighted mean diameter of different samples was calculated using following equation:

$$d_{wm} = \sum_{i=1}^{N} f_i \, d_i \qquad (3.1)$$

Where N is the number of particle size groups, f_i is the solid fraction; d_i is the mean diameter of the two successive sizes of sieves.

3.1.2 Specific Gravity

The specific gravity of solid material is an important parameter in the design of a slurry transportation system. It decides the settled concentration of the solid liquid mixture. The specific gravity of fly ash and bottom ash were determined using standard pycnometer method.

3.1.3 Static Settled Concentration

The static settled concentration of slurry suspension is representing the maximum value of solid concentration, which can be determined by gravitational settling method. The static settled concentration value depends on the large number of parameters like particle shape, particle size distribution, specific gravity, and viscosity of solid –liquid suspension etc. It is well accepted that the optimum value of solid concentration for slurry transportation is around 5 to 10% lower than the static settled value.

The static settled concentration value has been determined by preparing a solid-liquid suspension of initial solid concentration i.e. 20% (by weight). The slurry level was

noted during the process of settling of the slurry suspension at regular intervals of time. Static settled concentration for all the solids are obtained from the settling characteristics of the mixture. The method of calculating static settled concentration has been described here.

$$\text{Initial concentration of the slurry} = \frac{W_s}{\rho_w V_w + W_s} \quad (3.2)$$

$$\text{Volume of water in the settled slurry} = V_{wm} = V_w - (V_{mi} - V_m) \quad (3.3)$$

$$\text{The static settled concentration (by weight)} = C_{ws} = \frac{W_s}{(\rho_w V_{wm} + W_s)} \quad (3.4)$$

3.1.4 pH Value

A digital pH meter was used to determine pH value of the coal ash slurry suspension at any given solid concentration. The pH meter electrode was first moistened with distilled water and then calibrated with known pH value of buffer solution. It is cleaned with distilled water and then immersed in the slurry suspension of coal ash sample whose pH value was to be determined.

3.1.5 Zeta Potential

Zeta potential is a physical property exhibited by suspension particles in any suspension. There are three fundamental states of matter namely solids, liquids and gases. If any one of these states of matter is finely dispersed in another then it is called the colloidal system. The zeta-potential is used in colloid chemistry for observing the behavior of dispersive systems in liquids.

The zeta potential value represents the potential stability of any slurry suspension solution. The particle suspension at which the surface charge of a particle is zero is referred as the point of zero charge (PZC) or isoelectric point (IEP). However, if the particles have low zeta potential value then there will be no force to prevent the particles coming together and flocculating. If the slurry suspensions show the large positive or negative zeta potential value then they will repel to each other. Some of the investigators (Salopek et al. 1992 and Hunter 2001) reported the methodology to measure the zeta potential of various minerals.

Zeta Plus (manufactured by Brookhaven Instruments Corporation, U.S.A) was used to measure Zeta potentials of bottom ash slurry with and without addition of fly ash.

The Zeta Plus instrument utilize the shift in frequency of scattered laser when, particles move perpendicularly to the laser beam due to an applied electric field (Doppler effect). The frequency shift is proportional to the electrophoresis mobility, which in turn is related to the zeta potential of the particles.

3.2 RHEOLOGICAL BEHAVIOUR OF SOLID-LIQUID MIXTURE

The most important data required for design a slurry transportation system is the rheological characteristics of the slurry suspension at various solid concentrations and flow conditions. The rheological characteristic of slurry depends on several parameters such as particle size distribution, solid concentration, viscosity etc.

3.2.1 Rheometer

A standard Rheometer (Rheolab Q-C Manufactured by Anton Paar Company Ltd, Germany) was used to determine the shear strain rate and shear stress relationship of the ash slurries. The rheometer (Rheolab-QC) works on the Searle principle. It consists of a high-precision encoder and a highly dynamic electronically commutated (EC) synchronous drive. The Rheometer (Rheolab Q-C) is shown in Figure 3.1. The rheological properties were determined by measuring the shear stress at various shear strain rates. The rheometer has a co-axial cylindrical cup and bob measuring system. The stationary concentric cylinder was used as a cup, which houses the slurry, into the rotating bob mounted vertically. The slurry suspension undergoes shearing action by rotation of the rotating bob. The detailed specifications of the rheometer are given in Table 3.1.

3.2.2 Preparation of the Slurry Samples

For rheological data, 100 ml of the slurry suspension was prepared by mixing required quantity of bottom ash or fly ash with tap water to obtain desired solid concentration. The ash was weighed accurately using an electronic single pan balance. The resolution of the electronic balance is ±0.1 mg. The slurry suspension was prepared gently using a glass rod with due care to avoid the particles attrition. Before conducting the experimentation, the

cup and bob assembly was fixed with a locking device. The slurry suspension was poured into cup (stationary cylinder) up to the specified mark. The slurry suspension was again stirred with a glass rod and the bob was quickly lowered into the cup so that the free surface touches the top of the bob. The bob was then rotated inside the cylinder at the required speed. The tests were conducted at the shear rate of 50, 100, 150, 200, 250 and 300 s^{-1} at constant temperature of 26°C at all concentrations. To ensure the precision of the rheological data, measurement was repeated with the same shear rate. For each solid concentration, experiments were conducted on at least two samples of the same material to check the repeatability of the data.

3.2.3 Range of Parameters

The rheological experiments were carried out with the slurry suspension of bottom ash, fly ash, and mixtures of fly ash and bottom ash. The rheology of the fly ash and bottom ash slurry was measured in the solid concentration range of 10 to 50% (by weight). For mixtures of fly ash and bottom ash, the total solids was used to determine the solid concentration and the proportion of fly ash in the mixture was varied as 10%, 20% and 30% (by weight) as percent of total weight of solids. The effect of the temperature on the rheology of bottom ash slurry with and without addition of fly ash was studied at the concentration of 20% (by weight). The constant temperature circular bath was connected to rheometer for variation of temperature of slurry. The slurry suspension temperature was varied from 26ºC to 41ºC for all the shear rate conditions.

3.3 PHYSICAL AND CHEMICAL PROPERTIES OF FLY ASH AND BOTTOM ASH

The materials used in the present work were fly ash and bottom ash. The pycnometer method has been used to determine the specific gravity of ash samples. The specific gravity of the bottom ash and fly ash was determined as 2.25 and 1.99. The particle size distribution of bottom ash and fly ash sample was determined by using sieve analysis. The particle size distributions of both coal samples are given in Table 3.2 and shown in Figure 3.2. From Figure 3.2, it is observed that the biggest particle size of bottom ash is 2000µ m. More than 79.4% particles are coarser than 150 µ m and only 3% particles are finer than

75μ m. In the fly ash, the biggest particle size is 355μ m and 69% particles are finer than 75μ m. The weighted mean and median diameter of bottom ash particles were found as 230μ m and 162μ m, respectively. The fly ash weighted mean and median diameters were determined as 54μ m and 48μ m, respectively.

The static settled concentrations of the fly ash and bottom ash slurries were measured by taking an initial mixture of 20% concentration (by weight). The final static settled concentration of bottom ash and fly ash slurries was observed as 49% and 57% (by weight), respectively. The static settled concentration value with variation of time is tabulated in Table 3.3 and shown in Figure 3.3. The higher static settled concentration of the bottom ash was attributed to its coarse irregularly shaped particles whereas the fly ash leads to low value of static settled concentration owning to fine spherical shaped particles. The SEM analysis photograph (Figure 3.4) shows that the bottom ash particles are irregular in shape which may be causing more drag for flow of particles in hydraulic pipelines.However shape of fly ash particles is nearly spherical.

The pH value of the bottom ash and fly ash slurry suspension was determined using digital pH meter. The pH values with variation of the solid concentration (by weight) of fly ash and bottom ash slurry shown in Table 3.4. The pH values have been measured at various concentrations in the range of 10 to 50% (by weight). The pH value of bottom ash and fly ash varies with the solid concentration in the range of 7.60 to 7.75 and 7.44 to 7.61 respectively. The pH values of both samples depict non- reactive nature of both the ash slurries. It can be inferred that the concentration of the fly ash and bottom ash slurries has negligible effect on pH value.

Energy-dispersive X-ray spectroscopy (EDX) was used to measure the chemical compositions of fly ash and bottom ash sample which is listed in Table 3.5. From the Table 3.5, it is observed that in both samples, the proportion of aluminum oxide and silica oxide are more as compared to other elements like iron, potassium, calcium, copper, magnesium, zinc etc. The percentage of aluminum oxide and silica oxide in the bottom ash and fly ash were found as 33.0% and 51.5%, and 26.57%, and 45.18 % respectively.

The X-ray diffraction (XRD) analysis of the bottom ash and fly ash samples were carried out at the room temperature between position $10° \leq 2\theta \leq 80°$, which is shown in Figure 3.5. The XRD result showed that both the samples, bottom ash and fly ash, are

amorphous in nature, as indicated by the presence of major proportion of the crystalline phases of SiO_2 and Al_2O_3. The elements FeO, TiO_2, CO_2 and ZnO are presence in small proportions. This shows that the particles of Al and Si having highly surface enrichment. These elements also act as more uncreative inert fillers causing drag effects on the flow behavior of the fly ash and bottom ash.

In order to evaluate the zeta potential value of bottom ash slurry with and without addition of fly ash samples were prepared at concentration of 10% and 20% (by weight). The mixtures of bottom and fly ash were in the ratios of 9:1, 8:2 and 7:3 respectively. The zeta potential results of bottom ash with and without addition of fly ash are given in Table 3.6. From the results it is observed that the zeta potential value of bottom ash was negative -22.4 mV and -22.7 mV at solid concentration of 10 and 20% (by weight), respectively. As the fly ash is added in the bottom ash, surface of bottom ash becomes negatively charged and zeta potential value of bottom ash was found as -25.7, -28.9, -29.2 mV for mixture ratio of 9:1, 8:2 and 7:3, respectively, at solid concentration of 10% (by weight). At the solid concentration of 20% (by weight) of bottom ash slurry, the value of zeta potential found was as -25.8, -28.6, -29.4 mV for mixture ratio of 9:1, 8:2 and 7:3 respectively. The addition of the fly ash modified the surface properties of the bottom ash particles keeping the suspension in the stable condition.

It is also observed that with increasing the proportion of fly ash in the bottom ash, the suspension becomes more negative. The study indicates that the bottom ash slurry will be more stable with the addition of fly ash in the bottom ash. From the Table 3.6, it is seen that the zeta potential value of bottom ash slurry does not change significantly with solids concentration. Few investigators (Cho et al. 2005 and Naik et al. 2009) also studied the stability of fly ash slurry with the help of zeta potential measurement.

3.4 RHEOLOGIGAL CHARACTERISTICS OF BOTTOM ASH WITH AND WITHOUT ADDITION OF FLY ASH

The shear stress - shear rate data for above range of solid concentration were obtatined for each bottom and fly ash sample.The Bingham fluid behaviour of the slurry suspension can be expressed in Equation 3.5.

$$\tau = \tau_y + \eta \frac{du}{dy} \quad (3.5)$$

Relative viscosity is defined as the ratio of viscosity of the slurry to the viscosity of water under identical conditions. In case of Bingham fluid, the coefficient of rigidity is used as viscosity of slurry for determining the relative viscosity. To evaluate the viscosity of all the slurry suspensions, a straight line equation was fitted to all sets of data. The shear stress-shear rate data of bottom ash and fly ash at different concentrations are presented in Figures 3.6 and 3.7. From Figure 3.6, it is observed that shear stress increases linearly with increase in shear strain rate at all slurry suspension of bottom ash. The value of τ_y is zero for all suspensions of bottom ash slurry up to 50% solid concentration (by weight). This implies that bottom ash slurry suspensions show Newtonian behaviour up to 50% solid concentration (by weight). Fly ash slurry shows the Newtonian flow characteristics up to 30% concentration (by weight) and beyond which it depicts non Newtonian flow characteristics as shown in Figure 3.7. The rheology data of bottom ash slurry and fly ash slurry with variation of the solid concentrations are presented in Table 3.7. The result indicated that the slurry viscosity of both the suspension is a function of solid concentration. For Bingham flow characteristics of fly ash slurry, the value of yield stress also increases with the concentration. As the solid concentration of slurry increases, a relatively larger numbers of solid particles were present in the suspensions and hence a high value of shear stress is required to start the shearing process. Similar observation was also drawn by many investigators (Gandhi et al. 1998 and 2000; Senapati et al. 2009 and 2010; Seshadri et al. 2008; Chandel et al. 2009b and Naik et al. 2011) with fly ash slurry.

3.4.1 Effect of Addition of Fly Ash on the Rheology of Bottom Ash Slurry

The experimental rheology data of bottom ash slurry with and without fly ash are presented in Figure 3.8 .The coarse particulate bottom ash was mixed with the finer particles of fly ash in the ratio of 9:1, 8:2 and 7:3 (by weight). The total solid concentration of the slurry suspension varies from 10 to 50% (by weight) at the temperature environment of 26ºC. From the Figure 3.8, it is seen that the shear stress value increases monotonically with increase in the solid concentration. It is also observed that shear stress value increases with increase in the proportion of fly ash in the bottom ash slurry at any shear rate value.

The relative viscosity of mixture of the bottom and fly ash suspension at different solid concentrations is shown in Figure 3.9. It is observed that the value of relative viscosity increases with increasing the proportion of fly ash in the bottom ash slurry. The relative viscosity of 10% concentration ash slurry increases to maximum 8.89% for 30 % proportion of the fly ash. Whereas for 50% concentration, the ash slurry shows an increase of 25.23% for 30% proportion of the fly ash. Thus the effect of addition of fly ash appears more pronounced on bottom ash slurries at higher concentrations.

3.4.2 Effect of Temperature on the Rheology

The rheology of the slurry suspension of bottom ash with and without addition of fly ash has been evaluated with the variation of the temperature from 26ºC to 41ºC for all the shear rates. The temperature of the slurry suspension was increased in the step of 5ºC at the solid concentration of 20% (by weight). The shear stress – shear rate data of the bottom ash slurry with and without addition of fly ash at the temperature of 26ºC is shown in Figure 3.8 (b) and similar variation at 41ºC is shown in Figure 3.10.

From Figure 3.10, it is observed that the shear stress value was decreased with increase in the temperature of slurry suspension at fixed shear rate. With the increases of slurry temperature from 26ºC to 41ºC, the maximum decrease in shear stress value is 6.84% for bottom ash, 8.34% for mixture ratio of 9:1, 9.96 % for mixture ratio of 8:2 and 6.20 % for mixture ratio of 7:3. The decrease in viscosity of the suspension with increase in temperature is attributed to the decrease in viscosity of carrier fluid with temperature and insignificant increase in area of solid phase with temperature rise.

The relative viscosity of slurry suspension with the variation of the temperature is shown in Figure 3.11. The relative viscosities of all the slurry suspensions decrease with increase in the temperature which follows the trend of a viscous fluid.

With increase in the slurry temperature, the kinetic energy of the slurry particles increase which promote to reduce the intermolecular forces between adjacent layers which results in decrease in relative viscosity of the slurry suspension. When slurry suspension temperature increases from 26ºC to 31ºC, relative viscosity of bottom ash slurry and mixture ratio of 9:1, 8:2 and 7:3 are reduced by 2.93, 3.32, 4.05 and 3.38%,respectively. The relative viscosity of bottom ash slurry and mixture ratio of 9:1, 8:2 and 7:3 were

decreased by6.05, 6.65, 8.54 and 5.70 % for increase in temperature from 31ºC to 36ºC and decreased by2.95, 2.84 , 3.56 and 2.90% for increase in temperature from 36ºC to 41ºC respectively.

Based on the relative viscosity data, the rate of decrease in the slurry viscosity with temperature increases up to temperature of 36 ºC and there after it decreases with further increase in temperature. The relative viscosity reduction was marginal with increase in the temperature from 36ºC to 41ºC for the tested range of shear rates. It is also observed that the maximum drop in relative viscosity of bottom ash slurry is approximately 13.84 %. This result may help to design the pipeline for possibility of the transportation of slurry with minimum energy consumptions.

Some of the investigators (Mishra et al.2002; Senapati et al. 2009 and Naik et al. 2011) also studied the rheology of coal-water slurry, limestone-water slurry and fly ash slurry with variation of temperature and observed similar phenomena.

3.5 PRACTICAL RELEVANCE OF THE PRESENT STUDY

On the basis of the rheological behaviour model of the slurry suspension a designer may adopt the prediction methodology to select the slurry pump and pipeline. Several empirical correlations have been developed to predict the pressure drop for different flow regimes like laminar, transition and turbulent flow in the slurry pipeline.

The rheological parameters obtained from the bench scale tests could be used for prediction of flow behavior at high concentration bottom ash slurry disposal system. Bottom ash and fly ash is the solid residue by-products produced by coal-burning utilities. In the present study, a comparison of shear stress and viscosity for bottom ash, and mixtures of bottom ash and fly ash in the ratio 9:1, 8:2 and 7:3 showed that the viscosity and shear stress increases with the addition of fly ash in the bottom ash.

Based on the present work on the rheological characteristics of bottom ash slurry with and without fly ash, the following observations were made.

- Bottom ash slurries showed Newtonian fluid behavior up to 50% concentration (by weight). The behavior does not change with the addition of fly ash up to 30% proportion (by weight).

- The measurement of zeta potential indicates that the bottom ash slurry will become more stable by addition of fly ash in the bottom ash.
- The relative viscosity of the bottom ash was increased with increase in the proportion of fly ash in the bottom ash slurry.
- The relative viscosity decreases with increasing the temperature of the bottom ash slurry with and without addition of fly ash.

Table 3.1: Specification of the rheometer (Rheolab QC)

Sr. No.	Component	Specification
1.	Motor Type	Synchronous Electric motor
2.	Torque Range	0.25 – 75, mN-m
3.	Speed Range	0.01 to 1200, min^{-1}
4.	Shear Stress Range	0.5 to 3 x 10^7, mPa
5.	Shear Rate Range	0.01 to 4000, sec^{-1}
6.	Viscosity Range	0.1 to 10^9, mPa-s
7.	Temperature Range	-20 to 180, ^oC

Table 3.2: Particle size distribution of bottom ash and fly ash

Particle size distribution of Bottom ash (% fine by weight) $d_{wn}(\mu m) = 162$ $d_{50}(\mu m) = 230$												
Particle size, μ m	> 2000	1400	710	355	300	250	212	180	150	125	90	75
% finer	100	89.5	85.5	72.6	65	58.8	46.8	44.1	20.6	17.4	13.5	3
Particle size distribution of Fly ash (% fine by weight) $d_{wn}(\mu m) = 48$ $d_{50}(\mu m) = 54$												
Particle size, μ m	-	-	355	300	250	212	180	150	125	90	75	53
% finer	-	-	100	99	98.5	97	95	92	88	80	69	48

Table 3.3: Settling characteristics of bottom ash and fly ash

Initial concentration of suspension = 20% by weight													
Time(Minute)	0	1	2	3	4	5	15	30	60	120	180	240	480
Conc. ($\%C_w$) Fly ash	20	24.97	25.28	29.8	32.2	44.4	53.9	53.9	54.5	55.7	55.7	57	57
Conc. ($\%C_w$) Bottom ash	20	28.12	33.16	42.37	45.25	47.4	47.4	47.4	48.5	48.5	48.5	49	49

Table 3.4: pH values of bottom ash and fly ash

Concentration (% by weight)	0	10	20	30	40	50
pH of bottom ash	7.75	7.72	7.67	7.66	7.63	7.62
pH of fly ash	7.75	7.61	7.59	7.51	7.46	7.44

Table 3.5: Chemical composition analysis of the fly and bottom ash

Chemical composition (%by weight)										
Material	CO_2	Al_2O_3	SiO_2	K_2O	CaO	TiO_2	FeO	CuO	ZnO	others
Fly ash	10.38	26.57	45.18	1.53	1.96	1.95	4.98	2.97	3.03	1.45
Bottom ash	2.33	33.03	51.54	0.70	1.87	4.02	4.34	1.11	1.05	0.01

Table 3.6: Zeta potential value of bottom ash slurry with and without addition of fly ash

Sample number	**Bottom ash (g)**	**Fly ash (g)**	**Water (g)**	**Solid concentration (% by weight)**	**Zeta Potential (m V)**
I.	10	0	90	10	-22.4
II.	9	1	90	10	-25.7
III.	8	2	90	10	-28.9
IV.	7	3	90	10	-29.2
V.	20	0	80	20	-22.7
VI.	18	2	80	20	-25.8
VII.	16	4	80	20	-28.6
VIII.	14	6	80	20	-29.4

Table 3.7: Rheological properties of bottom ash and fly ash at temperature of 26°C

Concentration (Cw) %	Bottom ash			Fly ash		
	Yield stress (Pascal)	Relative viscosity	Flow behaviour	Yield stress (Pascal)	Relative viscosity	Flow behaviour
0	0	1	Newtonian	0	1	Newtonian
10	0	1.02	Newtonian	0	1.41	Newtonian
20	0	1.61	Newtonian	0	1.92	Newtonian
30	0	2.21	Newtonian	0	2.8	Newtonian
40	0	4.32	Newtonian	0.17	7.93	Non-Newtonian
50	0	5.62	Newtonian	0.28	15.86	Non-Newtonian

Figure 3.1: Rheometer (Anton Paar, Germany)

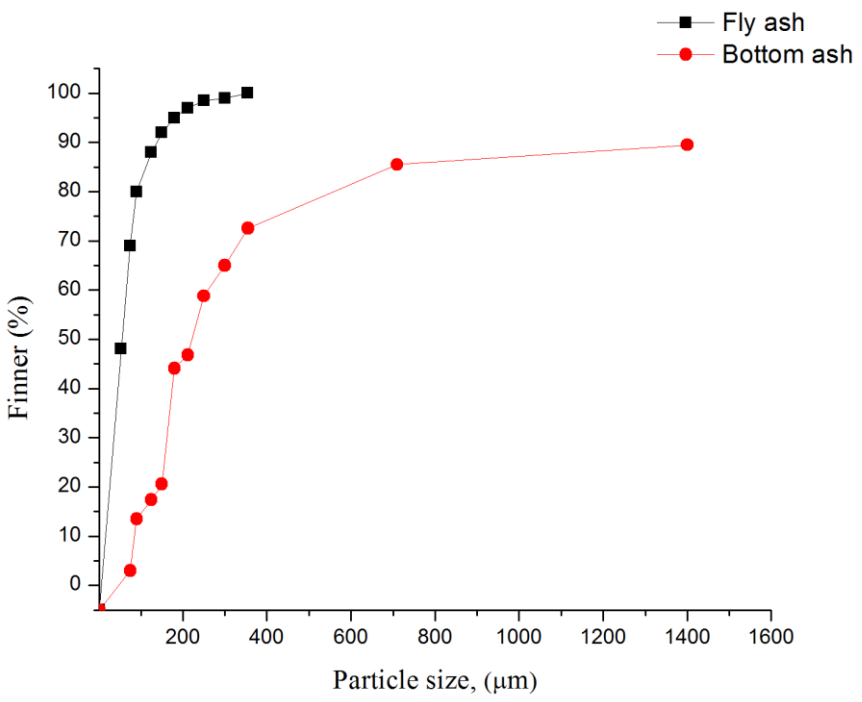

Figure 3.2: Particle size distribution of fly and bottom ash

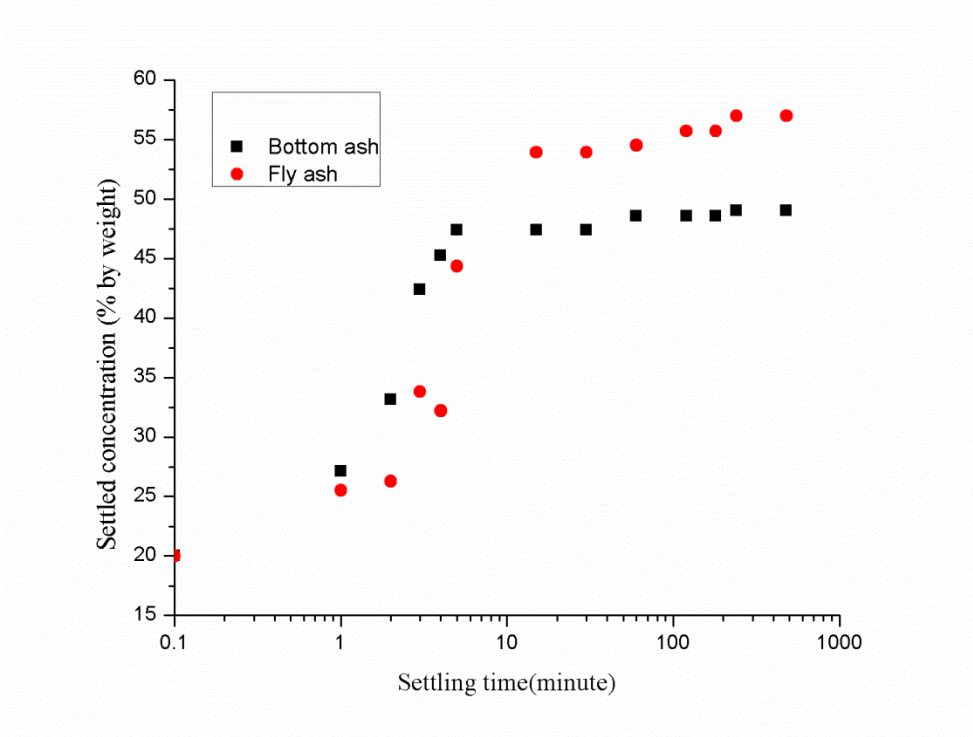

Figure 3.3: Settled concentration of fly and bottom ash

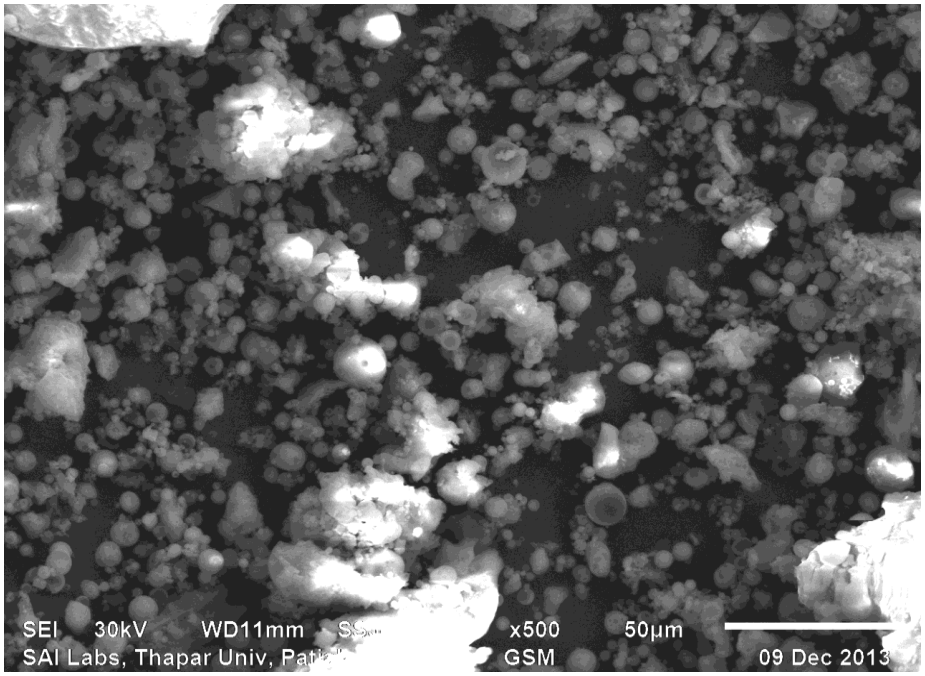

(a) Fly ash

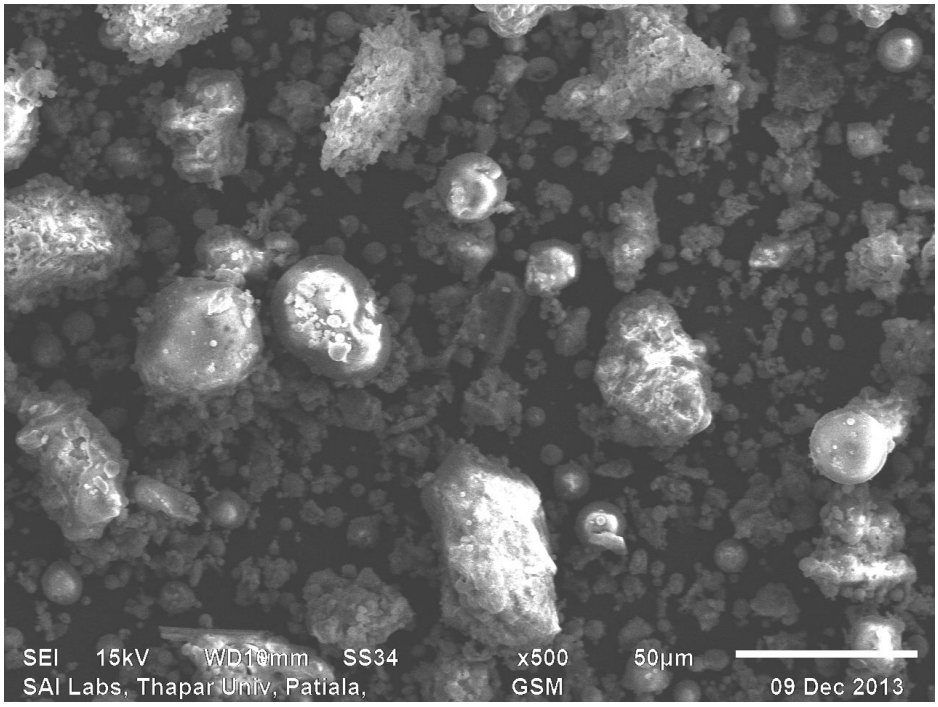

(b) Bottom ash

Figure 3.4: SEM photomicrograph of ash samples at 500×500 magnification

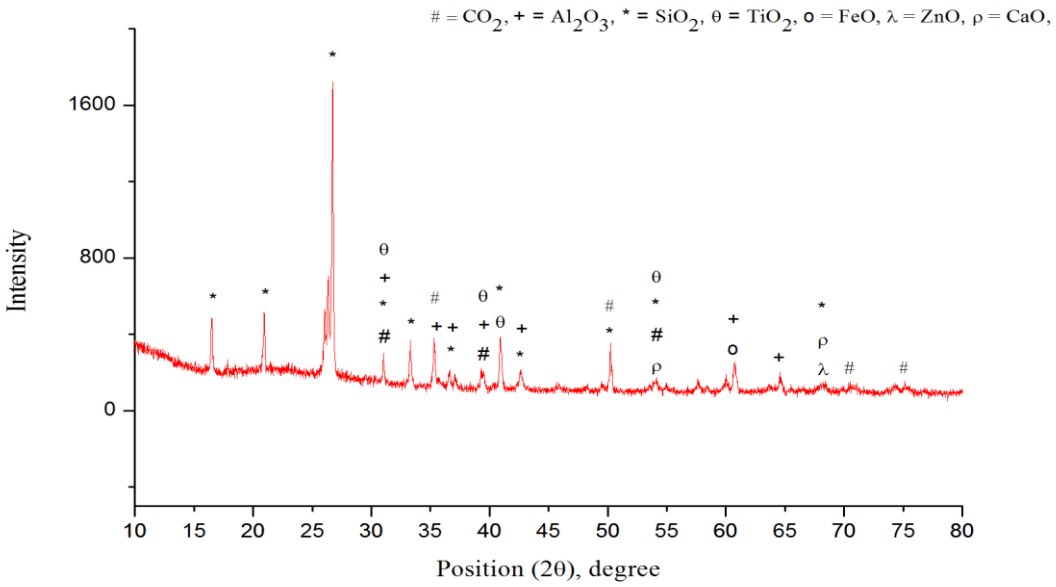

(a) Fly ash

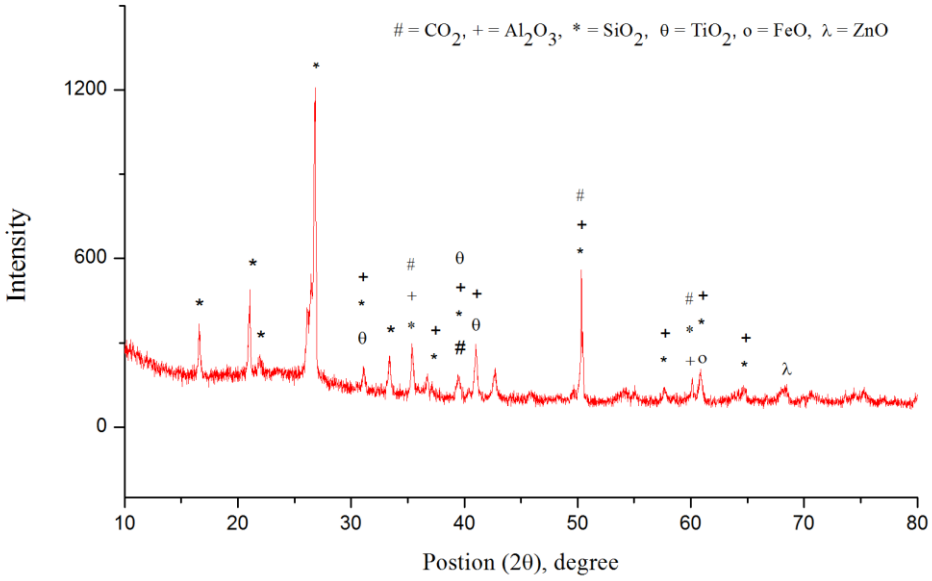

(b) Bottom ash

(c) Figure 3.5: X-ray diffraction pattern of fly ash and bottom ash

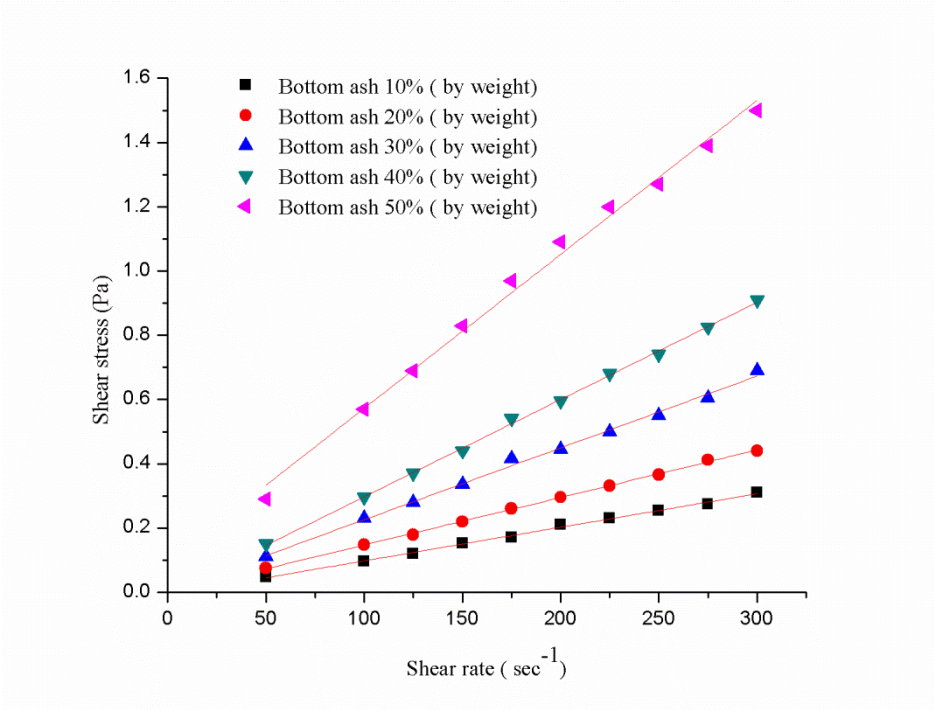

Figure 3.6: Shear stress- strain rate curve of bottom ash at different concentrations

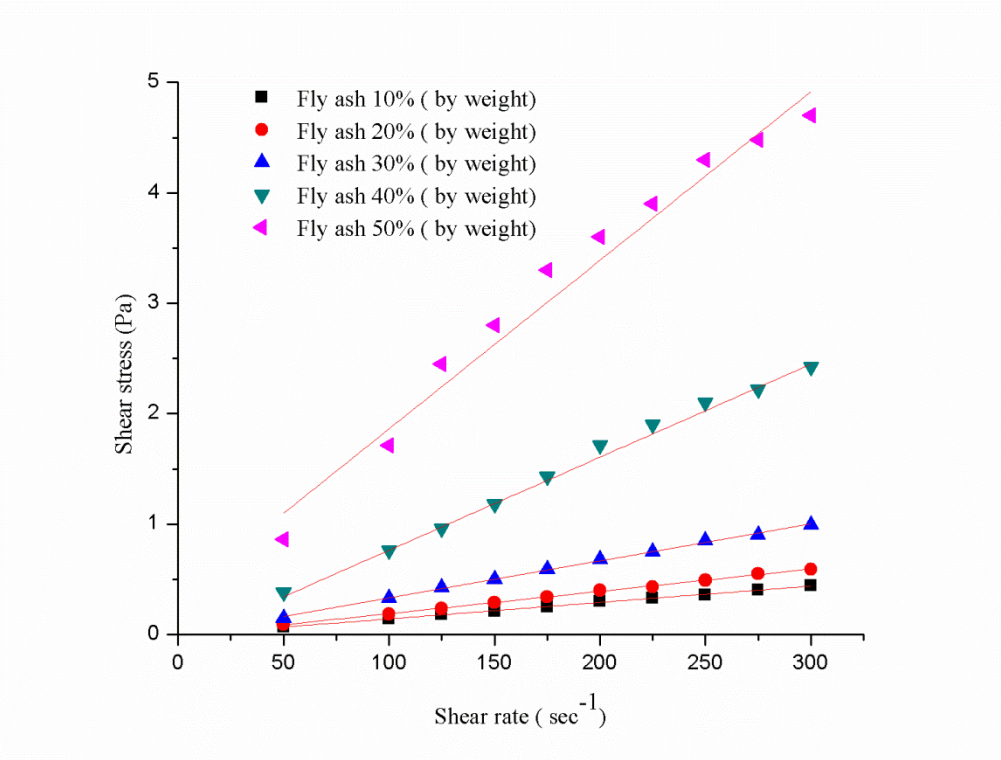

Figure 3.7: Shear stress- strain rate curve of fly ash at different concentrations

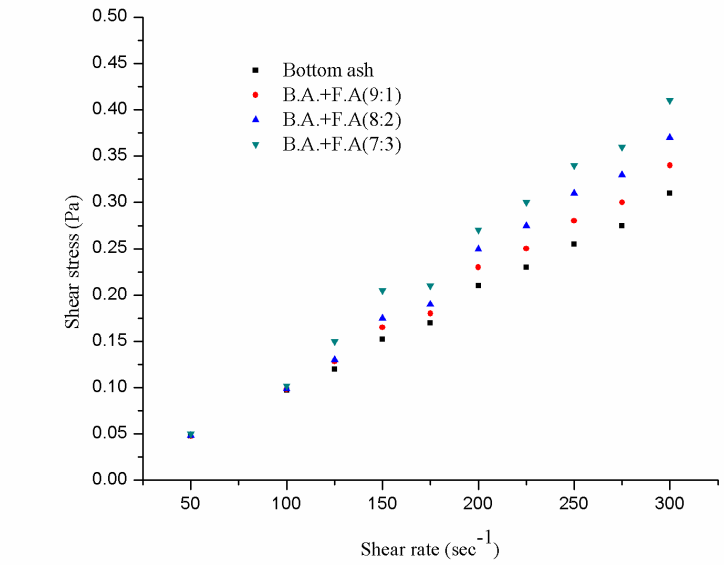

(a) Solid concentration 10% (by weight)

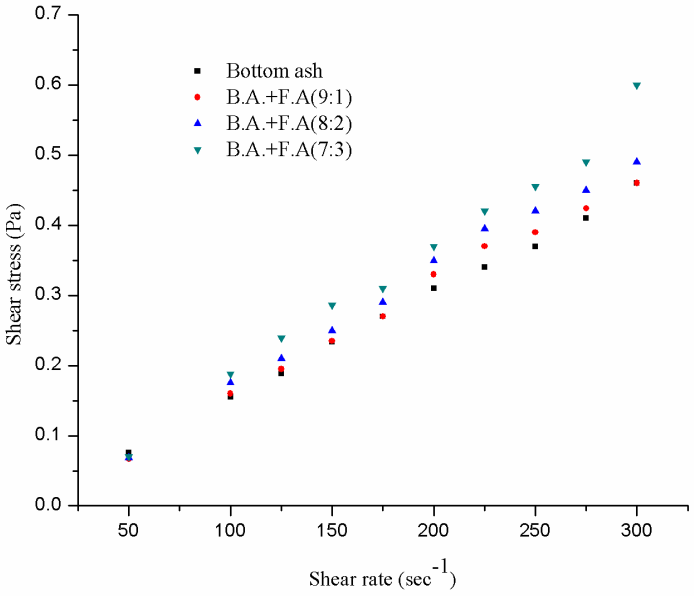

(b) Solid concentration 20% (by weight)

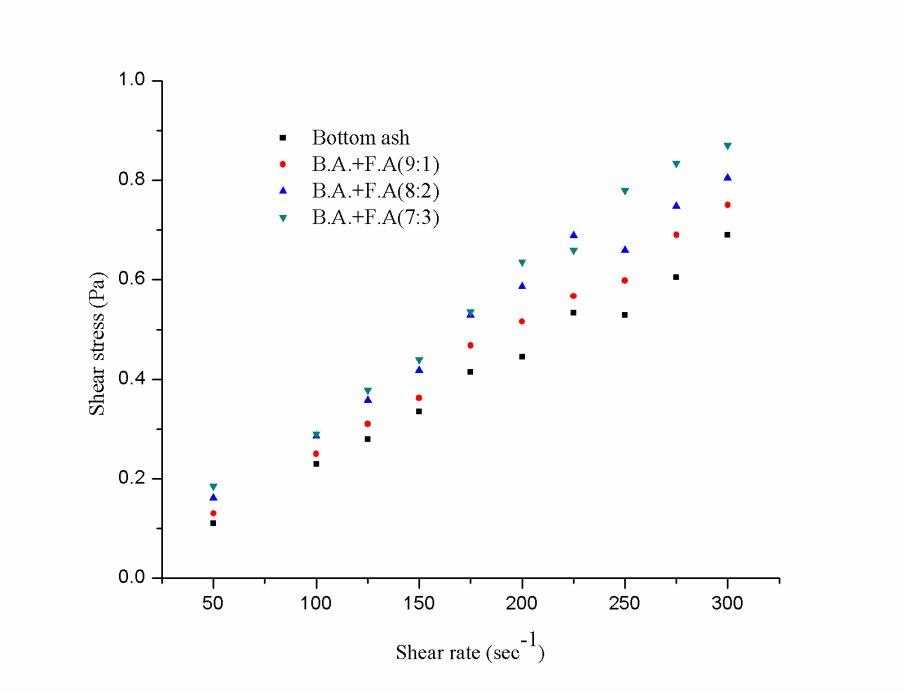

(c) Solid concentration 30% (by weight)

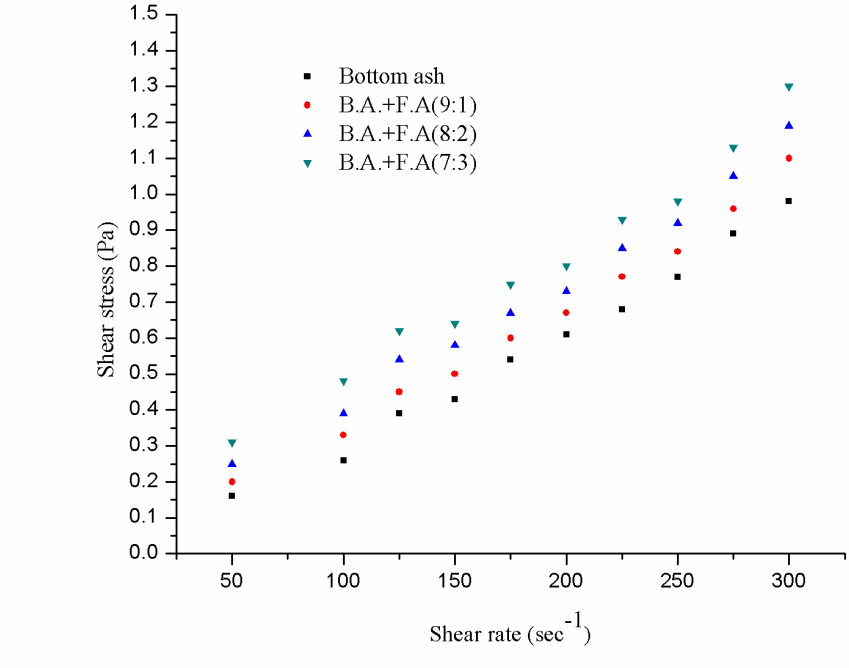

(d) Solid concentration 40% (by weight)

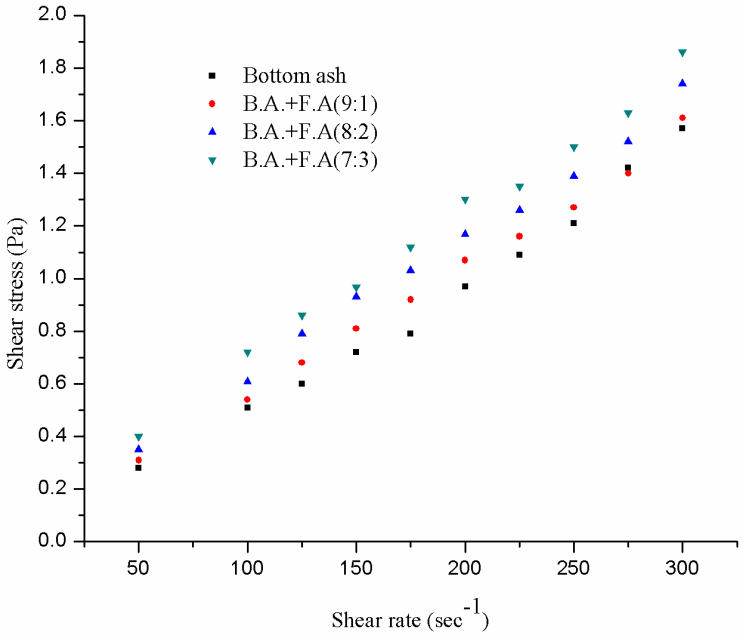

(e) Solid concentration 50% (by weight)

Figure 3.8: Rheogram of bottom ash with and without addition of fly ash at temperature of 26ºC

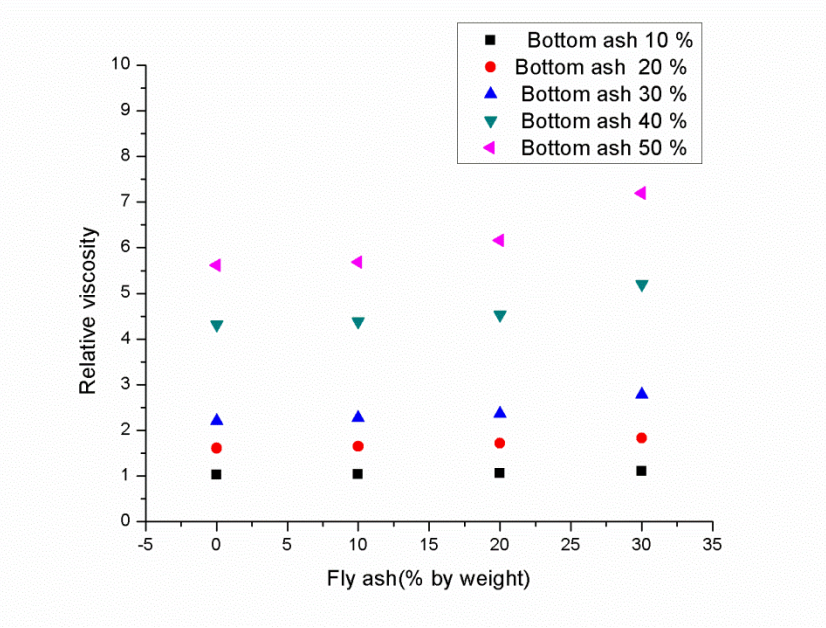

Figure 3.9: Variation of relative viscosity of bottom ash slurry with addition of fly ash

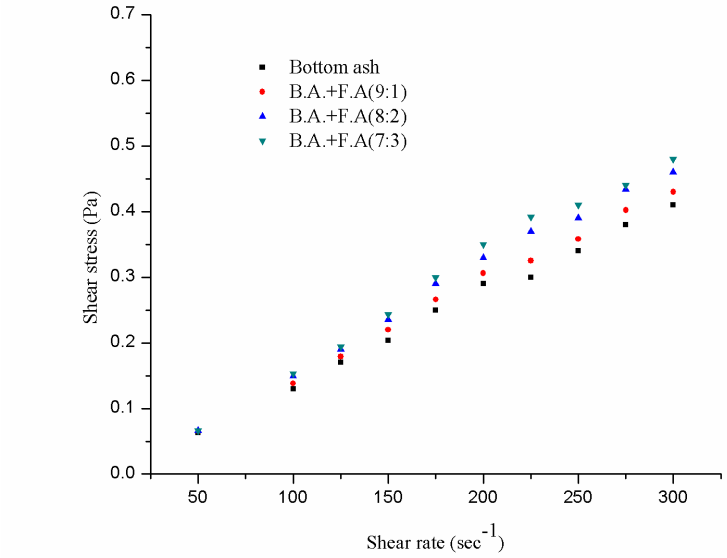

Figure 3.10: Rheogram of bottom ash with and without fly ash at concentration of 20% (by weight) in the temperature environment of 41ºC

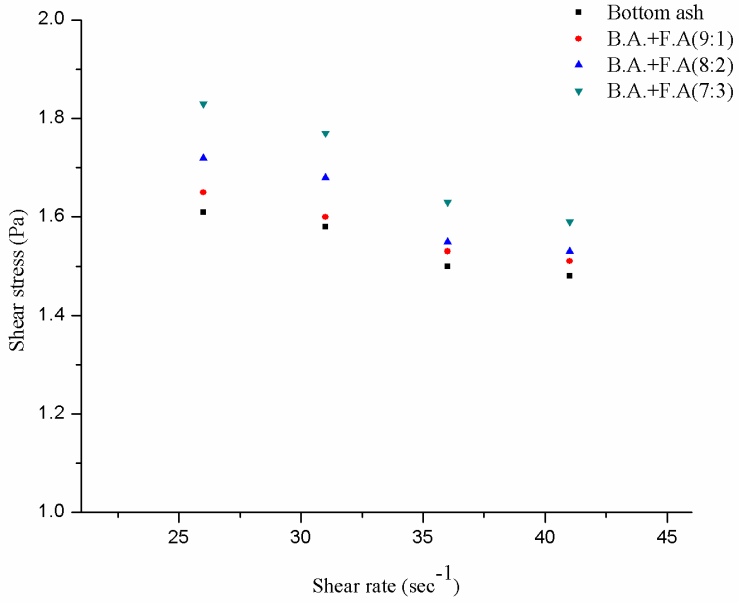

Figure 3.11: Variation of relative viscosity bottom ash slurry with temperature at concentration of 20% (by weight)

CHAPTER 4

EXPERIMENTAL PERFORMANCE OF CENTRIFUGAL SLURRY PUMP

The pump is the heart of any hydraulic conveying system. Centrifugal slurry pumps are used to transport solid particulate materials for a wide range of applications such as dredging, dewatering of open mines, and transportation of solids in mineral plants, disposal of ash in thermal power stations etc. They are popular due to consistent flow rate, low maintenance cost and excellent stability. Construction of these pumps is different as compared to the conventional pumps. The design of a centrifugal pump for slurry transportation system needs special consideration to ensure that the flow passages should offer any smooth passage of solids with minimum erosion.

The efficiency of centrifugal slurry pump is lower as compared to that of a conventional centrifugal pump because of robust impeller and nearly concentric casing design, large running clearances and relatively wide throat impeller clearance. The difference in the geometrical parameter causes more hydraulic losses and hence results in relatively poor pump performance characteristics.

The performance characteristics of centrifugal slurry pumps depend on the characteristics of the slurry when handling solid-liquid mixture. Any variation in the requirement of head and/or flow rate is generally met by changing the operating speed of the pump. The enhance requirement of the slurry pump for total head and flow rate are generally met by adjusting the pump operating speed. The change in the impeller diameter is not possible due to hard metal construction of slurry pump. Thus for design or selection of a centrifugal slurry pump, extensive experimental data is required for evaluating the deviation in the pump performance due to slurry suspension. The extensive tests need to be carried out on centrifugal slurry pump at different operating speeds for pumps handling solid-liquid suspension with different solid concentrations and particle size distribution. This chapter describes the experimental study carried out on a centrifugal slurry pump handling bottom ash slurry with and without addition of fly ash.

4.1 EXPERIMENTAL SET-UP

Figure 4.1 shows the schematic diagram of the experimental setup used for the present study to evaluate the performance of the pump with water and slurries. The photographic view of the centrifugal slurry pump with short and long test loop is shown in Figure 4.2. The long loop consists of a closed circuit pipe test loop of 50 mm NB pipe having a length of around 40m, along with the other necessary components. The short loop is generally used for performance evaluation of the pump only and slurry does not flow through the 40 m long pipeline.

The slurry for the pump performance tests was prepared in the hopper shaped mixing tank having a suitable stirring arrangement for keeping the slurry always in a well-mixed state during experimentation. The mixing tank is made of 4 mm thick stainless steel sheet. The height of the tank is 1.55 m and has a square shape at the top (1.00 m x 1.00 m). The maximum capacity of the tank is 0.76 m^3. The slurry is drawn from the mixing tank by the pumps and returned after circulation through the test loops to either the mixing tank or the measuring tank.

The flow rate is determined by monitoring the level of the slurry in the measuring tank collected over a known time interval. The return line from the measuring tank enables to empty this tank after each measurement. A stirrer, being fabricated by welding plates on 50 mm pipe which will be rotate around 50 rpm by a 3 phase induction motor using 1:30 reduction gear, for keeping the slurry always in a well-mixed state during experimentation. The plug valves are provided in the test loop and the bypass pipeline to vary the flow rate over a wide range. The nucleonic density meter provided in long test loop is used to measure the density of the slurry suspension.

For monitoring of the flow rate, pre-calibrated electro-magnetic flow meters were installed in the vertical pipe section of each test loop as shown in schematic diagram (See Figure. 4.2). The short test loop was provided with an efflux sampling tube fitted with a plug valve, in the vertical pipe section for collection of the slurry sample to monitor solid concentration. Measuring tank is placed near the mixing tank. Both tanks are provided with drain plugs. Flow deflector is provided in-between mixing and measuring tank to divert the fluid during the calibration of flow meters. The pump delivers the water or slurry back to

the tank for recirculation. Separators are installed in suction and delivery sides of centrifugal slurry pump. The purpose of a separator is to eliminate entrance of solid particles in the tube connected to pressure transmitter. The arrangement of the separator is shown in Figure 4.3.

Pressure transducers are attached to measure the suction and delivery pressures of the pump. Pressure is measured at the suction and delivery side of the pump by SMAR pressure transducer (LD 290 and LD301). Air is purged off from the pipeline and the pressure transducer before taking measurements. Pump is driven by 7.5 kW, 440 V and 14.5A variable speed induction motor (Type: 3 phase square cage). For the variation of motor speed, frequency modulator is used. The pump speeds were measured using digital electronic tachometer (Type: Digital photo type tachometer, Make: Systems Limited). The pump input power is determined by measurement of torque by using a torque transducer (T22-M, Make: M/s. HBM LTD, Germany) and speed at pump shaft. The manufacturer's specifications for centrifugal slurry pump (WILFLEY model, Make: Hindustan Dorr-Oliver Ltd. Bombay) are given in Table 4.1. The impeller of the pump was closed type having 5 blades for pump. The sectional view of the centrifugal slurry pump is shown in Figure 4.4.

4.2 INSTRUMENTATION

Different instruments are used for the measurement of various operating parameters of the pump. Instrument specifications, calibration and measurement procedure are described in the following paragraphs.

4.2.1 Flow Rate Measurement

Flow rate was measured by an electro-magnetic flow meter. A Measuring tank was used to calibrate the electro-magnetic flow meter at regular intervals.

For calibration, the flow of slurry in the test loop is diverted to the measuring tank of 0.206 m3 having a height of 0.8 m for known time interval. The level of water or slurry in the tank for a given time interval was measured using a scale having a least count of 1 mm. The least count of the stop watch was 0.01 second. Flow rate by this method could be evaluated with an accuracy of $\pm$ 0.5%. An electromagnetic flow meter (Magmaster, Make: M/s ABB

Kent Taylor Ltd., UK) was used to measure the flow rate in test loop. Before installation, both the flow meters were calibrated with water using gravimetric method. In this method, the time for a known amount of fluid passing through the meter at a given flow rate is measured accurately. By this method, the flow rate could be evaluated with an accuracy of $\pm$ 0.25% at full scale. This procedure was repeated at various flow rates over the entire range of operation of the magnetic flow meter. The calibration curve of magnetic flow meter -1 is shown in Figure 4.5. It is seen that the deviations are within $\pm$ 0.5%. The flow meter was fitted in the vertical section of the return pipeline of the loop (Figure 4.2). The calibration of the meter was also checked with slurries at selected solid concentrations using the measuring tank method.

4.2.2 Pressure Measurement

The suction and delivery pressures of the pump were measured by providing pressure taps with separation chambers at two diameters upstream and downstream of the suction and delivery flanges respectively. The separation chambers were provided to have an interface separation for slurry and manometric fluid/ pressure gauge material, water being the intermediate fluid.

These pressure transducers arebased on a capacitive principle that provides reliable operation and high performance. At suction side, LD301 smart pressure transducer was used in order to measure absolute pressure, similarly at delivery side, LD290 smart pressure transducer was used for gauge pressure measurement. The accuracy of both the transducers is± 0.75% of full scale. The pressure gauge transmitter LD290 was calibrated using dead weight pressure gauge tester. The calibration curve of the transmitter is shown in Figure 4.6.

4.2.3 Speed Measurement

Non contacting type tachometer (Manufacturer: System Pvt. Ltd, New Delhi) was used for measurement of speed having least count of 1.0 rpm. During measurement of speed, shaft surface was cleaned properly and reflector is attached at one location.The number of pulse counted through the reflector is indicated as speed of the shaft.

4.2.4 Measurement of Input Power

The input power to the pump was also measured by providing a torque transducer (T22-M, Make: M/s.HBM LTD, Germany) between the pump and the motor shafts during the test. This measures both the torque and speed of the shaft. The range of the torque transducer is 0.1 Nm to 200 Nm with the accuracy of ±0.2% and that of speed is ±1 rpm.

4.3 UNCERTAINTY IN MEASUREMENTS

All the experimental measurements involve uncertainty in spite of all care and precaution to eliminate all possible sources of error from the measurements. This error may be due to geometrical in-accuracy of the test apparatus and accuracy of measuring instruments.

The uncertainty was estimated for experimental measurements (Klein and McClintock 1953 and Holman, 1994). The procedure of the uncertainty estimation is given below:

Let F is a parameter calculated using certain measured value as,

$$F = F(x_1, x_2, x_3, ..., x_n) \tag{4.1}$$

Then uncertainty in measurement of F is given as follows:

$$\delta F = \left[\left(\frac{\partial F}{\partial x_1} \delta x_1 \right)^2 + \left(\frac{\partial F}{\partial x_2} \delta x_2 \right)^2 + \left(\frac{\partial F}{\partial x_3} \delta x_3 \right)^2 + ... + \left(\frac{\partial F}{\partial x_n} \delta x_n \right)^2 \right]^{0.5} \tag{4.2}$$

Where, $\delta x_1, \delta x_2, \delta x_3, \ldots\ldots\ldots\ldots, \delta x_n$ are the errors in measurements of parameter x_1, x_2, $x_3 \ldots x_n$, δF is absolute uncertainty ;

4.3.1 Sources of Errors

Uncertainty are involved in the measurement of various parameters like specific gravity, efflux concentration and flow velocity by electromagnetic flow meter and pressure head by pressure transducer. In view of the fact that absolute accuracy can never be achieved in any experimentation, it is essential to estimate accuracy achieved in the present experiments. The measurements accuracy is the function of resolution of the instruments. In the present case, the instruments used are the electro-magnetic flow meter, measuring jars, pressure transducers, torque analyzer and the weighing scales.

The least count of these instruments are:

(i)	Pressure transducer	±0.75% of full scale
(ii)	Electro-magnetic flow meter	±0.5% of full scale
(iii)	Measuring jars	±10ml
(iv)	Weighing Scale	±0.1mg
(v)	Efflux concentration	±1%
(vi)	Torque analyzer	±0.2% of full scale

The uncertainties in the centrifugal slurry pump head, input power and efficiency were obtained from equation 4.1 and 4.2. The uncertainty in the head, input power and efficiency were obtained as 0.9%, 0.23% and0.93% respectively.

4.4 RANGE OF PARAMETERS STUDIED

Experiments have been carried out on the centrifugal slurry pump to investigate the effect of bottom ash and mixture of fly and bottom ash slurries on the centrifugal slurry pump performance characteristics. The physical, chemical and rheological properties of the bottom ash with and without addition of fly ash have been discussed in chapter 3.

The head, power and efficiency of the pump for clear water and ash slurries have been measured at different flow rates to evaluate the head-flow rate, power- flow rate and efficiency -flow rate characteristics. These characteristics have been evaluated at four different speeds namely 1000, 1150, 1300 and 1450 rpm with clear water and bottom ash slurries with and without addition of fly ash. Experiments were conducted with bottom ash slurry at four different concentrations for each speed. Addition of fly ash in the bottom ash has been varied from 10 to 30% (by weight) Similarly, the experiments with addition of the fly ash in the bottom ash mixture in different proportional ratio namely 9:1, 8:2 and 7:3 were conducted at four concentrations in the range of 12 to 48% to determine the pump performance characteristics at all the above four speeds. The details of the range of parameters are presented in Table 4.2.

4.5 DATA ANALYSIS

The performance of the pump is determined with clear water before, as well as, after the

experiment. For this purpose, all the plug valves were first closed, and the mixing tank, separation chambers, suction and delivery pressure measurement tubes were properly filled up with water and purged off were all the air bubbles. To measure the head- flow characteristics of pump, the suction plug valve connected to the mixing tank was opened fully and the pump was run by starting the motor. The delivery plug valve was then opened and adjusted to the desired flow rate. The measurements indicated by different instruments namely pressure transducer, tachometer, torque meter and magnetic flow meter were noted. These measurements were repeated for various openings of the delivery valve to cover the entire operating range of the pump. Similar procedure was followed for pump at all four speeds namely 1000, 1150, 1300 and 1450 rpm. The pump input power is determined by measurement of torque using a torque transducer and speed at pump shaft. No variation in the pump performance with water is observed during the whole experiments.

After evaluating the performance characteristics of the pumps with water, the above procedure was repeated to evaluate the performance characteristics of the pump handling bottom ash with and without addition of fly ash up to 50% concentration (by weight). The mixtures of bottom ash and fly ash were in the ratios of 9:1, 8:2, and 7:3 respectively. The stirrer is continuously rotating for proper mixing of solid in the mixing tank.

During each test run, two efflux samples were collected to monitor the solid concentration and to analyze the particle size distribution in order to establish the extent of attrition of solid particles during the tests. The specific gravity of the slurry is calculated from the weight and volume of the efflux samples collected. The data collected in each test was analysed to determine the pump performance. The calculation of solid concentration, total head developed, shaft power, pump efficiency, head ratio, efficiency ratio and power ratio equations are given below:

$$H = \left(\frac{P_D}{\rho g} + Z_d\right) - \left(-\frac{p_S}{\rho g} + Z_s\right) + \frac{V_d^2}{2g} - \frac{V_s^2}{2g} \tag{4.3}$$

4.5.1 Data Reduction

Affinity laws are a set of three non-dimensional parameters which enable to determine the performance of the pump at a fixed speed (i.e. rated speed of 1450 rpm) from the results obtained at test speed (N). The head discharge and power is to be determined as below:

$$H_{1450rpm}=H_N\times\frac{1450^2}{N^2} \quad (4.4)$$

$$Q_{1450rpm}=Q_N\times\frac{1450}{N} \quad (4.5)$$

$$P_{1450rpm}=P_N\times\frac{1450^3}{N^3} \quad (4.6)$$

Measurement of Slurry Concentration (C_W)

$$C_w=\frac{\rho_s(\rho_m-\rho_l)}{\rho_m(\rho_s-\rho_l)} \quad (4.7)$$

Power Output

$$P_{out}=\rho gQH \quad (4.8)$$

Power input

$$P_{in}=T\times\acute{\omega}=2\pi NT/60 \quad (4.9)$$

Efficiency of Pump

$$\eta_{pump}=\frac{P_{out}}{P_{in}}\times 100 \quad (4.10)$$

The additional parameters required in equations 4.3 to 4.9 were evaluated as follows:

- The slurry suspension specific gravity was determined by the weight and volume of the efflux samples.
- The velocity of flow in the suction and delivery lines was calculated from the knowledge of the flow rate and pipe diameter.
- The total head of the pump was determined from the suction head, delivery head, velocity head and potential head.
- The pump input power was obtained from the torque and operating speed.

Typical data test sheet of the pump performance is given in Table 4.3.

4.6 RESULTS AND DISCUSSION

The performance characteristics of the centrifugal slurry pump have been evaluated experimentally with water and bottom ash slurries with and without addition of fly ash. The experimental result has been analysed extensively to investigate the effect of solid concentration, operating speed and addition of fly ash in the bottom ash slurry on the performance characteristics of centrifugal slurry pumps.

4.6.1 Performance Characteristics of Pump at Rated Speed

The performance characteristics of the centrifugal slurry pump have been evaluated experimentally for handling bottom ash slurries with and without addition of fly ash. The performance characteristics of the slurry pump with water at speed 1450 rpm is given in Table 4.3. The performance data at the different speed 1000, 1150 and 1300 rpm with water are tabulated in Table 4.4. The experimental performance of centrifugal slurry pump with water and different combinations of bottom and fly ash mixtures at the operating speed of 1450 rpm are presented in Figures 4.7–4.10 and given in Tables 4.5 -4.8.

From Figure 4.7(a), it is seen that the maximum head developed by the pump is 18.90 m (at 3.10 lps) and the maximum efficiency attained is 45.25% (at 13.20 lps). The head-flow rate characteristics presented in Figure 4.7(a), do not indicate any cavitation inception at high discharge rates. A gradually dropping nature of the curve from the shut-off head also shows that there is no unstable region of operation close to the shut-off conditions.

Figure 4.7(b) shows that the pump input power for water increases steadily with increase in flow rate and its maximum value is 5.22 kW at 14.05 lps flow rate (Table 4.3). The pump efficiency characteristic with water, shown in Figure 4.7(c), depicts that all the data points lie on a smooth curve and the maximum efficiency is 45.25% identified as BEP of the pump (Table 4.3). At the BEP, the head, the discharge rate and input power to the pump are 16.80 meter of water column, 13.20 lps and 4.83 kW respectively (Table 4.3).

The performance characteristics of the centrifugal slurry pump were evaluated with bottom ash by preparing the slurry in the mixing tank. The bottom ash slurry concentration was varied from 14 % to 44.3 % (by weight). The head, flow rate, input power and efficiency of the pump were measured at each concentration of bottom ash slurry. These experimental

data are given in Table 4.5 and are presented graphically in Figure. 4.7(a)-(c). The head-flow rate curves for bottom ash slurries shown in Figure 4.7(a) shows the dropping nature similar to water data. The total head developed decreases with increase in concentration of the bottom ash slurry.The total head developed at BEP reduces with increase in concentration (by weight) from 14% to 44.30% with the maximum drop of 1.28 m of water column.

From the Figure 4.7(b), it is observed that the pump input power increases with increase in the flow rate at all concentrations. The input power also increases monotonically with increases in the concentration of bottom ash. With further increase in solid concentration, the input power increases at a rate that is lower compared to the rate of increase of mixture specific gravity. At concentration (C_w) of 44.30%, the specific gravity of the mixture is increased by33% relative to water whereas the increase in the input power relative to water performance is around 14.16% at BEP (See Table 4.5). This implies that the increase in pump power required for handling bottom ash slurries at any concentrations does not increase in the same proportion as the increase in specific gravity of the mixture. At BEP, it is seen that input power increases by 8.24% with increase in concentration by weight from 14% to 44.30 %.

From the Figure 4.7(c), it is seen that the efficiency of the pump decreases with increase in the solid concentration. Similar observations have also been reported by (Gahlot et al. 1992 and Gandhi et al. 2001 and 2002) for nearly similar type of solid materials.

4.6.2 The Effect of Addition of Fly Ash with Bottom Ash on Performance of the Slurry Pump

The pump performance is evaluated with addition of fly ash in the bottom ash slurry in the ratio of 9:1, 8:2 and 7:3 respectively. It is seen that particle size distribution of the fly ash and bottom ash shows that the biggest particle size of fly ash is 355 μm and 69% particles are finer than 75μm. The biggest particle size of bottom ash was 2000μm and only 3% particles were finer than 75μm. The weighted mean particle diameter for fly ash was nearly one third of that of the bottom ash (Table 3.2). This shows that the bottom ash is coarse without significant amount of fine particles whereas fly ash is a fine particulate material (See Figure 3.3).

The head –flow rate characteristics observed with all mixtures of the fly and bottom ash slurries follow similar trends as that of the bottom ash slurry and are shown in Figures 4.8-4.10. The head developed reduces with increase in concentration at any given flow rate for all concentrations. At the BEP, the drop of the head observed is 2.04 m for bottom ash slurry, 1.95 m for mixture of bottom ash and fly ash in the ratio of 9:1, 1.82 m for mixture ratio of 8:2 and 1.80 m for mixture ratio of 7:3.

This observation shows that with addition of the fly ash in the bottom ash mixture, the pump head drop reduces approximate 0.09 m for mixture of bottom ash and fly ash in the ratio of 9:1, 0.22 m for mixture ratio of 8:2 and 0.24m for mixture ratio of 7:3 at BEP. These data shows that maximum pressure drops in the pump reduces for the mixture of bottom ash and fly ash in the ratio of 8:2. The pump performance reduces very marginal for the mixture of bottom ash and fly ash in the ratio of 7:3.

The similar nature of variation of input power with flow rate was observed at all concentrations of the bottom ash mixture with fly ash. All data show that the input power increases linearly with the flow rate at all the concentrations. The input power also increases with increase in the concentration of bottom ash and fly ash mixture. At BEP, the increase in input power is observed as 14.16%, 13.45%, 11.96% and 11.81% with bottom ash slurry, and bottom and fly ash in the mixture ratio of 9:1, 8:2 and 7:3 respectively.

The efficiency of the pump improves with addition of the fly ash in the bottom ash slurry. These data show that the maximum input power decreases for the mixture of bottom ash and fly ash in the ratio of 8:2 as compared to that of the ratio 9:1 and 7:3. It is also observed that with addition of the fly ash in the bottom ash, pump efficiency also increases. This phenomenon can be explained from the particle motion of the solids in the slurry. The bottom ash slurry settled rapidly due to coarser particles and head loss is more due to the extra energy required to keep coarser particles in motion.

The mixing of the finer particles of fly ash in the coarse particulate bottom ash slurry help to suspend the larger particles of the bottom ash and hence the energy spent is lower which result to improve the developed pump head. As developed head increases and input power decreases, it may results in the lower power consumption for the transportation of the bottom ash in pipelines. But more mixing of the finer particles of fly

ash in the bottom coarse particulate in the ratio of 7:3 the frictional losses in the pump increases so that head drop with the bottom and fly ash ratio of 7:3 is marginal.

4.6.3 Variation of Head Ratio and Power Ratio

The variation in head ratio (HR) of bottom ash slurry with and without fly ash is shown in Figure 4.11 and given in Table 4.9. It is observed that the HR decreases with the increase in the concentration of the slurry for all the bottom ash slurry with and without fly ash. For both types of slurries with and without addition of fly ash, head ratio is not the function of the flow rate. Similar observations have been reported by Gandhi et al. (2001) and Chandel et al. (2011).

It is also seen that the values of HR for bottom ash slurry decreases more rapidly with concentration up to 10-15% (by weight). The decrease HR is lower with increase in fly ash in the bottom ash. Further increase in the solid concentration shows comparatively lower decrease in HR as compared to initial rate of change. The trend is similar for bottom ash and mixture of fly ash and bottom ash in different proportions.

The bottom ash slurry is coarse and have very small amount of fine particles (See Table 3.2) to provide support to the larger particles for suspension at low velocities. Therefore, the head loss for coarse slurry is greater as higher energy is required to push the coarse slurry across the pump. With addition of fly ash in the bottom ash slurry the presence of finer particles of fly ash provides the support to the coarse particles of bottom ash and hence additional losses decreases as the addition of the fly ash increases in the bottom ash slurry. Thus HR value increases with the addition of fly ash in the bottom ash.

The variation of HR with solid concentration for all the cases with and without addition of fly ash does not show an exact linear variation with solid concentration but depends on particle size distribution, rheological behavior of the mixture and the percentage of finer particles present with the coarser particles. The comparison of the trends of variation of head ratio of bottom ash slurries with and without addition of fly ash shows that the value of head ratio varies between 0.87–1.0 for all the concentrations tested.

Figure 4.12 shows the variation of PR for pump with solid concentrations of the bottom ash slurry with and without addition of fly ash. The PR increases with increase in solid concentration. However the increase in the PR is not equals to the increase in the

specific gravity of the mixture. The efficiency ratio of the bottom ash slurry with and without the ash varies in the range of 0.92-1 for all the concentrations (See Table 4.9). This shows that the values of ER are always lower than 0-5.0% of the corresponding HR values for all the mixtures of the bottom and fly ash slurry. This phenomenon has also been observed by Gahlot et al. (1992) and Gandhi et al. (2001). Gahlot et al. (1992) evaluated the HR and PR value with the coal water slurry and zinc tailing slurry whereas Gandhi et al. (2001) evaluated the performance with slurries of bottom ash, fly ash and zinc tailing.

4.6.4The Effect of Speed on the Performance of Pump

The performance of pump has been evaluated at different speeds namely 1000 ,1150 ,1300 and 1450 rpm for bottom ash slurry with and without addition of fly ash to study the effect of speed on the pump performance. The performance characteristics of slurry pump with water at operating speeds of 1000, 1150, 1300 and 1450 rpm are given in Tables 4.4. Figures 4.13 - 4.24, show the performance characteristics of the centrifugal slurry pump of bottom ash slurry with and without addition of fly ash at different operating speed 1000, 1150, 1300 and 1450 rpm.

From the head-flow rate characteristics with water, it is seen that the maximum head developed by the pump is measured near shut-off condition as 18.90, 15.34, 12.68 and 9.66m at the operating speed of 1450, 1300, 1150 and 1000 rpm respectively. All the head flow rate curve show nearly similar nature. These curves also do not indicate any sign of cavitation inception or unstable region of operation in the complete operating range. The input power curves at different speeds (Figures 4.7b, 4.13b, 4.17b and 4.21b) also appear to follow nearly similar nature. Lower input power values are seen at lower speed and higher input power values for higher speed at all flow rates (Figures 4.21b and 4.7b). The maximum input power to the pump was measured as 5.22 kW (14.05 lps), 3.80 k W (13.40lps), 3.05 k W (13.05lps) and 1.99 kW (12.46 lps) at the speed of 1450, 1300, 1150 and 1000 rpm respectively.

The efficiency curve at different pump speeds with water passes through all the data points (Figures 4.7c, 4.13c, 4.17c and 4.21c) and appear to be nearly similar. It is seen that the maximum efficiency attained by the pump is 41.37% at 1000 rpm and corresponding values of the head and flow rate are 7.37 m and 10.59 lps respectively (Table 4.4). At the speed 1150 rpm, the maximum efficiency attained is 42.31% (11.33 lps) and corresponding value of head

as 10.97m, responding (Table 4.4). Similar at the speed 1300rpm, the maximum efficiency and corresponding values of the head measured as 43.75% (11.79 lps) and 12.84m (Table 4.4) respectively. At the 1450 rpm, the maximum efficiency attained is 45.25 %(13.2 lps) is 45.25% and corresponding values of head is 16.80 m (Table 4.4).

The observations show that the maximum efficiency of the pump increases with increase in pump speed and is in line with the findings on conventional pumps reported in literature Gandhi et al. (2001). For the conventional pumps, the frictional losses decrease with increase in pump Reynolds number which incidentally increases with increase in pump speed. Results on the centrifugal slurry pump also show similar trends i.e. higher pump efficiency at 1450 rpm compared to that for 1000, 1150 or 1300 rpm.

The experimental data on the performance of the pump with bottom ash slurry are given in Tables 4.5,4.10, 4.14 and 4.18 and presented graphically in Figures 4.7, 4.13, 4.17 and 4.21 for speed of 1450,1300,1150 and 1000 rpm respectively. The variation in head, power and efficiency with solid concentrations at all four speeds shows the similar trend with minor deviations.

The drop in head is less at 1000 rpm and is only 1.19 m at BEP for 43.0% concentration by weight (Figure 4.21) while it is 2.05 m at BEP for 44.3% concentration by weight at 1450 rpm (Figure 4.7). At 1150 rpm, the decrease in head is 1.48m at BEP for 45.0% concentration by weight (Figure 4.17). At BEP, pump head is reduced by 1.63 m for 43.0% concentration (by weight) for 1300 rpm (Figure 4.13).

The input power curves at all the speeds (Figure. 4.7b, 4.13b, 4.17b and 4.21b) also appear to be nearly similar in nature. Lower input power values are seen at lower speed and higher input power values for higher speed at all flow rates (Figures. 4.7b and 4.21b). The maximum input power to the pump at 1450 rpm was measured as 5.27 kW(14.05 lps) and at 1000 rpm, it was measured as 3.05 kW(11.70 lps). At the speed of 1150 and 1300 rpm, the maximum input power of the pump were measured as 3.53 kW(12.85 lps) and 4.08 kW(12.21 lps) respectively. The efficiency curve at all the operating speeds with water pass through all the data points (Figures 4.7, 4.13, 4.17 and 4.21)and appear to be nearly similar.

To further understand the effect of speed on the performance of the centrifugal slurry pump for water and slurries, the non-dimensional parameters namely specific head, specific flow rate and specific power defined for conventional pumps (affinity laws) were evaluated.

These are presented graphically in Figure 4.25 - 4.28. Figure 4.25 shows the variation in specific head with specific flow rate at all the four speeds namely1450, 1300, 1150 and 1000 rpm with water. The trend of the specific head decreases with increase in specific flow rate at all the operating speeds.

It is also seen that there is not much variation in these curves at the all four speeds. The maximum deviations in the specific head observed at all four speed at any given specific flow rate is within $\pm$ 4.5 %. Hence, one can say that the relationships for non-dimensional head and flow rate under affinity laws for conventional pumps are valid even for slurry pumps despite constructional differences. Similar variation has also been reported by (Gandhi et al. 2002**)**.

Fig 4.26 shows the variation in specific input power with specific flow rate at all the four speeds namely1450, 1300, 1150 and 1000 rpm with water.The specific power increases linearly with the specific flow rate at all the operating speeds.

The specific power at any specific flow rate decreases with increase in speed, the decrease being nearly equal from 1000 to 1150 rpm, 1150 to 1300 rpm and then from 1300 to 1450 rpm at all specific flow rate. This could be attributed to increase in frictional losses with reduction in pump Reynolds number with pump speed as explained earlier. The specific power decreases by nearly 9% for 13 % increase in pump speed viz. from 1000 rpm to 1450 rpm. The above observation shows that the affinity laws relationship for pump input power for slurry pumps is not exactly applicable and depends on the speed. However due to small variation in specific power, it is still feasible to use the relationship for narrow variation in pump speeds (Fairbank 1942; Maz 1984; Kazim et al. 1997; and Gandhi et al. 2002)

The non-dimensional head- flow rate characteristics of the slurry pump with bottom ash slurry at different concentrations are shown in Figure 4.27 (a) - (d). Each Figure depicts the variation in specific head for four speeds at nearly equal values of solid concentration. The specific head developed decreases with increase in pump speed for nearly equal values of concentrations. Further increase in concentration shows a decrease in specific head at all speeds. This is due to increase in hydraulic losses with increase in solid concentration at all flow rates. It is also seen that increase in solid concentration increases the deviations in specific head characteristics observed at different speeds. The deviations are within $\pm$ 5% up to solid concentration of 22% (by weight) and are 8% or higher at higher concentrations. This

observation suggests that the affinity laws can be used to derive specific head relationship at various speeds for slurry pump handling concentrate slurry with significant errors.

Figure 4.28(a) - (d) shows the specific power- flow rate characteristics of the pump for bottom ash slurries at different speeds for nearly equal values of solid concentration. From the Figure 4.28(a) - (d), it is seen that the deviations in specific power characteristics with speed, increase with increase in concentration. This could be attributed to smaller increase in power ratio compared to the increase in specific gravity of the mixture for higher concentrations. It is seen that the deviations are almost equal for all the solid concentration values and are in the approximate same range as observed with water. Hence, the relationship for specific power is also not exactly applicable to this pump handling bottom ash slurries at all solid concentrations and depends on pump speed.

Similar measurements were repeated at speed of 1000, 1150, 1300 and 1450 rpm for bottom ash and fly ash mixture in the ratio of 9:1, 8:2 and 7:3 respectively. The head, power and efficiency characteristics of the pump at speeds of 1000, 1150 and 1300 rpm depict the similar trend of variation as seen for 1450 rpm for the same slurry and the variation in magnitude is observed. At BEP of 1450 rpm, the drop of the head reduced by 0.10 m for the mixture ratio of 9:1, 0.28 m for the mixture ratio of 8:2 and 0.32 for the mixture ratio of 7:3. At the speed of 1300 rpm, pump head drop at BEP reduces approximate 0.08 m for mixture of bottom ash and fly ash in the ratio of 9:1, 0.22 m for mixture of bottom ash and fly ash in the ratio of 8:2 and 0.26 m for mixture of bottom ash and fly ash in the ratio of 7:3.

At the speed of 1150 rpm, pump head drop at BEP reduces approximate 0.07 m for mixture of bottom ash and fly ash of ratio of 9:1, 0.24 m for mixture of bottom ash and fly ash of ratio of 8:2 and 0.28 m for mixture of bottom ash and fly ash of ratio of 7:3. At the speed 1000 rpm, the pump head drop at BEP reduces approximate 0.05 m for mixture of bottom ash and fly ash of ratio of 9:1, 0.13 m for mixture of bottom ash and fly ash of ratio of 8:2 and 0.16 m for mixture of bottom ash and fly ash of ratio of 7:3.

These data also shows that the maximum pressure drop in the pump reduces for the mixture of bottom ash and fly ash of ratio of 8:2 at all speeds. The results for the pump performance at different speeds of 1000, 1150, 1300 and 1450 rpm for bottom ash with and without addition of fly ash show that the pump head drop and efficiency is the function of

slurry properties and solid concentration. The head and efficiency of the pump also affects with operating speed at any solid concentration.

From the present experimental investigations on the pump characteristics for bottom ash slurry with and without addition of the fly ash at different speeds, following observations are made:

- The head and efficiency of the pump decreases with increase in solid concentration, whereas input power to the pump increases with increase in the concentration of solid.
- The pump input power is not directly proportional to the specific gravity of slurry.
- The relationship for specific head under the affinity laws is valid for centrifugal slurry pumps with water whereas the specific power relationship for significant change in pump speed needs to be corrected for the speed.
- The specific head relationship in the affinity laws may be applicable for slurry pump at concentrations less than 22% for bottom ash slurry. For higher concentrations this law is not applicable.
- The presence of the finer particles of the fly ash in the coarse particulate bottom ash slurry improves the performance characteristics of the centrifugal slurry pump.
- The head ratio decreases with the increase in the concentration of the slurry for all the bottom ash slurries with and without fly ash. For both type of slurry, with and without addition of fly ash, head ratio is not a function of the flow rate.

Table 4.1: Geometrical details of centrifugal slurry pump

Specification	
(a) Impeller	
Type	Closed
Material	Ni-hard
Number of blade	5
Impeller eye diameter(mm)	110
Impeller outlet diameter(mm)	265
Impeller width at eye(mm)	44.2
Impeller inlet vane angle(degree)	23
Impeller outlet vane angle(degree)	25
Impeller width at outlet(mm)	68.59
Blade thickness(mm)	22.40
(b) Casing	
Type	Single volute
Material	Ni-hard
Base volute diameter (mm)	275
Volute width(mm)	85
(c) Inlet passage diameter(mm)	100
(d) Out let passage diameter(mm)	50
Operating speed(rpm)	1450
Non-dimensional Specific speed	0.06957
Minimum Rated speed (rpm)	1450
Best efficiency point head (mwc)	15.1
Rated discharge (lps)	15.1
Maximum efficiency (%)	46%
Pump input power (kW)	4.86

Table 4.2: Range of parameters for centrifugal slurry pump performance

Slurry	Concentration range (% by weight)	Characteristics evaluated	Speed range (rpm)
Bottom ash	13.0 - 45 (4 concentrations)	Complete head-flow rate and efficiency-flow rate characteristics	1000-1450
B.A+FA(9:1)	12 - 45 (4 concentrations)	Complete head- flow rate and efficiency- flow rate characteristics	1000-1450
B.A+FA(8:2)	12.0 - 45.0 (4 concentrations)	Complete head- flow rate and efficiency- flow rate characteristics	1000-1450
B.A+FA(7:3)	12.0 - 48.0 (4 concentrations)	Complete head- flow rate and efficiency- flow rate characteristics	1000-1450

Table 4.3: Data sheet of performance of the centrifugal slurry pump with water at 1450 rpm speed

Slurry density -1000 kg/m^3 slurry temperature-26 °C

Sr. No	Flow Rate ,(lps)	Suction pressure (m of water column) Absolute	Delivery pressure (kg/m^2) Gauge	velocity at inlet ,v_s (m/s)	velocity at outlet, v_d, (m/s)	Velocity head at inlet pipe,$Vs^2/2g$ (m of water column)	Velocity head at outlet pipe, $V_d^2/2g$ (m of water column)	head (m of water column)	Torque (N-m)	Input Power (kW)	Pump Efficiency (%)
1.	14.05	10.36	1.50	1.66	7.28	0.14	2.70	16.15	31.58	5.22	43.33
2.	13.20	10.46	1.55	1.56	6.82	0.12	2.37	16.80	30.95	4.83	45.25
3.	11.00	10.59	1.67	1.34	5.96	0.09	1.77	17.38	30.37	4.61	41.03
2.	9.30	10.73	1.70	1.13	5.62	0.09	1.71	17.56	29.86	4.26	39.28
4.	8.00	11.51	1.99	1.08	4.81	0.06	1.12	18.04	26.32	4.10	33.95
5.	6.00	11.80	2.01	0.93	4.04	0.04	0.82	18.30	23.69	3.66	28.43
6.	4.70	11.92	2.07	0.70	3.06	0.02	0.47	18.70	21.90	3.54	22.45
7.	3.10	11.96	2.18	0.55	2.39	0.02	0.29	18.90	20.73	3.23	15.90

Table 4.4: Performance of the pump with water at different speed

Speed 1450 rpm						
Flow rate (lps)	**Head (m)**	**Input Power(kW)**	**Efficiency (%)**	**HR**	**PR**	**ER**
14.05	16.15	5.22	43.33	1.00	1.00	1.00
13.20	16.80	4.83	45.25	1.00	1.00	1.00
11.00	17.38	4.61	41.03	1.00	1.00	1.00
9.50	17.56	4.26	39.28	1.00	1.00	1.00
7.95	18.04	4.10	33.95	1.00	1.00	1.00
6.20	18.30	3.66	28.43	1.00	1.00	1.00
4.80	18.70	3.54	22.45	1.00	1.00	1.00
3.10	18.90	3.23	15.90	1.00	1.00	1.00
Speed 1300 rpm						
13.42	12.14	3.80	38.22	1.00	1.00	1.00
11.79	12.84	3.45	43.75	1.00	1.00	1.00
9.91	13.27	3.13	40.30	1.00	1.00	1.00
8.20	13.63	3.01	38.93	1.00	1.00	1.00
7.75	14.08	2.73	34.64	1.00	1.00	1.00
6.00	14.40	2.62	30.43	1.00	1.00	1.00
4.23	14.81	2.42	24.98	1.00	1.00	1.00
2.92	15.34	2.20	20.20	1.00	1.00	1.00
Speed 1150 rpm						
13.02	10.45	3.05	40.77	1.00	1.00	1.00
11.33	10.97	2.90	42.31	1.00	1.00	1.00
10.20	11.25	2.62	40.40	1.00	1.00	1.00
8.13	11.66	2.49	38.60	1.00	1.00	1.00
6.43	11.92	2.21	34.10	1.00	1.00	1.00
5.24	12.13	2.01	29.40	1.00	1.00	1.00
4.15	12.47	1.89	25.10	1.00	1.00	1.00
2.91	12.68	1.80	18.10	1.00	1.00	1.00
Speed 1000 rpm						
12.46	6.81	1.99	40.79	1.00	1.00	1.00
10.59	7.37	1.85	41.37	1.00	1.00	1.00
8.66	8.11	1.74	39.56	1.00	1.00	1.00
6.74	8.58	1.69	33.54	1.00	1.00	1.00
4.45	8.91	1.57	24.75	1.00	1.00	1.00
3.50	9.19	1.52	20.73	1.00	1.00	1.00
2.15	9.66	1.39	14.64	1.00	1.00	1.00

Table 4.5: Performance of the pump at 1450 rpm with bottom ash slurry

Concentration 14.0% (S =1.08)						
14.10	15.31	5.32	40.50	0.91	0.99	0.93
12.50	15.82	5.04	43.05	0.91	0.99	0.94
10.60	16.53	4.69	38.06	0.92	1.00	0.96
9.10	16.70	4.54	36.71	0.92	1.00	0.94
7.80	17.09	4.29	32.31	0.93	1.01	0.94
5.90	17.45	3.97	25.45	0.93	1.01	0.93
4.60	17.51	3.73	20.83	0.94	1.02	0.95
3.30	17.96	3.53	14.89	0.95	1.03	0.97
Concentration 22.0% (S =1.14)						
14.00	14.76	5.43	40.60	0.90	1.03	0.94
13.40	15.32	5.37	41.10	0.90	1.04	0.95
10.80	16.01	4.99	40.23	0.91	1.05	0.93
9.50	16.18	4.68	39.16	0.91	1.06	0.92
8.00	16.50	4.47	35.52	0.92	1.07	0.94
7.20	16.96	4.28	30.35	0.92	1.07	0.94
5.40	17.21	3.99	23.70	0.93	1.08	0.95
4.10	17.48	3.85	20.08	0.94	1.09	0.95
2.80	17.70	3.62	16.92	0.93	1.09	0.95
Concentration 32.0% (S=1.22)						
14.00	14.55	5.60	39.58	0.89	1.06	0.93
13.20	15.05	5.48	40.27	0.89	1.07	0.93
11.30	15.46	5.10	38.90	0.89	1.08	0.95
9.10	16.06	4.77	36.50	0.89	1.09	0.94
7.70	16.29	4.54	33.80	0.90	1.10	0.96
5.90	16.76	4.26	28.40	0.90	1.11	0.96
4.80	16.97	4.04	21.54	0.91	1.13	0.97
2.80	17.33	3.83	15.29	0.91	1.18	0.94
Concentration 44.3% (S =1.33)						
13.90	14.55	5.66	38.90	0.87	1.14	0.93
11.50	15.16	5.30	38.90	0.87	1.17	0.95
9.20	15.58	4.98	30.87	0.88	1.18	0.95
8.05	15.90	4.69	31.76	0.88	1.19	0.93
7.10	16.14	4.41	26.24	0.89	1.23	0.92
5.25	16.53	4.28	21.70	0.89	1.24	0.94
3.60	16.85	4.08	19.80	0.89	1.26	0.92
2.40	16.90	3.88	15.60	0.91	1.27	0.94

Table 4.6:Performance of the pump at 1450 rpm with bottom and fly ash mixture (9:1)

Concentration 13% (S=1.07)						
14.15	15.23	5.31	40.92	0.92	1.01	0.94
12.50	15.73	5.13	43.17	0.93	1.01	0.93
11.20	16.44	4.83	38.58	0.92	0.99	0.95
10.00	16.60	4.58	36.93	0.93	1.01	0.93
9.00	17.00	4.45	32.60	0.94	1.03	0.94
6.50	17.36	4.05	25.71	0.93	1.04	0.94
5.10	17.60	3.81	20.95	0.94	1.06	0.96
3.30	18.41	3.55	15.65	0.95	1.04	0.95
Concentration 19% (S =1.12)						
13.90	14.84	5.41	40.94	0.90	1.01	0.94
13.50	15.40	5.35	41.40	0.91	1.04	0.95
10.90	16.10	4.97	40.70	0.90	1.04	0.92
9.50	16.26	4.67	39.42	0.91	1.05	0.94
7.30	16.59	4.45	32.85	0.91	1.07	0.93
5.90	17.10	4.26	26.79	0.92	1.05	0.94
4.60	17.29	3.97	22.85	0.92	1.08	0.94
2.70	17.57	3.84	17.87	0.93	1.08	0.95
Concentration 31% (S=1.19)						
14.10	14.63	5.58	39.58	0.91	1.04	0.93
13.36	15.07	5.46	40.27	0.90	1.06	0.93
10.50	15.54	5.09	38.90	0.90	1.08	0.93
9.30	16.08	4.84	36.50	0.92	1.10	0.95
6.00	16.36	4.43	29.58	0.92	1.10	0.93
5.10	16.85	4.25	23.40	0.92	1.12	0.94
3.50	17.08	4.02	20.54	0.93	1.18	0.95
Concentration 40.5 % (S=1.28)						
14.00	14.44	5.60	39.10	0.88	1.15	0.93
13.40	14.71	5.53	40.20	0.89	1.16	0.94
11.30	15.23	5.30	39.20	0.89	1.17	0.95
9.90	15.64	5.05	31.57	0.90	1.19	0.94
7.20	15.98	4.73	28.87	0.91	1.19	0.94
5.10	16.21	4.40	27.50	0.90	1.21	0.95
3.90	16.62	4.26	22.90	0.91	1.22	0.93

Table 4.7: Performance of the pump at 1450 rpm with bottom ash and fly ash mixture(8:2)

Concentration 15% (S =1.08)						
14.32	15.32	5.31	40.56	0.92	1.01	0.93
13.34	15.79	5.13	42.70	0.93	1.01	0.94
10.81	16.49	4.79	38.54	0.94	1.02	0.92
9.30	16.70	4.55	35.76	0.95	1.03	0.94
6.64	17.25	4.24	31.16	0.95	1.06	0.93
5.10	17.64	4.04	23.89	0.95	1.04	0.97
4.60	17.87	3.82	20.67	0.96	1.07	0.95
2.90	18.27	3.54	15.46	0.95	1.07	0.96
Concentration 21% (S =1.13)						
13.56	15.41	5.42	40.87	0.93	1.03	0.94
11.00	16.09	4.96	39.98	0.92	1.03	0.92
9.10	16.30	4.66	36.68	0.94	1.04	0.93
7.91	16.65	4.46	32.50	0.95	1.06	0.95
5.70	17.20	4.25	28.94	0.94	1.04	0.94
4.45	17.38	3.98	23.81	0.93	1.08	0.94
2.71	17.60	3.83	14.87	0.93	1.08	0.95
Concentration 29% (S =1.185)						
13.41	15.10	5.50	39.08	0.91	1.06	0.93
11.26	15.67	5.16	38.70	0.92	1.06	0.91
9.15	16.00	4.87	35.96	0.91	1.09	0.93
8.00	16.28	4.65	33.56	0.93	1.11	0.92
5.63	16.66	4.32	29.80	0.92	1.13	0.93
4.23	16.95	4.20	22.48	0.93	1.15	0.94
2.71	17.10	3.92	16.26	0.93	1.16	0.94
Concentration 42.0% (S=1.29)						
14.20	14.66	5.58	39.67	0.90	1.13	0.91
13.60	14.98	5.50	38.89	0.89	1.12	0.92
10.81	15.38	5.24	38.20	0.91	1.16	0.93
8.91	15.78	5.00	31.70	0.90	1.18	0.93
7.42	15.99	4.73	27.87	0.91	1.19	0.92
5.33	16.28	4.40	23.53	0.93	1.21	0.93
4.31	16.63	4.27	22.50	0.92	1.23	0.93
3.00	16.80	4.05	15.38	0.93	1.22	0.94

Table 4.8:Performance of the pump at 1450 rpm with bottom ash and fly ash mixture (7:3)

Concentration 13.5 % (S=1.07)						
14.21	15.35	5.35	40.20	0.94	1.01	0.93
13.40	15.85	5.19	41.75	0.95	1.01	0.94
10.90	16.54	4.80	38.06	0.95	1.01	0.94
9.20	16.74	4.56	33.71	0.94	1.02	0.94
6.80	17.29	4.25	30.10	0.95	1.03	0.94
5.00	17.70	3.92	24.60	0.95	1.03	0.95
3.80	17.90	3.77	20.63	0.96	1.05	0.96
2.60	18.34	3.50	14.49	0.94	1.09	0.95
Concentration 23% (S =1.135)						
13.51	15.45	5.43	39.81	0.93	1.02	0.92
11.00	16.11	4.97	38.58	0.94	1.02	0.93
9.11	16.33	4.68	35.28	0.93	1.04	0.93
7.90	16.68	4.48	31.57	0.95	1.04	0.93
5.70	17.22	4.26	28.53	0.94	1.06	0.93
4.41	17.40	3.98	23.88	0.94	1.05	0.93
2.70	17.64	3.82	14.94	0.93	1.06	0.93
Concentration 32% (S =1.20)						
13.40	15.12	5.51	39.50	0.91	1.04	0.93
11.26	15.71	5.15	38.73	0.93	1.05	0.93
9.14	16.10	4.86	34.49	0.91	1.06	0.94
8.00	16.34	4.65	31.56	0.93	1.08	0.92
5.62	16.70	4.33	27.20	0.94	1.10	0.94
4.20	16.99	4.20	22.80	0.93	1.11	0.92
2.71	17.16	3.93	13.63	0.93	1.15	0.93
Concentration 39.0% (S =1.28)						
14.15	14.70	5.60	39.69	0.90	1.11	0.92
13.62	15.00	5.49	38.81	0.90	1.13	0.94
10.70	15.42	5.24	36.65	0.91	1.14	0.93
9.00	15.82	5.00	31.75	0.90	1.16	0.94
7.60	16.04	4.75	27.89	0.90	1.18	0.95
5.52	16.31	4.41	23.58	0.92	1.15	0.92
4.20	16.66	4.28	22.50	0.92	1.14	0.93
2.64	16.85	4.06	13.38	0.93	1.16	0.94

Table 4.9: Variation of head ratio, power ratio and efficiency ratio with solid concentration of bottom ash slurry with and without addition of fly ash at B.E.P at 1450 rpm

Bottom ash				**Bottom ash+Fly ash (8:2)**			
Concentration	Head ratio	Power ratio	Efficiency ratio	Concentration	Head ratio	Power ratio	Efficiency ratio
0	1	1	1	0	1	1	1
14	0.91	1.01	0.93	15	0.93	1.01	0.94
22	0.90	1.05	0.94	21	0.92	1.03	0.92
32	0.89	1.08	0.93	29	0.92	1.06	0.91
44	0.87	1.16	0.94	42	0.89	1.14	0.92
Bottom ash+Fly ash (9:1)				**Bottom ash+Fly ash (7:3)**			
13	0.92	1.01	0.93	13.5	0.95	1.01	0.93
19	0.915	1.04	0.95	23	0.94	1.02	0.93
31	0.90	1.06	0.93	32	0.93	1.05	0.94
40.5	0.885	1.15	0.94	39	0.90	1.13	0.91

Table 4.10: Performance of the pump at 1300 rpm with bottom ash slurry

Concentration 16.0% (S =1.09)						
12.71	12.04	3.83	38.04	0.94	1.01	0.96
9.92	12.93	3.56	41.01	0.95	1.01	0.96
8.20	13.05	3.43	39.30	0.93	1.00	0.96
6.53	13.38	3.09	37.29	0.96	1.00	0.97
5.10	13.70	2.94	32.39	0.93	1.00	0.96
4.20	14.04	2.85	29.70	0.96	1.01	0.96
3.15	14.83	2.60	22.83	0.94	1.01	1.00
Concentration 23.0% (S =1.15)						
12.51	11.94	3.89	37.87	0.95	1.08	0.96
9.84	12.62	3.62	40.75	0.95	1.05	0.94
8.30	12.95	3.49	38.30	0.94	1.04	0.97
6.52	13.08	3.16	35.29	0.94	1.05	0.95
5.20	13.30	2.99	30.39	0.94	1.03	0.96
4.00	13.94	2.98	27.70	0.93	1.06	0.95
3.00	14.65	2.69	19.83	0.93	1.06	0.95
0.00			0.00			
Concentration 31.0% (S=1.21)						
12.65	11.65	3.99	39.87	0.94	1.08	0.94
9.70	12.40	3.74	39.75	0.90	1.10	0.92
8.12	12.76	3.60	37.30	0.92	1.11	0.91
6.60	12.88	3.27	34.29	0.93	1.12	0.96
5.25	13.00	3.03	29.90	0.92	1.13	0.90
4.00	13.78	3.00	25.01	0.92	1.13	0.98
2.97	14.48	2.79	18.26	0.92	1.14	0.98
Concentration 4 3% (S =1.32)						
12.21	11.16	4.08	39.40	0.92	1.15	0.92
10.10	12.01	3.89	38.50	0.89	1.15	0.91
8.20	12.30	3.68	37.85	0.91	1.17	0.95
6.70	12.51	3.59	34.80	0.91	1.16	0.94
5.00	12.85	3.38	32.65	0.90	1.18	0.93
3.80	13.45	3.09	28.73	0.89	1.17	0.91
2.70	14.20	2.73	20.80	0.89	1.19	0.97

Table 4.11: Performance of the pump at 1300 rpm with bottom ash and fly ash mixture (9:1)

Concentration 13.50% (S =1.08)						
12.50	12.09	3.60	39.54	0.97	1.00	0.95
10.15	12.96	3.46	40.07	0.97	1.00	0.96
8.63	13.10	3.33	39.89	0.96	1.00	0.95
7.12	13.43	3.03	36.91	0.95	1.01	0.95
5.21	13.77	2.80	33.37	0.95	1.01	0.94
4.10	14.09	2.71	28.65	0.97	1.02	0.98
3.00	14.88	2.47	21.64	0.94	1.00	0.96
Concentration 22.0% (S=1.135)						
12.81	11.98	3.81	38.70	0.96	1.03	0.92
10.45	12.68	3.54	39.61	0.93	1.01	0.94
8.50	13.00	3.43	38.92	0.95	1.02	0.96
6.88	13.14	3.06	34.72	0.95	1.04	0.93
5.63	13.38	2.93	30.83	0.94	1.04	0.94
4.20	13.99	2.87	25.66	0.94	1.06	0.97
3.12	14.73	2.60	20.11	0.93	1.07	0.90
Concentration 32.0% (S =1.21						
12.75	11.70	3.90	39.87	0.95	1.06	0.93
10.15	12.48	3.68	39.75	0.92	1.08	0.96
8.43	12.80	3.53	37.30	0.93	1.09	0.94
6.51	12.97	3.21	34.29	0.94	1.10	0.92
5.36	13.07	2.98	29.90	0.93	1.11	0.94
4.10	13.86	2.90	25.01	0.94	1.10	0.91
2.82	14.55	2.70	18.26	0.92	1.11	0.93
Concentration 4 5% (S=1.323)						
12.80	11.12	4.01	39.56	0.92	1.07	0.94
10.43	11.90	3.82	39.96	0.90	1.09	0.95
8.70	12.18	3.63	38.50	0.91	1.11	0.93
7.31	12.49	3.55	33.86	0.91	1.12	0.96
5.80	12.93	3.28	30.58	0.91	1.13	0.93
4.25	13.52	3.03	27.35	0.91	1.13	0.91
2.82	14.27	2.92	18.96	0.90	1.15	0.94

Table 4.12:Performance of the pump at 1300 rpm with bottom ash and fly ash mixture (8:2)

Concentration 15.0% (S =1.08)						
12.60	12.13	3.57	39.95	0.96	1.00	0.96
9.88	13.02	3.40	40.25	0.98	1.00	0.96
8.15	13.15	3.27	38.92	0.96	1.00	0.99
6.60	13.48	3.01	36.27	0.97	1.01	0.95
4.56	13.85	2.75	30.37	0.98	1.02	0.98
3.80	14.17	2.65	28.66	0.97	1.01	0.96
2.61	14.93	2.41	20.88	0.95	1.02	0.98
Concentration 23.0% (S =1.141)						
12.85	11.90	3.79	39.23	0.95	1.00	0.97
10.20	12.50	3.53	39.85	0.95	1.01	0.96
8.61	12.97	3.40	38.72	0.95	1.03	0.98
6.85	13.07	3.04	34.95	0.96	1.01	0.98
5.50	13.36	2.91	30.67	0.96	1.03	0.96
4.12	13.89	2.86	26.77	0.93	1.02	0.98
3.13	14.55	2.57	22.56	0.95	1.02	0.99
Concentration 32.0% (S=1.21)						
12.83	11.75	3.88	39.98	0.95	1.01	0.97
9.90	12.40	3.66	38.61	0.92	1.03	0.96
8.35	12.85	3.51	36.72	0.94	1.05	0.98
6.60	12.99	3.20	33.23	0.94	1.06	0.98
5.21	13.07	2.97	28.89	0.94	1.07	0.96
4.20	13.86	2.89	24.01	0.93	1.07	0.98
3.12	14.58	2.69	20.88	0.93	1.08	0.99
Concentration 44.0% (S=1.31)						
12.41	11.22	3.97	38.86	0.94	1.06	0.94
9.70	11.99	3.77	40.26	0.90	1.07	0.95
8.23	12.29	3.59	38.39	0.92	1.08	0.97
6.50	12.63	3.50	32.96	0.92	1.08	0.95
5.65	12.96	3.26	30.88	0.92	1.10	0.98
4.32	13.55	3.00	26.65	0.91	1.12	0.97
3.20	14.30	2.88	21.06	0.91	1.14	0.96
0.00			0.00			

Table 4.13: Performance of the pump at 1300 rpm with bottom ash and fly ash mixture (7:3)

Concentration 12.5% (S=1.08)						
12.80	12.17	3.55	40.02	0.99	1.00	0.97
9.90	13.05	3.40	39.25	0.97	1.00	0.95
8.80	13.18	3.24	36.22	0.97	1.01	0.97
7.10	13.50	3.01	33.31	0.96	1.00	0.96
5.20	13.88	2.71	28.69	0.97	1.03	0.95
4.20	14.20	2.63	25.77	0.98	1.02	0.97
3.10	14.97	2.38	22.81	0.95	1.02	0.96
Concentration 24.0% (S =1.145)						
12.75	12.00	3.77	39.73	0.98	1.01	0.96
10.12	12.64	3.50	39.03	0.96	1.02	0.97
8.62	13.07	3.38	38.96	0.96	1.03	0.96
6.50	13.16	3.02	32.53	0.95	1.03	0.97
5.23	13.61	2.90	29.89	0.96	1.02	0.95
4.17	14.08	2.84	26.92	0.96	1.01	0.97
3.00	14.61	2.55	19.96	0.95	1.01	0.96
Concentration 32.0% (S =1.23)						
12.90	11.75	3.87	39.20	0.94	1.01	0.96
10.26	12.40	3.64	38.60	0.93	1.02	0.97
8.50	12.85	3.49	34.64	0.95	1.03	0.96
6.75	12.99	3.18	31.35	0.94	1.04	0.97
5.50	13.07	2.94	26.79	0.95	1.05	0.98
4.24	13.86	2.88	23.66	0.95	1.04	0.96
2.86	14.58	2.68	20.06	0.94	1.06	0.97
Concentration 42.5% (S=1.29)						
12.80	11.27	3.95	39.06	0.95	1.04	0.95
9.92	12.04	3.74	40.56	0.91	1.06	0.97
8.31	12.36	3.56	38.67	0.93	1.07	0.96
6.50	12.68	3.47	32.93	0.93	1.09	0.94
5.36	13.00	3.24	30.89	0.92	1.10	0.99
4.24	13.64	2.98	26.95	0.92	1.10	0.96
2.90	14.38	2.86	19.46	0.91	1.12	0.96

Table 4.14: Performance of the pump at 1150 rpm with bottom ash slurry

Concentration 15.0% (S =1.08)						
12.91	10.02	3.20	39.56	0.94	1.00	0.96
11.30	10.48	3.08	41.80	0.97	1.00	0.98
9.81	10.90	2.78	38.40	0.96	1.01	0.97
7.35	11.30	2.56	35.60	0.95	1.00	0.95
5.32	11.70	2.30	30.10	0.95	1.01	0.94
4.00	12.02	2.09	23.40	0.95	1.00	0.98
2.83	12.35	1.91	16.50	0.97	1.02	1.00
0.00			0.00			
Concentration 24 % (S =1.15)						
12.71	9.81	3.29	39.02	0.93	1.04	0.94
9.91	10.15	3.00	41.40	0.95	1.03	0.94
8.00	10.60	2.76	37.20	0.95	1.05	0.95
6.92	11.03	2.57	33.40	0.93	1.05	0.96
5.15	11.34	2.36	29.70	0.92	1.04	0.96
4.23	11.63	2.21	22.60	0.94	1.06	0.97
3.00	12.02	2.07	18.60	0.95	1.07	0.98
0.00			0.00			
Concentration 33 % (S=1.230)						
12.91	9.52	3.40	38.86	0.91	1.05	0.96
9.81	9.95	3.07	41.20	0.93	1.06	0.93
8.34	10.20	2.90	36.68	0.94	1.07	0.92
7.15	10.70	2.73	32.87	0.91	1.09	0.95
5.35	11.05	2.48	28.58	0.90	1.10	0.93
4.00	11.20	2.27	21.90	0.93	1.10	0.93
3.15	11.80	2.08	16.95	0.94	1.11	0.93
0.00			0.00			
Concentration 45.0 % (S =1.33)						
12.85	9.26	3.53	38.70	0.89	1.11	0.94
10.14	9.68	3.24	41.13	0.91	1.10	0.92
8.44	10.00	3.01	36.85	0.92	1.12	0.95
7.00	10.38	2.85	31.80	0.89	1.12	0.92
5.41	10.75	2.64	26.51	0.89	1.13	0.94
4.11	10.98	2.37	20.53	0.91	1.11	0.95
2.81	11.45	2.23	17.23	0.93	1.15	0.98

Table 4.15: Performance of the pump at 1150 rpm with bottom ash and fly ash mixture (9:1)

Concentration 12.0% (S =1.07)						
13.00	10.00	3.17	39.50	0.94	1.00	0.97
11.50	10.44	3.01	41.83	0.98	1.00	0.98
10.00	10.82	2.75	38.30	0.96	1.00	0.97
7.52	11.25	2.59	35.70	0.95	1.00	0.95
5.41	11.77	2.31	29.30	0.96	1.01	0.95
4.16	12.06	2.02	24.20	0.95	1.00	0.94
3.00	12.39	1.90	18.60	0.97	1.01	1.02
Concentration 22.5 % (S =1.13)						
12.94	9.77	3.33	39.80	0.93	1.03	0.96
10.15	10.45	3.08	39.40	0.96	1.03	0.94
8.20	10.65	2.84	35.80	0.95	1.04	0.96
7.00	11.07	2.65	32.49	0.93	1.04	0.95
5.25	11.29	2.43	27.84	0.93	1.04	0.96
4.30	11.58	2.19	23.85	0.94	1.05	0.98
2.85	12.05	2.02	17.95	0.96	1.06	0.99
Concentration 34 % (S=1.230)						
13.00	9.59	3.43	39.38	0.91	1.04	0.94
10.20	10.00	3.15	40.15	0.94	1.05	0.94
8.00	10.26	2.90	35.90	0.94	1.06	0.92
7.25	10.75	2.76	31.96	0.92	1.08	0.95
5.00	11.13	2.54	26.24	0.91	1.08	0.92
4.10	11.26	2.26	22.65	0.94	1.10	0.94
2.78	11.88	2.07	18.23	0.95	1.10	0.92
Concentration 43.0 % (S=1.30)						
12.81	9.20	3.55	38.94	0.89	1.10	0.93
10.15	9.78	3.27	40.05	0.90	1.09	0.96
8.40	9.96	3.02	35.56	0.89	1.10	0.95
7.00	10.32	2.85	30.40	0.89	1.11	0.95
5.43	10.64	2.68	25.85	0.90	1.12	0.94
4.15	10.88	2.39	21.96	0.91	1.13	0.93
2.81	11.38	2.26	16.58	0.93	1.13	0.92

Table 4.16:Performance of the pump at 1150 rpm with bottom ash and fly ash mixture (8:2)

Concentration 14.0% (S=1.08)						
12.90	10.20	3.15	40.23	0.94	1.00	0.96
11.20	10.52	3.00	41.33	0.98	1.00	0.97
9.85	10.88	2.74	39.20	0.96	1.00	0.96
7.64	11.36	2.53	36.90	0.96	1.00	0.95
5.45	11.80	2.26	31.50	0.96	1.02	0.95
4.05	12.10	2.00	25.60	0.96	1.00	0.95
2.94	12.22	1.88	19.80	0.97	1.02	0.95
Concentration 24.0 % (S=1.15)						
13.10	9.86	3.28	39.90	0.93	1.03	0.95
10.95	10.23	3.09	38.80	0.94	1.02	0.93
9.80	10.72	2.84	33.87	0.95	1.01	0.95
7.50	11.10	2.60	30.95	0.93	1.03	0.95
5.26	11.44	2.32	25.56	0.93	1.03	0.97
4.22	11.69	2.14	22.78	0.94	1.05	0.95
2.94	12.08	2.01	19.80	0.95	1.05	0.96
Concentration 33 % (S =1.220)						
13.00	9.59	3.37	39.74	0.92	1.03	0.95
10.50	10.16	3.03	40.56	0.93	1.04	0.94
8.23	10.42	2.78	37.60	0.94	1.06	0.93
7.05	10.90	2.60	30.94	0.92	1.07	0.92
5.36	11.20	2.39	25.93	0.91	1.08	0.93
4.27	11.34	2.22	21.92	0.94	1.09	0.94
3.15	11.76	2.09	17.60	0.95	1.09	0.92
Concentration 46.0 % (S=1.33)						
12.92	9.32	3.47	39.50	0.87	1.07	0.93
10.60	9.90	3.20	40.34	0.90	1.08	0.95
8.57	10.03	2.95	36.80	0.90	1.09	0.92
7.12	10.44	2.72	31.73	0.90	1.10	0.92
5.84	10.75	2.60	26.58	0.90	1.11	0.93
4.00	10.99	2.29	22.80	0.92	1.11	0.93
2.94	11.50	2.15	15.60	0.93	1.12	0.94

Table 4.17:Performance of the pump at 1150 rpm with bottom ash and fly ash mixture (7:3)

Concentration 16.0% (S=1.09)						
13.05	10.15	3.19	39.56	0.95	1.00	0.96
11.32	10.50	3.00	40.67	0.97	1.00	0.98
9.92	10.90	2.76	38.40	0.97	1.00	0.98
7.92	11.37	2.54	35.57	0.96	1.00	0.96
5.82	11.64	2.28	30.97	0.96	1.01	0.97
4.11	12.06	2.02	23.96	0.96	1.00	1.00
3.05	12.27	1.90	18.56	0.98	1.01	1.00
Concentration 25.0 % (S=1.15)						
13.01	9.86	3.25	39.60	0.93	1.02	0.95
10.93	10.43	3.02	39.90	0.95	1.01	0.98
9.74	10.80	2.85	35.70	0.96	1.01	0.95
7.72	11.14	2.60	31.54	0.93	1.02	0.97
5.16	11.48	2.31	24.80	0.95	1.03	0.97
4.15	11.70	2.15	22.90	0.95	1.02	0.95
2.88	12.10	2.00	17.67	0.95	1.06	0.98
Concentration 34.5 % (S=1.230)						
12.9	9.56	3.32	39.89	0.92	1.03	0.95
11.02	10.05	3.12	40.23	0.93	1.04	0.96
8.45	10.30	2.83	36.90	0.94	1.06	0.94
6.86	10.80	2.57	30.34	0.92	1.07	0.95
5.25	11.16	2.33	25.50	0.91	1.07	0.94
4.21	11.39	2.19	21.23	0.94	1.08	0.96
2.82	11.70	2.09	16.80	0.95	1.07	0.97
Concentration 48.0 % (S=1.34)						
12.82	9.35	3.45	39.20	0.88	1.07	0.94
10.55	9.94	3.23	38.89	0.91	1.08	0.95
8.61	10.10	3.02	35.70	0.91	1.09	0.97
7.11	10.30	2.85	31.50	0.90	1.05	0.92
5.56	10.66	2.60	24.80	0.90	1.08	0.93
4.24	10.86	2.36	21.90	0.92	1.10	0.93
2.85	11.37	2.19	16.90	0.94	1.10	0.94

Table 4.18: Performance of the pump at 1000 rpm with bottom ash slurry

Concentration 13.0% (S =1.08)						
12.20	6.36	2.08	38.79	0.94	1.00	0.96
10.55	7.04	1.95	40.17	0.96	1.01	0.97
8.26	7.71	1.86	35.45	0.95	1.02	0.97
6.58	8.22	1.78	30.24	0.96	1.00	0.98
4.30	8.59	1.67	23.45	0.97	1.00	0.99
3.30	8.77	1.60	19.12	0.95	1.02	0.97
2.45	9.03	1.50	14.26	0.94	1.04	0.96
Concentration 22.0% (S =1.14)						
11.80	6.16	2.17	38.25	0.93	1.02	0.94
10.30	6.92	2.05	39.54	0.95	1.03	0.97
8.95	7.33	1.95	34.41	0.94	1.05	0.95
7.30	7.80	1.88	31.69	0.96	1.04	0.98
5.60	8.16	1.79	26.94	0.94	1.06	0.96
4.20	8.39	1.70	23.55	0.95	1.07	0.97
2.73	8.73	1.60	16.33	0.93	1.08	0.96
Concentration 34% (S=1.23)						
11.33	6.10	2.25	38.56	0.92	1.06	0.94
9.80	6.77	2.13	39.03	0.93	1.07	0.96
8.42	7.21	2.03	35.16	0.93	1.07	0.95
7.00	7.63	1.96	30.93	0.93	1.08	0.94
5.40	8.02	1.87	25.42	0.91	1.09	0.93
4.15	8.17	1.79	20.73	0.94	1.09	0.96
2.65	8.55	1.67	18.24	0.93	1.1	0.95
Concentration 4 3% (S =1.32)						
11.40	5.89	2.34	38.96	0.92	1.08	0.94
9.90	6.61	2.22	38.49	0.91	1.09	0.93
7.60	7.08	2.09	33.40	0.90	1.10	0.91
6.23	7.57	2.01	28.53	0.91	1.10	0.94
4.71	7.92	1.94	22.48	0.91	1.12	0.92
3.55	7.95	1.84	19.83	0.92	1.14	0.93
2.53	8.41	1.77	13.71	0.89	1.14	0.94

Table 4.19: Performance of the pump at 10 00 rpm with bottom ash and fly ash mixture (9:1)

Concentration 15.0% (S =1.09)						
12.30	6.41	2.07	39.21	0.96	1.00	0.97
10.38	7.08	1.94	39.74	0.95	1.00	0.94
8.60	7.78	1.85	36.04	0.95	0.99	0.93
6.91	8.26	1.76	30.37	0.94	1.01	0.97
4.85	8.64	1.65	24.04	0.97	1.02	0.96
3.57	8.81	1.59	19.15	0.95	1.01	0.93
2.67	9.05	1.49	13.82	0.95	1.03	0.97
Concentration 24.0% (S =1.15)						
12.10	6.20	2.16	38.58	0.94	1.00	0.96
10.80	6.94	2.04	39.24	0.96	1.00	0.93
9.10	7.35	1.94	32.64	0.96	1.01	0.97
7.50	7.83	1.86	27.93	0.96	1.03	0.92
5.82	8.18	1.78	22.42	0.97	1.05	0.94
4.35	8.40	1.69	18.83	0.96	1.06	0.93
2.95	8.76	1.59	12.82	0.94	1.07	0.93
Concentration 33.0% (S =1.22)						
11.90	6.14	2.24	38.24	0.94	1.05	0.92
9.60	6.81	2.12	38.64	0.94	1.07	0.93
8.20	7.24	2.01	34.40	0.93	1.08	0.92
7.10	7.67	1.95	30.37	0.96	1.09	0.93
5.60	8.08	1.85	23.67	0.92	1.09	0.93
4.40	8.20	1.78	18.94	0.94	1.10	0.93
2.80	8.59	1.65	14.14	0.95	1.11	0.93
Concentration 45.0% (S =1.32)						
11.80	5.94	2.33	38.01	0.93	1.07	0.93
9.50	6.65	2.20	38.97	0.92	1.08	0.94
7.80	7.11	2.07	30.90	0.91	1.09	0.95
6.40	7.60	2.01	22.59	0.93	1.09	0.94
4.10	7.95	1.92	19.68	0.92	1.10	0.93
3.30	7.98	1.82	16.95	0.92	1.10	0.93
2.50	8.44	1.75	13.85	0.90	1.13	0.94

Table 4.20: Performance of the pump at 1000 rpm with bottom ash and fly ash mixture (8:2)

Concentration 13.0% (S =1.075)						
12.50	6.56	2.05	39.79	0.96	1.00	0.97
10.73	7.18	1.93	39.91	0.97	1.00	0.95
8.80	7.83	1.82	33.06	0.96	1.01	0.95
6.74	8.30	1.74	29.69	0.97	1.02	0.94
4.95	8.67	1.64	24.94	0.97	1.02	0.98
3.50	8.89	1.57	20.83	0.97	1.01	0.96
2.80	9.10	1.50	15.14	0.94	1.03	0.93
Concentration 25.0% (S=1.16)						
12.43	6.25	2.13	38.87	0.95	1.02	0.93
10.65	7.00	2.03	39.31	0.96	1.03	0.94
9.25	7.39	1.92	32.99	0.95	1.04	0.96
7.86	7.89	1.85	27.30	0.94	1.04	0.96
5.59	8.23	1.76	24.48	0.94	1.05	0.96
4.20	8.45	1.68	19.98	0.93	1.05	0.92
3.13	8.80	1.58	13.71	0.94	1.06	0.93
Concentration 34.0% (S =1.22)						
12.10	6.20	2.23	38.83	0.94	1.04	0.96
9.80	6.89	2.10	38.81	0.95	1.06	0.94
8.10	7.28	2.00	35.90	0.93	1.07	0.92
7.45	7.72	1.94	30.76	0.94	1.08	0.93
5.54	8.13	1.83	24.89	0.92	1.08	0.91
4.23	8.25	1.76	19.98	0.94	1.09	0.92
2.69	8.65	1.63	16.29	0.94	1.10	0.92
Concentration 44.5 % (S=1.323)						
11.93	6.11	2.32	39.07	0.92	1.06	0.91
9.38	6.86	2.15	38.66	0.92	1.07	0.93
7.94	7.15	2.05	34.82	0.94	1.08	0.92
6.56	7.64	1.99	23.71	0.93	1.08	0.94
4.57	7.99	1.90	19.38	0.94	1.09	0.92
3.62	8.02	1.81	16.47	0.92	1.10	0.93
2.71	8.49	1.74	15.42	0.93	1.10	0.95

Table 4.21: Performance of the pump at 10 00 rpm with bottom ash and fly ash mixture (7:3)

Concentration 15.0% (S =1.09)						
12.00	6.64	2.03	39.43	0.97	1.01	0.95
10.24	7.20	1.93	38.49	0.98	1.00	0.95
8.95	7.78	1.86	37.99	0.96	1.00	0.98
6.77	8.31	1.82	31.35	0.97	1.01	0.98
5.56	8.66	1.77	25.94	0.96	1.03	0.96
3.96	8.88	1.70	19.88	0.97	1.03	0.96
2.78	9.10	1.66	14.16	0.95	1.02	0.98
Concentration 24.0% (S =1.15)						
12.25	6.27	2.05	38.98	0.96	1.02	0.93
10.92	6.97	2.00	39.86	0.95	1.03	0.97
9.85	7.40	1.93	33.65	0.96	1.03	0.95
7.66	7.90	1.87	26.35	0.94	1.05	0.96
5.36	8.23	1.80	22.80	0.94	1.06	0.92
4.10	8.47	1.73	19.56	0.96	1.06	0.94
2.90	8.81	1.71	15.42	0.94	1.07	0.96
Concentration 35.0% (S=1.23)						
12.18	6.21	2.09	39.30	0.95	1.05	0.96
10.43	6.90	2.02	38.54	0.94	1.06	0.93
8.63	7.29	1.95	34.67	0.93	1.07	0.91
7.68	7.74	1.91	28.47	0.95	1.08	0.93
5.85	8.15	1.80	22.90	0.92	1.08	0.90
4.19	8.25	1.77	19.14	0.93	1.09	0.91
2.88	8.67	1.72	16.56	0.95	1.09	0.93
Concentration 47.0% (S =1.33)						
12.10	6.15	2.10	39.75	0.93	1.07	0.94
10.38	6.90	2.04	37.59	0.94	1.07	0.92
8.29	7.17	1.97	33.72	0.94	1.08	0.92
6.37	7.65	1.93	26.83	0.94	1.08	0.96
4.86	8.04	1.84	20.68	0.94	1.09	0.93
3.66	8.04	1.81	17.57	0.93	1.09	0.91
2.81	8.50	1.75	15.48	0.93	1.11	0.96

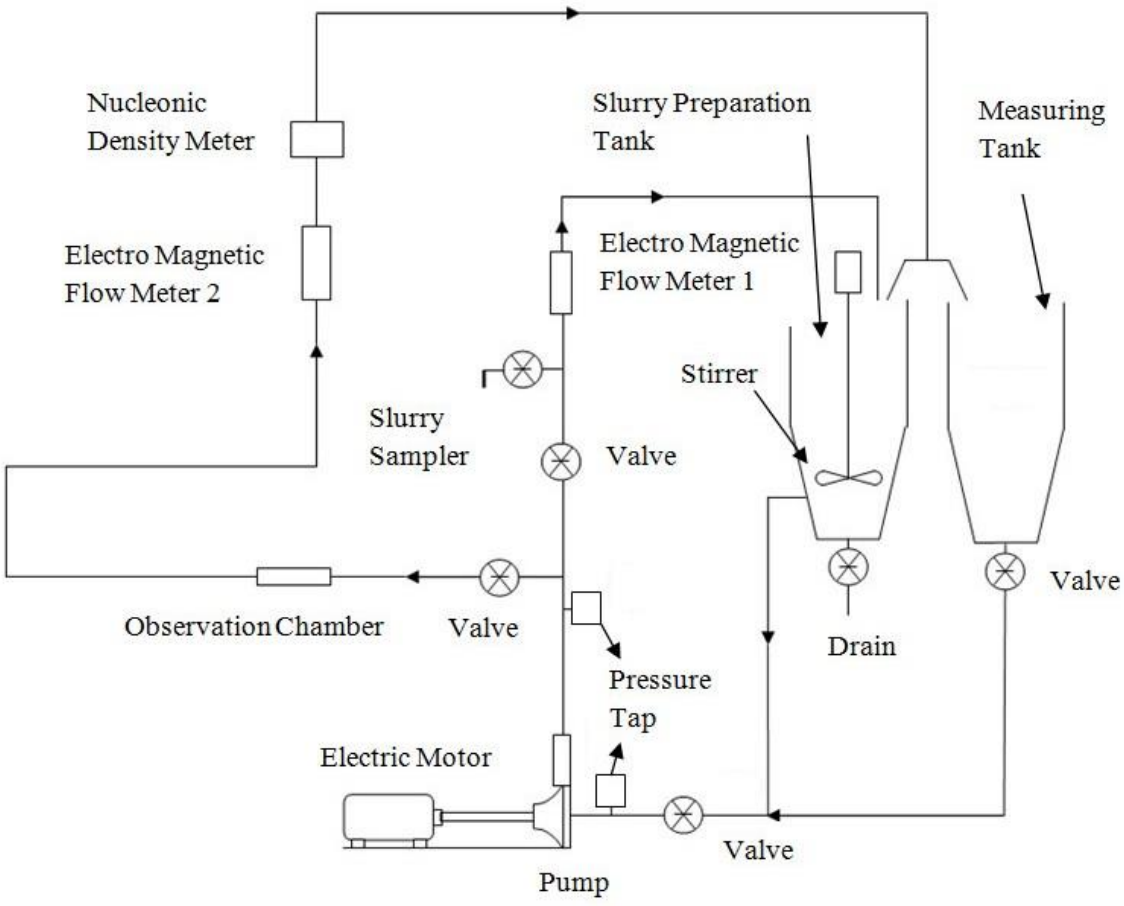

Figure 4.1:Schematic diagram of the experimental setup

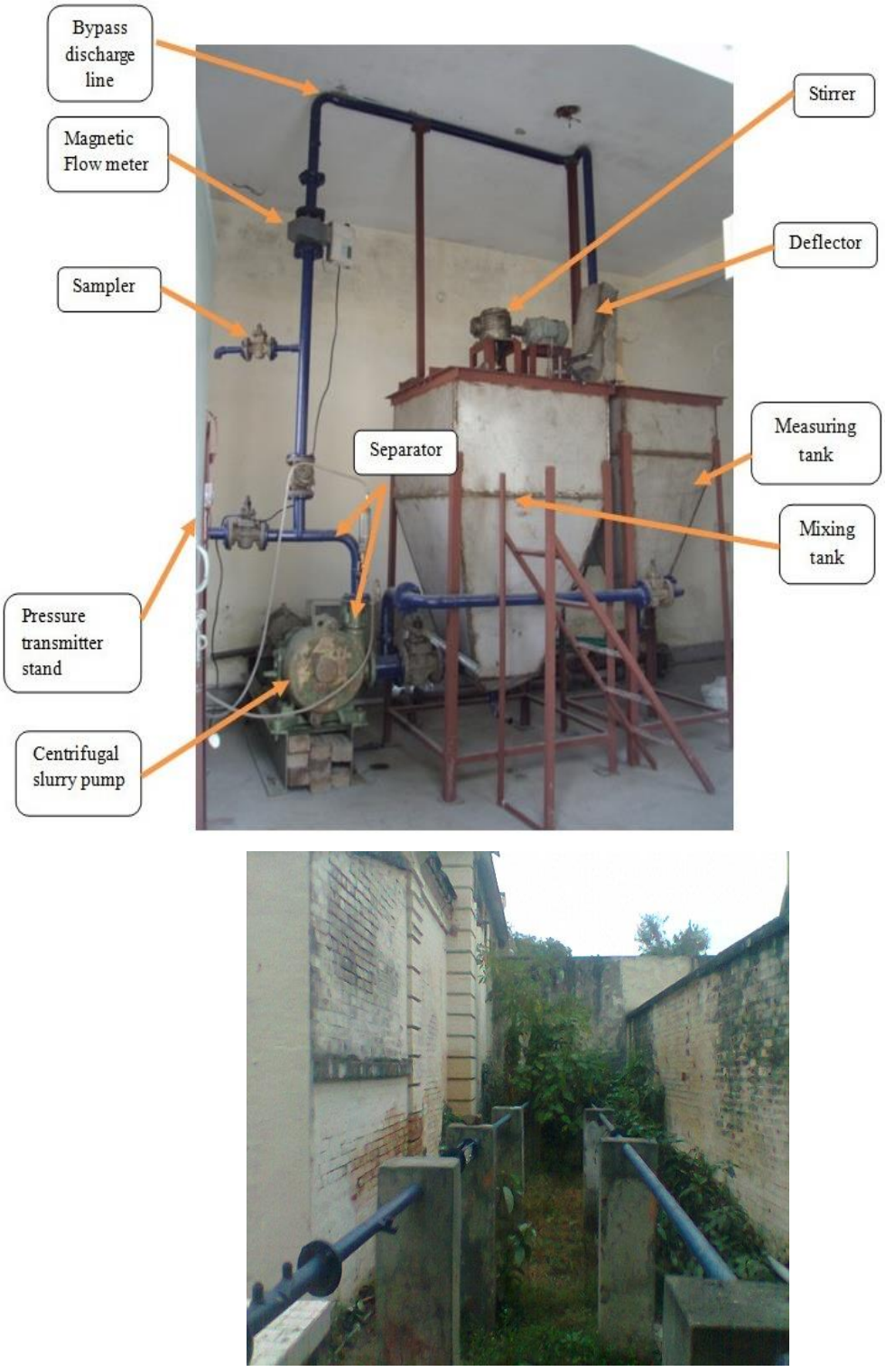

Figure 4.2:Photographic view of experimental set-up

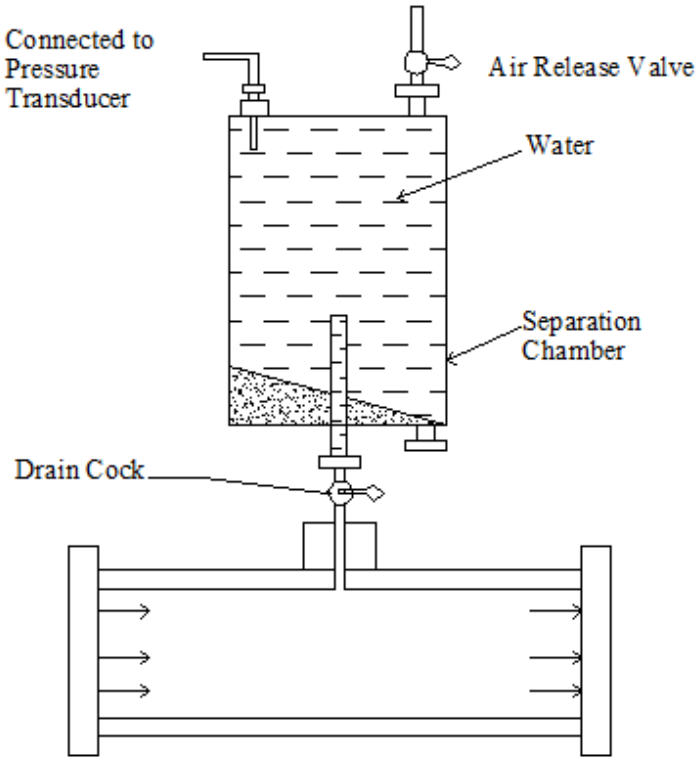

Figure 4.3: Schematic diagram of the separation chamber

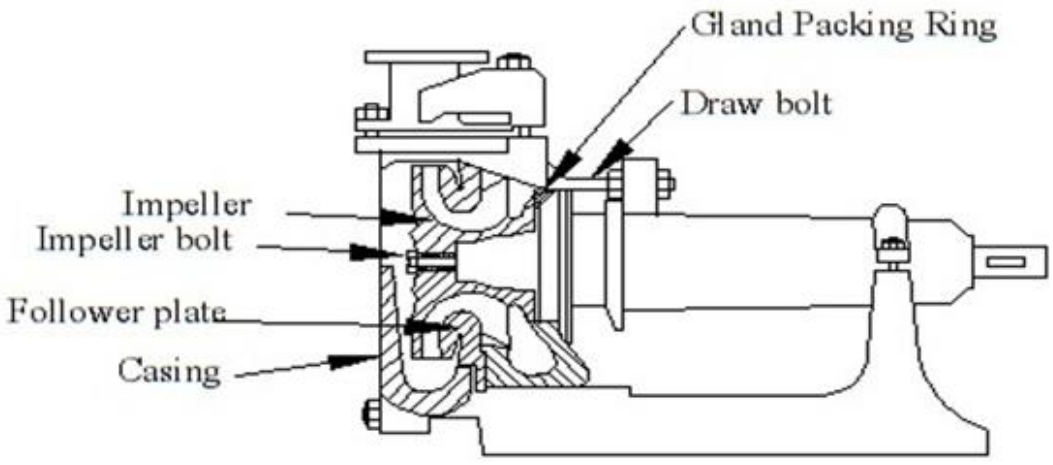

Figure 4.4: Sectional view of centrifugal slurry pump (Wilfley 2002)

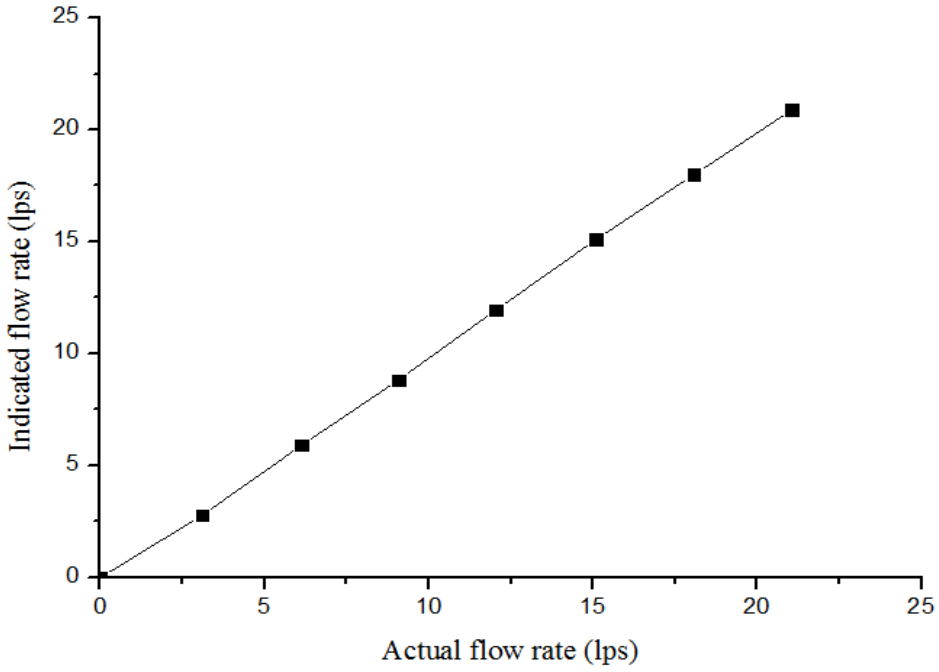

Figure 4.5: Calibration curve of Electromagnetic flow meter

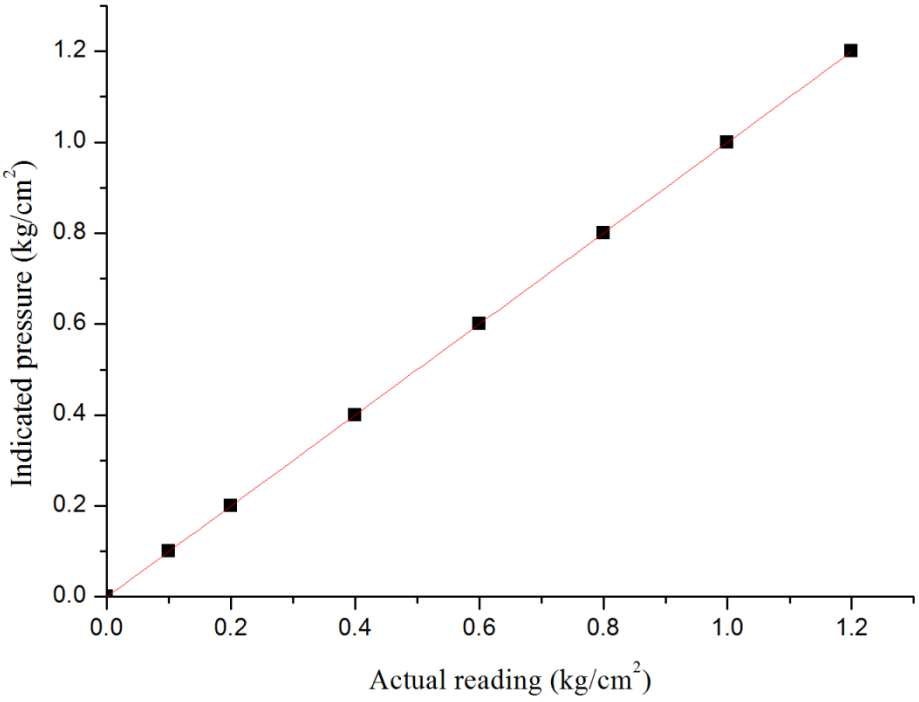

Figure 4.6: Calibration curve of LD290 pressure transmitter

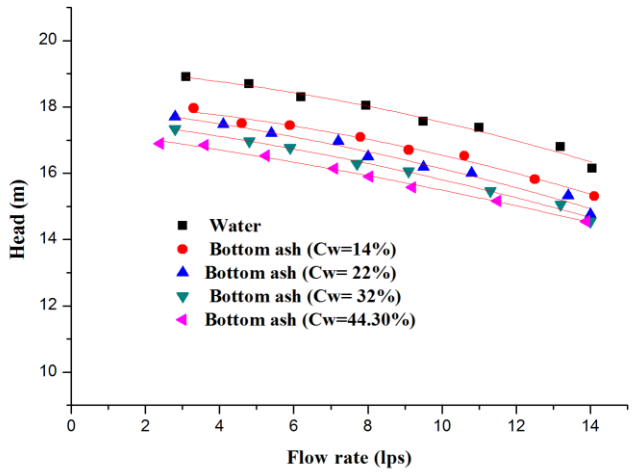

(a) Head-flow rate characteristics

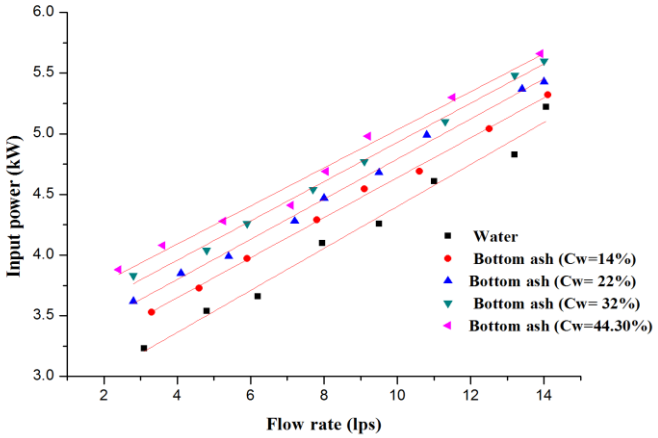

(b) Input power-flow rate characteristics

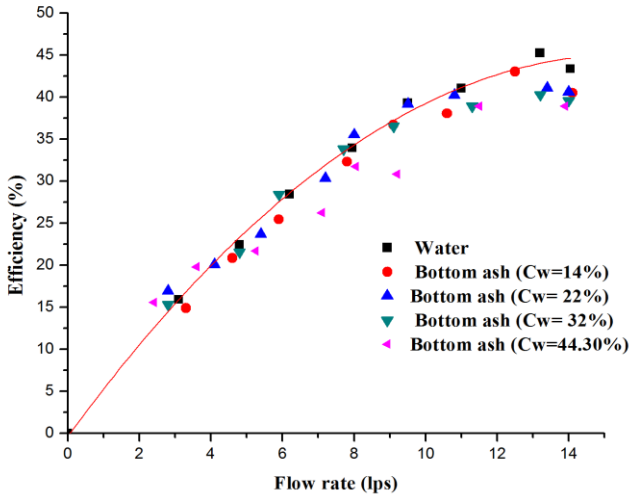

(c) Efficiency-flow rate characteristics

Figure 4.7: Performance characteristics of the centrifugal slurry pump with bottom ash slurry at 1450 rpm

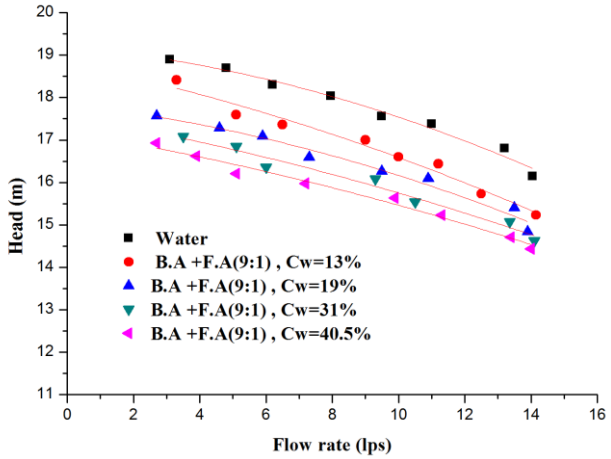

(a) Head-flow rate characteristics

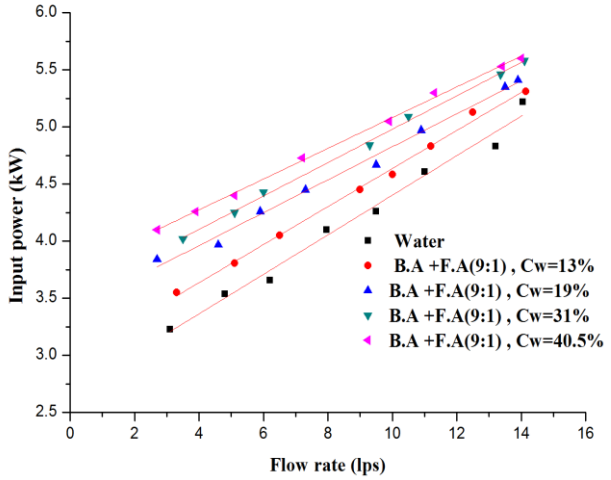

(b) Input power-flow rate characteristics

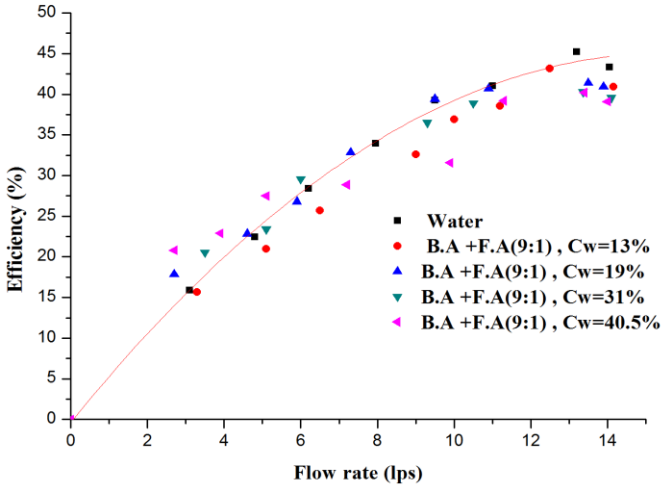

(c) Efficiency-flow rate characteristics

Figure 4.8: Performance characteristics of the centrifugal slurry pump with bottom ash and fly ash mixture (9:1) at 1450 rpm

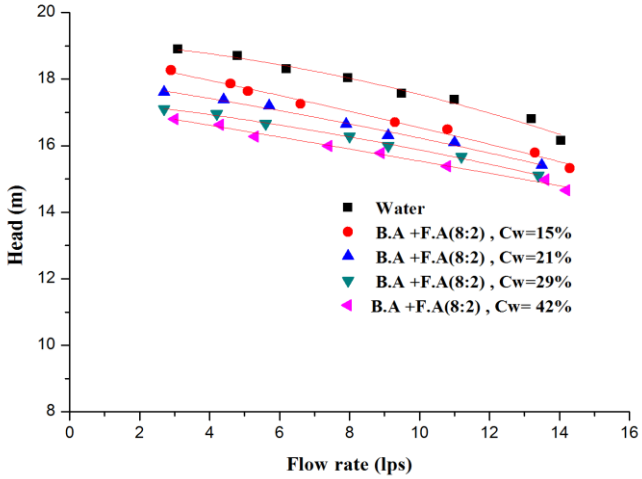

(a) Head-flow rate characteristics

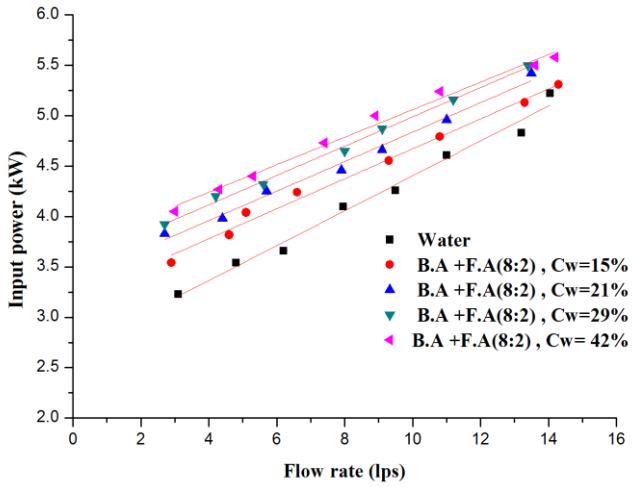

(b) Input power-flow rate characteristics

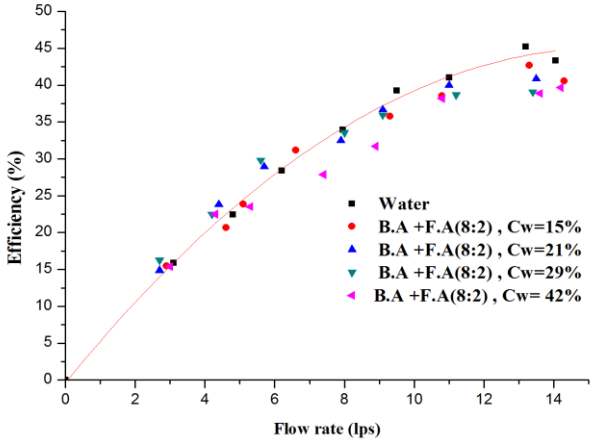

(c) Efficiency-flow rate characteristics

Figure 4.9: Performance characteristics of the centrifugal slurry pump with bottom ash and fly ash mixture (8:2) at 1450 rpm

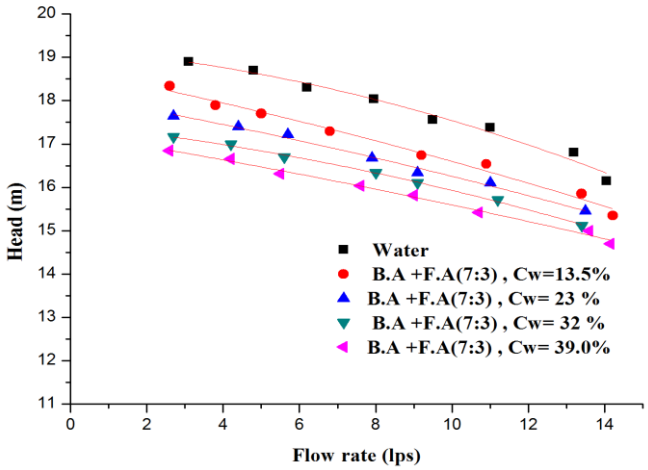

(a) Head-flow rate characteristics

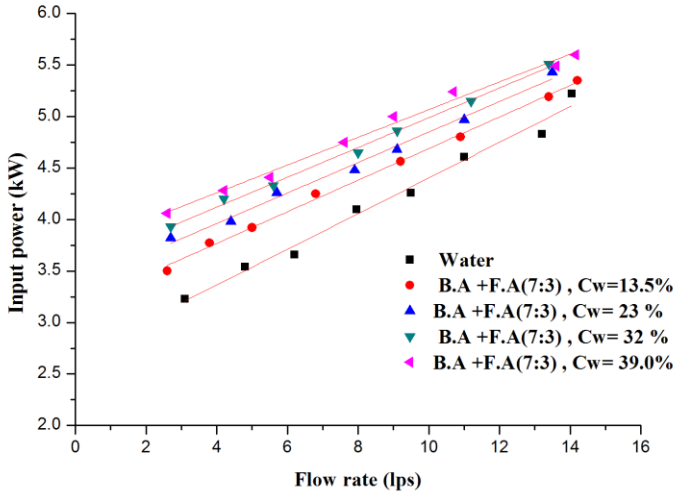

(b) Input power-flow rate characteristics

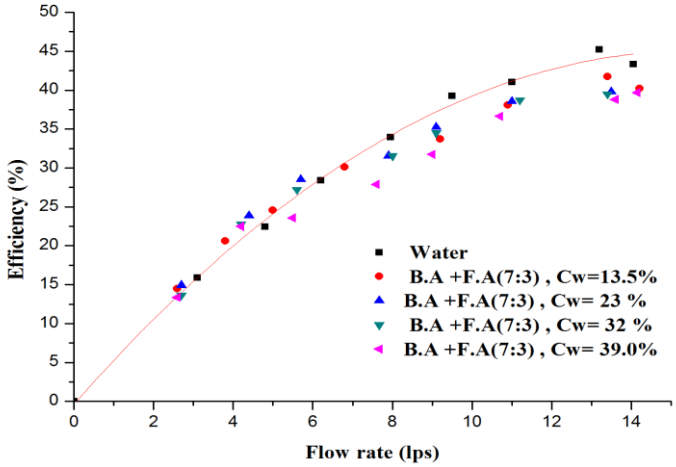

(c) Efficiency-flow rate characteristics

Figure 4.10: Performance characteristics of the centrifugal slurry pump with bottom ash and fly ash mixture (7:3) at 1450 rpm

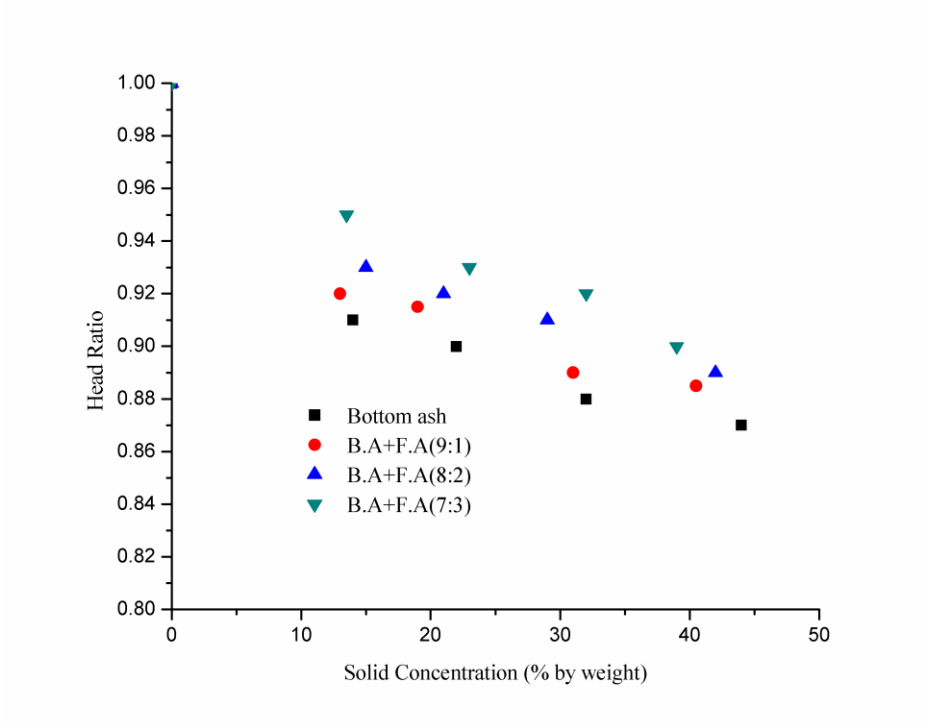

Figure 4.11: Variation of head ratio with solid concentration for bottom ash slurry with and without addition of fly ash at 1450 rpm at B.E.P

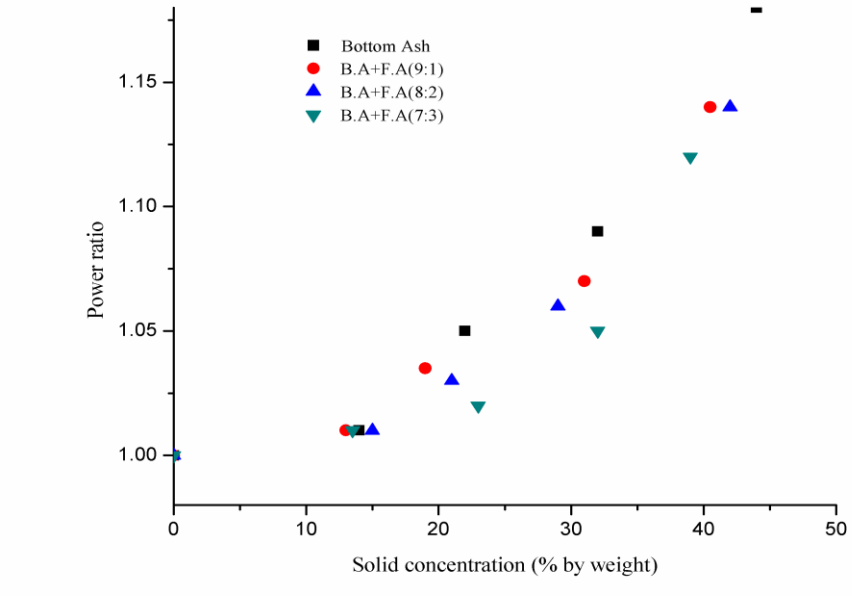

Figure 4.12: Variation of Power ratio with solid concentration for bottom ash slurry with and without addition of fly ash at 1450 rpm at B.E.P

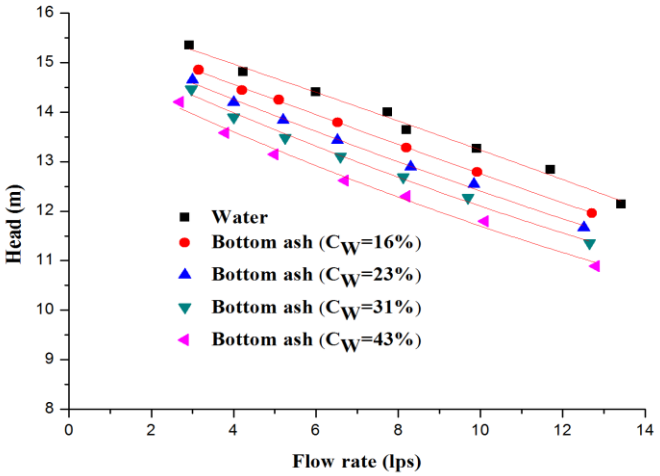

(a) Head-flow rate characteristics

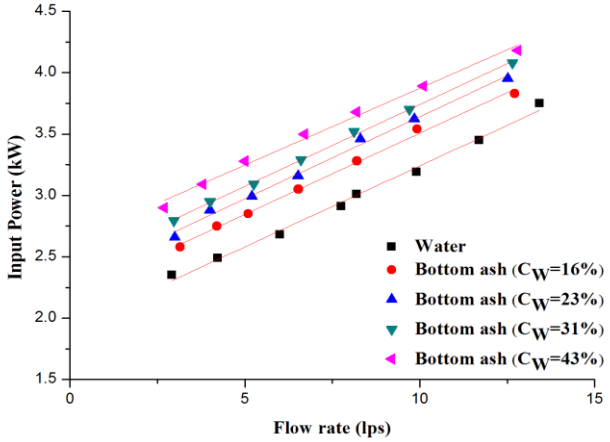

(b) Input power-flow rate characteristics

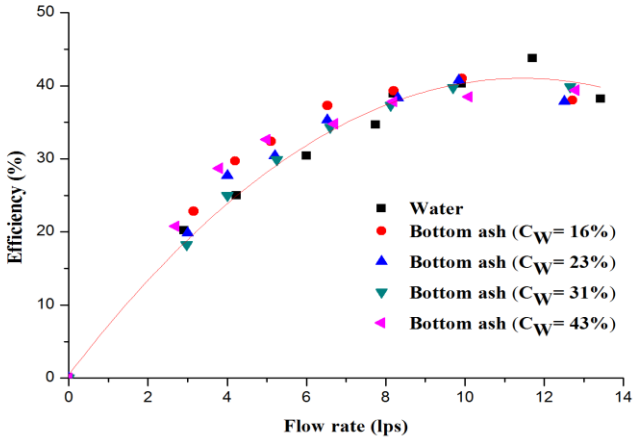

(c) Efficiency-flow rate characteristics

Figure 4.13: Performance characteristics of the centrifugal slurry pump with bottom ash slurry at 1300 rpm

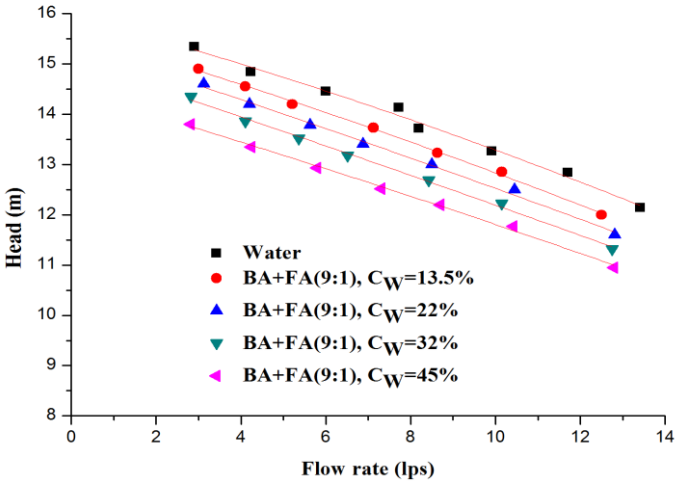

(a) Head-flow rate characteristics

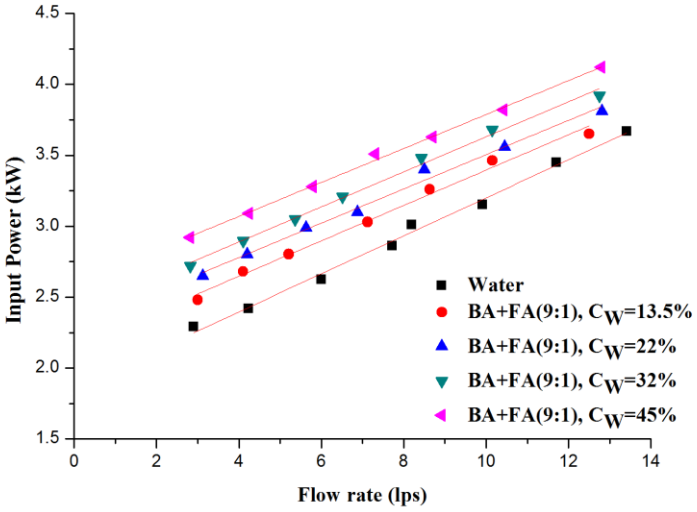

(b) Input power-flow rate characteristics

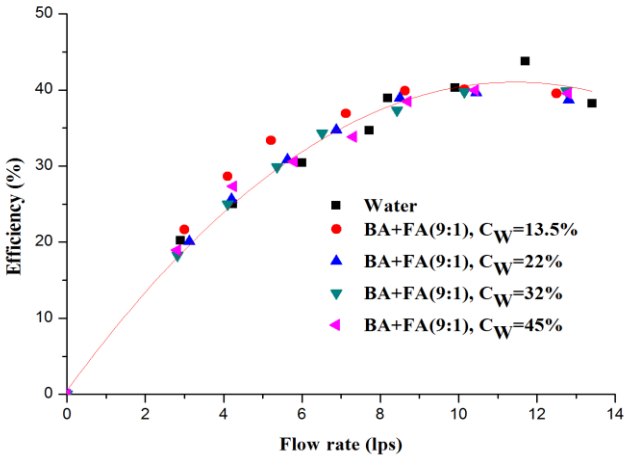

(c) Efficiency-flow rate characteristics

Figure 4.14: Performance characteristics of the centrifugal slurry pump with bottom ash and fly ash mixture (9:1) at 1300 rpm

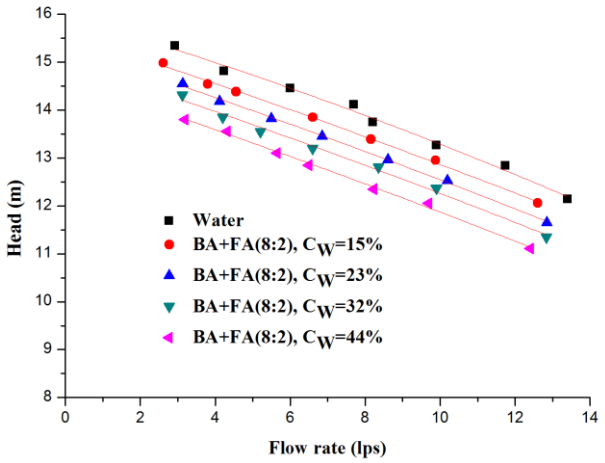

(a) Head-flow rate characteristics

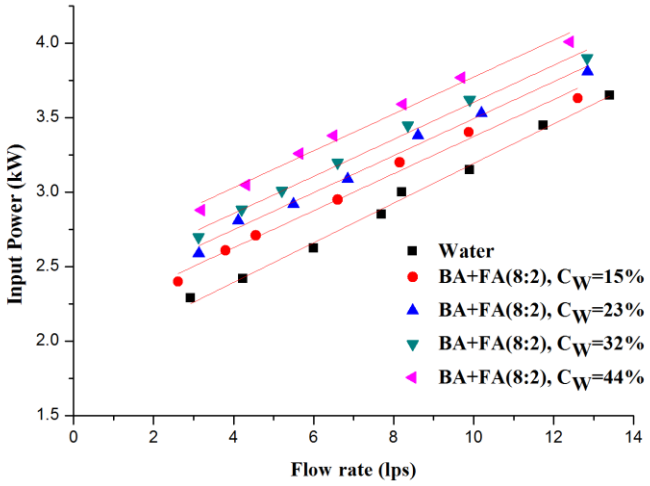

(b) Input power-flow rate characteristics

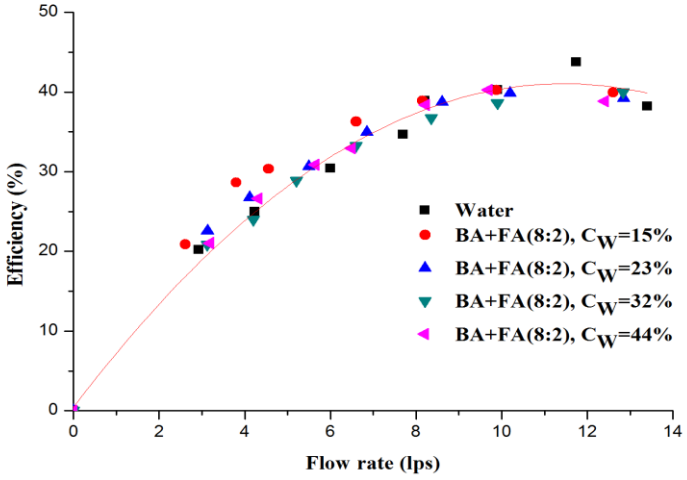

(c) Efficiency-flow rate characteristics

Figure 4.15: Performance characteristics of the centrifugal slurry pump with bottom ash and fly ash mixture (8:2) at 1300 rpm

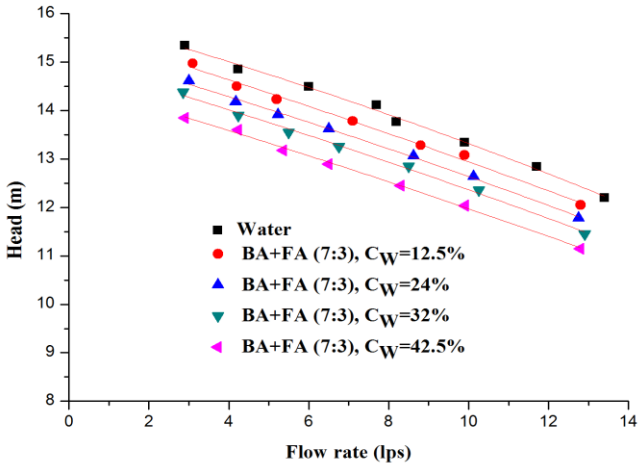

(a) Head-flow rate characteristics

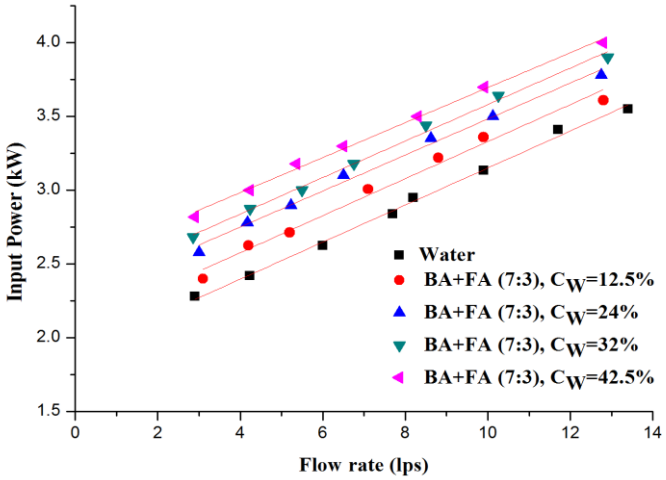

(b) Input power-flow rate characteristics

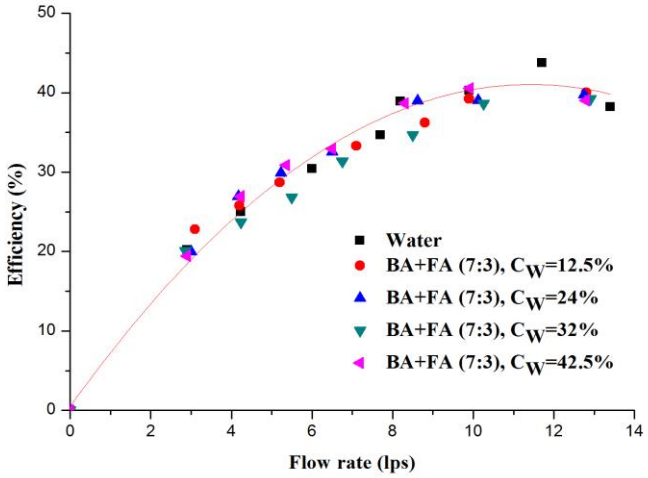

(c) Efficiency-flow rate characteristics

Figure 4.16: Performance characteristics of the centrifugal slurry pump with bottom ash and fly ash mixture (7:3) at 1300 rpm

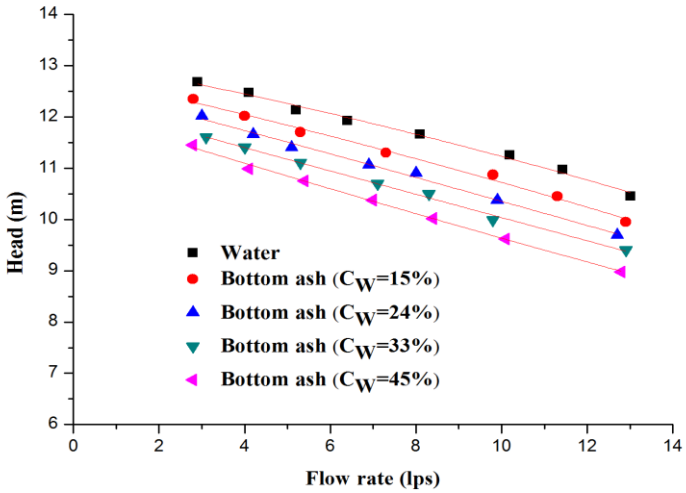

(a) Head-flow rate characteristics

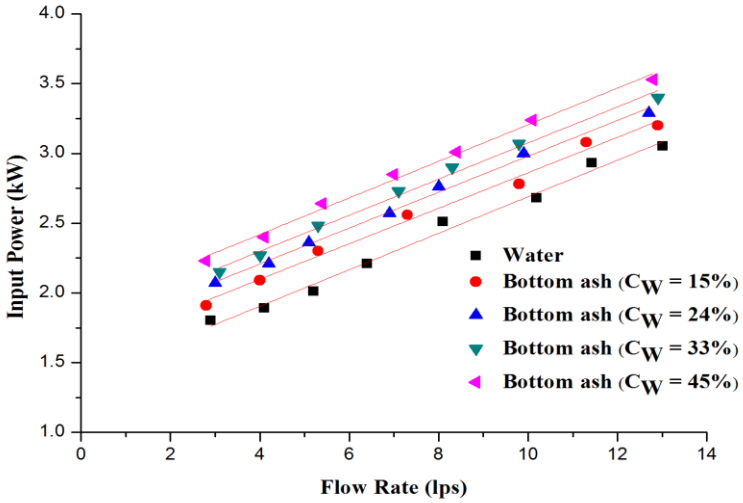

(b) Input power-flow rate characteristics

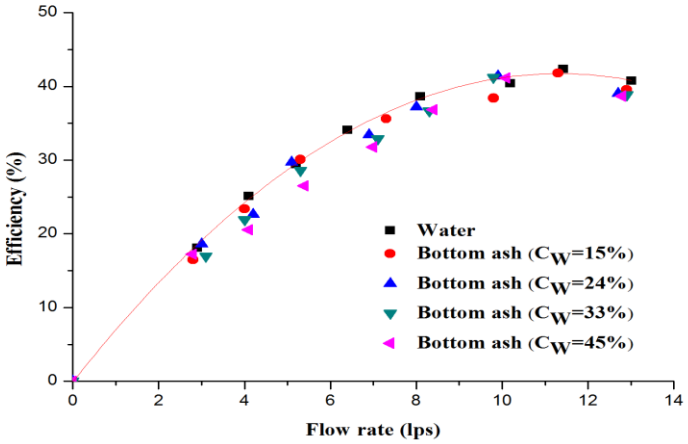

(c) Efficiency-flow rate characteristics

Figure 4.17: Performance characteristics of the centrifugal slurry pump with bottom ash slurry at 1150 rpm

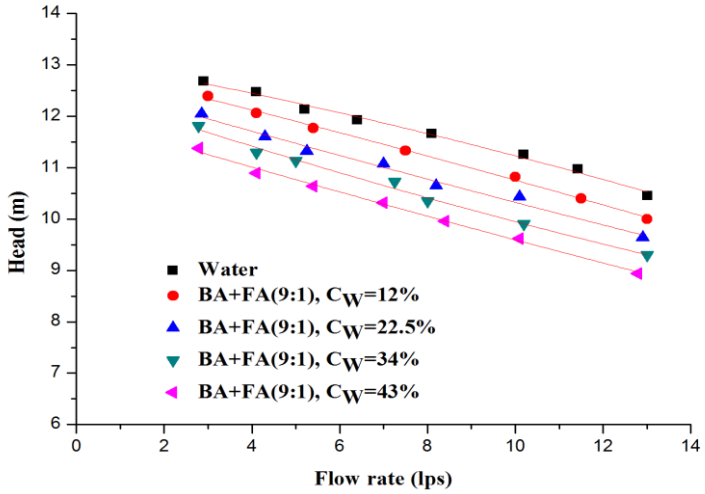

(a) Head-flow rate characteristics

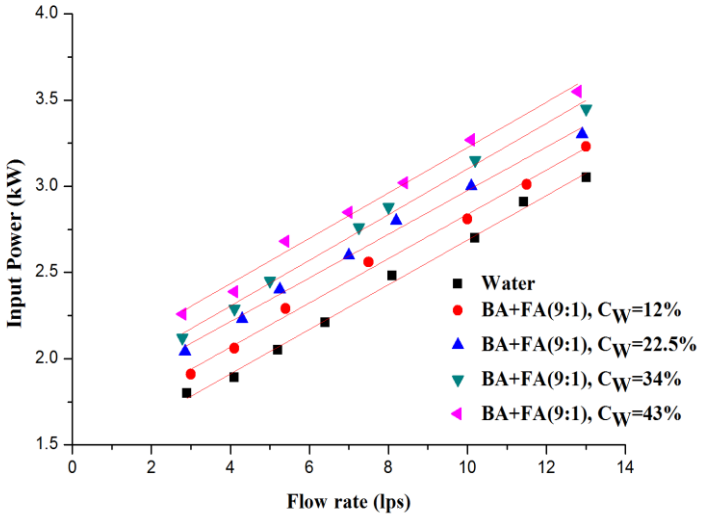

(b) Input power-flow rate characteristics

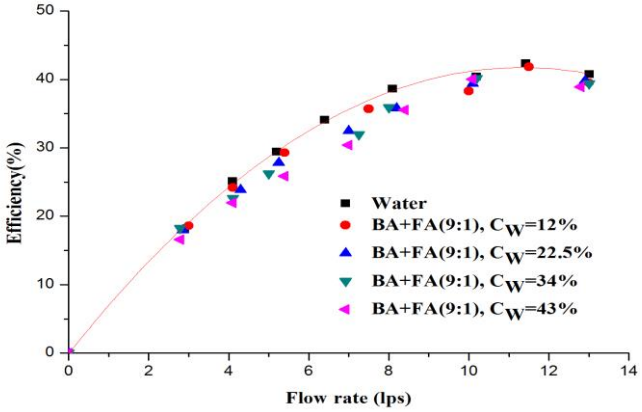

(c) Efficiency-flow rate characteristics

Figure 4.18: Performance characteristics of the centrifugal slurry pump with bottom ash and fly ash mixture (9:1) at 1150 rpm

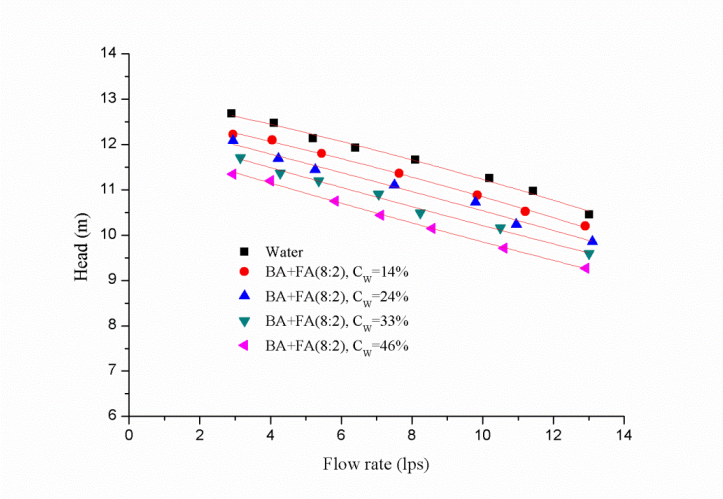

(a) Head-flow rate characteristics

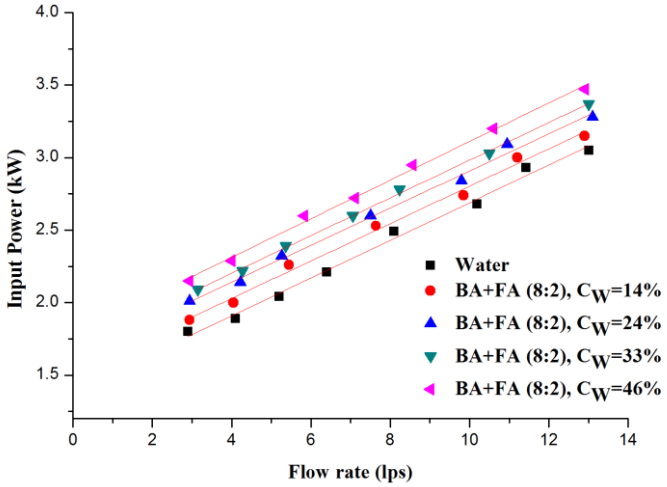

(b) Input power-flow rate characteristics

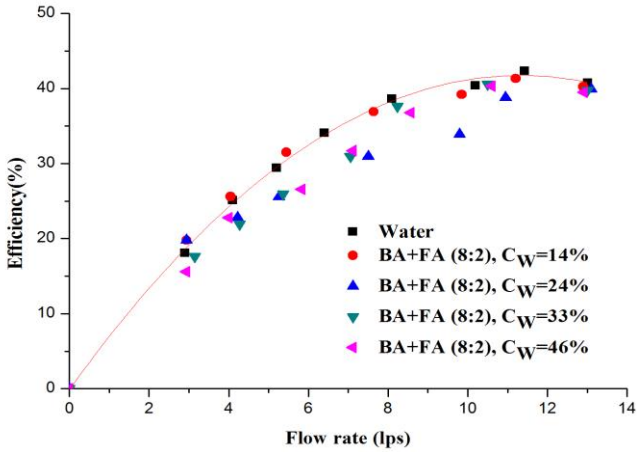

(c) Efficiency-flow rate characteristics

Figure 4.19: Performance characteristics of the centrifugal slurry pump with bottom ash and fly ash mixture (8:2) at 1150 rpm

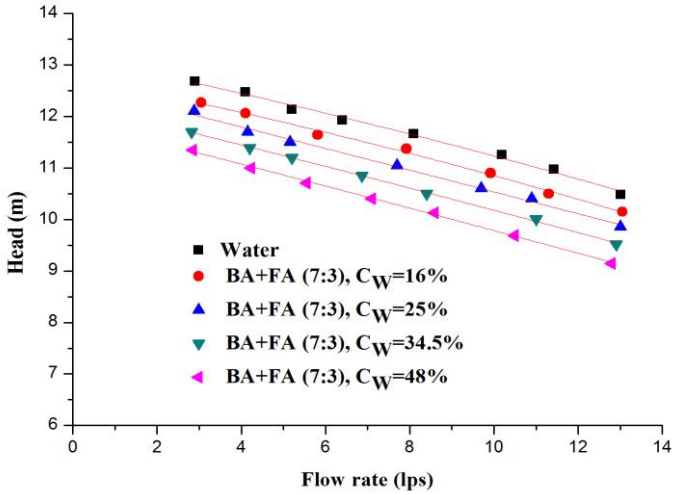

(a) Head-flow rate characteristics

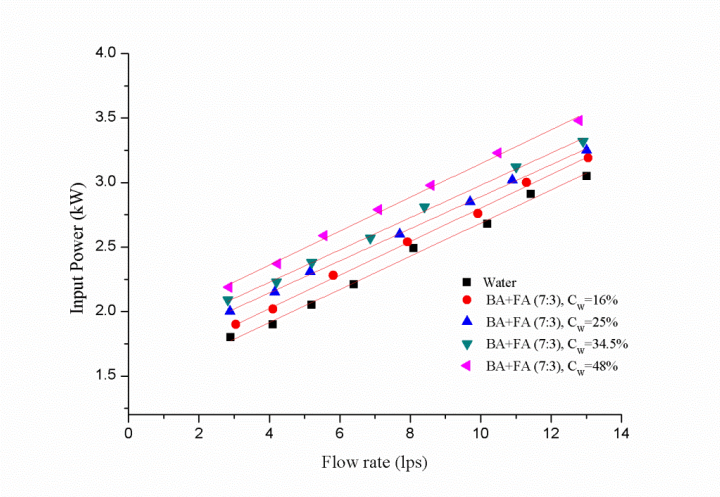

(b) Input power-flow rate characteristics

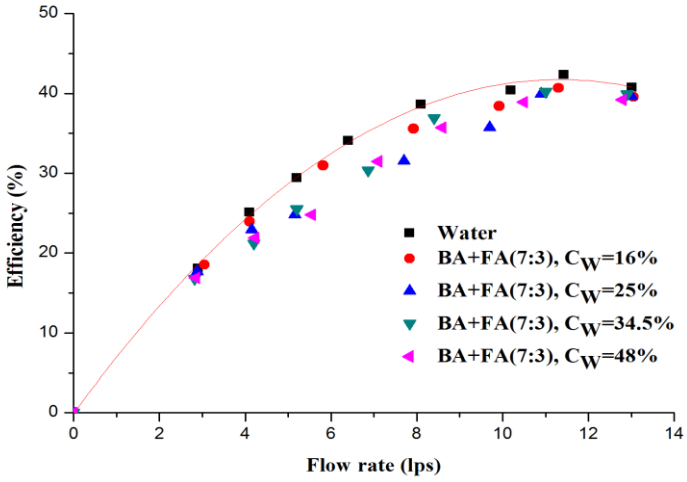

(c) Efficiency-flow rate characteristics

Figure 4.20: Performance characteristics of the centrifugal slurry pump with bottom ash and fly ash mixture (7:3) at 1150 rpm

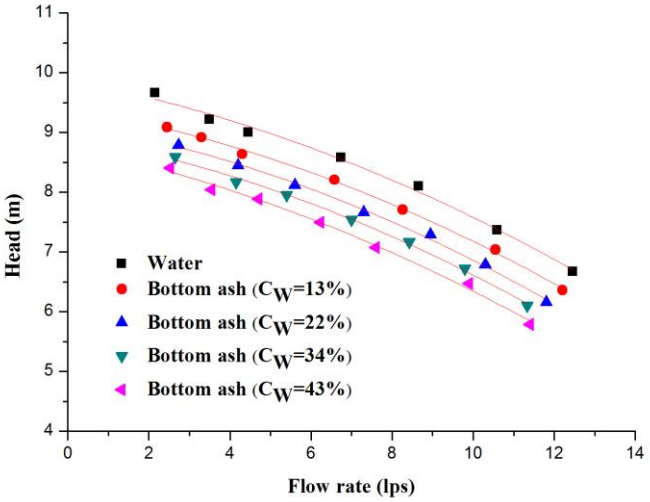

(a) Head-flow rate characteristics

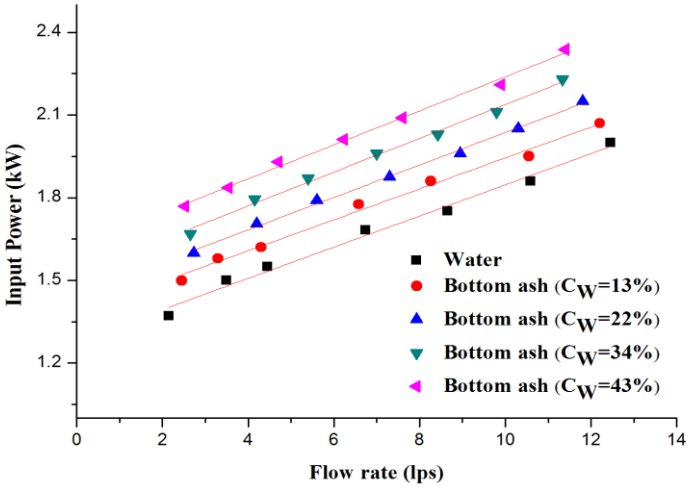

(b) Input power-flow rate characteristics

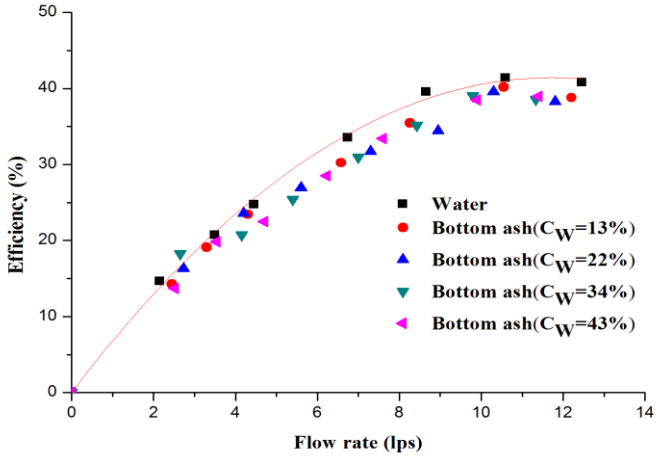

(c) Efficiency-flow rate characteristics

Figure 4.21: Performance characteristics of the centrifugal slurry pump with bottom ash slurry at 1000 rpm

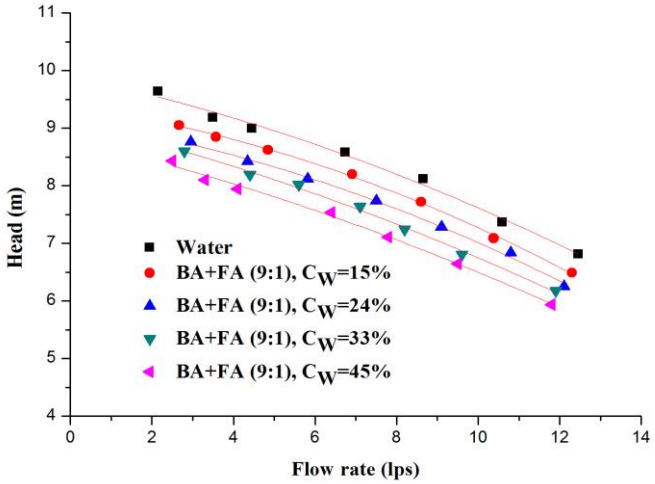

(a) Head-flow rate characteristics

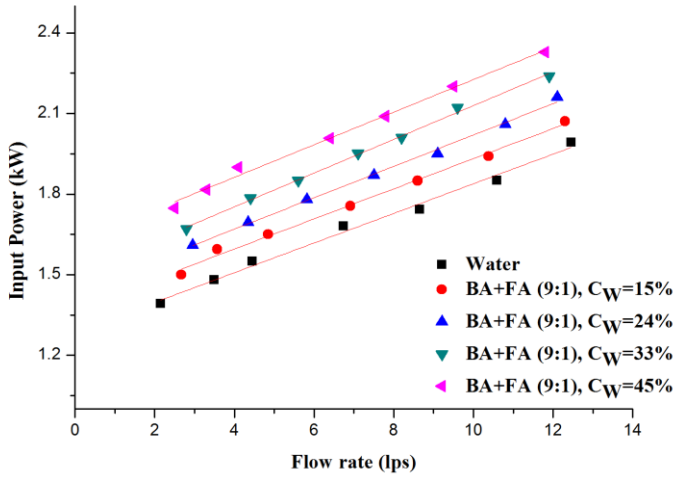

(b) Input power-flow rate characteristics

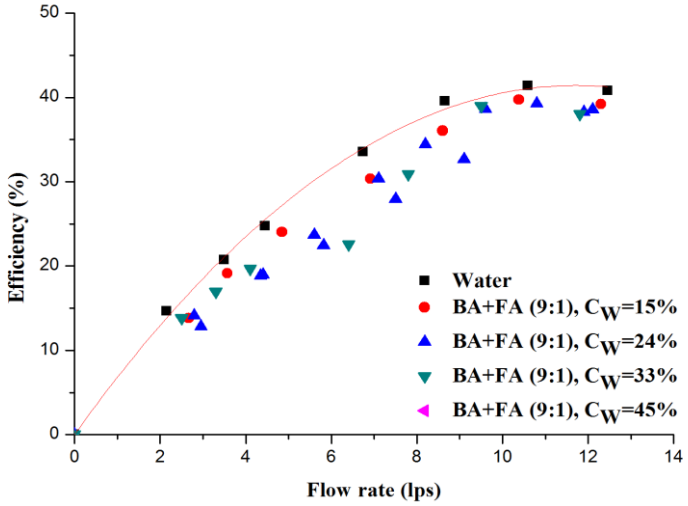

(c) Efficiency-flow rate characteristics

Figure 4.22: Performance characteristics of the centrifugal slurry pump with bottom ash and fly ash mixture (9:1) at 1000 rpm

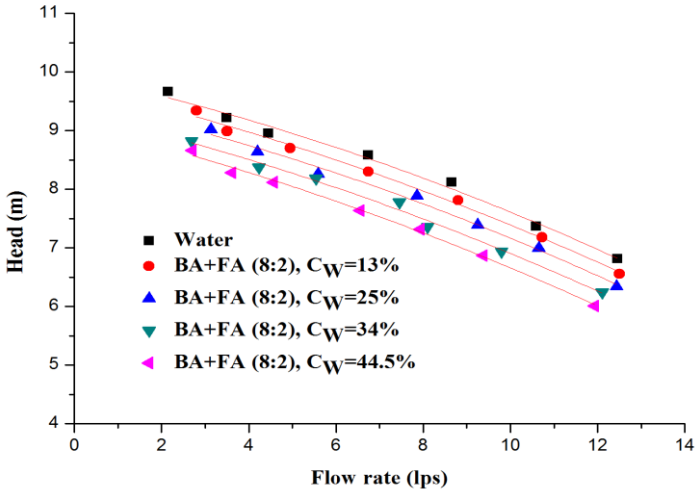

(a) Head-flow rate characteristics

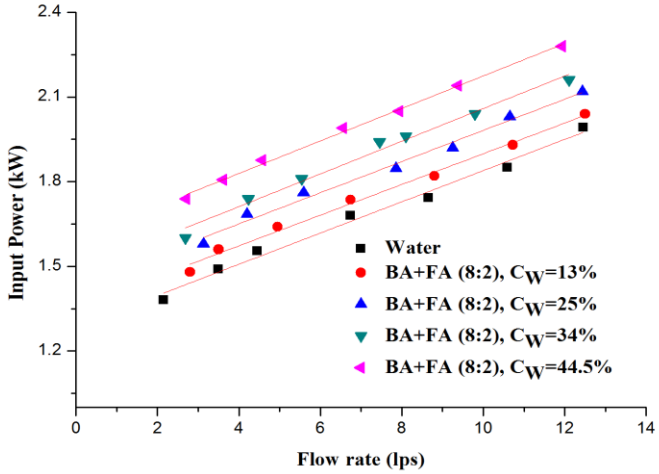

(b) Input power-flow rate characteristics

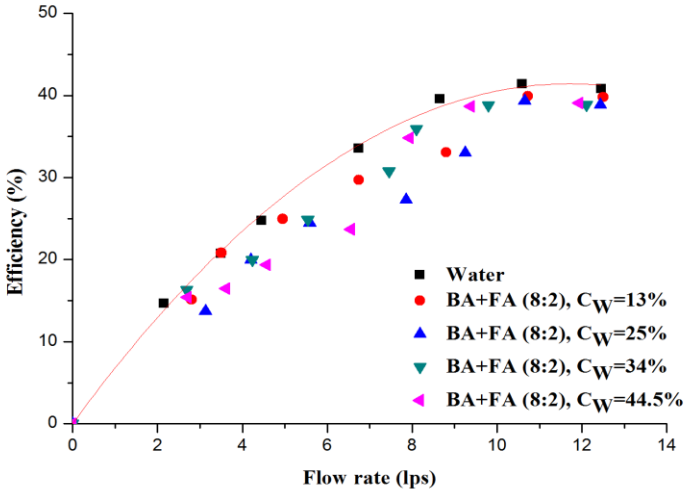

(c) Efficiency-flow rate characteristics

Figure 4.23: Performance characteristics of the centrifugal slurry pump with bottom ash and fly ash mixture (8:2) at 1000 rpm

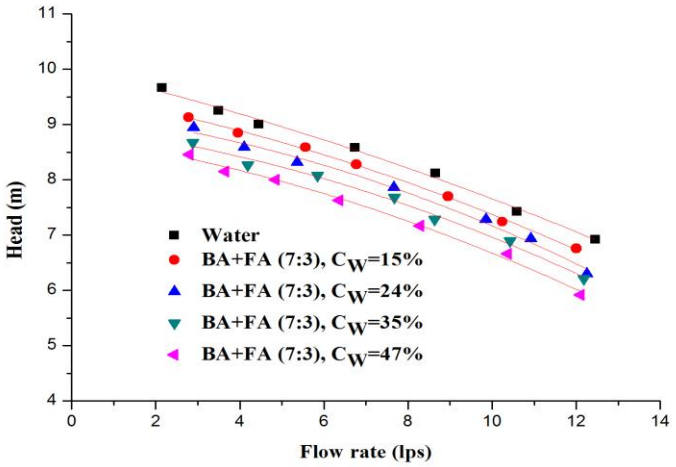

(a) Head-flow rate characteristics

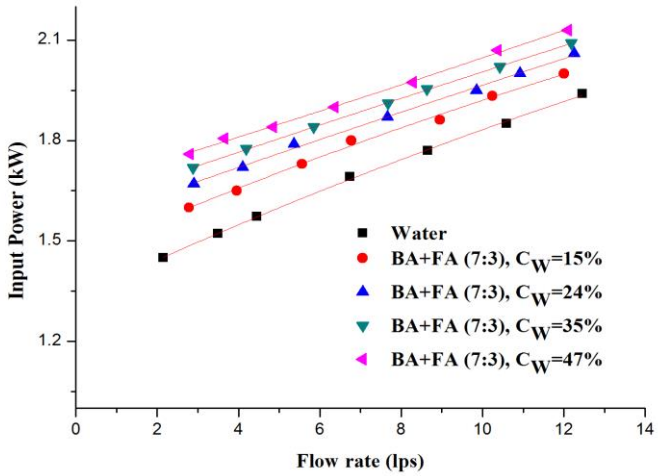

(b) Input power-flow rate characteristics

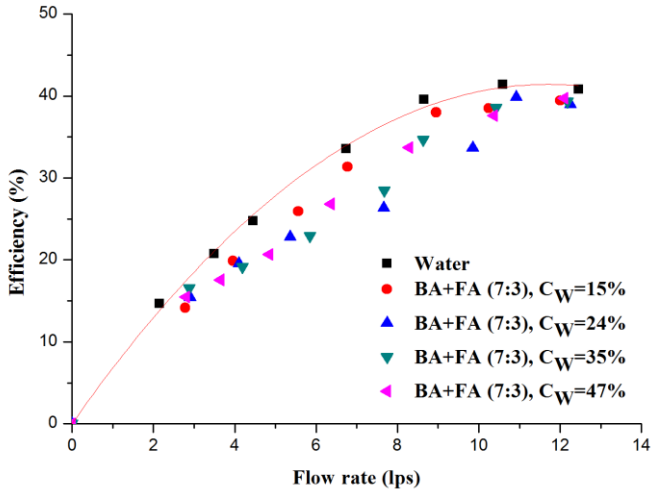

(c) Efficiency-flow rate characteristics

Figure 4.24: Performance characteristics of the centrifugal slurry pump with bottom ash and fly ash mixture (7:3) at 1000 rpm

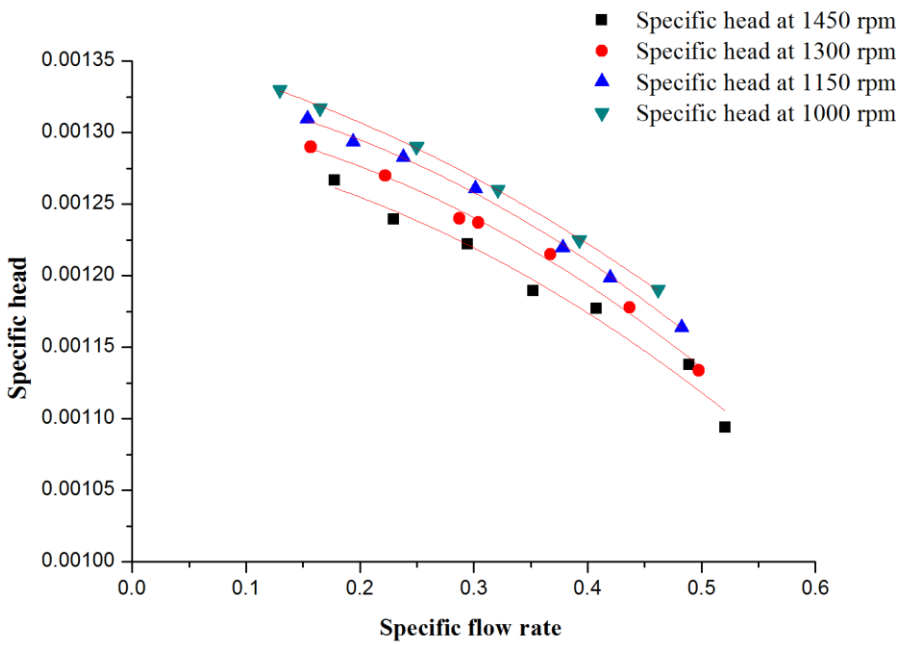

Figure 4.25: Specific head- flow rate characteristics of pump with water

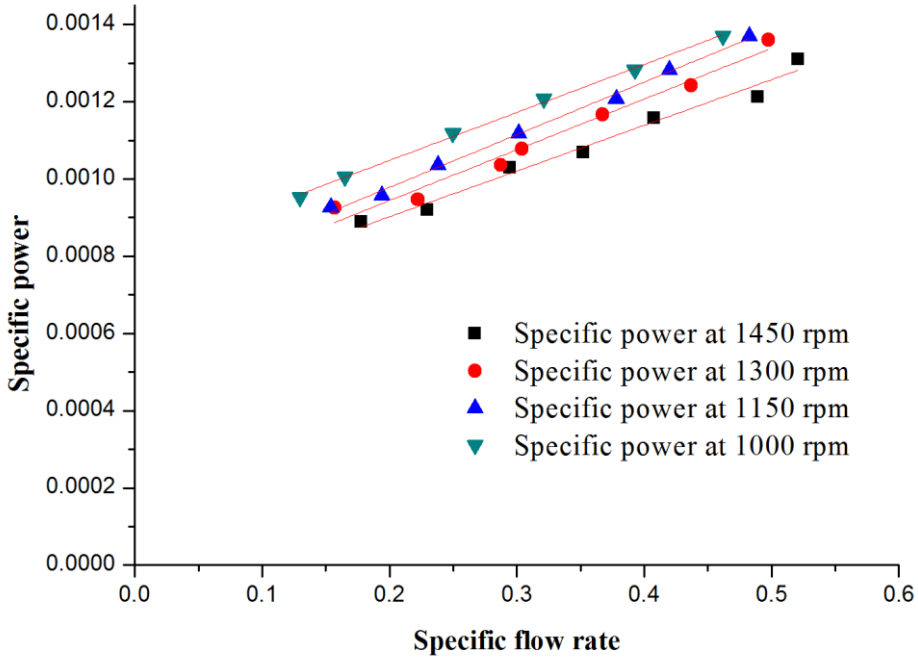

Figure 4.26: Specific power - flow rate characteristics of pump with water

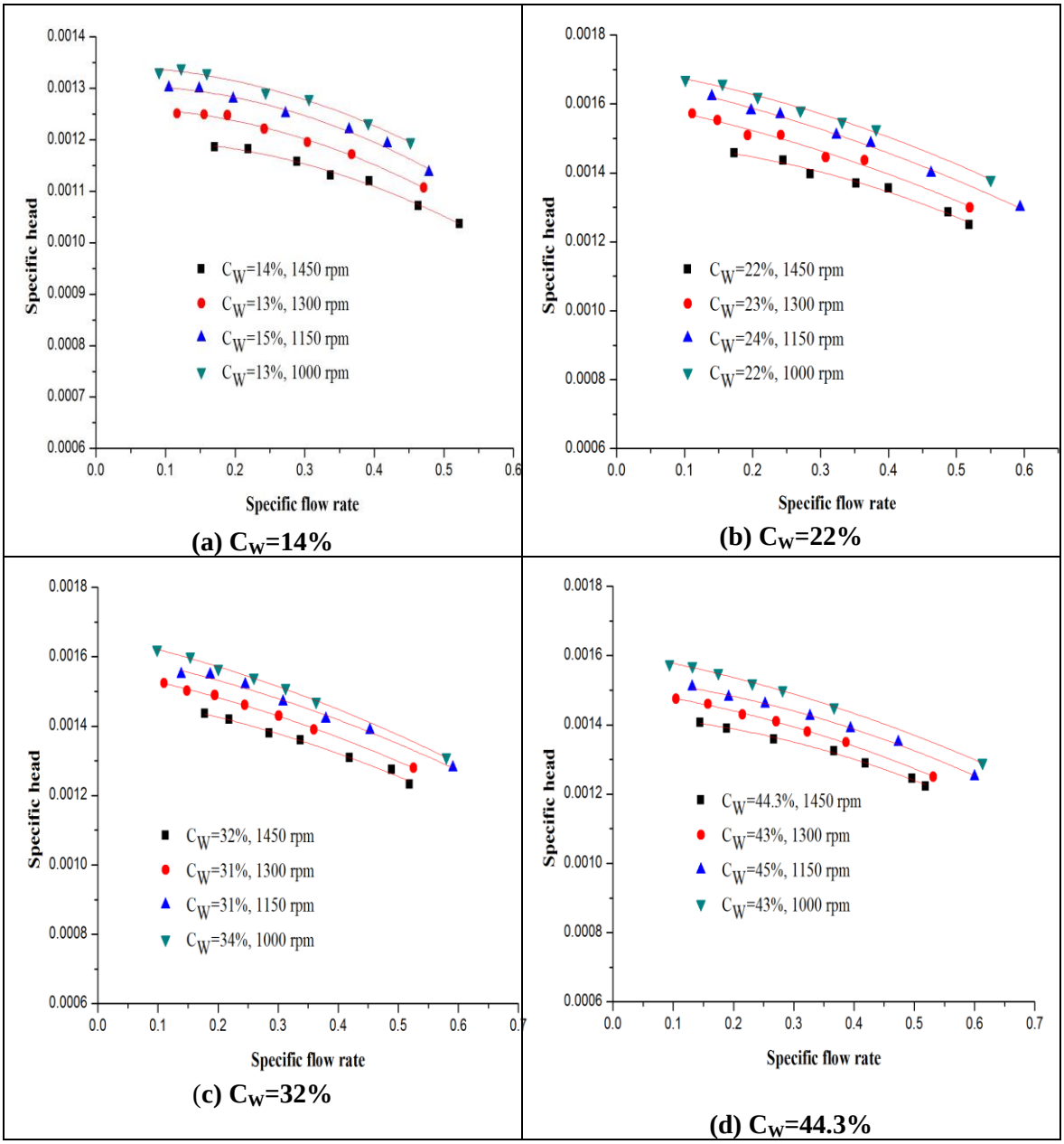

Figure 4.27: Specific head - flow rate characteristics of pump with bottom ash slurry at different concentration

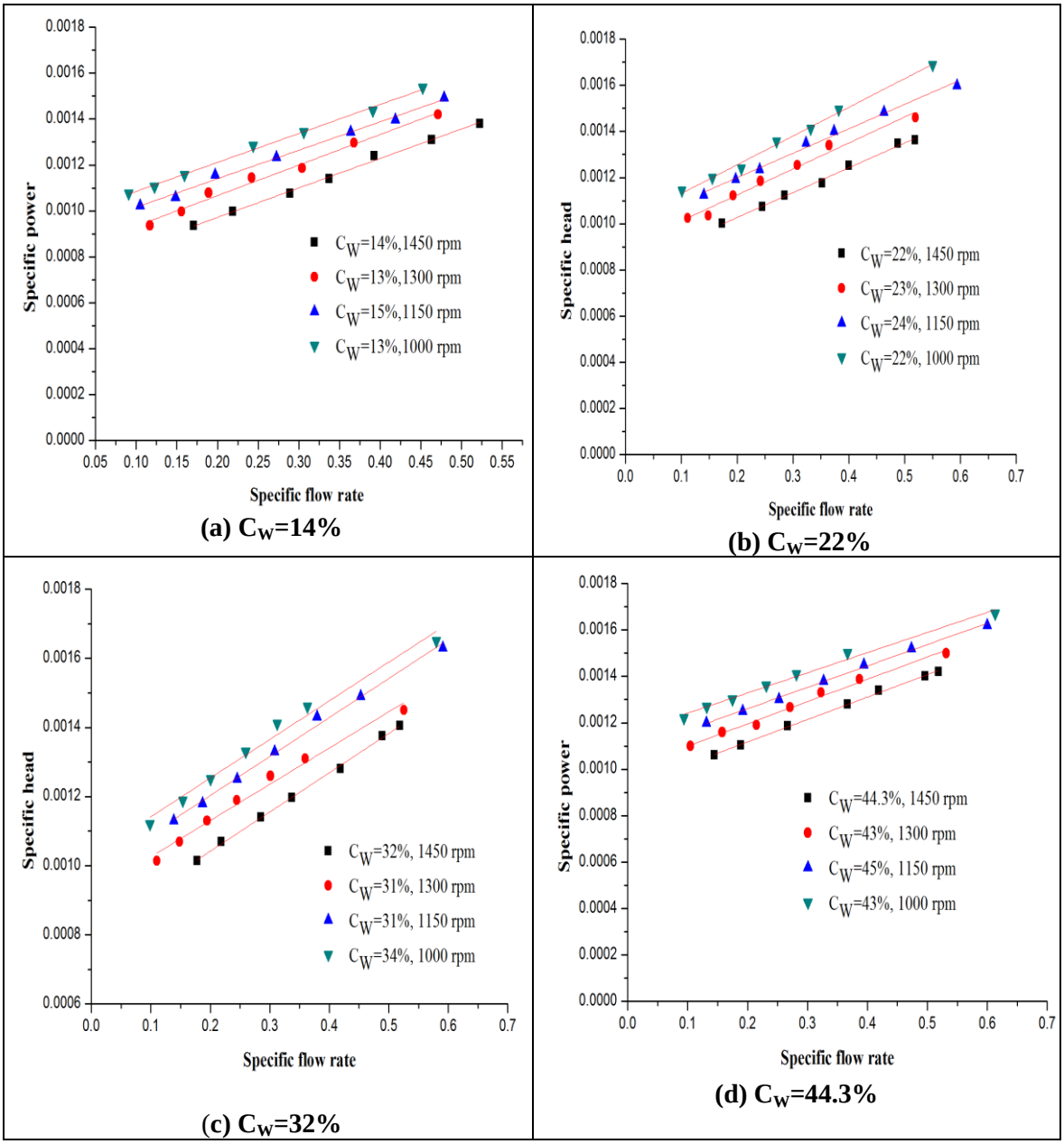

Figure 4.28: Specific power - flow rate characteristics of pump with bottom ash slurry at different concentration

CHAPTER 5

NUMERICAL EVALUTION OF CENTRIFUGAL SLURRY PUMP PERFORMANCE

In the recent years, Computational fluid dynamics (CFD) is being increasingly applied to design of the pumps. Simulation study makes it possible to visualize the flow field inside the centrifugal pump passages and provides the valuable information for hydraulic design. Currently user friendly commercial computational code like Fluent, CFX, and COMSOL are available which can be used directly for simulation purpose.

All CFD codes contain three main components:

i. A **pre-processor** which is used for modeling of the components. It includes geometry generation, mesh generation and the boundary conditions.
ii. A **flow solver** which is used to solve the governing equations of the fluid flow. Three methods are used to solve the problem.
    - Finite difference method
    - Finite element method
    - Finite volume method
iii. A **post-processor** which is used for obtaining the results in data format, graphical form and vector plots etc.

5.1 GOVERNING EQUATIONS OF CFD

Fluid flows are governed by the following three fundamental principles:

- Conservation of mass
- Conservation of momentum
- Conservation of energy

5.1.1Conservation of Mass Equation

The equation for conservation of mass is written as follows:

$$\nabla(\rho \vec{V}) = S_m \tag{5.1}$$

The equation is valid for incompressible as well as compressible flows. The source (S_m) is the mass addition in the continuous phase from the dispersed second phase.

For steady state incompressible fluid flow the continuity equation is given by:

$$\rho(\nabla \vec{V}) = 0$$

Where, $\nabla = \frac{\partial}{\partial x_i}\hat{i} + \frac{\partial}{\partial x_i}\hat{j} + \frac{\partial}{\partial x_i}\hat{k}$ and $V = u_i\,\hat{i} + u_j\,\hat{j} + u_k\,\hat{k}$

5.1.2 Conservation of Momentum Equation

Conservation of momentum equation is described as:

$$\nabla.(\rho \vec{V}\vec{V}) = -\nabla p + \nabla(\bar{\bar{\tau}}) + \rho \vec{g} + \vec{F} \tag{5.2}$$

Where,

The stress tensor $\bar{\bar{\tau}}$ is given as:

$$\bar{\bar{\tau}} = \mu[(\nabla \vec{V} + \nabla \vec{V}^T)] = -\frac{2}{3}\nabla.\vec{V} I \tag{5.3}$$

For steady state incompressible fluid flow, the momentum conservation equation is given by

$$\nabla.(\rho \vec{V}\vec{V}) = -\nabla p + \nabla.(\bar{\bar{\tau}}) + \rho \vec{g} + \vec{F}$$

5.1.3 Conservation of Energy Equation

$$\nabla.(\rho_i v) = -p\nabla.v + \nabla.(k\nabla T) + \varphi + S \tag{5.4}$$

5.2 TURBULENCE MODELS

Turbulence is characterized by fluctuations in the velocity flow field. Turbulence occurs when the inertia forces in the liquid dominant the viscous forces.

Turbulent flow variables say velocity may be divided in two components, one component is the time-averaged component$\bar{u}_i$ which is independent of time and other component is the fluctuating component (u_i'). Whose sum aggregate over a lay time period is zero.

$$u_i = \bar{u}_i + u_i'$$

The fluctuating quantities mix with the transport quantities like concentration, momentum and energy and produce the fluctuation in transported quantities. The amount of fluctuation may be small scale but have high frequency; they are very expensive to solve computationally in engineering calculation. The instantaneous governing equations can be assemble with time-averaged equations, or manipulated to minimize the small scale. Modified sets of governing equations can be solved numerically. Hoverer, modified governing equation contains additional parameters and turbulence models, are needed to obtain these variable. There is no single turbulence modeling scheme which is accepted to solve all types of the problems. The selection of the turbulence modeling scheme depends on the flow behavior, type of the problem, level of the accuracy, computational resources and time of the simulation process.

5.2.1 Reynolds Averaged Approach

For the complex geometry it is very difficult to determine the time- dependent solution of Navier –Strokes equations. Reynolds averaged method is an alternative method, which can be used to transform Navier –Strokes equations in such a way that the small scale turbulent fluctuations do not required to be solved directly (Fluent6.1 User's Guide, 2003). The continuity and momentum equation of Reynolds Averaged Navier stokes (RANS)arewritten as:

$$\frac{\partial}{\partial x_i}(\rho u_i) = 0 \tag{5.5}$$

$$\frac{\partial}{\partial x_j}(\rho u_i u_j) = -\frac{\partial p}{\partial x_i} + \frac{\partial}{\partial x_j}\left[\mu\left(\frac{\partial u_i}{\partial x_j} + \frac{\partial u_j}{\partial x_i} - \frac{2}{3}\delta_{ij}\frac{\partial u_l}{\partial x_l}\right)\right] + \frac{\partial}{\partial x_i}(-\rho\overline{u_i' u_j'}) \tag{5.6}$$

The Reynolds-averaged approach is used for solving many engineering problems, using turbulence models like **k-ε,k- ώ,** Spalart-Allmaras and RSM etc.

5.2.2 Boussinesq Approach

In the Reynolds-averaged approach of turbulence modeling scheme requires the Reynolds stresses in the equation (5.6). A common method employs the Boussinesqhypothesis to relate the Reynolds stresses to the mean velocity gradients:

$$-\rho\overline{u_i'u_j'} = \mu_t\left(\frac{\partial U_i}{\partial x_j}+\frac{\partial U_j}{\partial x_i}\right)-\frac{2}{3}\left(\rho k+\mu_t\frac{\partial U_i}{\partial x_i}\right)\delta_{ij} \quad (5.7)$$

Where μ, is turbulent viscosity and δ_0 is Kroneker delta which is 1 for i = j and 0 for i ≠ j. The convention of this notation is that i or j = 1 corresponds to x- direction, i or j = 2 corresponds to y direction. The left hand side of the equation (5.7) in terms of x and y can be written as follows:

$$-\rho\overline{u'v'} = \mu_t\left(\frac{\partial U}{\partial y}+\frac{\partial V}{\partial x}\right) \quad (5.8)$$

This hypothesis expresses the Reynolds stresses in terms of velocity gradients of mean velocities $\frac{\partial U}{\partial y}$ and $\frac{\partial V}{\partial y}$and a term μ called turbulence viscosity. It thus replaces the fluctuating components. Equation 5.7 and takes the following form:

$$(U.\nabla)U = -\frac{1}{\rho}\frac{\partial P}{\partial x}+\frac{\partial}{\partial x}\left[(\nu+\nu_t)\frac{\partial U}{\partial x}\right]+\frac{\partial}{\partial y}\left[(\nu+\nu_t)\frac{\partial U}{\partial y}\right] \quad (5.9\text{ a})$$

$$(U.\nabla)V = -\frac{1}{\rho}\frac{\partial P}{\partial x}+\frac{\partial}{\partial x}\left[(\nu+\nu_t)\frac{\partial V}{\partial x}\right]+\frac{\partial}{\partial y}\left[(\nu+\nu_t)\frac{\partial V}{\partial y}\right] \quad (5.9b)$$

The Boussinesq hypothesis is used by taking k-ε models, k-ω models and Spalart-Allmaras model for turbulence. Advantage of the Boussinesq approach is the low cost associated to solve turbulent viscosity terms. In the Spalart-Allmaras model, only one transport equation for turbulence viscosity is solved. While in the k-ε and k-ω models, two transport equations (turbulence kinetic energy (k) and turbulence dissipation rate (ε) or specific dissipation rate (ω) are solved.

5.2.3 Standard k-ε Model

The standard k-ε model is a semi-empirical model, based on model transport equations for the turbulence kinetic energy (k) and its dissipation rate (ε). The model transport equation for k is derived from the exact equation, while the model transport equation for ε as obtained using physical reasoning and bears little resemblance to its mathematical

counterpart. In the derivation of the k-ε model, it was assumed that the flow is fully turbulent, and the effects of molecular viscosity are negligible.

The turbulence kinetic energy and rate of dissipation is obtained from the following equations:

$$\frac{\partial}{\partial x_i}(\rho k u_i) = \frac{\partial}{\partial x_j}\left[\left(\mu + \frac{\mu_t}{\sigma_k}\right)\frac{\partial k}{\partial x_j}\right] + G_k + G_b - \rho\varepsilon - Y_M + S_k \tag{5.10}$$

and

$$\frac{\partial}{\partial x_i}(\rho \varepsilon u_i) = \frac{\partial}{\partial x_j}\left[\left(\mu + \frac{\mu_t}{\sigma_\varepsilon}\right)\frac{\partial \varepsilon}{\partial x_j}\right] + C_{1\varepsilon}\frac{\varepsilon}{k}\left(G_k + C_{3\varepsilon}G_b\right) - C_{2\varepsilon}\rho\frac{\varepsilon^2}{k} + S_\varepsilon \tag{5.11}$$

$$\mu_t = \rho C_\mu \frac{k^2}{\varepsilon} \tag{5.12}$$

For standard k-ε model, value of constant used is:

$C_{1\varepsilon}$=1.44, $C_{2\varepsilon}$= 1.92, C_μ = 0.09, σ_k = 1.0 and σ_ε= 1.3.

5.2.4 RNG k-ε Model

The RNG-based k-ε turbulence model is derived from the instantaneous Navier-Stokes equations, using a mathematical technique called “renormalization group" (RNG) methods.

$$\frac{\partial}{\partial x_i}(\rho k u_i) = \frac{\partial}{\partial x_j}\left(\alpha_k \mu_{eff}\frac{\partial k}{\partial x_j}\right) + G_k + G_b - \rho\varepsilon - Y_M + S_k \tag{5.13}$$

and

$$\frac{\partial}{\partial x_i}(\rho \varepsilon u_i) = \frac{\partial}{\partial x_j}\left(\alpha_\varepsilon \mu_{eff}\frac{\partial \varepsilon}{\partial x_j}\right) + C_{1\varepsilon}\frac{\varepsilon}{k}\left(G_k + C_{3\varepsilon}G_b\right) - C_{2\varepsilon}\rho\frac{\varepsilon^2}{k} - R_\varepsilon + S_\varepsilon \tag{5.14}$$

5.2.5 k- ώ Model

This is two-transport-equation model used by solving kinetic energy k and turbulent frequency ω. This model allows for a more accurate near wall treatment with switch from wall function to a low-Reynolds number formulation based on cell space. The model does not involve the complex non-linear damping functions.

Turbulence kinetic energy and turbulent frequency relation is given as:

$$\mu_t = \frac{k}{w} \tag{5.15}$$

5.3 MOVING REFERENCE FRAME (MRF)

When the momentum equation is solved in a rotating frame of reference, the acceleration of the fluid terms is appearing in the momentum equations. FLUENT allow to solve rotating frame problems using either absolute velocity or relative velocity.

$$\vec{v_r} = \vec{v} - (\vec{\omega} \times \vec{r}) \tag{5.16}$$

The left-hand sides of momentum equation with inertial reference frame is as follows:

$$\nabla.(\rho \vec{v}\vec{v}) \tag{5.17}$$

For rotating reference frame, the left-hand side is written as:

$$\nabla.(\rho \vec{v_r}\vec{v}) + \rho(\vec{\omega} \times \vec{v}) \tag{5.18}$$

In terms of relative velocities the left-hand side is written as:

$$\nabla.(\rho \vec{v_r}.\vec{v_r}) + \rho(2\vec{\omega} \times \vec{v_r} + \vec{\omega} \times \vec{\omega} \times \vec{r}) + \rho.\frac{\partial \vec{\omega}}{\partial t} \times \vec{r} \tag{5.19}$$

$$\nabla.(\rho \vec{v_r}) = S_m \tag{5.20}$$

The equation for torque calculation is given as:

$$T = \iint_S r v_\theta \rho \vec{v} \hat{n} dS \tag{5.21}$$

5.4 MULTIPHASE FLOW MODEL

The multiphase flow model is used for the simulation of the multiphase flow problem like solid-liquid, liquid-vapour, solid-vapor etc. The multiphase flow model is designed with local variables of each individual phases. The multi-phase flow problems are solved by the following two approaches:

- Euler-Lagrange approach
- Euler-Euler approach

In the Euler-Lagrange approach, liquid phase is treated as a continuous phase and mass and momentum conservation equations are solved in Eulerian framework using the time averaged Navier-Stokes equations with or without additional coupling terms, The dispersed phase is solved by tracking a large number of particles, bubbles or droplets in the Lagrangian framework. The dispersed phase can exchange conservation of mass, momentum

and energy with the liquid phase. Eulerian-Lagrangian approach is generally used for simulation of the small volume dispersed phase problems like simulation of fuel combustion, spray dryers and particle-laden flow etc. Eulerian-Eulerian approach is based on the principle of interpenetrating continuum and RANS form of the mass and momentum equations are solved for both the faces. As the volume of a phase cannot be carried by the other phases, concept of volume fraction is introduced. There are three different models used in Euler-Euler multiphase approach:

- Volume of fraction method (VOF)
- Mixture model
- Eulerian model

The VOF approach is generally applicable for separated flow where dispersed phase is well separated from the continuous phase with a distinct interface. In theVOF model, the momentum equations are shared by fluids and volume fraction of each fluid in computational cell is tracked throughout the domain. The Eulerian model is the most complex model among the other available multiphase models. It solves set of mass and momentum equations for each phase. Couplings are achieved through the pressure and inter phase exchange coefficients. The Eulerian model is used for the simulation of multi-phase flow problems like simulation of bubble columns, risers, particles suspension, and fluidized bed etc. The mixture model is used for simulation of two of more phases (liquid or particulate). It can also be used for modeling of homogenous two phase flow with very strong coupling. The mixture model solves for the mixture momentum equation and prescribes relative velocity for dispersed phase. The mixture model is used to simulate the sedimentation, bubbly flows and cyclone separators etc.

5.4.1 Governing Equation of Mixture Model

The mixture model solves the conservation of mass, momentum and energy equations for the mixture of both phases. The concept of slip velocity is used in the mixture model which allows the phases to move with different velocity.

Continuity Equation

$$\nabla(\rho_m \vec{v}_m) = 0 \qquad (5.22)$$

Mass average velocity is given by:

$$\vec{v}_m = \frac{\sum_{k=1}^{n} \alpha_k \rho_k \vec{v}_k}{\rho_m} = \frac{\alpha_s \rho_s \vec{v}_s \vec{v}_s + \alpha_f \rho_f \vec{v}_f}{\alpha_s \rho_s + \alpha_f \rho_f} \quad (5.23)$$

Mixture density is given by:

$$\rho_m = \sum_{k=1}^{n} \alpha_k \rho_k \quad (5.24)$$

Where subscript *k* represents *f* (fluid) or *s* (solid), and *m* represents mixture.

Momentum Equation.

$$\nabla(\rho_m \vec{v}_m \vec{v}_m) = -\nabla \mathrm{P} + \nabla . [\mu_{\mathrm{m}} (\nabla \vec{v}_m + \vec{v}_m^T)] + \rho_m \vec{g} + \nabla . \{ (\alpha_f \mu_f + \alpha_s \mu_s) \vec{v}_{dr} \vec{v}_{dr} \} \quad (5.25)$$

Where μ_{m} is the mixture viscosity given by:

$$\mu_m = \alpha_f \mu_f + \alpha_s \mu_s \quad (5.26)$$

Drift velocity $\vec{v}_{dr}$ takes the following form in mixture model:

$$\vec{v}_{dr} = \vec{v}_k - \vec{v}_m \quad (5.27)$$

The drift velocity and relative velocity ($\vec{v}_{kc}$) are determined by the following expression:

$$\vec{v}_{dr} = \vec{v}_{kc} - \sum_{k=1}^{n} c_k \vec{v}_{mk} \quad (5.28)$$

$$\vec{v}_{kc} = \frac{\tau_s}{f_{drag}} \frac{(\rho_s - \rho_m)}{\rho_s} a \quad (5.29)$$

Where τ_s is the particle relaxation time $\tau_s = \frac{\rho_s d_s^2}{18 \mu_s}$

$$f_{drag} = \begin{cases} 1 + 0.15 Re^{0.687} & Re \leq 1000 \\ 0.0183 ReRe & > 1000 \end{cases}$$

Acceleration $\vec{a}$ is expressed as

$$\vec{a} = \vec{g} - (\overrightarrow{v_m} . \nabla) \overrightarrow{v_m} - \frac{\partial \overrightarrow{v_m}}{\partial t} \quad (5.30)$$

The granular kinetic viscosity of solid –liquid mixture calculated using (Syamlal et al. 1993) and given in following expression

$$\mu_{s,kin} = \frac{\alpha_s d_s \rho_s \sqrt{\Theta_s \pi}}{6(3-e_{ss})} \left[1 + \frac{2}{5}(1+e_{ss})(3e_{ss}-1)\alpha_s g_{0,ss}\right] \quad (5.31)$$

The bulk viscosity of solid –liquid mixture calculated using (Lun et al. 1984) and given in following expression

$$\lambda_s = \frac{4}{3}\alpha_s \rho_s d_s g_{0,ss}(1+e_{ss})\left(\frac{\Theta_s}{\pi}\right)^{1/2} \quad (5.32)$$

5.5 MODELLING OF PUMP COMPONENT

For numerical analysis of the pump, the geometrical data of pump was required to generate a model in the software. In the present work, centrifugal slurry pump (50 M WILFLEY) as shown in Figure 5.1 is taken for the simulation. The pump impeller consists of five identical blades enclosed in a volute casing. For taking the dimensions of components, reverse engineering technique was used. The test loop was shut off and all the valves were closed to prevent any leakage of water or slurry.

The pump was first disconnected from the pipes of the test loop and the water in the pump assembly was drained. The pump assembly was disassembled and all the parts were separated. The assembly consisted of the casing, impeller and suction discs (frame and follower plate). The geometry of impeller, volute casing and inlet passage modelled by using Pro-E and imported in pre-processor Gambit2.3.16 (Fluent6.1 User's Guide, 2003). In the present work the clearance gap between casing and impeller was kept as 2.5 mm. Three-dimensional modelling of the pump components like impeller, inlet passage and volute casing are shown in Figure 5.2. The geometrical details of the pump are discussed in previous chapter 4 and given in Table 4.1. One of the most important tasks in CFD simulation is generation of the computational grid. Geometry is decomposed in to sub - domains for generation of unstructured mesh in Gambit. Actual flow domain is divided into different volumes namely inlet pipe, inlet passage, impeller hub, blade flow passage, volute casing and outlet pipe. In the present work, mixed hexahedral and tetrahedral mesh

is used in pump domain. In addition, quality of mesh is checked using the tools available in GAMBIT. The quality of mesh plays a significant role in the accuracy and stability of the numerical computation. The mesh quality parameters are skewness and aspect ratio.

5.5.1 Skewness of Mesh Element

Skewness of element affects the accuracy of the CFD simulation. Each element will have the value of skewness between 0 and 1. The skewness is classified in two ways, equi-angle skew and equi-size skew. The smaller value of equi angle skew and equisize skew are more acceptable. It is also important to verify that all of the elements in mesh have positive area/volume otherwise the simulation in 'FLUENT' solver is not possible.

The Equi-angle skew (Q_{ea}) is defined as follows:

$$Q_{ea} = \max imum\left\{\frac{\theta_{\max} - \theta_e}{180 - \theta_e}, \frac{\theta_q - \theta_{\min}}{\theta_e}\right\} \tag{5.33}$$

Where,

θ_{max}&θ_{min} = maximum and minimum angles between the edges of the element, degrees

θ_q = characteristic angle corresponding to an equilateral cell of similar form. For triangular and tetrahedral elements, $\theta e = 60^\circ$, for quadrilateral and $\theta eq = 90^\circ$ for hexahedral elements.

The Equi-size Skew (Q_{EvS}) is defined as follows:

$$Q_{EVS} = \frac{(S_e - S)}{S_e} \tag{5.34}$$

Aspect ratio is defined as the ratio of the maximum distance between the cell centroid and face centroids to the minimum distance between the nodes of the cell. For good quality of mesh the aspect ratio should be between 1 to10.

For the pump geometry, Equi-angle skew coefficient and aspect ratio of the grid was kept less than 0.82 and 3.25 respectively. Meshed pump assembly is shown in Figure 5.3 and detail of the pump component with different mesh size is given in Table 5.1.

Assumptions

The simulation of flow inside the centrifugal slurry pump is done on basis of following basic assumptions:

- Steady state condition.

- Incompressible fluid flow.
- Constant fluid properties.
- The impeller blades and casing walls are hydraulically smooth.

Boundary Conditions

The boundary conditions are specified as follows:

- Mass flow inlet is given at suction pipe entering section.
- Inlet passage faces, rotating faces of impeller and fixed faces of volute casing are considered as wall.
- At outlet face of delivery pipe section pressure outlet is applied.
- The suction pipe, impeller passages, volute casing, inlet passage and delivery pipe are considered as fluid zone.

Solution Parameters

- 3-D double precision solver was used to solve the simulation.
- Multiple Reference Frame technique (MRF) is used to simulate the pump performance.
- Clear water was taken as working fluid.
- Standard k - ε turbulence modeling scheme was used.
- A convergence criterion for continuity and momentum equation was set as 10^{-5}.
- First order scheme is used for pressure correction as well as for solving momentum turbulent kinetic energy and turbulence dissipation rate.
- SIMPLE scheme is used for pressure velocity coupling.
- To achieve convergence in less time under relaxation factor applied are 0.3 for pressure, 0.7 for momentum, 0.8 for kinetic energy and 0.8 for dissipation rate.

5.5.2 Grid Independent Test

In the present work three types of mesh namely type-A, type-B and type-C have been taken for checking of the grid independence test. The details of mesh quality inside the pump components for all the three types of mesh are given in Table-5.1. These simulation results are compared at best efficiency point of the pump with those obtained by the experimental measurement at 1450 rpm. The total pressure head developed by the pump with simulation of all the three types of the mesh is listed in Table 5.2. The deviation between predicted head and experimental head with type-A mesh is 6.96%, type-B mesh is 5.55% and type-C mesh is 3.16%. The mesh type-C shows the closer results with the experimental data and is, used for present work.

5.5.3 Turbulence Model for Pump Performance Characteristics

The different standard turbulence models k-ε, k-ώ RSM and RNG k- ε have been used and the numerical results obtained with water for each of turbulence models at best efficiency point of 1450 rpm speed are compared with experimental results as shown in Table 5.3.

From the Table 5.3, it can be observed that the deviation in head with standard k-ε model, k-ω model, RSM model and RNG k- ε model is 3.16 %, 7.32 %, 8.45 % and 6.25 %, respectively. The result shows that the lowest deviation in head is observed with standard k-ε turbulence model. Further Simulation time for k-ω model, RSM model and RNG k- ε is around 1.7, 2.8 and 2.5 times of that of the standard k-ε model. Thus the standard k-ε model requires lowest computational time compared to the other models and also results in better predictions.

Thus it is used for simulation of flow through the pump with water and solid – liquid mixture in the present work. Many researchers (Miner 2000; Tamm et al. 2001; and Zhou et al. 2003) have also used the k- ε turbulent model for CFD analysis of conventional centrifugal water pump.

5.6 PREDICTION OF CENTRIFUGAL SLURRY PUMP PERFORMANCE CHARACTERISTICS WITH WATER

The centrifugal slurry pump performance characteristics have been numerically estimated at different operating speeds of 1000, 1150, 1300 and 1450 rpm for water using standard k-ε turbulence model. The performance characteristics obtained in terms of head, power and efficiency are compared with the experimental results.

Figure 5.4 shows the numerical and experimental results of the performance characteristics of the pump at different operating speeds of 1000, 1150, 1300 and 1450 rpm with water. The head curve trend for both numerical and experimental results shows a decrease in head with increase in flow rate at all the operating speeds. The maximum deviation of the head developed experimentally and numerically is 3.16%, 4.39%, 4.75% and 4.89 % at the operating speeds of 1450, 1300, 1150 and 1000 rpm respectively.

Figure 5.5 shows the input power variation of the pump with flow rate. It is observed that the numerical results follow the same trends as experimental results and input power increases linearly with the flow rate at both the operating speeds. The maximum deviation of the experimental and numerical values of input power is 4.48 %, 4.24%, 4.79% and 4.97% at the operating speeds of 1450, 1300, 1150 and 1000 rpm respectively.

Figure 5.6 shows the efficiency variation of the pump with flow rate. It is observed that numerical results follow the same trend as that of experimental results at all the operating speeds. It is seen that the maximum pump efficiency obtained experimentally and numerically are 45.02% and 45.25% at 1450 rpm, 44.36% and 43.75% at 1300 rpm, 42.56 % and 42.31% at 1150 rpm, 41.37% and 42.28% at 1000 rpm, respectively. The above results show that pump efficiency calculated numerically is close to the experimental value at all pump speed. The maximum deviation of the numerical and experimental value of head, input power and efficiency are within 5%.These simulation data shows reasonable agreement with the experimental water data at the different speeds.

From the simulation results of head-flow rate characteristics with water (Figure 5.4), it is seen that the maximum head developed by the pump near shut of condition is 19.98 m (3.00lps), 15.86 m (3.00lps), 13.39 m (3.00lps), and 10.12 m (3.00lps), at the operating speed

of 1450, 1300, 1150 and 1000 rpm, respectively. The maximum input power to the pump was determined as 5.36 kW (14.00 lps), 3.96 k W (13.50lps), 3.28 k W (13.00 lps) and 2.25kW (13.00 lps) at the speed of 1450, 1300, 1150 and 1000 rpm, respectively.

5.7 PERFORMANCE PREDICTION OF THE CENTRIFUGAL SLURRY PUMP WITH BOTTOM ASH SLURRY

The mixture model is used for the numerical simulation of solid liquid flow through centrifugal slurry pump. The water and bottom ash are taken as a primary phase and secondary phase respectively. The concentration of bottom ash is taken in the terms of volume fraction. The volume fraction of the slurry is defined as ratio of volume of secondary phase in the cell to the total volume of the cell. The volume fraction of the bottom ash slurry is calculated as 0.09, 0.13, 0.19 and 0.26 at weight concentration of 15%, 25%, 35% and 45% respectively. The 3D segregated solver is used for simulation of bottom ash slurry. The particle diameter of the bottom ash is taken as 162 μ m (see Table 3.2). The granular viscosity and granular bulk viscosity is calculated using (Syamlal et al. 1993 and Lun et al. 1984) model. The First order scheme is used for pressure correction as well as for solving momentum turbulent kinetic energy and turbulence dissipation rate. SIMPLE scheme is used for pressure velocity coupling.

The performance characteristics of the centrifugal slurry pump is numerically estimated with bottom ash slurry for concentration of 15%, 25%, 35% and 45% (by weight) at rated speed of 1450 rpm. The numerically simulated performance characteristics of the pump with bottom ash slurry in the terms of parameters like flow rate, total head, input power, efficiency are shown in Figure 5.7 and tabulated in Table 5.4 at constant pump speed of 1450 rpm.

The performance characteristics of the slurry pump with water are shown in Figure 5.4. It can be observed from the Figure 5.4 that the maximum head developed by the pump is 19.98 m (at 3.0 lps) and the maximum efficiency attained is 45.02% (13.2 lps). Figure 5.5 shows that the pump input power for water increases steadily with increase in flow rate and its maximum value is 5.36 kW at 14.00 lps flow rate.

The head-flow rate curves for bottom ash slurry at any given concentration is shown in Figure 5.7 (a) which shows the drooping nature similar to experimental data (See Figure

4.7). The total head developed decreases with increase in concentration of the bottom ash slurry. The total head developed at BEP reduces with increase in concentration by weight from 15% to 45% with the maximum drop of 0.96 m of water column. From the Figure 5.7 (b), it is observed that the input power increases with increase in the flow rate at all concentrations similar as the experimental results. At BEP it is seen that input power increases 9.93 % with increase in concentration by weight from 15 % to 45 %. From Figure 5.7 (c), it is seen that the efficiency of the pump decreases with increase in the solid concentrations.

The pump performance is evaluated with addition of fly ash in the bottom ash slurry in the ratio of 9:1, 8:2 and 7:3 respectively. The weighted mean particle diameter for fly ash was nearly one third of that of the bottom ash (Table 3.2). The bottom ash is coarse particulate whereas fly ash is a fine particulate material. When the fly ash added in the bottom ash, the weighted mean particle diameter gets reduced. The weighted mean particle diameter of the mixture of bottom ash and fly ash in the ratio of 9:1.8:2 and 7:3 found as 138, 117 and 105 µ m.The specific weight of the mixture determined as 2.18, 2.14 and 2.11 of the mixture of bottom ash and fly ash in the ratio of 9:1.8:2 and 7:3.

The particle diameter, density, solid concentration and viscosity of the slurry are the key parameters, which change the flow distribution inside the pump passage (Liu et al. 2011; Yi et al. 2011 and Yuliang et al. 2013). Though the viscosity of the bottom ash slurry increases slightly with addition of the fly ash in the bottom ash (see Figure 3.9), it seems that it has little effect on increase in the head losses. Due to reduction in the particle diameter and density of the mixture with addition of fly ash in bottom ash, the pump performance characteristics has improved for mixture of fly ash and bottom ash at any given concentration. The simulation performance characteristics of the pump with all mixtures of fly ash and bottom ash at 1450 rpm are shown in Figures 5.8- 5.10.

Figures 5.8- 5.10 show nearly similar nature of pump performance with all mixtures of the fly and bottom as depicted by the experimental results (Figure 4.8-4.10). The head developed reduces with increase in concentration at any given flow rate for all concentrations. At the BEP, the drop of the head observed is 1.55 m for bottom ash slurry, 1.48 m for mixture of bottom ash and fly ash in the ratio of 9:1, 1.44 m for mixture ratio of 8:2 and 1.38 m for mixture ratio of 7:3. This observation show that with addition of the fly

ash in the bottom ash mixture, the pump head drop reduces approximately 0.07 m for mixture of bottom ash and fly ash in the ratio of 9:1, 0.11 m for mixture ratio of 8:2 and 0.14m for mixture ratio of 7:3 at BEP.

The simulation data of the performance characteristics of the centrifugal slurry pump with bottom ash slurry at different speeds of 1450, 1300, 1150 and 1000 rpm are presented in Figures 5.7, 5.11, 5.12 and 5.13 respectively. The variation in head, power and efficiency with solid concentrations at the all four speeds shows the similar trend as experimental result (Figure 4.7, 4.13, 4.17 and 4.21) with minor deviations.

The reduction in head is less at 1000 rpm and is only 0.51 m (Figure 5.13 a) with increase in concentration by weight from 15 % to 45 % (by weight). Similar the value of reduced 0.64, 0.72 and 0.96m with increase in same solid concentration of bottom ash at the speed 1150, 1300 and 1450 rpm which is shown in (Figure 4.12 a), (Figure 5.10 a), and (Figure 5.7 a) respectively. The input power curves at all the speeds (Figures 5.7b, 5.11b, 5.12b and 5.13 b) also appear to be nearly similar nature. Lower input power values are seen at lower speed and higher input power values for higher speed at all discharge rates (Figure. 5.7 b and 5.13 b). The maximum input power to the pump at 1450 rpm was determined as 6.15kW (14.00 lps) and 1000 rpm was determined as 2.62 kW (13.00 lps). At the speed 1150 and 1300 rpm, the maximum input power of the pump were determined as 3.68 kW (13.00 lps) and 4.18 kW (13.50 lps). The efficiency curve at the all the operating speeds with water pass through all the data points (Figures 5.7c , 5.11 c , 5.13c and 5.17c) and appear to be nearly similar observation.

5.8 VARIATION OF HEAD RATIO AND POWER RATIO

The comparison of pump performance in the terms of head ratio and power ratio at 1450 rpm through simulation result at B.E.P for different solid concentrations is given in Table 5.5 and Figure 5.14. From Figure 5.14, it is observed that head ratio decreases with increase in the concentration of the slurry with all the bottom ash slurries with and without fly ash similar to the experimental data (see Table 4.9). For both types of slurry with and without addition of fly ash, head ratio is not a function of flow rate. With addition of the fly ash proportion in bottom ash head ratio value improves. The comparison of the trends

of variation of head ratio with bottom ash slurries with and without addition of fly ash shows that the value of head ratio is varies 0.91–1.0 for all the concentrations tested through simulation studies. Figure 5.15 shows the variation of Power ratio for pump with solid concentrations of the bottom ash slurry with and without addition of fly ash. The power ratio increases with increase in solid concentration of the bottom ash. With addition of the fly ash proportion in bottom ash, power ratio decreases. The power ratio of the bottom ash slurry with and without the ash varies 1-1.18 for all the concentrations (Table 5.5).

Figure 5.16 and 5.17 show the comparison of experimental data of head ratio and power ratio with the predicted data. The *x*-axis represents the experimental value and *y*-axis the predicted value. A straight line shows the zero residual or the fitted model line. Implying that, all the points would have been lying on that if there is zero residual or no residual. Thus a reasonable agreement can be observed. Also, 100% of the data points of the head ratio and power ratio lie within the deviation limits of +6%, and ±8% (Figures 5.16-5.17).

5.9 STATIC PRESSURE AND VELOCITY DISTRIBUTION OF PUMP WITH WATER

The numerical simulation can provide information on the flow characteristics inside the pump and helps the engineer to design the particular pump. Numerical simulation also helps to reduce the cost and time of fabricating and testing of the prototype pumps and reduces the profit of manufacturers. For this reason, CFD analysis was used for flow structure analysis of many different pumps (Hornsby 2002; Cao et al. 2005). Effort was made by many researchers in the past few years to simulate the flow field of a conventional centrifugal pump to establish its performance characteristics with water. Many researchers (Gayo et al. 2002; Gonz´alez et al.2002; Byskov et al.2003; Asuaje et al.2005; Gonzalez and Santolaria 2006) studied the performance analysis of conventional centrifugal pumps using CFD code.

Static pressure distribution in an orthogonal plane at the middle of the impeller section and the volute section for pump at B.E.P ($Q/Q_{bep}=1$) and low flow ($Q/Q_{bep}=0.2$) for 1450 speed are presented in Figure 5.18. It is observed that static pressure gradually

increases from inlet to outlet of impeller at both flow rate conditions. The static pressure in the impeller and volute channels is asymmetry distributed. The maximum static pressure appears at outlet regions of impeller and the minimum one at the back of blade at impeller inlet section. At the impeller-volute interaction section non uniform pressure distribution is observed. The high pressure drop is found at the diffuser duct of the casing.

The static pressure distribution at the off design condition (Q/Q_{bep}=0.2) for 1450 speed is shown in Figure 5.18 (b). It is observed that the static pressure increases with decrease in flow rates (Q/Q_{bep}=0.2). The low pressure area is observed at the suction side of the blade inlet at small flow rate condition. The static pressure on diffusion section of volute outlet also increases at flow rates (Q/Q_{bep}=0.2) while the static pressure on the same place decreases clearly at larger flow rate. Almost same pressure rise in all the channels of the impeller, no much pressure increase in the volute casing of the nozzle section. At the volute and impeller interface position, pressure fluctuation is observed. The rate of pressure fluctuation found more at low flow rate rates (Q/Q_{bep}=0.2) as compared to design flow rate (Q/Q_{bep}=1).

Velocity vectors are useful to identify directional motion of fluid particles in the flow domain of impeller and volute casing. The absolute velocity distribution in the mid plane of the impeller and casing at the design condition (Q/Q_{bep}=1) and low flow condition (Q/Q_{bep}=0.2) for 1450 speed are shown in Figure 5.19. As shown in the Figure 5.19, the absolute velocity increases from impeller inlet to outlet and reaches maximum value at impeller outlet and lower at impeller inlet and volute outlet. In all the channels of the impeller, absolute velocity is almost uniform. The absolute velocity distribution is also found uniform in casing section, but in the discharge section velocity increases and pressure decreases.

It is also observed that there is good guidance of the flow in the volute section but recirculation zone appears at the diverging section of the volute casing at 20% of BEP flow rate. Inside the impeller flow velocities are relatively uniform for all blade passages at design flow rate condition, but backflow occurs near the pressure surface of the pump impeller at 20% of BEP flow rate.

The velocity vector contour at the tongue of the impeller and volute interface are shown in the Figure 5.20 at the design condition (Q/Q_{bep}=1) and off design condition

(Q/Q_{bep}=0.2) for speed 1450 rpm. From the Figure 5.20, it is clearly visible the flow separation between the tongue and the impeller passage. At the impeller outlet due to the interaction between the impeller blades and the tongue of the volute casing, amplitudes of pressure fluctuation can be observed. The static pressure value is very low near the tongue region.

At the off design condition, pressure fluctuation in the tongue region was observed higher as compared to the design flow rate. The static pressure distribution of the centrifugal slurry pump at operating speed 1450 and 1000 rpm are shown in Figure 5.18 and 5.21. From the Figures 5.18 and 5.21, it is seen that the static pressure increases with the increase in rotational speed of the pump. At 100 rpm speed, pump shows the similar pressure and velocity distribution as 1450 rpm speed at both design and low flow rates (Figure 5.22).

5.10 VOLUME FRACTION DISTRIBUTION OF BOTTOM ASH SLURRY

The volume fraction distributions of the bottom ash slurry suspension inside the centrifugal slurry pump are shown in Figure 5.23**.** The simulation data were analyzed with solid concentration of 15, 25, 35 and 45% (by weight) at the B.E.P flow rate operating conditions. It is found that the volume fraction distribution is uneven in both the impeller and the volute casing. In the impeller, particles mainly flow along the pressure surface and hub, due to the influence of centrifugal and inertial force; in the volute, particles mainly accumulate in the region near to the exit of volute, and the largest volume fraction is observed at the tongue.

The volume faction increases with increase in solid concentration of the bottom ash suspension. With increasing solid concentration of the slurry, it enhances uniformity in the solid distribution due to enhancement of interference effect between solid particles. The ash pariculate suspension becomes almost homogeneous, which suggests that the interaction and interference effect between solid particles having the controlling factor of the slurry flow. At high concentrations, it minimizes the erosion wear and improves the performance of the pump.

Numerical simulations were carried out to estimate the performance characteristics of the centrifugal slurry pump handling bottom ash slurry with and without fly ash. Following observations are made:

- Standard k- ε shows reasonable agreement with the experimental results as compared to the other turbulence models.
- The difference between the predicted and experimental values of head, input power and total efficiency are less than 5%.Thus CFD results show good agreement with experimental data for complete operating range of the pump.
- The deviation of predicted value of head ratio and power ratio with experimental data is lie within the limits of ±8%.
- At the low concentration of bottom ash slurry, volume fraction distribution is inhomogeneous and at high concentration the pariculate suspension becomes almost homogeneous which may help to reduce the erosion wear and also improves the performance of pump .

Table 5.1: Mesh quality of the centrifugal slurry pump component

Mesh type	Component	Mesh Size (mm)	Tetrahedral element	Hexahedral element	Total element	Equie size Skewness	Aspect ratio
A	Inlet Passage	4	241871	31008	272879	0.8	3.12
	Casing	3.5	542864	55626	598490	0.81	3.05
	Impeller	2	142081	310083	272879	0.82	3.09
					1021132	0.78	3.07
B	Inlet Passage	4	241871	31008	272879	0.78	3.12
	Casing	2.5	686744	74240	760984	0.82	3.25
	Impeller	2.5	142081	7682	149763	0.82	3.09
					1183626	0.79	3.21
C	Inlet Passage	3	494366	132180	626546	0.77	3.03
	Casing	3	545790	56474	602264	0.81	3.04
	Impeller	3	163390	8303	171693	0.76	3.09
					1400503	0.77	3.06

Table 5.2: Grid independency test

Description	Flow rate (kg/s)	Head (mwc)	% Deviation
Experimental water data at B.E.P	13.2	16.80	----
Mesh type-A	13.2	17.97	6.96
Mesh type-B	13.2	17.69	5.55
Mesh type-C	13.2	17.33	3.16

Table 5.3: Numerical performance data with different turbulence models

Turbulence model	Total head (mwc)	% deviation
Experimental data at B.E.P (13.2 lps)	16.80	-------
Standard k-ε	17.33	3.16
Standard k-ώ	18.03	7.32
RSM	18.22	8.45
RNG, k- ε	17.85	6.25

Table 5.4 : Numerical performance of the pump at 1450 rpm with bottom ash slurry

Water						
Flow rate (lps)	**Head (m)**	**Input Power(kW)**	**Efficiency(%)**	**HR**	**PR**	**ER**
14	16.75	5.36	43.13	1	1	1
13.2	17.33	5.01	45.02	1	1	1
11	18.02	4.85	40.15	1	1	1
9	18.45	4.36	37.27	1	1	1
8	18.9	4.26	34.76	1	1	1
6	19.27	3.72	30.42	1	1	1
4.5	19.36	3.35	27.19	1	1	1
3	19.98	3.06	20.90	1	1	1
Concentration 15.0% (S =1.09)						
14	15.61	5.40	40.27	0.952	1.008	0.980
11	16.91	4.91	42.50	0.936	1.018	0.992
9	17.30	4.40	37.41	0.954	1.014	0.951
7	17.59	4.10	33.37	0.961	1.02	0.981
5	18.59	3.58	28.53	0.953	1.032	0.984
3	19.16	3.15	21.46	0.96	1.031	0.993
Concentration 25.0% (S=1.16)						
14	15.24	5.51	40.97	0.921	1.05	0.950
11	16.88	5.01	41.35	0.937	1.04	0.092
9	16.97	4.53	35.04	0.92	1.04	0.941
7	17.02	4.22	32.67	0.93	1.05	0.960
5	18.25	3.69	27.65	0.938	1.06	0.985
3	18.63	3.30	20.12	0.925	1.08	0.962
Concentration 35.0% (S =1.24)						
14	14.74	5.83	38.68	0.910	1.13	0.920
11	16.31	5.44	40.55	0.905	1.12	0.954
9	16.77	4.88	34.29	0.909	1.12	0.921
7	16.96	4.62	31.98	0.936	1.15	0.940
5	17.69	4.04	26.47	0.920	1.16	0.943
3	18.54	3.58	19.67	0.929	1.17	0.941
Concentration 45.0% (S=1.33)						
14	14.64	6.15	38.97	0.900	1.18	0.950
11	16.07	5.69	40.46	0.892	1.16	0.970
9	16.54	5.19	33.55	0.902	1.17	0.901
7	16.85	4.86	31.28	0.909	1.17	0.919
5	17.31	4.25	27.06	0.910	1.16	0.964
3	18.26	3.76	19.22	0.915	1.21	0.920

Table 5.5: Simulation head ratio and Power ratio

Bottom ash			BFA 9:1		BFA 8:2		BFA 7:3	
Concentration	HR	PR	HR	PR	HR	PR	HR	PR
0	1	1	1	1	1	1	1	1
15	0.95	1.02	0.96	1.01	0.96	1.01	0.96	1.01
25	0.94	1.05	0.95	1.04	0.95	1.03	0.95	1.03
35	0.93	1.14	0.93	1.12	0.94	1.10	0.94	1.09
45	0.91	1.18	0.92	1.18	0.94	1.17	0.94	1.15

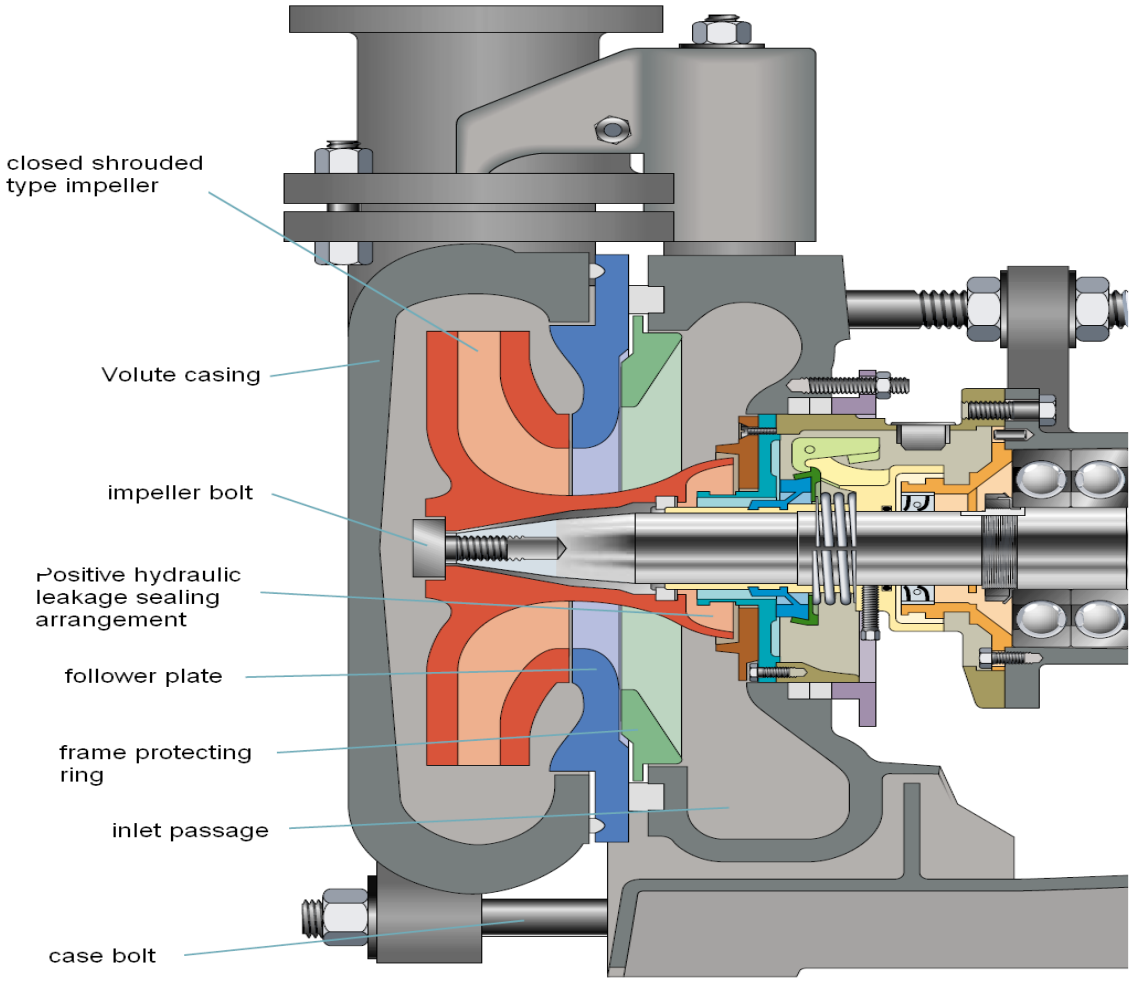

Figure 5.1: Cross sectional view of centrifugal slurry pump (Wilfley, 2002)

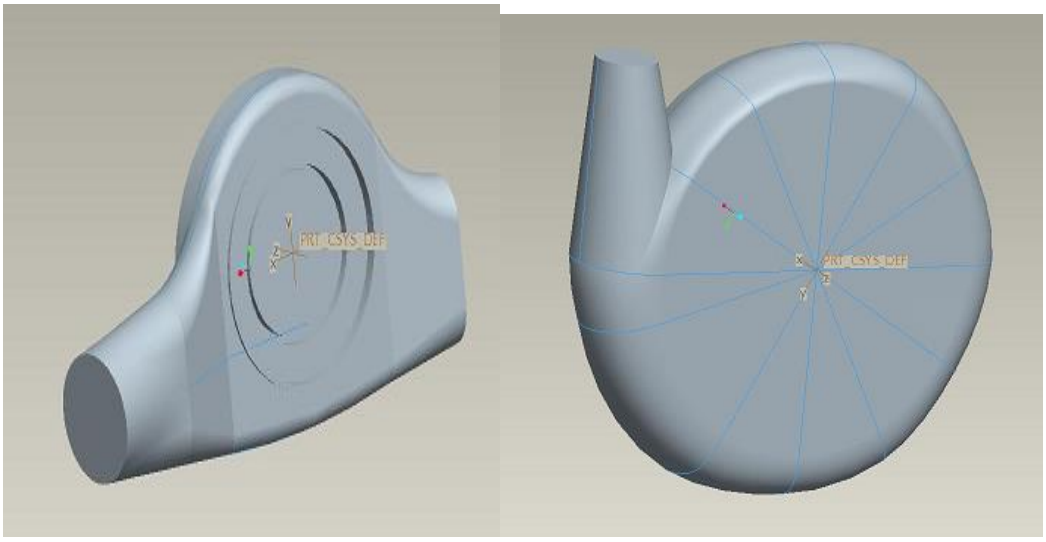

(a) Inlet passage (b) Casing

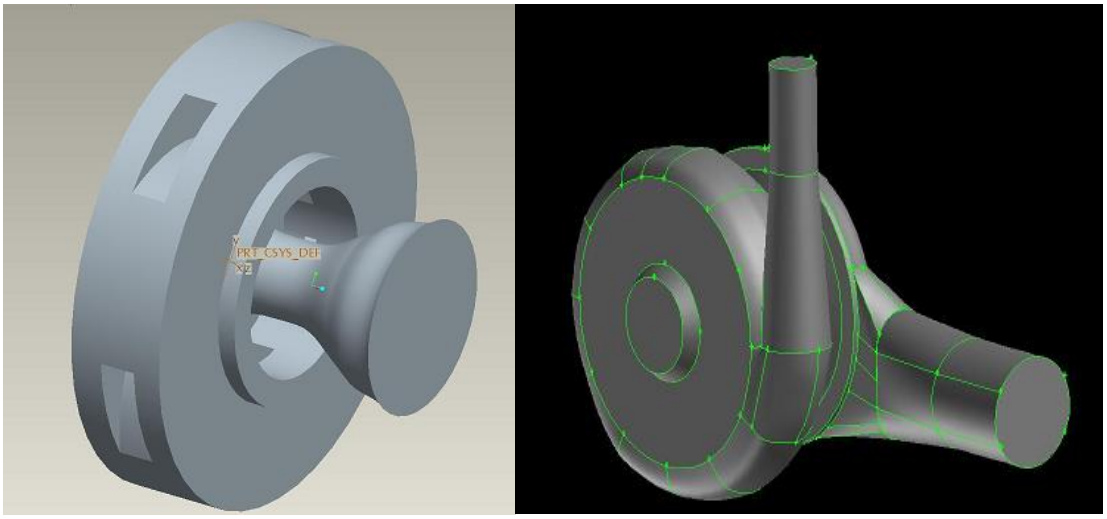

(c) Impeller domain (d) Pump assembly

Figure 5.2: Modelling of pump component

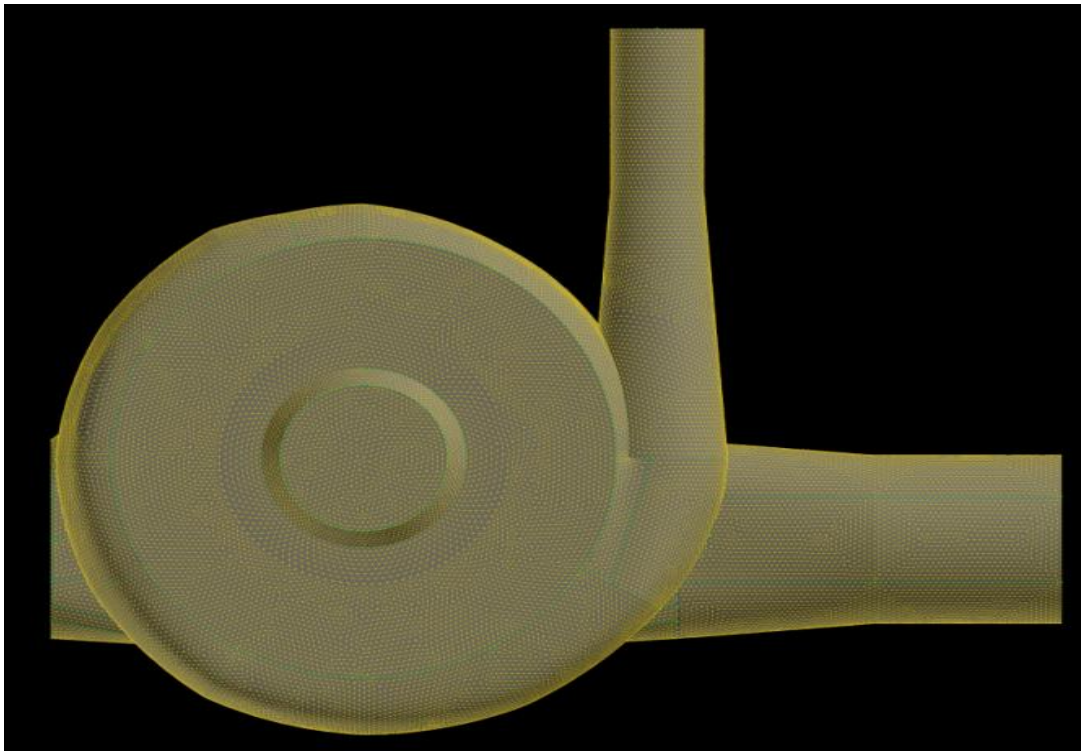

Figure 5.3: Meshed Pump Assembly

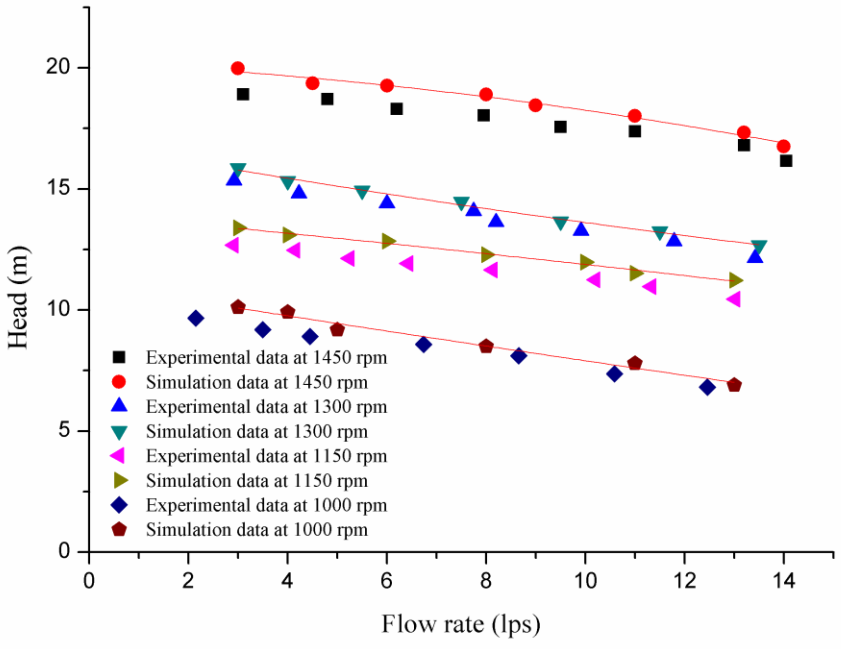

Figure 5.4: Head-flow rate characteristics of pump at different speeds

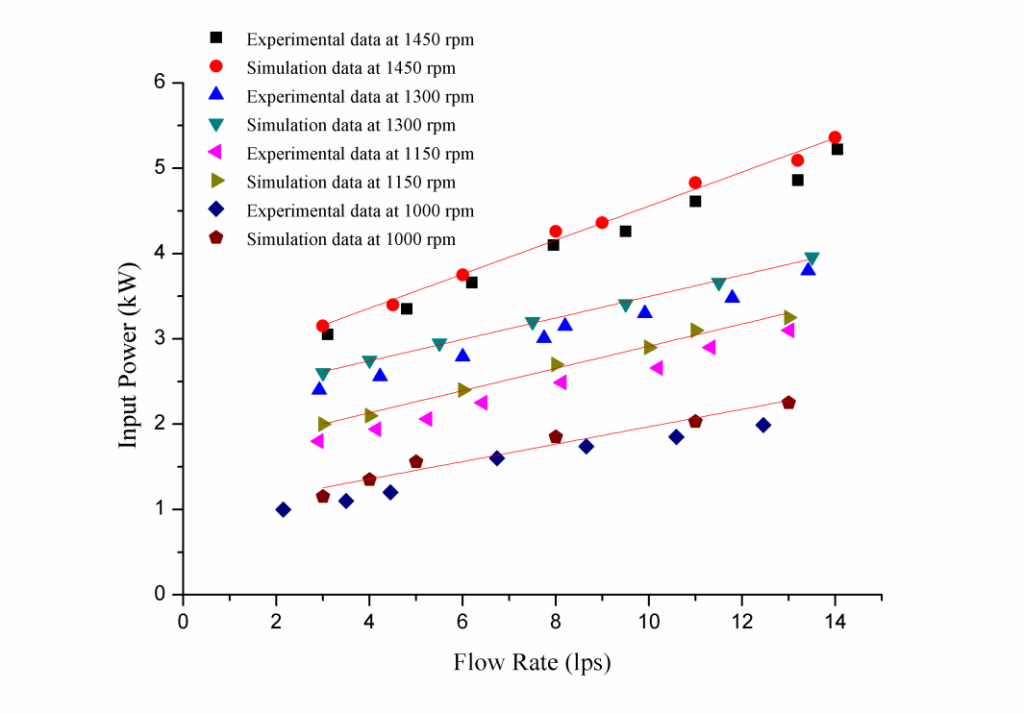

Figure 5.5: Input power-flow rate characteristics of pump at different speeds

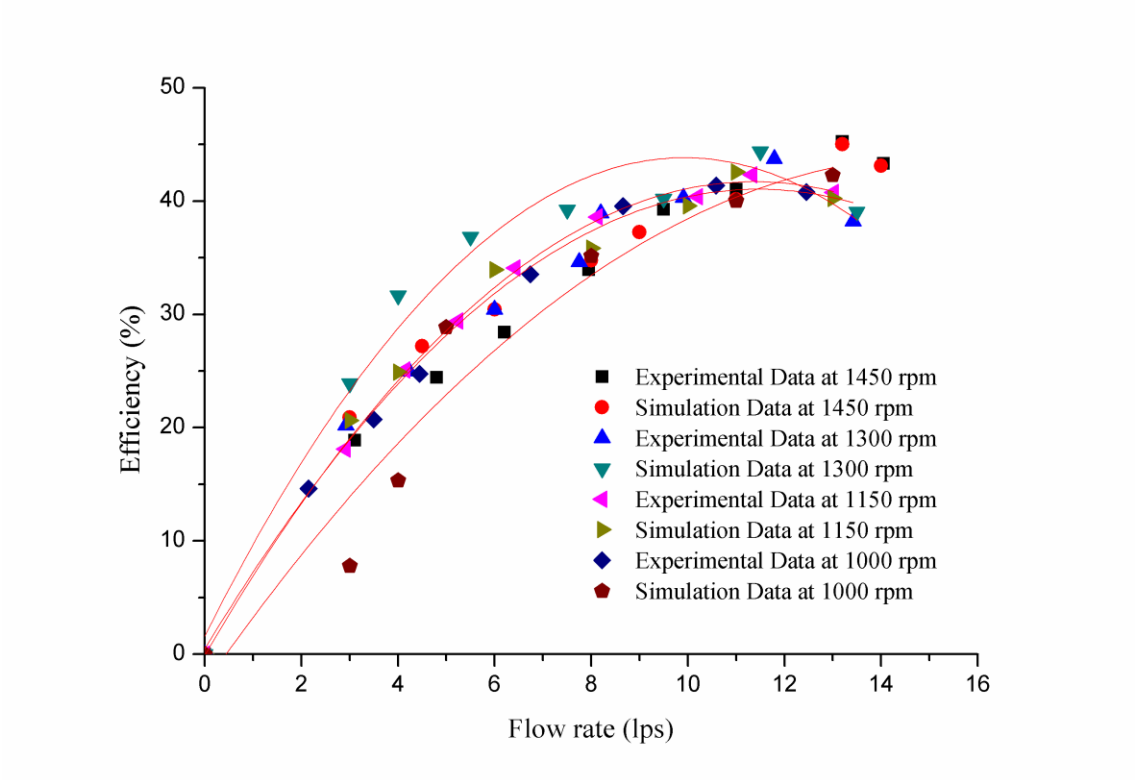

Figure 5.6: Efficiency -flow rate characteristics of pump at different speeds

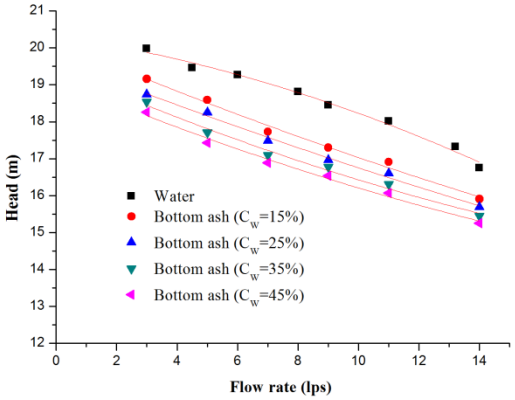

(a) Head-flow rate characteristics

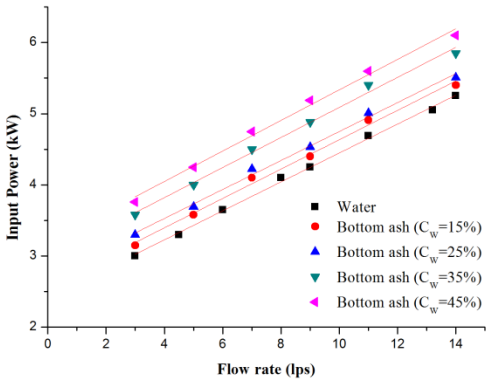

(b) Input power-flow rate characteristics

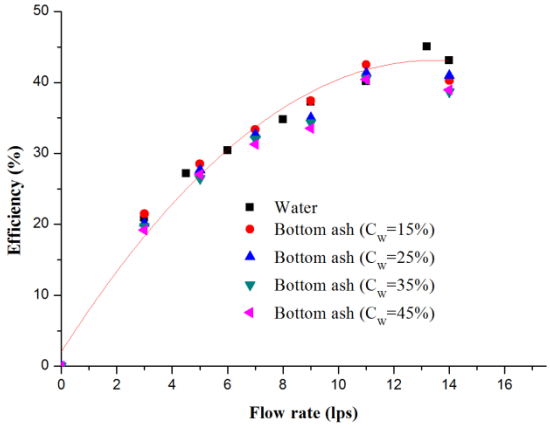

(c) Efficiency -flow rate characteristics

Figure: 5.7: Numerical performance characteristics of pump with bottom ash slurry at 1450rpm

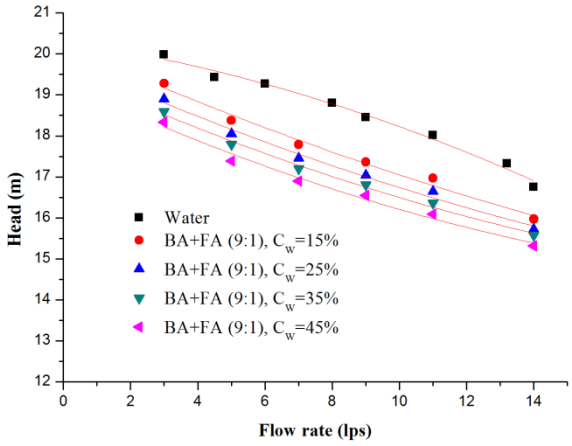

(a) Head-flow rate characteristics

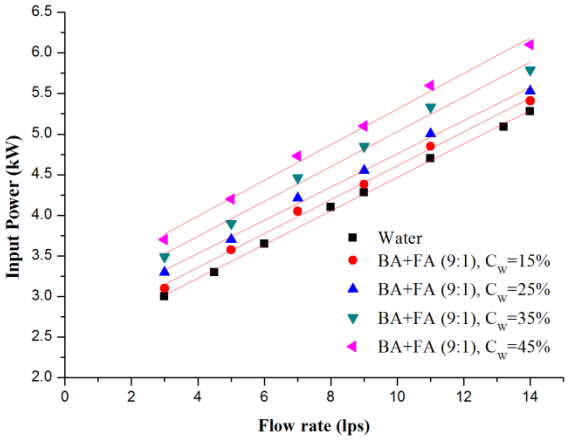

(b) Input power-flow rate characteristics

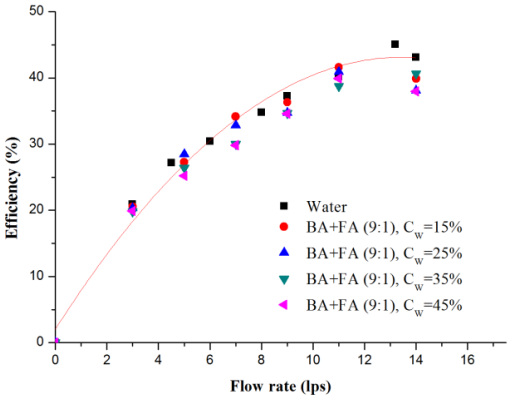

(c) Efficiency -flow rate characteristics

Figure: 5.8: Numerical performance characteristics of pump with bottom ash and fly ash mixture (9:1) at 1450rpm

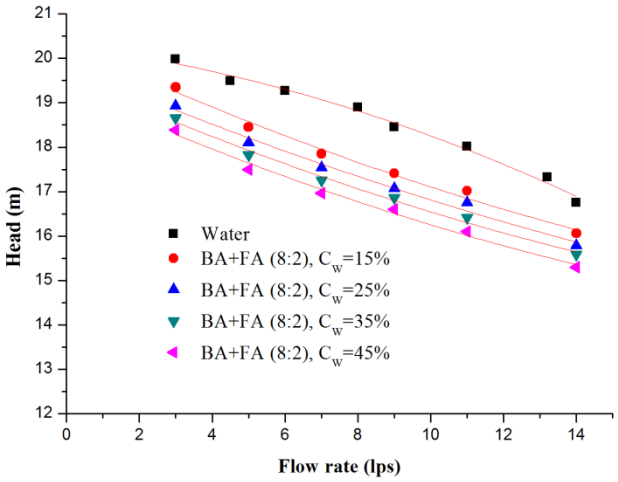

(a) Head-flow rate characteristics

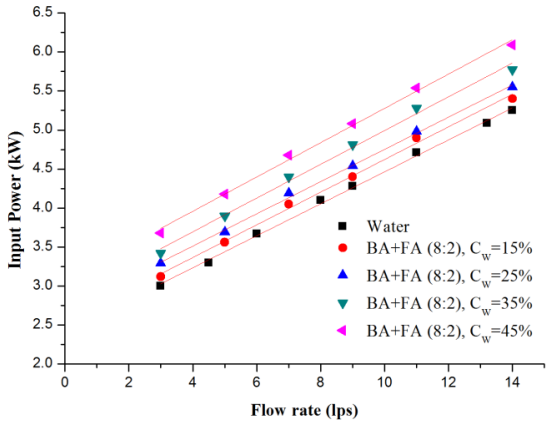

(b) Input power-flow rate characteristics

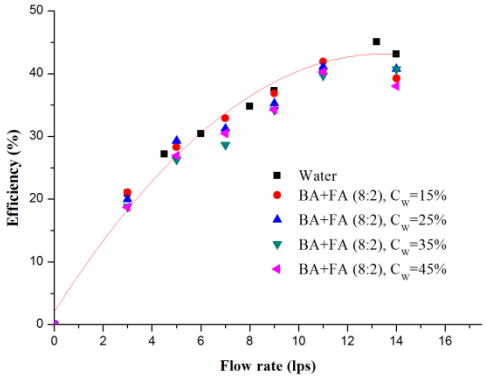

(c) Efficiency -flow rate characteristics

Figure: 5.9: Numerical performance characteristics of pump with bottom ash and fly ash mixture (8:2) at 1450rpm

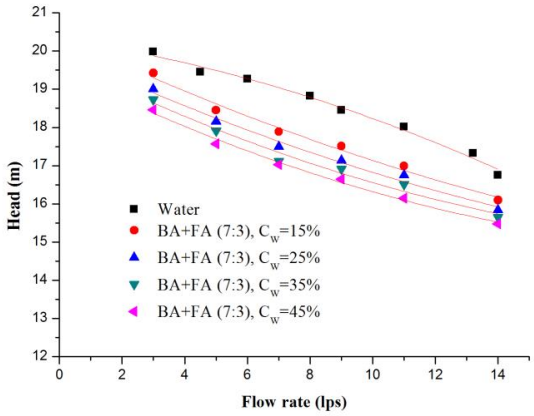

(a) Head-flow rate characteristics

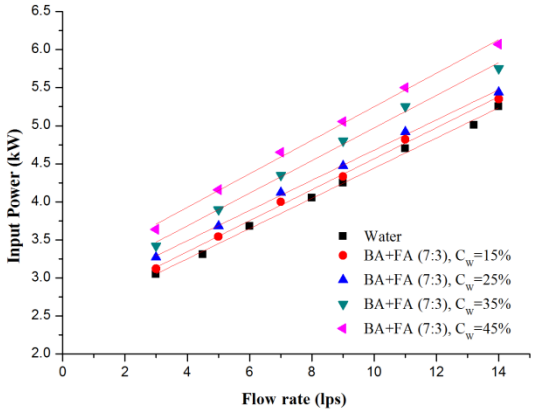

(b) Input power-flow rate characteristics

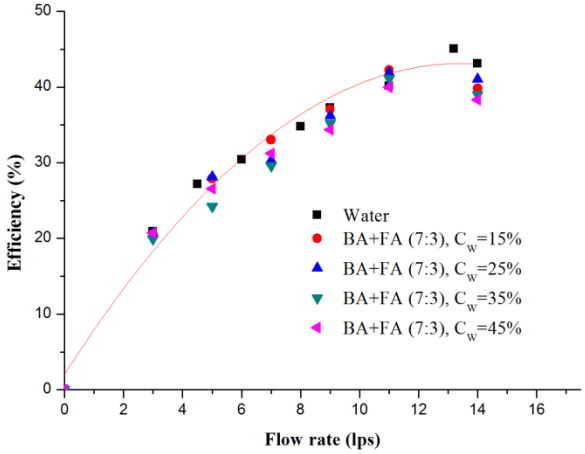

(c) Efficiency -flow rate characteristics

Figure: 5.10: Numerical performance characteristics of pump with bottom ash and fly ash mixture (7:3) at 1450rpm

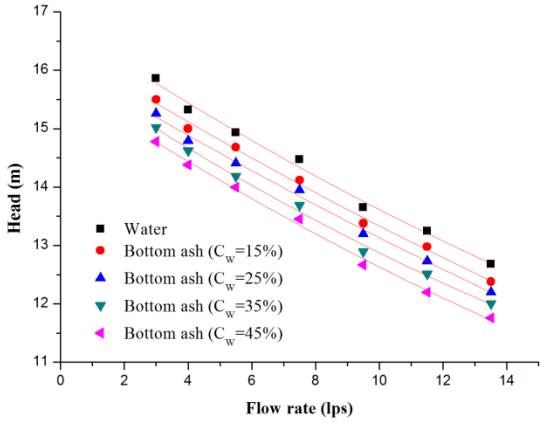

(a) Head-flow rate characteristics

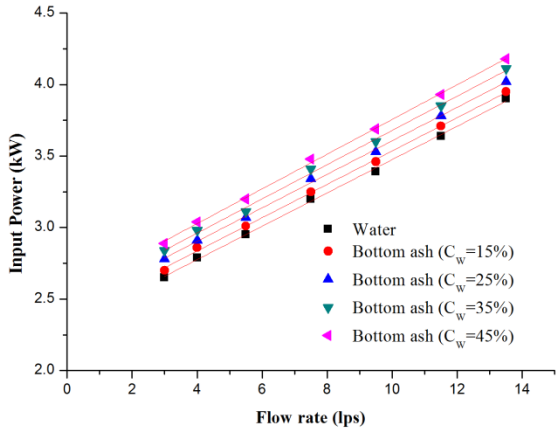

(b) Input power-flow rate characteristics

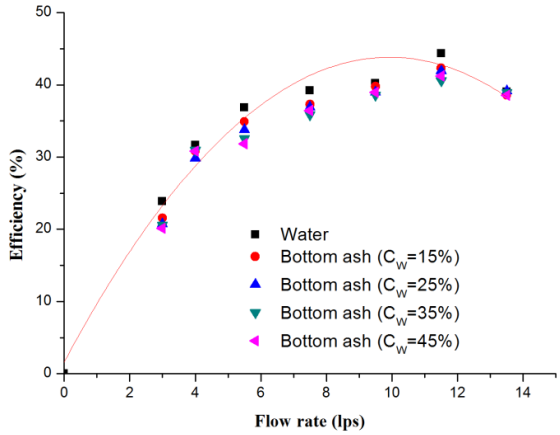

(c) Efficiency -flow rate characteristics

Figure: 5.11: Numerical performance characteristics of pump with bottom ash slurry at 1300rpm

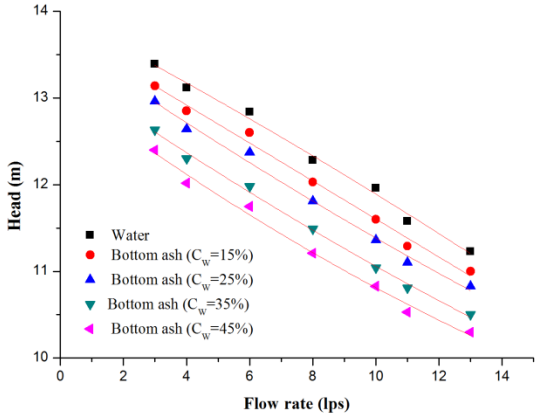

(a) Head-flow rate characteristics

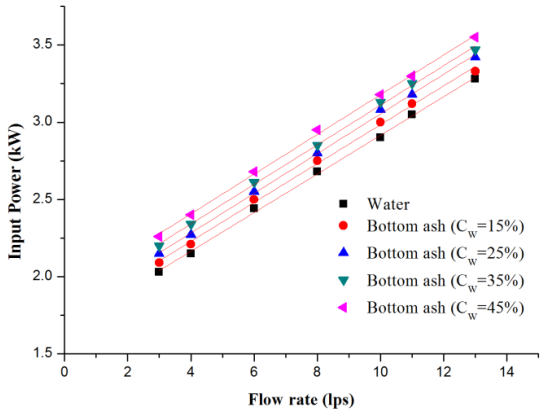

(b) Input power-flow rate characteristics

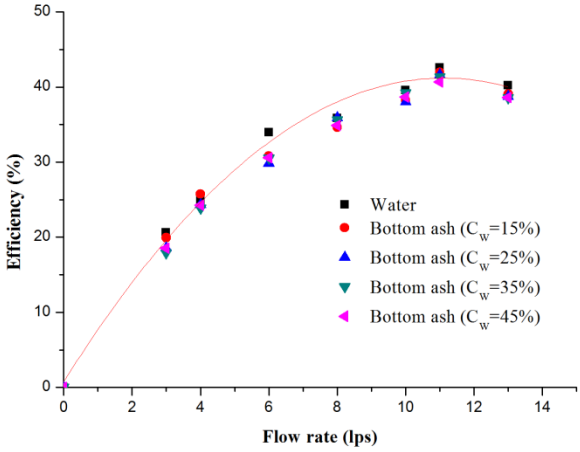

(c) Efficiency -flow rate characteristics

Figure: 5.12: Numerical performance characteristics of pump with bottom ash slurry at 1150rpm

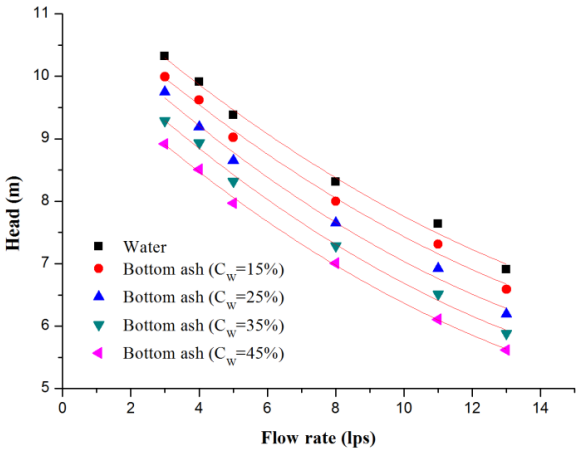

(a) Head-flow rate characteristics

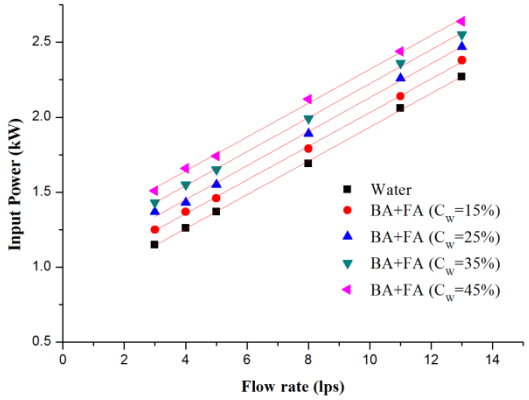

(b) Input power-flow rate characteristics

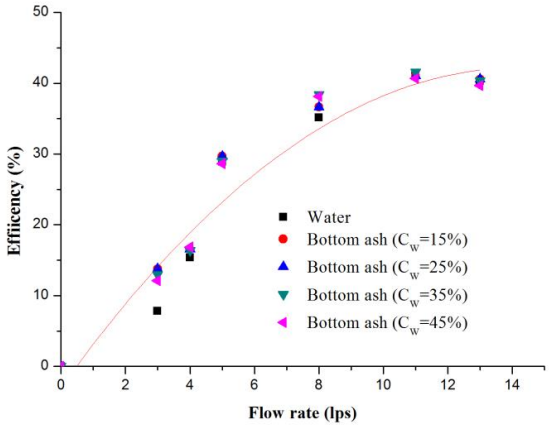

(c) Efficiency -flow rate characteristics

Figure: 5.13: Numerical performance characteristics of pump with bottom ash slurry at 1000rpm

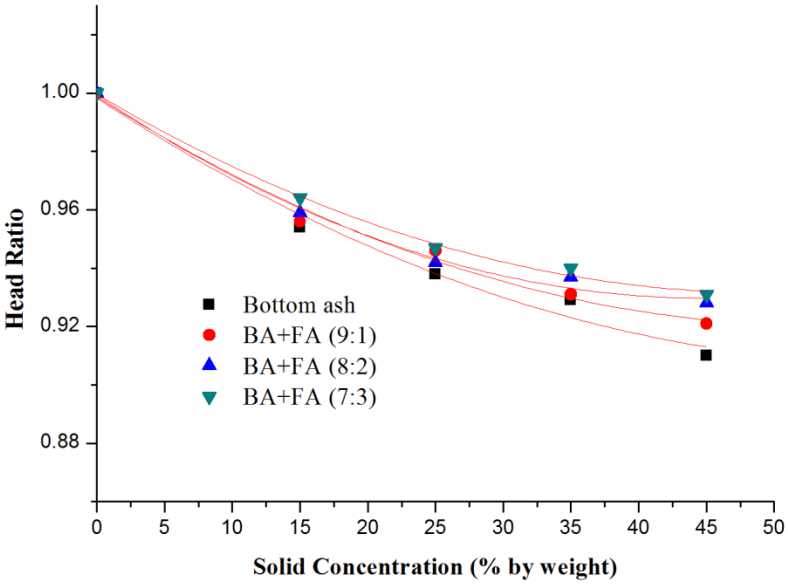

Figure 5.14: Head ratio variation of bottom ash at B.E.P

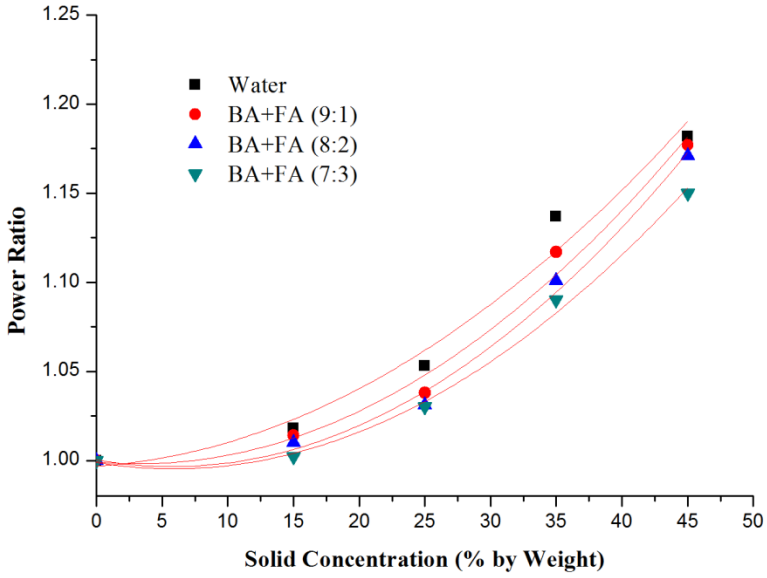

Figure 5.15: Power ratio variation of bottom ash at B.E.P

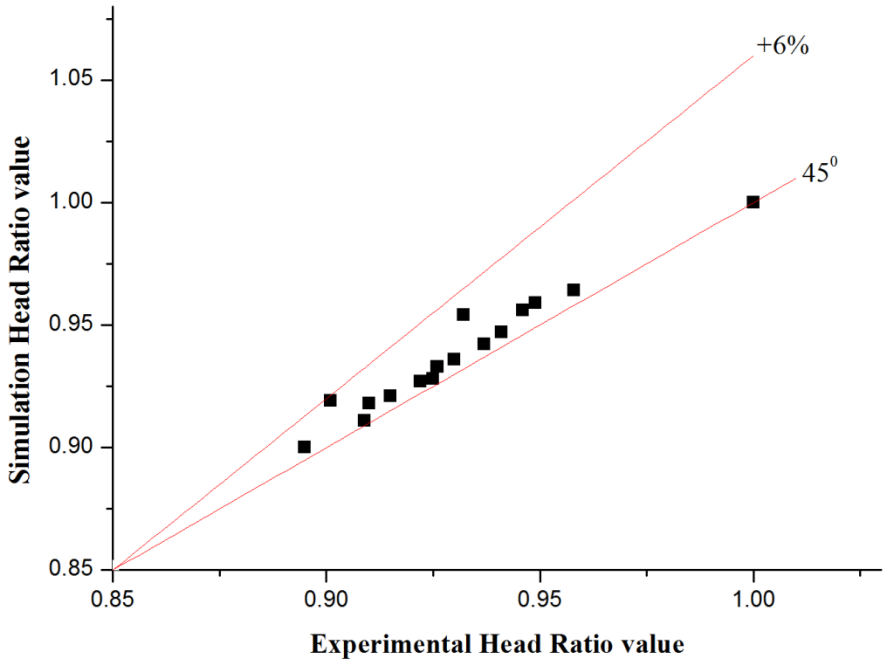

Figure 5.16: Comparison of experimental values and predicted value of Head ratio

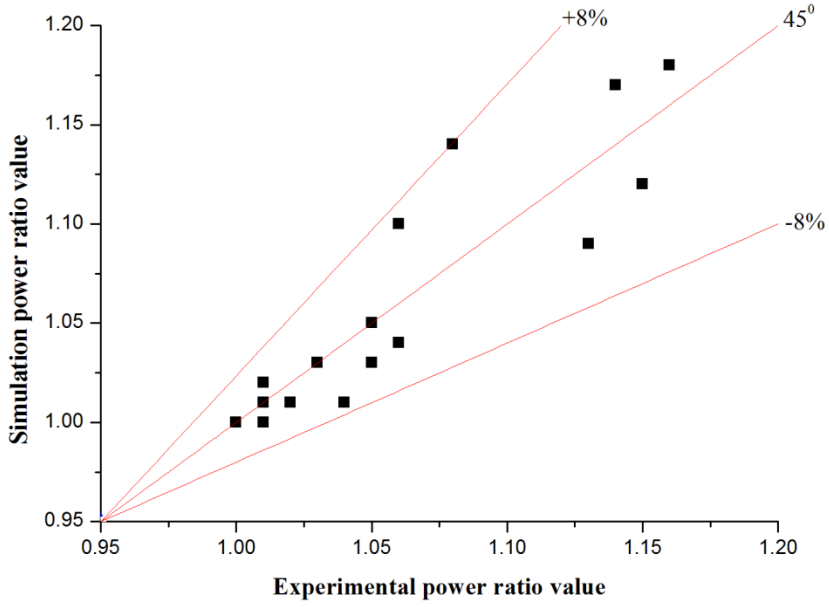

Figure 5.17: Comparison of experimental values and predicted value of Power ratio

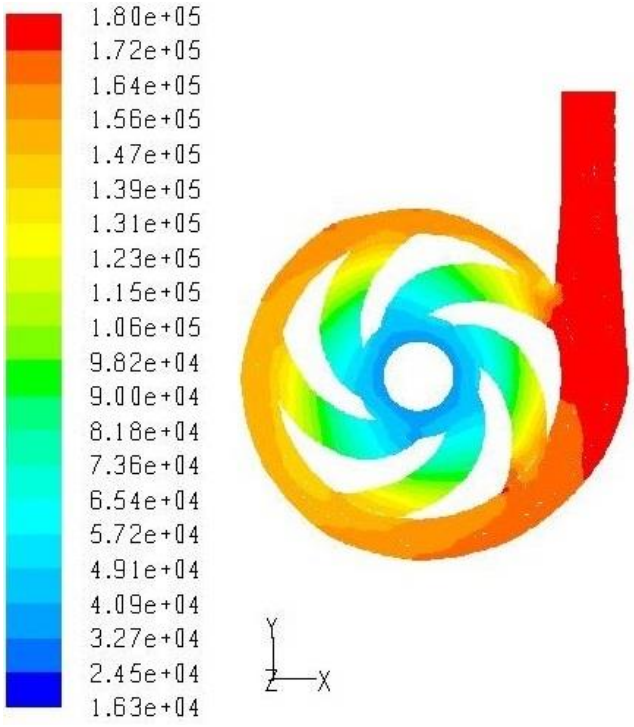

(a) Q/Q_{bep}=0.25

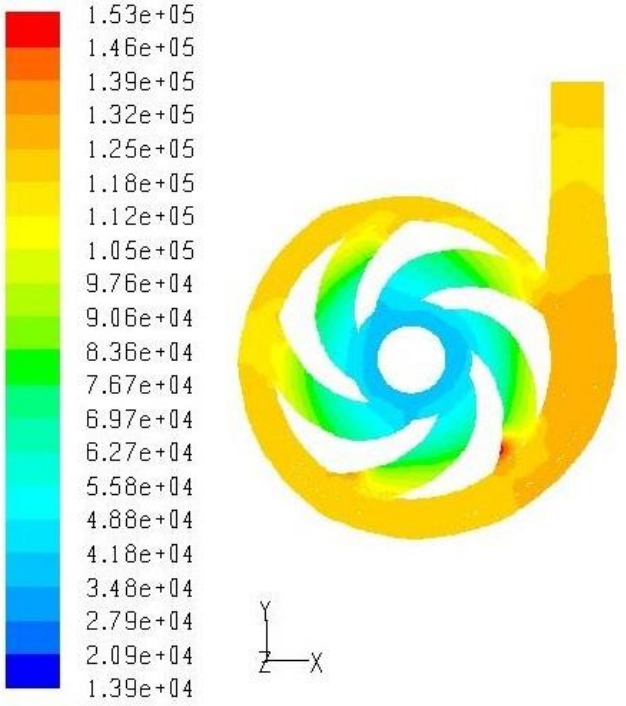

(b) Q/Q_{bep}= 1

Figure 5.18: Static pressure distribution of pump at 1450 rpm

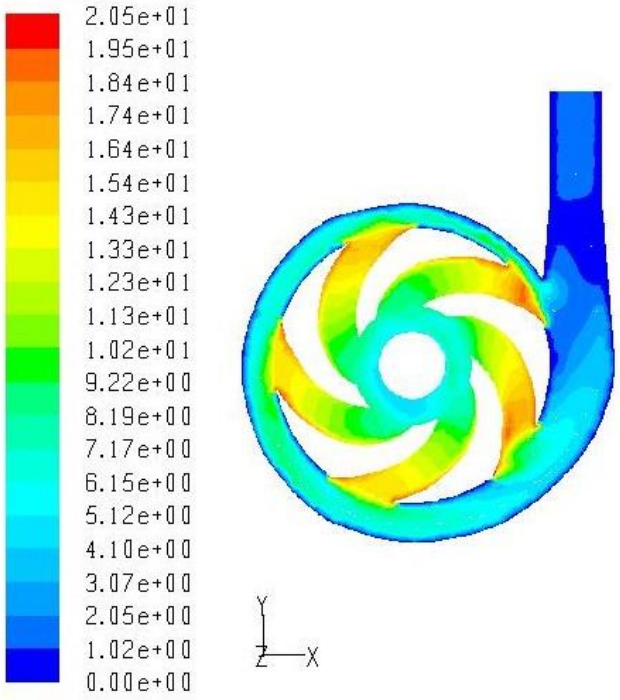

(a) Q/Q_{bep}=0.25

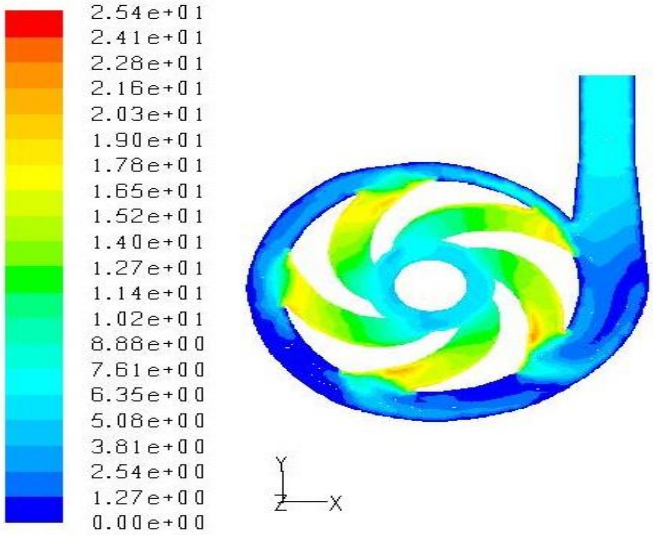

(b) Q/Q_{bep}= 1

Figure 5.19: Absolute velocity distribution of pump at 1450 rpm

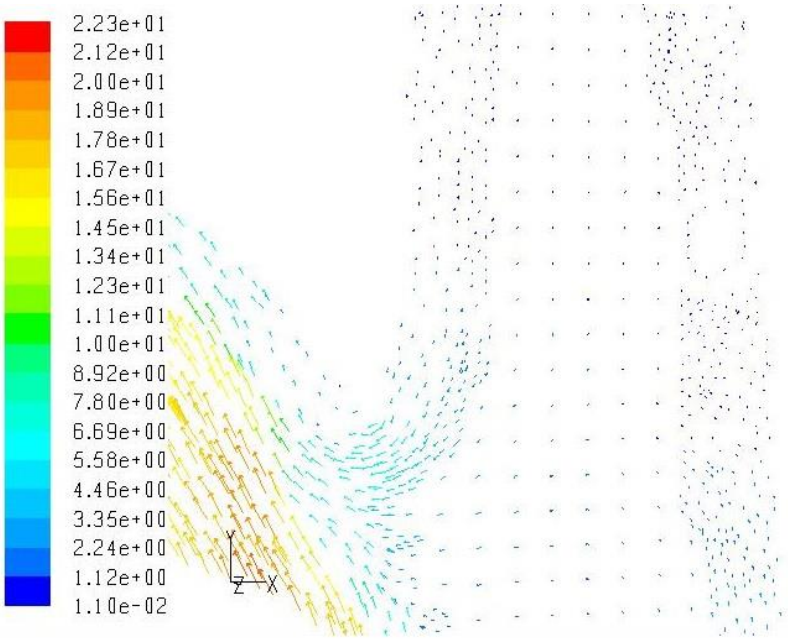

(a) Q/Q_{bep}=0.25

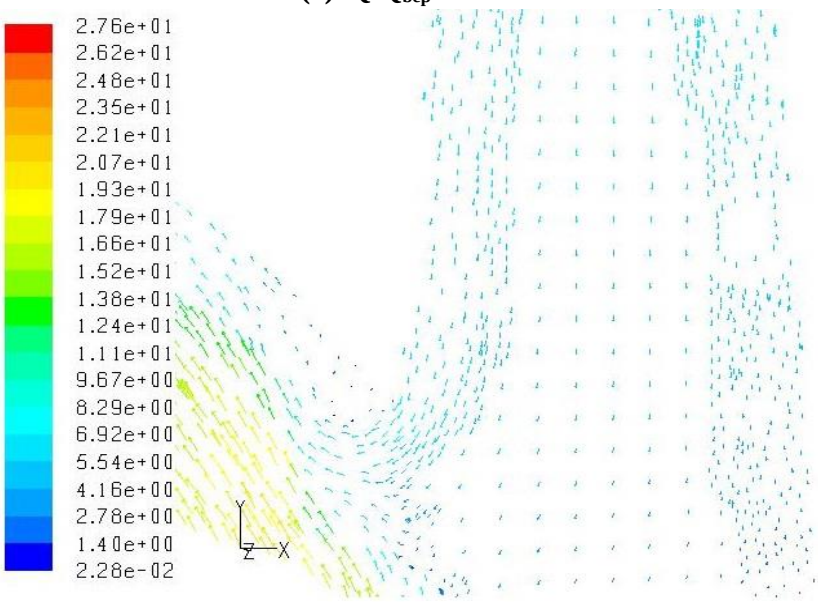

(b) Q/Q_{bep}= 1

Figure 5.20: Velocity vector contour at the tongue of the impeller and volute Interface

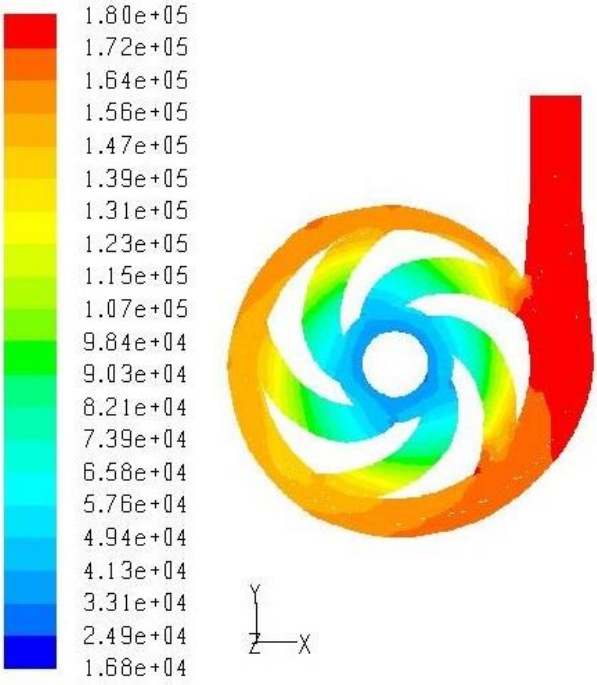

(a) Q/Q_{bep}=0.25

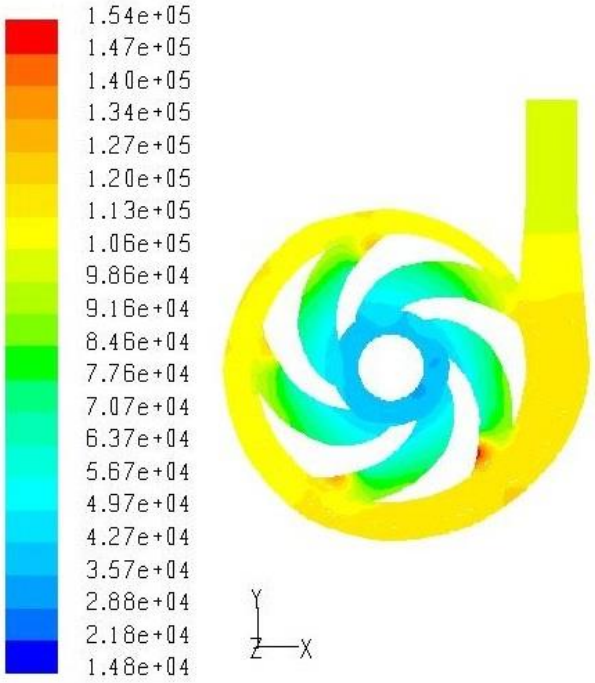

(b) Q/Q_{bep}= 1

Figure 5.21: Static pressure distribution of pump at 1000 rpm

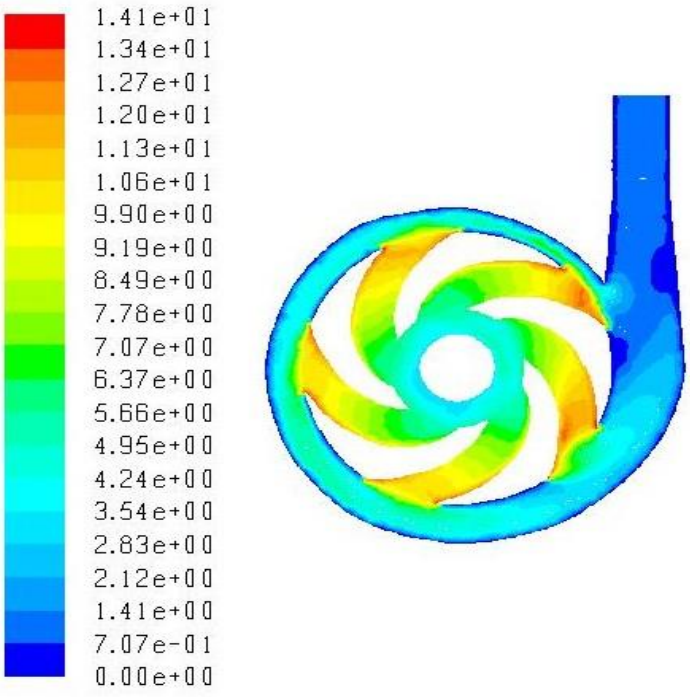

(a) (Q/Q_{bep}=0.25)

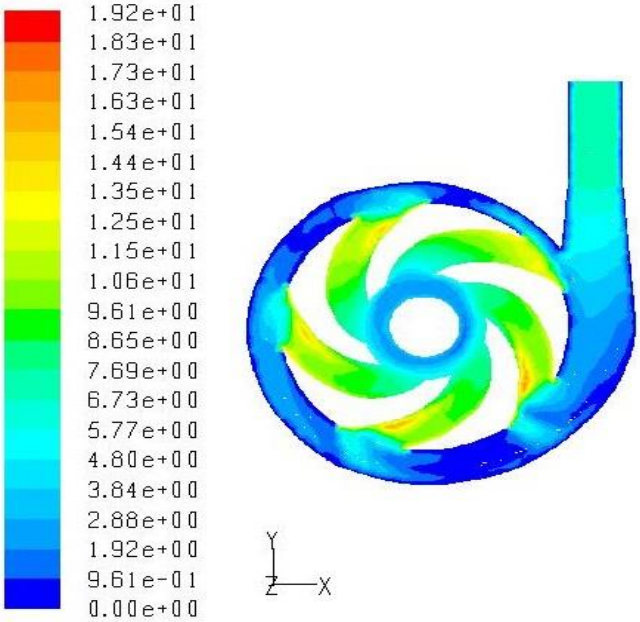

(c) (Q/Q_{bep}=1)

Figure 5.22: Absolute pressure distribution of pump at 1000 rpm

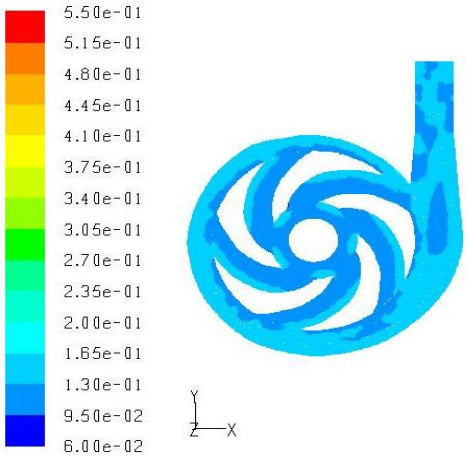

(a) 15%(by weight)

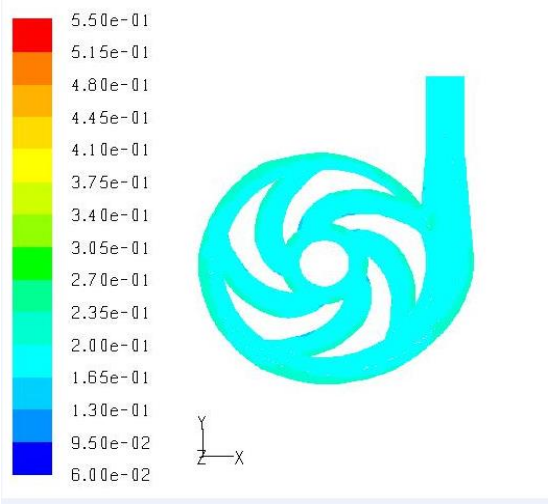

(b) 25%(by weight)

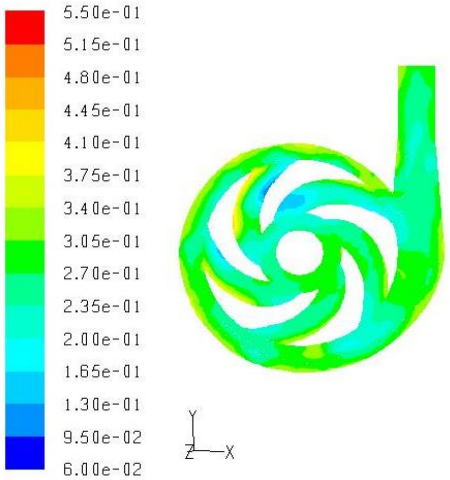

(c) 35%(by weight)

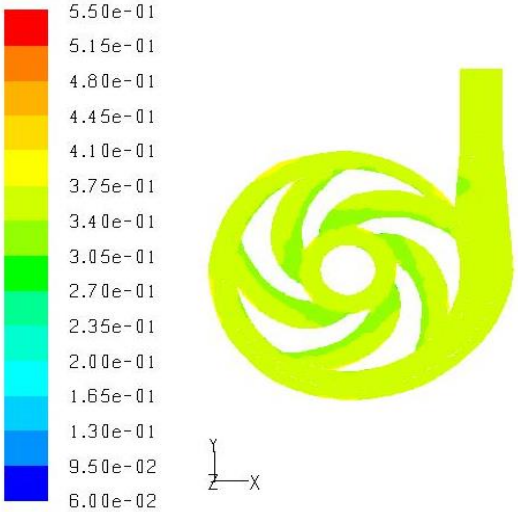

(d) 45% (by weight)

Figure 5.23: Volume fraction distribution of bottom ash slurry at 1450 rpm

CHAPTER6

CONCLUSION AND FUTURE SCOPE

6.1 CONCLUSION

The centrifugal slurry pump performance characteristics for handling multi sized coal ash particulate slurry have been evaluated at different concentration at different speed. Based on study the specific conclusion drawn have already been mentioned an individual chapter. Hence only generic conclusions are listed here:

1. The addition of fine particles of fly ash with coarse particles of bottom ash increases the viscosity of bottom ash slurry.
2. The relative viscosity is reduced with increase in the temperature of the bottom ash slurry, with and without addition of fly ash. The optimum modification temperature was found as 36 ºC.
3. The head and efficiency of centrifugal slurry pump decreases with increase in solid concentration whereas shaft input power increases. Also the head ratio and efficiency ratio is not the function of discharge at any given solid concentration.
4. The specific head relation given by affinity law is valid for centrifugal slurry pump with water whereas the specific power relation needs to be corrected for large changes in the pump speed. The specific head relation which is valid for water flow is also applicable for bottom slurry at low solid concentrations (below 20% by weight)
5. Addition of fly ash improves the performance of centrifugal slurry pump handling bottom ash slurry. Addition of fly ash in proportion of 20% (by weight) of the total weight of the ash slurry improved the maximum head ratio and efficiency ratio.
6. The present study can be useful for transporting bottom ash with addition of fly ash at higher concentrations, so that large amount of water and power can be saved.
7. From the analysis of flow distribution inside the centrifugal slurry pump, following problems have been identified for improving the design of the pump for better hydraulic performance.

- From the flow distributions near the tongue region of the pump clearly visible the flow separation. This separation can be minimized by optimizing the space between tongue and impeller blade.
- The slurry particles mainly accumulate in the region near to the exit of volute, and the largest volume fraction is observed at this location. The discharge nozzle slope may be modified to reduce the accumulation of solid particles at this location.
- The flow area of the existing impeller blade passages also can be optimized by changing number of blades.

6.2 FUTURE SCOPE WORK

The design of slurry transportation system is dependent on large number of parameters and the focus of the present study is on hydraulic parameters of the slurry pump. The following aspects of work need greater attention for better understanding of the flow mechanism of highly concentrated slurry through pipes and pumps:

1. To study the shut-down/re-start characteristics of the slurry pipeline and pump at higher concentration.
2. To carry out detailed flow field analysis of the solid–liquid flow through centrifugal type pump as well as positive displacement pumps using CFD tools or sophisticated instrument like laser Doppler velocimeter (LDV) etc.
3. To study the wear characteristics of different pump and piping materials with help of erosion wear tester.
4. To investigate the performance of the slurry suspension at high concentration with addition of different suitable additives.
5. To study the effect of various clearance on the performance and erosion characteristics of slurry pump. This will enable the optimization of these parameter.

REFERENCE

1. Addie, G.R. and Sellgren, A. 2007. The new ANSI/HI centrifugal slurry pump standard, *BHRA 17th International Conference on the Hydraulic Transport of Solids,Cape Town, South Africa,*.205–218.
2. Ahmad, M. Singh, S.N. and Seshadri, V. 1995. Pressure drop in a long radius 90º horizontal bend for the flow of multi sized heterogeneous slurries, *International Journal of Multiphase Flow*, 2(2):329-334.
3. Ahmad, M. Singh, S.N. and Seshadri, V. 1997. Prediction of concentration and size distribution of solids in a slurry pipeline, *Indian Journal of Engineering and Materials Science*, 4(1):1-9.
4. Aman, A. Sileshi, K. and Edessa, D. 2011. Flow simulation and performance prediction of centrifugal pumps using CFD tool, *Journal of the European Economic Association*, 28:59-65.
5. Asuaje, M. Bakir, F. Kouidri, S. Kenyery, F. and Rey, R. 2005. Numerical modelization of the flow in centrifugal pump: volute influence in velocity and pressure fields, *International Journal of Rotating Machinery*, 3:244–255.
6. Aude, T.C. Thompson, T.L. and Wasp, E.J. 1974. Economics of slurry pipeline system, *3rd International Conference on the Hydraulic transport of Solids in Pipe,Golden, Color., USA*, 2-13.
7. Aude, T.C. Thompson, T.L. and Wasp, E.J. 1975. Slurry pipe line system oil and gas, *Journal of Pipelines*, 66-73.
8. Bacharoudis, E.C. Filios, A.E. Mentzos, M.D. andMargaris, D.P. 2009. Parametric study of a centrifugal pump impeller by varying the outlet blade angle, *The Open Mechanical Engineering Journal*, 2:75-83.
9. Bain, A.G. and Bonnington, S.T. 1970. The hydraulic transport of solids by pipe line, *Pergamon Press*.

10. Baiz, A. 1984. Performance of irrigation pumps in muddy waters, *Multiphase flow and heat transfer III. Part B: Application*, Elsevier science publication, 527-540.

11. Bbraganca, S.R. Goncalves, M.R.F. Bergmann, C.P. and Rubio, J. 2009. Coal ash transportation as paste like highly loaded pulps in Brazil: characterization and main features, *International Journal of Coal Preparation and Utilization*, 29:203-215.

12. Behrouz, J. Hajari, A. and Mehdi M. 2010. The flow simulation of a low- specific-speed, high-speed centrifugal pump,*Applied Mathematics and Modeling*, 19:425-432.
13. Benretem, A. Iiaddouche, A. Cheghib. S. 2007. Influence of solid particles on centrifugal pump characteristics, Journal of Engineering and Applied Sciences, 2(1): 244-247.

14. Biswas, A. Gandhi, B.K. Singh, S. N. and Seshadri, V. 2000. Characteristics of coal ash and their role in hydraulic design of ash disposal pipelines, *Indian Journal of Engineering and Material Science*, 7:1-7.

15. Boylu, F. Dincer, H. and Atesok, G. 2004. Effect of coal particle size distribution, volume fraction and rank on the rheology of coal–water slurries, *Fuel Processing Technology*, 85: 241-250.
16. BS 5316 Part 1. 1976. Acceptance tests for centrifugal mixed flow and axial pumps part 1 class C tests Gr 8, *British Standards Institution*,London.
17. Bunn, T.F. Chambers, A.J. and Goh, C.M. 1990. Rheology of some fly ash slurry, *Proceeding of International Coal Engineering Conference,Sydney Australia*, 7-14.
18. Bunn, T.F. and Chambers, A.J. 1991. Rheology of some fly ash slurries, *Powder Handling and Processing*, 3(3):221-256.

19. Bunn, T.F. and Chambers, A.J. 1993. Experiences with dense phase hydraulic conveying of vales point fly ash, *International Journal of Powder Handling and Processing*, 5(1):35-44.

20. Buranasrisak, P. and Narasingha, M.H. 2012. Effects of particle size distribution and packing characteristics on the preparation of highly-loaded coal-water slurry, *International Journal of Chemical Engineering and Applications*, 3:31-35.

21. Burgess, K.E. and Riezes, J.A. 1976. The effect of sizing, specific gravity and concentration on the performance of centrifugal slurry pumps, *Proceeding of Institutional Mechanical Engineers*, 190 (36/76): 391-398.

22. Byskov, R.K. Jacobsen, C.B. and Padersen, N. 2003. Flow in a centrifugal pump impeller at design an off-design conditions-Part Ⅱ: large eddy simulations, *Journal of Fluids Engineering*, 125:73-83.

23. Cader, T. Masbernet, O. and Roco, M.C. 1992. LDV measurements in centrifugal slurry pump for water and dilute slurry flow,*Transaction Actions of ASME, Journal of Fluid Engineering*, 114: 606-613.

24. Cader, T. Masbernet, O. and Roco, M.C. 1994. Two-phase velocity distributions and overall performance of a centrifugal slurry pump,*Transaction Actions of ASME, Journal of Fluid Engineering*, 116: 316-323.

25. Cao, S. and Peng, G. 2005. Hydrodynamic design of rotodynamic pump impeller for multiphase pumping by combined approach of inverse design and CFD analysis, *ASME Transaction: Journal of Fluids Engineering*, 127: 330–338.

26. Cave, I. 1976. Effect of suspended solids on the performance of centrifugal pumps, *4th International Conference on the Hydraulic Transaction port of Solids in Pipes, Paper H3-35 BHRA Fluid Engineers.1-9.*

27. Chakraborty, S. Pandey, K.M. Roy, B. 2012. Numerical analysis on effects of blade number variations on performance of centrifugal pumps with various rotational speeds, *International Journal of Current Engineering and Technology*, 143-152.

28. Chakraborty S. Choudhari, K. Dutta, P. and Debbarma, B. 2013. Prediction of centrifugal pumps with variations of blade number, *Journal of Scientific & Industrial Research*, 72: 373-378.

29. Chand, P. Adinaryana, B. and Singh, R.P., 1985. Effect of drag reduction polymer on slurry pump characteristics; Bulk *solid Handling*, 5(4): 807-811.

30. Chandel, S. Singh, S. N. and Seshadri, V. 2009a. Deposition characteristics of coal ash slurries at higher concentrations, *Advanced Powder Technology*, 20:383–389.

31. Chandel, S. Singh, S.N. and Seshadri, V. 2009b. Effect of additive on pressure drop and rheological characteristics of fly ash slurry at high concentration, *Journal of Particulate Science and Technology*,27:271-284.

32. Chandel, S. Singh, S.N. and Seshadri, V. 2011. A comparative study on the performance characteristics of centrifugal and progressive cavity slurry pumps with high concentration fly ash slurries,*Particulate Science and Technology*, 29:378-396.

33. Cheah, K.W. Lee, T.S. Winoto, S.H. and Zhao, Z.M. 2007. Numerical flow simulation in a centrifugal pump at design and off-design conditions, *International Journal of Rotating Machinery*, 200:126-134.

34. Cheng, D.C.H. 1980. Viscosity-concentration equations and flow curves for suspensions, *Chemical & Industrial*, 1:403-406.

35. Cheng, X.R. Li, R.N. Gao, Y. and Guo, W.L. 2013. Numerical research on the effects of impeller pump-out vanes on axial force in a solid-liquid screw centrifugal pump, *International Conference on Pumps and Fans with Compressors and Wind Turbines*, 1-6.

36. Cho, H. Oh, D. and Kim, K. 2005. A study on removal characteristics of heavy metals from aqueous by fly ash, *Journal of Hazardous Materials*, 127(1-3):187-195.

37. Convery, M. Downing, L. Yin, C.Y. Goh, B.M. and Sharifah, A.S.A.K. 2010. Characterization of glass-ceramics produced from vitrification of class f Malaysian coal fly ash, *International Journal of Mechanical and Materials Engineering*, 5(1):1-4.

38. Cui, B. Zuchao, Z. Jianci, Z. and Ying, C. 2006. The flow simulation and experimental study of low-specific-speed high-speed complex centrifugal impellers, *Chinese Journal of Chemical Engineering*, 14(4): 435–441.

39. Darby, R. and Melson, J. 1981. How to predict the friction factor for the flow of Bingham plastics, *Chemical Engineering Journal*, 88 (26):59-61.

40. Das, D. 2008. Effect of organized assemblies. part 4 formulation of highly concentrated coal-water slurry using a natural surfactant, *Energy & Fuels*, 22:1865–1872.

41. Das, S. Das, P.K. and Maiti, B. 1998. CAD of centrifugal pump impeller with blades of single curvature, *25th National and 1st International Conference on Fluid Mechanics & Fluid Power*, India, 214-223.
42. Dick, E. Vierendeels, J. Serbruyns, S. and Voorde, J.V. 2001. Performance prediction of centrifugal pumps with CFD-tools, *Task Quarterly,* 5(4):579–594.
43. Dobson, T. 1971. User's guide to slurry pumps, *Technical and Supervisory Publication of the AVEW.*
44. Einstein, A. 1956. Investigation on the theory of the Brownian movement, *Dover Publications,* New York.
45. Engin, T. and Gur, M. 2001. Performance characteristics of a centrifugal pump impeller with running tip clearance pumping solid-liquid mixtures, *Journal of Fluids Engineering*, 193:532-538.
46. Engin, T. and Gur, M. 2003. Comparative evaluation of some existing correlations to predict head degradation of centrifugal slurry pumps, *Journal of Fluids Engineering*, 125:125-157
47. Fairbank, L.C. 1942. Effect on the characteristic of centrifugal pump, *Solid in Suspension Symposium ,Transaction of ASME*, 107:1564-1575
48. Feng, J. Benra, F.K. and Dohmen, H.J. 2007. Numerical investigation on pressure fluctuations for different configurations of vaned diffuser pumps, *International Journal of Rotating Machinery,* 1-10.
49. Fluent 6.1 User's Guide, 2003. Fluent Inc.
50. Frei, B. and Huber, H. 2005. Characteristics of different pump types operating with ice slurry, *International Journal of Refrigeration*, 28:92-97.
51. Gahlot, V.K. Seshadri, V. and Malhotra, R.C. 1988. A method for the experimental determination of the rheological parameters of multi-sized course particulate slurries, *International symposium on hydraulic transportation of coal and other minerals,* IIT Delhi, 283-295.

52. Gahlot, V.K. Seshadri, V. and Malhotra, R.C. 1992. Effect of density, size distribution, and concentration of solid on the characteristics of centrifugal pumps, *Transaction actions of ASME, Journal of Fluid Engineering*,114: 386-389.
53. Gandhi, B.K. Singh, S.N. and Seshadri, V. 1998. Predictions of performance characteristics slurry pump handling clear liquid, *Indian Journal of Engineering & Materials Sciences*, 5: 91-96.
54. Gandhi, B.K. Singh, S.N. and Seshadri, V. 2000. Improvement in the prediction of performance of centrifugal slurry pump handling slurries,*Proceeding of Intuition Indian Journal of Mechanical Engineers*, 214:473-486.
55. Gandhi, B.K. Singh, S.N. and Seshadri, V. 2001, Performance characteristics of centrifugal slurry pumps, *Transaction actions of ASME, Journal of Fluid Engineering*, 123:271-280.
56. Gandhi, B. K. Singh, S. N. and Seshadri, V. 2002. Effect of speed on the performance characteristics of a centrifugal slurry pump, *Transaction Actions of ASCE, Journal of Hydraulic Engineering*, 128: 225-233.
57. Gay, E.C., Nelson, F.A. and Armstrong, W.P. 1969 Flow properties of suspensions with solid concentration, *American Institute of Chemical Engineers Journal*, 15 (6): 815.
58. Gayo, J.L. Gonzalez, J. and Francos, F.J. 2002, The effect of the operating point on the pressure fluctuations at the blade passage frequency in the volute of a centrifugal pump, *Transactions of the ASME: Journal of Fluids Engineering*, 124 (3):784–790.
59. Ge, X.F. Gao, Z.X. Zheng, Y. and Shen, M.H. 2012, Efficiency calculation and the vortex characteristics research of centrifugal pump,*Earth and Environmental Science*, 15:1-6.
60. Ghanta, K.C. and Purohit, N.K. 2002. Effect of particle size distribution (psd) on the viscosity of suspension of bi-dispersed particles, *Proceedings Hydro transport 15, (*Cranfield, Bedfort), England, 299-313.

61. Gillies, R. Haas, D.B. Husband, W.H.W. Small, M. and Shook, C.A. 1982.A system to determine simple pass particle degradation by pump, *Hydro Transaction Port, BHRA Fluid Engineers*, Johannesburg, South Africa.
62. Gonz´alez, J. Fernandez-Francos, J. Blanco, E. and Santolaria-Morros, C. 2002. Numerical simulations of the dynamic effects due to impeller-volute interaction in a centrifugal pump, *Transactions of the ASME, Journal of Fluids Engineering*, 124 (2):348–355.
63. Gonz'alez, J. and Santolaria, M.C. 2006. Unsteady flow structure and global variables in a centrifugal pump, *Journal of FluidsEngineering*, 28: 937-946
64. Holman, J. P. 1994 Experimental Methods for Engineers, McGraw-Hill, Sixth Edition.
65. Herbitch, J. B. 1962. Modification in design improve dredge pump Efficiency, *Fritz Engineer Lab, Report*, 277-350.
66. Heywood, N.I. Mehta, K.B. Poplar, D. and Moore, C.D. 1993. Assesment of the flow characteristics of pulverised fuel ash slurries at higher concentration, *12th International conference on slurry handling and pipeline transport, Hydrotransport-12*, Belgium,
67. Hornsby, C. 2002. CFD – driving pump design forward, *World Pumps*, 1:18–22.
68. Horsely, R.R. 1982. Viscometers and pipe loop test on gold slime slurry at very high concentration (by weight) with and without additive, Proceedings *of Hydro transport 8, BHRA Fl Engineering*, Cranfield, Bedford, UK, 133.
69. Houlin, L. Yong, W. Shouqi, Y. Minggao, T. and Kai, W. 2010. Effects of blade number on characteristics of centrifugal pumps, *Chinese Journal of Mechanical Engineering*, 23:1-6.
70. Hunt, W.A. and Faddric, R.A. 1971. The effect of solids on centrifugal pump characteristics' Zandi, Advances *in Solid-Liquid Flow in Pipes and its Application*, 271, Pergomon Press.
71. Ippen, A. T. 1946. The influence of viscosity on centrifugal pump performance, *Transaction ASME*, 68 (8): 823-829.

72. Itaya, T. and Nishikana, T. 1964. Study on sand pump, *1st Report, on the Trajectories of solid particle in the pump impeller,Bulletin of the Japan Society of Mechanical Engineers*, 7(27): 577-582.

73. Jafarzadeh, B. Hajari, A. Alishahi, M.M. and Akhbari, M.H. 2011. The flow simulation of a low-specific-speed high-speed centrifugal pump, *Journal of Applied Mathematical Modeling*, 35: 242-249.

74. Johnson, M. 1981. *Some aspect of the design of system for non-Newtonian fluids*, 7th Tech. Conference of the BPMA: P17.

75. Jude, L. and Covshi, D.H. 1998, Numerical analysis of the inviscid incompressible flow in two-dimensional radial-flow pump impellers, *Engineering Analysis with Boundary Elements*, 22(4): 271-279.

76. Kawatra, S.K. and Eisele, T.C. 1988. Rheological effects in grinding circuits, *International Journal of Mineral Processing, 22*: 251-259.

77. Kazim, K.A. Maiti, B. and Chand, O. 1997. A correlation to predict the performance characteristic of centrifugal pump handling slurries, *Proceeding of Institutional Mechanical Engineer*, 211: 147-157

78. Kee, N.C.S. and Tan, R.B.H. 2002. CFD Simulation of solids suspension in mixing vessels, *The Canadian Journal of Chemical Engineering*, 80 (4):1-6.

79. Khalil, M.F. Sadek, Z.K. Ahmed, A.A and Azouz, N.A. 2013. Performance characteristics of centrifugal pump conveying soft slurry. *American Journal of Mechanical Engineering.* 1(5): 103-112.

80. Krieger, I.M. 1968. Shear rate in the couetta viscometer, *Transaction Society of Rheology*, 12: 5-13.

81. Kumar, S. Mohapatra, S. K. and Gandhi, B.K. 2013a.Effect of addition of fly ash and drag reducing on the rheological properties of bottom ash, *International Journal of Mechanical and Materials Engineering*,8(1): 1-8.

82. Kumar, S. Mohapatra, S. K. and Gandhi, B.K. 2013b. Investigation on centrifugal slurry pump performance with variation of operating speed, *International Journal of Mechanical and Materials Engineering,*8(1): 40-47.

83. Kumar, S. Gandhi, B.K. and Mohapatra, S. K. 2014.Performance characteristics of centrifugal slurry pump with multi-sized particulate bottom and fly ash mixtures, *Particulate Science and Technology.32:466-476.*

84. Kumar, U. Gandhi, B.K. Singh, S.N. Seshadri, V. and Gupta V.K. 2000. Performance characteristics of demonstration unit for transportation of solid-liquid flow at high concentration setup at NCPP,Dadri, *Proceedings International Seminar on Material handling Systems Indian Institute of Plant Engineers,* Delhi-Haryana Chapter,16(18):126-136.

85. Landel, R.F. Moser, B.G. and Baumann, A.J. 1965. Rheology of concentrated suspension : effect of surfactant, *4th International Congress on Rheology*, 663-673.

86. Lazarus, J.H. and Sive, A.W. 1984. A novel balance beam tube viscometer and rheological characteristics of high concentration fly ash slurries, *Ninth International Conference on Hydraulic Transport of Solids in Pipes,* Rome, Italy, 207-226.

87. Li, W.G. 2011. Blade exit angle effects on performance of a standard industrial centrifugal oil pump, *Journal of Applied Fluid Mechanics,* 4(2): 105-119.

88. Link, J.M. Faddick, R.R. and Lavingia, N.J. 1974. Slurry pipeline economics, *Society of Mining Engineering, AIME Annual meeting,* Dallas Texas.

89. Liu, Y. Jiang, Y. Han, Z. 2009. Research on the pattern of solid-liquid two-phase distribution in chemical process pump, *26th IAHR Symposium on Hydraulic Machinery and Systems.*1-8

90. Liu, H. Yong, W. Shouqi, Y. Minggao, T. and Kai, W. 2010. Effects of blade number on characteristics of centrifugal pumps,*Chinese Journal of Mechanical Engineering,* 23:1-5.

91. Liu, J. and Zhu, M. 2011. Numeration simulation of solid-liquid two-phase flow in centrifugal sewerage pump, *Applied Mechanics and Materials*, 44: 345-348.
92. Liu, Y. Jiang, Y. Han, Z.J. 2012. Research on the pattern of solid-liquid two-phase distribution in chemical process pump, *26th IAHR Symposium on Hydraulic Machinery and Systems*, 1-8.
93. Lun, C.K.K. Savage, S.B. Jeffrey, D.J. and Chepurniy, N. 1984. Kinetic theories for granular flow: In elastic particles in Couette flow and slightly inelastic particles in a general flow field, Journal of Fluid Mechanics, 54: 223–256.
94. Maclnnes, M.A. 2002. Investigation into effects of slurry thinners on the rheology of chalk slurries, *Proceeding Hydrotransport 15, BHRA Group, Fluid Engineering , Cranfield, Bedford, England:* 375-384.
95. Maz, 1984. The influence of solid concentration, solid density and grain size distribution on the working behaviour of centrifugal pump, *Hydro transport BHRA Fluid Engg*, Rome, Italy, paper H1.
96. Miner, S.M. 2000. Evaluation of blade passage analysis using coarse grids, *Transaction of ASME, Journal of Fluids Engineering*, 122:345-348**.**
97. Mishra, R., Singh, S.N. and Seshadri, V. 1998. Improved model for the prediction of pressure drop and velocity field in multi-sized particulate slurry flow through horizontal pipes, *Powder handling & processing*, 10(3):279-287.
98. Mishra, R. Fabien, C. Singh, S. and Seshadri, V. 2001. Holdup in multisized particulate solid-liquid flow through horizontal pipe,*Indian Journal of Engineering & Materials Sciences* , 8:84-89.
99. Mishra, S.K. Senapati, P.K. and Panda, D.2002. Rheological behavior of coal-water slurry,*Energy Sources Taylor & Francis*, 24: 159-167.
100. Mooney, M. 1951. The viscosity of a concentrated suspension of spherical particles, *Journal of Colloid Science*, 6:162-169.

101. Moreland, C. 1963. Viscosity of suspensions of coal in mineral oil, *Canadian Journal of Chemical Engineering,* 41:24-28.

102. Murakami, M. Kikuyama, K. and Asakura, E. 1980.Velocity and pressure distributions in the impeller passages of centrifugal pumps, *ASME Journal of Fluids Engineering, 102:420-426.*

103. Naik, H.K. Mishra, M.K. and Rao, U.M. 2009a. The effect of drag reducing additives on the rheological properties of fly ash water suspensions at varying temrature enviornment, *Journal of Coal Combustion And Gasification Products,*1: 25-31.

104. Naik, H.K. Mishra, M.K. Rao, U.M. and Debb, D.2009b.Evaluation of the role of a cationic surfactant on the flow characteristics of fly ash slurry, *Journal of Hazardous Materials,* 169:1134-1140.

105. Naik, H.K. Mishra, M.K. and Rao, U.M. 2011. Evaluation of flow characteristics of fly ash slurry at 40% solid concentration with and without additives, *World of Coal Ash Conference,* May 9-12, Denever, U.S.A., 1-15.

106. Neerken, R.F. 1979. Select the right pump, Fluid Movers-Pumps, Compressor, Fans and Blowers, *McGraw Hill Publication*.

107. Ni, F. Vlasblom, W.J. and Zwartbol, A. 1996. Effect of high solid concentration on characteristics of a slurry pump, *Hydro transaction port 14, BHRA Fluid Engineering.* Maastricht, Neatherland, 141–149.

108. Ogata, S. Kimura, A. and Watanabe, A. 2006 Effect of surfactant additives on centrifugal pump performance, *Journal of Fluids Engineering,* 128:794-798.

109. Osterwalder, J. and Ettig, C. 1977. Determination of individual losses and scale effect by model test with radial pump, *Proceeding of Institutional Mechanical Engineering Conference Publication Paper,* London, 185/77: 105-111.

110. Ozturk, A. Kadir, A. Besir, S. and Pinarbasi, A. 2009. Effect of impeller-diffuser radial gap ratio in centrifugal pump, *Journal of Scientific & Industrial Research,* 72: 203-213.

111. Pagalthivarthi, K.V. Kapoor, R. and Ramanathan, V. 1998. Finite element prediction of turbulent 2 D flow in centrifugal slurry casing, *1st International Conference on Fluid Power, December* 15(17):70-79.

112. Parida, A. Panda, D. Mishra, R.N. Senapati, P.K. and Murthy, J.S. 1995. Transportation of fly ash slurry, *proceeding of workshop on the fly ash management, Bhubaneswar,* 51-63.

113. Parida, A. Senapati, P.K. and Mishra, B.K. 2006. Slurry pipelines for fly ash-a design method for energy efficient fly ash disposal by hydraulic conveying, *Bulk solids handling*, 26(8):556-562.

114. Patidar, A. Gandhi, B.K. 2007. Numerical investigation of the flow field of a centrifugal slurry pump, *Proceedings of National Seminar on CFD- the New 3rd Dimension in Flow Analysis and Thermal Design*, Bhopal, India, 127-132.

115. Pullum, L. Graham, L.J. and Rudman, M. 2007. Centrifugal pump performance calculations for homogeneous and complex heterogeneous suspensions, *Hydro Transaction port 17, BHRA 17th International Conference on the Hydraulic Transport of Solids,* 239–253

116. Reddy, G.V. Mohapatra, S.K. and Sinha, R.K. 1994. Rheological properties of coal oil mixtures: influence of coal properties, *Fuel Science and Technology International*, 12 (9):1257-1270.

117. Remisz, J. 1983. Slurry pump; transformation of characteristics and design, *Proceedings of 8th technical Conference of BPMA,* Cambridge, UK, 13-22.

118. Roco, M.C. and Reinhart, E. 1980. Calculation of solid particles concentration in centrifugal pump impeller using finite element technique, *Proceedings of 7th International Conference onHydraulic Transport of Solids in Pipes, BHRA Fluid Engg.,* Sendai (Japan), Paper J3.

119. Roco, M.C. Addie, G.R. Dennis, J. and Nair, 1984. Modeling erosion wear in centrifugal slurry pump, *Hydro Transport 9, BHRA Fluid Engg*, Rome (Italy), Paper G1.

120. Roco, M. C. Marsh, M. Addie, G.L.R. and Mafett, J.R. 1986. Dredge pump performance predication, *Journal of Pipe line*, 5 (3):171-179.
121. Roco, M.C. Hamelin, P. and Davidson, G. 1989. Experimental study on centrifugal slurry pump, *Freight Pipeline, Proceeding of 6th symptoms freight pipelines Hemisphere Publishing,* New York, 235-244.
122. Roh, N. Shin, D.H. Kim, D.C. and Kim, J.D. 1994. Rheological behaviour of coal-water mixtures effects of coal type, loading and particle size, *Fuel*, 74: 1220-1225.
123. Roscoe, R. 1952. The viscosity of suspension of rigid spheres, *British Journal Applied Physics, 3: 267*-274.
124. Rutger, R., (1962), Relative viscosity of concentrated suspensions of rigid spheres in Newtonian fluids, *Rheology, Acta*, 2: 202-209.
125. Saeki, T. Tatsukawa, T. and Usui, H. 1999. Preparation techniques of coal water mixtures with upgraded low rank coals, *Coal Preparation,* 21:161-176.
126. Salopek, B. Krasi, D. and Filipovi, S. 1992. Measurement and application of zeta-potential, ActaTechnicaCorviniensis - Bulletin of Engineering, 4:147-151.
127. Schrick, W. Smith, L.G. Hass, D.B. and Husband, W.H.W. 1972. Experimental studies on the hydraulic transport of coal. *Engineering Division of Saskatchewan Research Council*, Canada.
128. Sellgren, A. 1979. Performance of centrifugal pump when pumping ores and Industrial Minerals, *6th International Conference on the Hydraulic Transactionport of Solids in Pipes, Paper G.1, 290 BHRA Fluid Engineers.*
129. Sellgren, A. Addie, G. and Scott, S. 2000. The effect of sand-clay slurries on the performance of centrifugal pump, *The Canadian journal of Chemical Engineering,* 78:764-769.
130. Sellgren, A. and Addie, G. 2002. Using centrifugal pump for highly concentrated tailing slurries, *Proceedings Hydro transport 15, BHRA Fluid Engineering,* Banff (Canada), 2: 669-677.

131. Senapati, P.K. Panda, D. and Parida, A. 2005. Studies on high concentration fly ash – bottom mixture slurry, *Bulk Solid Handling*, 25(6): 386-290.

132. Senapati, P.K. Das, D. Nayak, A. and Mishra, P.K. 2008. Studies on preparation of coal water slurry using a natural additive, *Energy Sources, Part A: Recovery, Utilization, and Environmental Effects*, 30:1788-1796.

133. Senapati, P.K. Panda, D. and Parida, A. 2009. Predicting viscosity of limestone water slurry, *International Journal of Minerals & Materials Characterization & Engineering*, 8(3): 203-221.

134. Senapati, P.K. Mishra, B.K. and Parida, A. 2010. Modeling of viscosity for power plant ash slurry at higher concentrations: Effect of solids volume fraction, particle size and hydrodynamic interactions, *Powder Technology*, 197:1-8.

135. Senapati, P.K. Mishra, B.K. Parida, A. 2013. Analysis of friction mechanism and homogeneity of suspended load for high concentration fly ash & bottom ash mixture slurry using rheological and pipeline experimental data, *Powder Technology*, 250:154-163.

136. Seshadri, V. Singh, S.N. Jain, K.K. and Verma, A.K. 2005. Effect of additive on head loss in the high concentration slurry disposal of fly ash, *Institution of Engineers*, 89:3-10.

137. Seshadri, V. Singh, S.N. Jain, K.K. and Verma, A.K. 2008**.** Effect of additive on head loss in the high concentration slurry disposal of fly ash, *Journal of Institution of Engineers*, 89:3-10.

138. Shojaeefard, M.H. Tahani, M. Ehghaghi, M.B. Fallahian, M.A. and Beglari, M. 2012. Numerical study of the effects of some geometric characteristics of a centrifugal pump impeller that pumps a viscous fluid, *Computer & Fluid*, 60: 61-70.

139. Sive, A.W. and Lazarus, J.H. 1987. Hydraulic transport system design for high concentration fly ash slurries, *Ash a Valuable Resource*, Pretoria, South Africa.

140. Spence, R. and Amaral-Teixeira, J. 2008.A CFD parametric study of geometrical variations on the pressure pulsations and performance characteristics of a centrifugal pump, Journal *of Computer and Fluid,* 38:1243-1257.

141. Stepnoff, A.J. 1957. Centrifugal and axial flow pumps theory, design and application, *John Wiley and Sons*.

142. Stepnoff, A.J. 1965. Pumps and blowers, two phase flow –flow and pumping of solids in suspension and fluid mixtures, John *Wiley and Sons. Inc,*

143. Sun, J. and Tsukamoto, H. 2001. Off design performance prediction for diffuser pump, *Proceeding of Intuition of Mechanical Engineers, Part A,* 215-224.

144. Sutton, M. 1968. Pump scale laws as affected by individual components losses, *Proceeding of Institutional Mechanical Engineers on Model Testing of Hydraulic Machinery and Associated Structure, 182, Pt 3 M.Cranfield ,Paper 10.*

145. Syamlal, M. Rogers, W. and Brien, T.J. 1993. NFX Documentation: Theory guide. National Technical Information Service, Springfield, VA.

146. Thomas, D.G. 1965. Transport characteristics of suspensions, a note on the viscosity of Newtonian suspension of uniform spherical particles, *Journal of Colloid Sci*ence, 20:267-273.

147. Thomas, A. and Sobota, J. 2002. Influence of additives on energy loss in pipeline flow of fly ash mixtures, *Proceedings of Hydro transport 15, BHRA Group, Fluid Engineering,*Cranfield, Bedford, England, 329-339.

148. Turian, R.M. Hsu, F.L. Avramidis, K.S. Sung, D.J. and Allendorfer R.K. 1992. Settling and Rheology of Suspensions of Narrow-Sized Coal Particles, *American Institute of Chemical Engineers Journal,* 38(7): 969-975.

149. Usui, H. Li, L. and Suzuki, H. 2001. Rheology and pipeline transportation of dense fly ash-water slurry, *Korea-Australia Rheology Journal,* 13:47-54.

150. Verma, A. K. Singh, S.N. and Seshadri, V. 2006. Pressure drop for the flow of high concentration solid liquid mixture 90˚ horizontal conventional circular pipe bends,*Indian Journal of engineering and Material Science*, 13:477-483.

151. Vlasak, P. Chara, Z. Stem, P. and Konfrst, J. 2002. Flow behavior and drag reduction of kaolin suspensions, *Proceedings of Hydro transport 15, BHRA Group, Fluid Engineering*,Cranfield, Bedford, England, 334-360.

152. Vlasak, P. and Z. Chara. 2007. Effect of particle size and concentration on flow behavior of complex slurries, *In Proceedings of the Seventh (2007) ISOPE Ocean Mining (& Gas Hydrates) Symposium.* Cupertino, California: International Society of Offshore and Polar Engineers, 188–196.

153. Vlasak, P. and Chara, Z. 2009. Conveying of solid particles in Newtonian and non-Newtonian fluids, *Particulate Science and Technology*, 27(5):428–443.

154. Vocaldo, J.J. Koo, J.K. and Prange, A.J. 1974. Performance of centrifugal pump in slurry service, *Hydro Transaction Part 3, BHRA Fluid engineering*, Colorado (USA) Paper 12.

155. Walker, C. I. and Gaulas, A. 1984. Performance characteristic of centrifugal pump when handling non-Newtonian homogeneous slurries, *Proceeding of Institutional Mechanical Engineers*, 41-48.

156. Walker, C. and SubbaRao, A.V. 1985. Design features of centrifugal slurry pumps and their applications in high pressure service, *Symposium on Hydraulic Transportation of Solids through Pipelines*, The Institution of Engineers, India, 2:E4.

157. Walker, C.I , P.J and Pomat ,C. 1993. The effect of impeller geometry on the performances of centrifugal slurry pumps, *Freight pipeline, Elsevier science of publisher, New York* : 247-258.

158. Wang, F. Wang, W. Wang, Y. Mao, Z.H. 2003. CFD simulation of solid-liquid two phase flow in baffled stirred vessel with Ruston impellers, *Third international conference on CFD in the minerals and process industries CSIRO,* Melbourne, Australia, 10-12, December, 287-292.

159. Wang, M. and Dong, L. 2005. Analysis of turbulent flow in the impeller of a chemical pump, *Journal of Science and Technology,* 2:218-225.

160. Wang, P. W. Zhao, J. Zou, W.J. and Hu,S.G. 2012. Experimental study and numerical simulation of the solid-phase particles' influence on outside characteristics of slurry pump, *Symposium on Hydraulic Machinery and Systems*, 1-8.

161. Wiedenroth, W. 1978. Experimental works on the transportation of solid-liquid mixture through pipeline and centrifugal pumps", Hydro transport 5, BHRA Fluid Engineering, Hnnover (Germany), Paper A2.

162. Wilfley Technical handbook, A.R. Wilfley& Sons, Inc., Denver, Colorado,2006

163. Williams, P.S. 1953. Flow of concentrated suspensions, *Journal of Applied Chemistry,* 3: 120-127.

164. Wilson, K.C. 1982. A dense phase option for coarse coal pipelining, *J. of Pipelines,* 5: 251-257

165. Wilson, K.C. Addie, G.R. and Clift, R. 1992. Slurry transport using centrifugal pumps, *ElsevierScience Publishers Limited.*, New York.

166. Wu, K.H. Lin, B.J. and Hung, C.I. 2008. Novel design of centrifugal pump impellers using generated marching method and CFD, *Engineering Applications of Computational Fluid Mechanics*, 2(2): 195-207.

167. Xu, J. Tipman, R. and Shook, C. 2002. Centrifugal pump performance with Newtonian and non-Newtonian slurries, *Proceedings Hydro transport 15, BHRA Fluid Engineering,* Banff Canada, 2:693-709.

168. Yang, S. Kong, F. and Chen, B. 2011. Research on pump volute design method using CFD, *International Journal of Rotating Machinery*, 1-7.

169. Yang, C.X. Dong, F.D. and Cheng, X.R. 2013. Numerical investigation of sediment erosion to the impeller in a double-suction centrifugal pump, *6th International Conference on Pumps and Fans with Compressors and Wind Turbines,* 1-7.

170. Yassine, K.C. 2010. Experimental investigations for centrifugal slurry pump performance, *Proceedings of ICFD 10:Tenth International Congress of Fluid Dynamics,*AinSoukhna, Red Sea, Egypt.

171. Yi, L. Zuchao, Z. Zhaohui, H. and Weiqiang, H. 2011. Abrasion characteristic analyses of solid-liquid two-phase centrifugal pump, *Journal of Thermal Science*, 20:283-287.

172. Yi, L. Zuchao, Z. Weiqiang, H. and Zhaohui, H. 2012. Numerical simulation and experimental research on the influence of solid phase characteristics on centrifugal pump performance, *Chinese Journal of Mechanical Engineering*, 25:1-10.

173. Yuliang, Z. Yi, L. Baoling, C. Zuchao, Z. and Huashu, D. 2013. Numerical simulation and analysis of solid liquid two phase flow, *Chinese Journal of Mechanical Engineering,* 26:1-8.

174. Zhou, W. Zhao, Z. and Winoto, S.H. 2003. Investigation of flow through centrifugal pump impeller using computational fluid dynamics, *International Journal of Rotating Machinery*, 9: 49-58.

LIST OF PUBLICATIONS

Journals:

1. Kumar Satish, Gandhi, B.K., and Mohapatra, S. K. 2014.Performance characteristics of centrifugal slurry pump with multi-sized particulate bottom and fly Ash mixtures, *Particulate Science and Technology.* 32:466-476.
2. Kumar Satish, Mohapatra, S. K., and Gandhi, B.K. 2013. Effect of addition of fly ash and drag reducing on the rheological properties of bottom ash,*International Journal of Mechanical and Materials Engineering,*8(1): 1-8
3. Kumar Satish, Mohapatra, S. K., and Gandhi, B.K.2013. Investigation on centrifugal slurry pump performance with variation of operating speed,*International Journal of Mechanical and Materials Engineering,*8 (1): 40-47.

Conference:

1. Kumar Satish, Mohapatra, S. K., and Gandhi, B.K. 2013. Modeling and simulation of flow distribution of centrifugal slurry pump, *The 28th international conference on solid wastetechnology and management, Widener University, Chester, Philadelphia, U.S.A,* 1, 1254-1260.
2. Kumar Satish, Mohapatra, S. K., and Gandhi, B.K. 2013. Numerical Simulation of Solid liquid two phase Flow behaviour in Centrifugal slurry Pump, *International conference on Powder, Granule and Bulk Solids: Innovations and applications, Thapar University, Patiala, India,* 1,170-175.

Paper in Under Review-

1. Influence of fly ash on flow characteristics of bottom ash multisized particulate slurry suspension at high concentration -Asia-Pacific Journal of Chemical Engineering.
2. Effect of addition of fly ash on the Rheological properties of bottom ash slurry at varying temperature- Particulate Science and Technology.
3. Numerical performance evaluation of the flow field of a centrifugal slurry pump handling bottom ash -International Journal for numerical methods in fluids.
4. Investigations of solid-liquid two-phase flow through centrifugal slurry pump impellers using Computational Fluid Dynamics - Journal of Scientific and Industrial Research.